Year : 2011

The JAK2/STAT3 pathway in the embryonic chick heart submitted to anoxia, reoxygenation and oxidant stress

PEDRETTI, Sarah

UNIL | Université de Lausanne
Faculté de biologie et de médecine

Département de Physiologie

The JAK2/STAT3 pathway in the embryonic chick heart submitted to anoxia, reoxygenation and oxidant stress

THESE DE DOCTORAT ES SCIENCES DE LA VIE (PhD)

présentée à la

Faculté de Biologie et de Médecine de l'Université de Lausanne

Par

Sarah Pedretti

Diplômée en Physiologie et Neurosciences
« Specialité Physiologie intégrée et Conditions extrêmes »
Université Claude Bernard, Lyon, France

Jury

Pr. Peter Clarke, Président
Pr. Eric Raddatz, Directeur de thèse
Pr. Lucas Liaudet, Expert
Pr. Jean-Marc Pequignot, Expert externe

LAUSANNE – 2011

UNIL | Université de Lausanne
Faculté de biologie
et de médecine

Ecole Doctorale

Doctorat ès sciences de la vie

Imprimatur

Vu le rapport présenté par le jury d'examen, composé de

Président	Monsieur	Prof. Peter	**Clarke**
Directeur de thèse	Monsieur	Prof. Eric	**Raddatz**
Experts	Monsieur	Prof. Lucas	**Liaudet**
	Monsieur	Prof. Jean-Marc	**Pequignot**

le Conseil de Faculté autorise l'impression de la thèse de

Madame Sarah Pedretti

Master de recherches physiologie université Claude Bernard, Lyon, France

intitulée

The JAK2/STAT3 pathway in the embryonic chick heart submitted to anoxia, reoxygenation and oxidant stress

Lausanne, le 18 février 2011

pour Le Doyen
de la Faculté de Biologie et de Médecine

Peter A.M. Clarke

Prof. Peter Clarke

REMERCIEMENTS

Je remercie bien évidemment le Pr Eric Raddatz de m'avoir fait confiance pendant toutes ces années et d'avoir été un aussi bon directeur de thèse. Merci pour tout ce que vous m'avez enseigné et permis de découvrir. Et comme on dit « le meilleur pour la fin » !!!

Je tiens également à remercier les membres de mon jury: le Pr Lucas Liaudet, le Pr Jean-Marc Pequignot et le Pr Peter Clarke d'avoir accepté de juger mon travail ainsi que pour tous leurs conseils et remarques avisés.

Un merci tout particulier à Stéphany Gardier. Grâce à toi je suis passée de « bébé chercheur » à Dr! Merci de t'être aussi bien occupée de moi avant même que je ne sois officiellement engagée! Cette thèse n'aurait pas été la même sans toi.

Je remercie la « chicken team »: Elodie Robin et Jessica Sabourin pour avoir partagé les derniers moments de ma thèse (et pas les plus faciles!) et pour m'avoir aussi bien conseillée pour mon manuscrit et mes présentations. Les filles je vous confie Eric, prenez-en soin! Merci à Anne-Catherine Thomas pour toute son aide pour les expériences.

Je tiens également à remercier tout le Département de Physiologie avec une pensée particulière pour Brigitte et Fabrice. Merci à vous deux pour tous les excellents moments partagés, je vous adore. Merci à l'équipe des « agrégats »: Denise, Marie-Gabrielle et Florianne, aux petits nouveaux de l'étage: Martine, Florent, Florian et Jacques-Antoine ainsi qu'à Touria, Valentine, Nathalie et Rachel, entre autres, pour tous les moments partagés à la cafèt'!

Merci à tous les « nouveaux » amis rencontrés au cours de ces années: Christine, Séverine, Antoinette, Irène, Jean-Jacques, Liliana, Alexandre, Isabelle: vous avez fortement contribué à rendre mon passage à Lausanne inoubliable!

Je remercie mes amis : Audrey, Jean-Christophe, Adeline, Stéphanie, Marjorie, Leslie, Mathilde, Sandrine et Charlène pour faire partie de ma vie et être mes amis tout simplement…

Une grosse pensée pour Yanick et ses « danseuses » pour m'avoir apportée un « échappatoire » dans les moments les plus stressants de ma thèse!

Et enfin un énorme merci à toute ma famille: mon papa qui me manque, ma maman pour son soutien inconditionnel, Julien et Cyril (ça y est je vous ai officiellement dépassés!!!), mes grands-parents, Jacques, Souad et Carole pour avoir fait entrer dans ma vie mes petits bouts que j'aime tant Elisa, Noane, Matis et Romain.

RESUME

Introduction: Le cœur embryonnaire et fœtal est très sensible au manque d'oxygène et une hypoperfusion utéroplacentaire transitoire peut conduire à une surproduction d'espèces radicalaires (ROS). Dans le cœur en développement les mécanismes moléculaires impliqués en situation d'ischémie-reperfusion (I-R) ne sont pas connus. La voie de signalisation JAK2/STAT3 (Janus Kinase 2 / Signal Transducer and Activator of Transcription 3), impliquée aussi bien dans la cardiogenèse précoce que dans la protection du cœur adulte contre l'I-R, pourrait jouer un rôle clé dans la réponse du myocarde fœtal à un déficit en oxygène. Cette étude a permis d'étudier le rôle de la voie JAK2/STAT3 et son interaction avec d'autres voies de signalisation dans un modèle de cœur embryonnaire soumis à un épisode anoxique. En outre, les effets du stress oxydant endogène provoqué par la réoxygénation ont été comparés à ceux du stress oxydatif exogène induit par du peroxyde d'hydrogène (H_2O_2).

Méthodes: Des cœurs isolés d'embryons de poulet âgés de 4 jours ont été soumis à une anoxie (30min) suivie d'une réoxygénation (80min) en présence ou non de l'antioxydant MPG et de l'inhibiteur de JAK2/STAT3 AG490 ou exposés à de l'H_2O_2 (50µM-1mM). L'évolution temporelle de la phosphorylation de STAT3α^{tyrosine705} (P-Tyr STAT3α) et celle de la phosphorylation des protéines de la voie RISK (Reperfusion Injury Salvage Kinase: PI3K, Akt, GSK3ß, glycogène synthase GS et ERK2) ont été déterminés dans l'homogénat et dans les fractions nucléaire et cytoplasmique du myocarde. La liaison de STAT3 à l'ADN a été déterminée par EMSA et l'expression de gènes cibles de STAT3 (iNOS, MnSOD, Cox2) par RT-PCR. Les effets chrono-, dromo- et inotropes ont été déterminés par les enregistrements de l'ECG et de l'activité contractile ventriculaire.

Résultats: STAT3 et GSK3ß étaient présents dans les fractions nucléaire et cytoplasmique tandis que PI3K, Akt, GS et ERK2 n'étaient détectées que dans la fraction cytoplasmique. L'augmentation de P-Tyr STAT3α provoquée par la réoxygénation était significativement réduite par le MPG ou l'AG490. La réoxygénation entraînait l'accumulation nucléaire de STAT3, mais étonnamment sans liaison avec l'ADN. A la réoxygénation l'AG490 diminuait la phosphorylation d'Akt, GS et ERK2 ainsi que celle de GSK3ß mais exclusivement dans la fraction nucléaire. L'inhibition de JAK2/STAT3 retardait également la récupération du rythme cardiaque et prolongeait la durée des arythmies. L'activité cardiaque n'était perturbée par de l'H_2O_2 qu'à des concentrations >500µM. A 1mM, l'H_2O_2 supprimait l'activité auriculaire dans 45% des cœurs et la conduction auriculo-ventriculaire dans 66% et augmentait la formation de P-Tyr STAT3α et sa liaison à l'ADN sans modifier l'expression des gènes cibles.

Conclusion: Les ROS produits par l'anoxie-réoxygénation activent STAT3α qui subit une translocation dans le noyau sans se lier à l'ADN et interagit rapidement avec des protéines de la voie RISK dans les compartiments nucléaire et cytoplasmique du cœur embryonnaire. Ce dernier, en particulier au niveau des oreillettes, se révèle très résistant au puissant stress oxydatif de l'H_2O_2 qui se différencie du stress lié à la réoxygénation en favorisant la liaison de STAT3 à l'ADN. Ces résultats originaux permettent une meilleure compréhension des mécanismes qui peuvent améliorer la récupération du cœur en développement après un épisode hypoxique intra-utérin.

SUMMARY

Aim: The embryonic/fetal heart is highly sensitive to oxygenation level and a transient uteroplacental hypoperfusion can lead to oxyradicals overproduction. Information about the molecular mechanisms underlying ischemia-reperfusion (I-R) injury in the developing heart is lacking. The Janus Kinase 2 / Signal Transducer and Activator of Transcription 3 (JAK2/STAT3) pathway, required for cardiogenesis and involved in protection of the adult heart against I-R, could also play a key role in the response of the fetal myocardium to transient oxygen deprivation. The aim of the study was to characterize the involvement of JAK2/STAT3 pathway and its interaction with other signalling pathways in the developing heart transiently submitted to anoxia. Furthermore, the response of the embryonic heart to an exogenous oxidant stress (H_2O_2) in comparison to reoxygenation-induced endogenous oxyradicals has been investigated.

Methods: Hearts isolated from 4-day-old chick embryos were submitted to anoxia (30min) and reoxygenation (80min) with or without the antioxidant MPG, the JAK2/STAT3 inhibitor AG490 or exposed to H_2O_2 (50µM-1mM). The time course of phosphorylation of STAT3$\alpha^{tyrosine705}$ and Reperfusion Injury Salvage Kinase (RISK) proteins (PI3K, Akt, GSK3ß, Glycogen Synthase and ERK2) was determined in homogenate and in enriched nuclear and cytoplasmic fractions. The STAT3 DNA-binding was determined by EMSA and the expression of STAT3 specific target genes by RT-PCR. The chrono-, dromo- and inotropic disturbances were also investigated by ECG and mechanical recordings.

Results: Phosphorylation of STAT3α^{tyr} (P-Tyr STAT3α) was increased by reoxygenation and reduced by MPG or AG490. STAT3 and GSK3ß were detected both in nuclear and cytoplasmic fractions while PI3K, Akt, GS and ERK2 were restricted to cytoplasm. Reoxygenation led to nuclear accumulation of STAT3 but unexpectedly without DNA-binding. AG490 decreased the reoxygenation-induced phosphorylation of STAT3α^{tyr}, Akt, GS and ERK2 and phosphorylation/inhibition of GSK3ß in the nucleus, exclusively. Inhibition of JAK2/STAT3 delayed recovery of atrial rate, worsened RR variability and prolonged arrhythmias compared to control hearts. Cardiac activity was altered only at concentrations >500µM of H_2O_2. Moreover, 1mM of H_2O_2 suppressed atrial activity in 45% of the hearts, atrioventricular conduction in 66% and augmented P-Tyr STAT3α which led to an increase in the DNA-binding but no change in the expression of three STAT3 specific target genes (iNOS, MnSOD, Cox-2).

Conclusion: In the developing heart, besides its nuclear translocation without transcriptional activity, ROS-activated STAT3α can rapidly interact with RISK proteins present in nucleus and cytoplasm and reduce the anoxia-reoxygenation-induced arrhythmias. Moreover, the embryonic heart is highly resistant to H_2O_2 and the atrial region is the less affected. The role of JAK2/STAT3 in the response to reoxygenation-induced oxyradicals is different from the response to strong exogenous oxidant stress where STAT3 DNA-binding activity is increased. Such findings provide a first step in understanding the modulation of signalling cascades in the fetal heart submitted to transient intrauterine oxygen deprivation.

CONTENTS

ABBREVIATIONS

Arg: Arginine

Ang: Angiotensin

AVB: Atrioventricular Block

ATP: Adenosine Triphosphate

BAD: Bcl-2-Associated Death promoter

Bax: Bcl-2-Associated X protein

Bcl: B-cell lymphoma

CC: Coiled-Coil

CNTF: Ciliary Neurotrophic Factor

COS: CV-1 (simian) in Origin and carrying the SV40 genetic material

Cox: Cyclooxygenase

CRM: Chromosome Region Maintenance

CSF: Colony Stimulating Factor

CT: Cardiotrophin

DMSO: Dimethylsulfoxide

Duox: Dual oxidase

E: Embryonic day

EB: Embryoid Body

E-C: Excitation-Contraction

ECG: Electrocardiogram

EGF: Epidermal Growth Factor

EMD: Electromechanical Delay

EMSA: Electrophoretic Mobility Shift Assay

EPO: Erythropoietin

ERK: Extracellular-signal-Regulated Kinase

ES: Embryonic Stem

ETC: Electron Transport Chain

GAS: Gamma interferon-Activated Site

G-CSF: Granulocyte-Colony Stimulating Factor

GF: Growth Factor

GH: Growth Hormone

GM-CSF: Granulocyte-Macrophage Colony Stimulating Factor

gp: glycoprotein

GPx: Glutathione Peroxidase

GR: Glutathione Reductase

GS: Glycogen Synthase

GSK: Glycogen Synthase Kinase

GTP: Guanosine Triphosphate

HGF: Hepatocyte Growth Factor

HIF: Hypoxia Inducible Factor

IL: Interleukine

INF: Interferon

IPC: Ischemic Preconditioning

IPoC: Ischemic Postconditioning

I-R: Ischemia-Reperfusion

JAK: Janus Kinase

JH: Janus Homology domain

JNK: c-Jun N-terminal Kinase

LIF: Leukemia Inhibitory Factor

LK: Linker

MAPK: Mitogen-Activated Protein Kinase

MEK: Mitogen-Activated Protein Kinase Kinase

MPG: N-(2-mercaptopropionyl)-glycine

mPTP: mitochondrial Permeability Transition Pore

MT: Metallothionein

mTOR: mammalian Target Of Rapamycin

NAC: N-Acetylcysteine

NADH: Nicotinamide Adenine Dinucleotide

NADPH: Nicotinamide Adenine Dinucleotide Phosphate

NES: Nuclear Export Signal

NFκB: Nuclear Factor-κB

NLK: Nemo-Like Kinase

NLS: Nuclear Localization Signal

NOS: Nitric Oxide Synthase

Nox: Nicotinamide adenine dinucleotide phosphate Oxidase

NP: Nucleoprotein

NPC: Nuclear Pore Complex

OSM: Oncostatin M

PASMC: Pulmonary Arterial Smooth Muscle Cells

PDGF: Platelet-Derived Growth Factor

PI3K: Phosphoinositide-3-Kinase

PK: Protein Kinase

PPC: Pharmacological Preconditioning

PTK: Protein Tyrosine Kinase

PTPase: Protein Tyrosine Phosphatase

RNS: Reactive Nitrogen Species

ROS: Reactive Oxygen Species

S: Serine

SH: Src-Homology

SHP: Src-Homology-containing Phosphatase

SIE: Sis-Inducible Element

SOD: Superoxide Dismutase

STAT: Signal Transducer and Activator of Transcription

TAD: Transactivation Domain

TYK: Tyrosine Kinase

TNF: Tumor Necrosis Factor

U-STAT: Unphosphorylated Signal Transducer and Activator of Transcription

VEGF: Vascular Endothelial Growth Factor

VSMC: Vascular Smooth Muscle Cells

v-Src: viral-Sarcoma

XDH: Xanthine Dehydrogenase

XO: Xanthine Oxidase

Y: tyrosine

INTRODUCTION

During gestation, any deterioration of the intrauterine environment may be the cause of congenital cardiopathies affecting about 8 ‰ neonates (Keller et al., 2007). Even if the embryo develops in a relatively hypoxic environment (Burton and Jaunaiux, 2001), the cardiovascular function can still be impaired by a transient intrauterine lack of oxygen resulting in myocardial hypoplasia and reduced heart rate (Ream et al., 2008). This can lead to possible long-term deleterious consequences, like emergence of cardiovascular diseases (hypertension, coronary heart disease…) in adulthood (Thornburg et al., 2010). It is therefore important to better understand the adaptative mechanisms of the immature heart to hypoxia to improve therapeutic strategies. Despite recent advances in fetal and perinatal cardiology and surgery, the signalling pathways underlying functional disturbances occurring during intermittent or prolonged ischemia, due, for example, to torsion of the umbilical cord or placental abnormalities are still poorly understood. This study in the embryonic chick heart model specifically focuses on the Janus Kinase 2 / Signal Transducer and Activator of Transcription 3 (JAK2/STAT3) pathway known to be involved in the response to ischemia-reperfusion (I-R) and protection of the adult heart (Negoro et al., 2000) and also required for normal cardiogenesis at early developmental stages (Foshay et al., 2005).

I. The Janus Kinase 2 / Signal Transducer and Activator of Transcription 3 (JAK2/STAT3) pathway

I.1 Definition of the JAK2/STAT3 pathway

I.1.a Components of the JAK/STAT pathway

The JAK proteins form a family of cytosolic non-receptor tyrosine kinases composed of four members in mammals: JAK1, JAK2, JAK3 and Tyrosine Kinase 2 (TYK2). The STAT proteins constitute a family of transcription factors composed of seven members in mammals: STAT1, STAT2, STAT3, STAT4, STAT5a, STAT5b and STAT6. It should be noticed that TYK2, STAT2, STAT5a and STAT6 are not present in the chick. JAKs are large tyrosine kinases (120-140kDa) ubiquitously expressed except JAK3 which is restricted to hematopoietic cells. JAK1 and JAK2 are the predominant members in cardiomyocytes. JAKs are characterized by seven highly conserved regions of homology called Janus Homology domain 1-7 (JH1-7) (fig. 1). JH1 is a kinase domain important for the enzymatic activity and contains conserved tyrosines (Y) necessary for JAKs activation (e.g. Y1038/Y1039 in JAK1, Y1007/Y1008 in JAK2, Y980/Y981 in JAK3 and Y1054/Y1055 in TYK2). JH2 is a pseudokinase domain, structurally similar to a kinase domain but lacking enzymatic activity, and can provide a potential docking site for STAT proteins. The JH3-JH4 domains share homology with Src homology 2 (SH2) domain but do not have phospho-Y binding ability. The amino terminal (NH_2) end (JH4-JH7) is a FERM domain (4.1, Ezrin, Radixin, Moesin) involved in association of JAKs with cytokine receptors and/or other kinases (Leonard and O'Shea, 1998).

Fig. 1: Domain structure of JAKs. JAKs are composed of several JAK homology domains (JH).

STATs are transcription factors (83-113kDa) ubiquitously expressed except STAT4 which is restricted to thymus, spleen and testis (Zhong et al., 1994). STATs are characterized by seven domains. The NH_2 domain is involved in dimerization, tetramerization, nuclear import and protein-protein interaction. The coiled-coil (CC) domain is implicated in receptor binding, nuclear import and export and is also an interacting domain with other proteins (fig. 2). The DNA-binding domain, which has an immunoglobulin-fold structure, binds to DNA as a dimer and is also involved in nuclear import and export and protein-protein interaction (e.g. Genes associated with Retinoid-IFN-induced Mortality-19 for STAT3). The linker (LK) domain is implicated in DNA-binding, transcriptional activity, nuclear export and is also an interacting domain with other proteins. The SH2 domain, the most conserved domain among STATs, is involved in receptor binding, dimerization, nuclear export and protein-protein interaction. The C-terminal part is a transactivation domain (TAD), the least conserved, implicated in dimerization, transcriptional activity, nuclear export and is also an interacting domain with other proteins (Lim and Cao, 2006).

All STATs contain a conserved Y residue in the TAD that undergoes phosphorylation upon activation and interacts with the SH2 domain of the dimer partner. In addition, STATs (except STAT2 and STAT6) contain a second conserved phospho-amino acid residue, a serine (S) also in the TAD (Decker and Kovarik, 2000).

The full-length STATs, the α isoforms, can undergo alternative splicing at the 3' end gene transcripts leading to shorter ß isoforms with truncated C-terminal TAD (Lim and Cao, 2006). More specifically STAT3ß lacks the 55 C-terminal amino acids of STAT3α, and consequently the phospho-S residue, but gains seven amino acids (fig. 2). STAT3α and STAT3ß are distinctly different in their activation, transcriptional activities, and biological functions (Schaefer et al., 1997). For example, granulocyte-colony stimulating factor (G-CSF)

activates only STAT3ß but not STAT3α in normal human $CD34^+$ bone marrow and HL60 cells (Chakraborty et al., 1996). In cells being CV-1 (simian) in Origin, and carrying the SV40 genetic material (COS) in the absence of cytokine or growth factor (GF) only STAT3ß is active and in response to epidermal GF (EGF) stimulation activated STAT3ß dimers have a greater DNA-binding activity and are more stable than STAT3α dimers (Park et al., 2000). However, relative to DNA-binding activity, STAT3α shows greater transcriptional activity than STAT3ß (Schaefer et al., 1997). STAT3ß acts as a dominant negative regulator of transcription in interleukine-5 (IL-5)-stimulated COS cells (Caldenhoven et al., 1996) but studies with mice deficient in STAT3α or STAT3ß show that STAT3ß is capable of activating distinct STAT3 target genes in response to IL-6, suggesting that STAT3ß may not be a dominant-negative factor of STAT3α *in vivo* (Maritano et al., 2004). Moreover, STAT3α and STAT3ß activate their own distinct set of genes and possess unique and non-redundant functions, as STAT3α but not STAT3ß, is required for viability (Maritano et al., 2004).

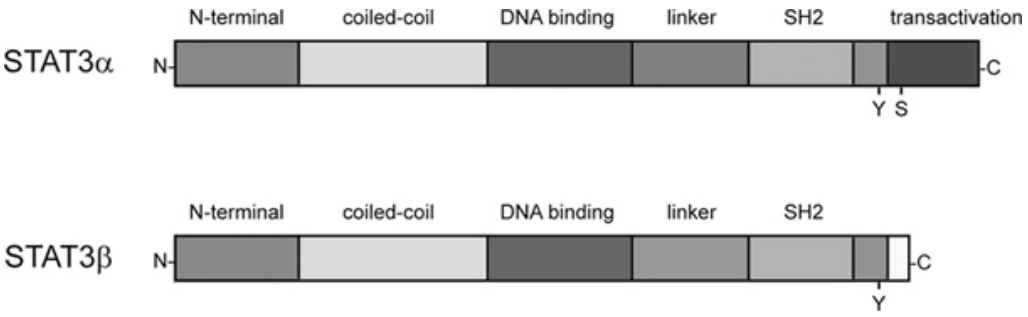

Fig. 2. Domain structure of STAT3α and STAT3ß. Src homology 2 (SH2), phospho-tyrosine^{705} (Y) and serine^{727} (S) motifs (Dewilde et al., 2008).

I.1.b Activation of the JAK2/STAT3 pathway

JAK2 activation is an immediate consequence of cytokine-induced receptor dimerization (Kurdi and Booz, 2009). The JAK2/STAT3 pathway is most often activated by

type I cytokines whose receptors share a common signal-transducing subunit glycoprotein 130 (gp130), like IL-6, IL-11, oncostatin M (OSM), ciliary neurotrophic factor (CNTF), leukemia inhibitory factor (LIF) and cardiotrophin-1 (CT-1) (Leonard and O'Shea, 1998). This pathway is also stimulated by interferon-α and -γ (INF-α and -γ) (Brierley and Fish, 2005) and hormones like growth hormone (GH), erythropoietin (EPO) (Piuhola et al., 2008) and leptin (McGaffin et al., 2008). JAK2 can also be activated in response to distinct ligands that bind to G-protein coupled receptors. Hormones, such as angiotensin II (Ang II) (Schieffer et al., 2000), or chemokines, like Chemokine (C-C motif) Ligand 5 (CCL5) (Wong and Fish, 1998) and α-chemokine interleukin 12 (CXCL12), bind to this type of receptor. JAK2 activation occurs upon dimerization and trans-autophosphorylation of conserved tandem Y found in the activation loop of JAK2 JH1 domain. Activated JAK2 phosphorylates Y sites on the cytoplasmic tail of the receptor that serve as docking sites for STAT3 SH2 domain (Kurdi and Booz, 2009) (fig. 3). STAT3 molecules are then phosphorylated on Y^{705} by JAK2 and form homodimers or STAT1-STAT3 heterodimers based on the interaction between the SH2 domains and the phosphorylated Y. Alternatively, STAT3 Y phosphorylation can be induced by other protein tyrosine kinases (PTKs) that are intrinsic to receptors or that are present in the cytoplasm or nucleus (fig. 3). PTKs are coupled to GF receptors such as EGF, platelet-derived GF (PDGF) (Reich and Liu, 2006), vascular endothelial GF (VEGF) (Ye et al., 2004), CSF-1, G-CSF and granulocyte macrophage-CSF (GM-CSF). In some cases, oncogenic derivatives of non-receptor tyrosine kinases such as viral-sarcoma (v-Src) or Bcr-Abl can phosphorylate STAT3 without receptor engagement (Buettner et al., 2002). STAT3 can also be phosphorylated independently of its Y residue on its S^{727} residue which is a substrate for extracellular-signal-regulated kinase 1/2 (ERK 1/2), p38 mitogen-activated protein kinase (MAPK) (Kovarik et al., 2001), mammalian target of rapamycin (mTOR) (Yonezawa et al., 2004), cyclin-dependent kinase 1 (CDK 1) (Shi et al., 2006), ZIP kinase (Sato et al., 2005)

and nemo-like kinase (NLK) (Kovarik et al., 2001, Brierley and Fish, 2005, Kojima et al., 2005, Kurdi and Booz, 2007a). Binding of STAT3 to DNA does not require S phosphorylation, however, S phosphorylation is essential for maximal STAT3 transcriptional activity (Wen et al., 1995b).

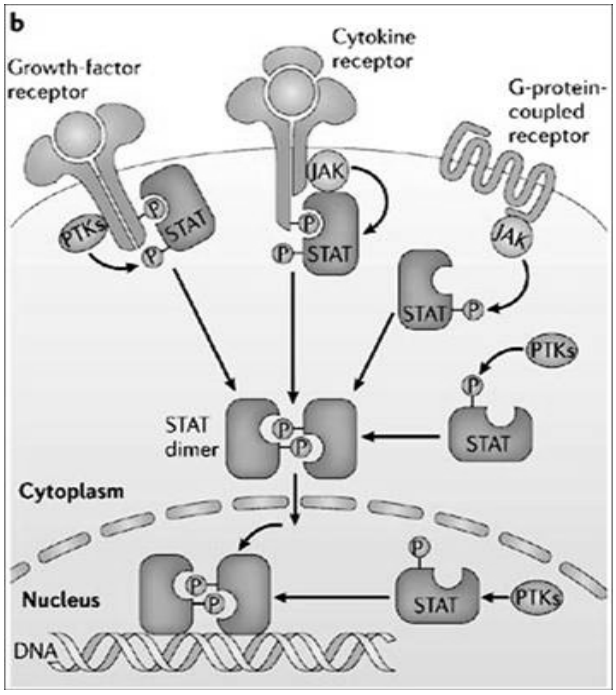

Fig. 3. Multiple mechanisms for STATs Y phosphorylation by JAKs or other protein tyrosine kinases (PTKs) (Reich and Liu, 2006).

Once phosphorylated dimers are stabilized by bivalent interactions and then translocate into the nucleus. Generally protein nuclear import involves importin-α which recognizes the protein nuclear localization signal (NLS) in the presence of importin-ß in the cytoplasm, and a nuclear pore complex (NPC) protein/importin-α/importin-ß is formed. Second, the NPC migrates into the nucleus via the interaction of importin-ß and several nucleoporins. Finally, Ran-GTP, the GTP-bound form of small GTPase Ran, directly binds to importin-ß in the complex, followed by disassembly of the complex inside the nucleus (Gorlich and Kutay, 1999) (fig. 4). In COS cells OSM-stimulated import of STAT3 into the nucleus is mediated by various importin-αs (importin-α5/nucleoprotein I-1 (NPI-1), importin-ß and Ran (Ushijima et al., 2005). In EGF-treated cells STAT3 nuclear import is mediated by active NLS present in

the CC domain (amino acids 150–162) recognized by importin-α3 (Liu et al., 2005). On the other hand in HeLa cells importin-α5 (strong interaction) and -α7 (weak interaction), but not importin-α1, -α3, and -α4, bind to STAT3 upon OSM stimulation. Binding domain of STAT3 and importin-α5 is an arginine (Arg)-214/215 motif in the CC domain (Ma and Cao, 2006).

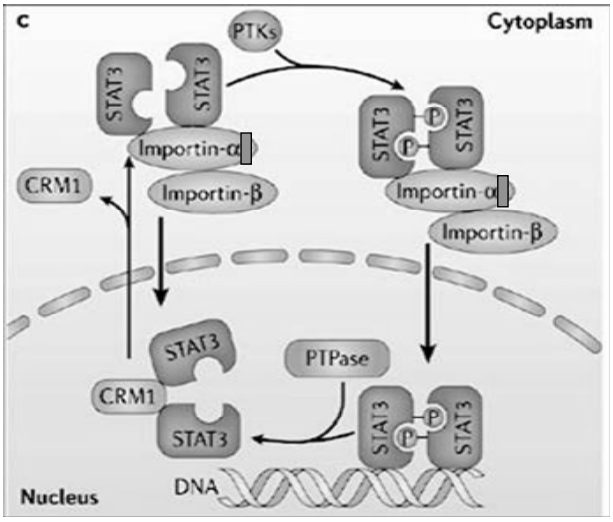

Fig. 4: STAT3 nuclear import and export. Chromosome region maintenance 1 (CRM1), protein tyrosine kinases (PTKs), protein tyrosine phosphatases (PTPases) (Reich and Liu, 2006).

Dimers translocate into the nucleus to bind DNA in order to activate transcription from specific target gene promoters containing a Gamma INF-Activated Site (GAS)-like element, sometimes referred to as the sis-inducible element (SIE) (Lew et al., 1991, Aaronson and Horvath, 2002).

Dissociation from DNA allows dephosphorylation of STAT3 by nuclear PTPases, such as TC45, SH2-containing phosphatase 1 and 2 (SHP1 and 2) (Kim et al., 2010). Dephosphorylated STAT3 are then export to the cytoplasm where they can be reactivated. Generally protein nuclear export involves an nuclear export signal (NES) sequence (Wen et al., 1995a) recognized by CRM1 (also known as exportin-1) (Fornerod et al., 1997) (fig. 4). The recognition of an NES by CRM1 requires it to associate with Ran-GTP to form a stable export complex (Petosa et al., 2004). The nuclear export of STAT3 is mediated by three NES

elements (amino acids 306-318, 404-414 and 524-535) (Bhattacharya and Schindler, 2003) recognized by exportin that remains to be identified.

The figure 5 shows a summary of the different ways leading to JAK2/STAT3 activation.

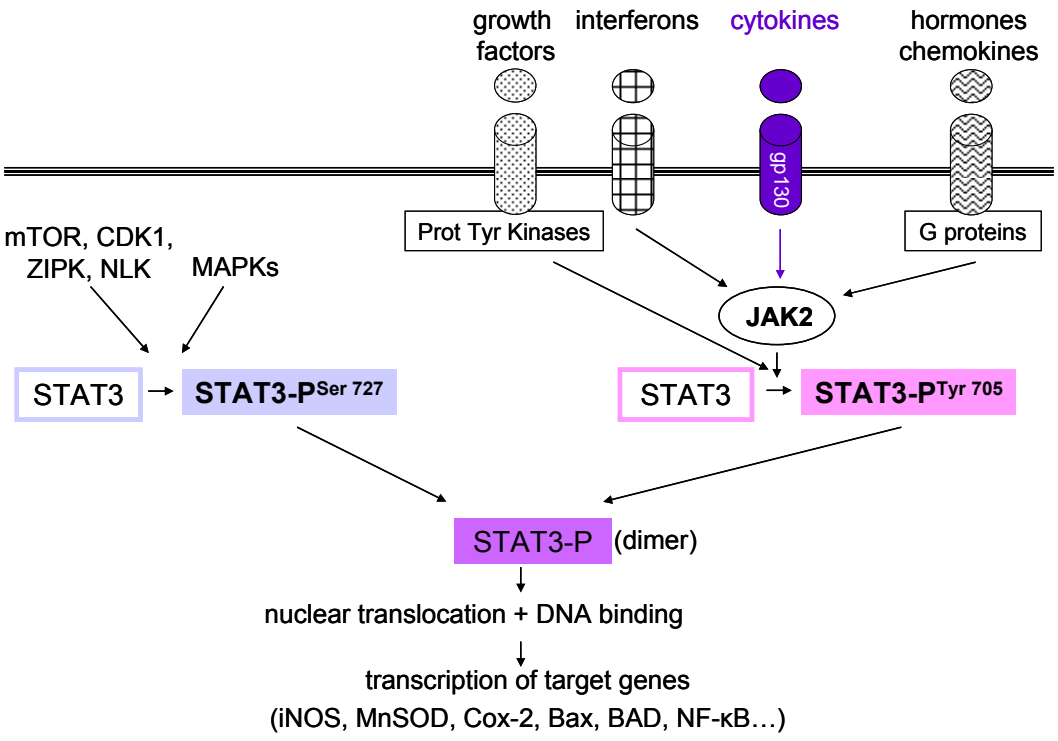

Fig. 5. Classical regulation of the JAK2/STAT3 pathway

I.1.c Localization of JAK2 and STAT3

JAK2 is a cytosolic kinase but can eventually be found in the nucleus. Indeed in unstimulated serum deprived chinese hamster ovary cells there is a constitutive nuclear localization of JAK2 and a GH stimulation caused the appearance of Y phosphorylated JAK2 in the nucleus (Lobie et al., 1996). In mouse mammary epithelial cells, prolactin activates JAK2 which translocates to the nucleus by an as-yet-unknown mechanism (Nilsson et al., 2006) and it has been shown that human JAK2 is present in the nucleus of haematopoietic cells (Dawson et al., 2009).

STAT3 is a cytoplasmic transcription factor shuttling between cytoplasmic and nuclear compartments once phosphorylated. But there is a constitutive presence of STAT3 in the nucleus independent of its phosphorylation state (Liu et al., 2005, Reich and Liu, 2006). Nuclear STAT3 continuously shuttles between nucleus and cytoplasm (Pranada et al., 2004, Liu et al., 2005). Nuclear translocation of STAT3 independent of phosphorylation occurs through association between a defined sequence in the CC domain (amino acids 152-163) and importin-α3 (Liu et al., 2005). STAT3 is also present in mitochondria from mice livers and hearts probably located in either the intermembrane space, the inner mitochondrial membrane [in the complex I and II of the electron transport chain (ETC)] and/or the matrix. The amount of STAT3 in mitochondria is about one-tenth that in the cytosol (Wegrzyn et al., 2009). STAT3 is also detected in mitochondria from mouse embryo fibroblasts, mammary epithelial cells and bladder carcinoma cells. The presence of STAT3 in mitochondria does not require Y phosphorylation or intact SH2 or DNA binding domains (Gough et al., 2009).

I.1.d Roles of the JAK2/STAT3 pathway in biological functions

STAT3 plays a crucial role in a variety of biological functions including cell growth and cell motility depending on the cell type and stimulus (Akira, 1999). For example, in murine hearts, LIF- and CT-1-stimulated STAT3 regulates VEGF expression and controls vessel growth during cardiac remodelling (Funamoto et al., 2000). STAT3 activation also mediates self-renewal in pluripotent embryonic stem cells (Boeuf et al., 1997, Niwa et al., 1998). In primary cortical neuroepithelial cells, STAT3 is involved in IL-6- or LIF-induced astrocyte differentiation (Bonni et al., 1997). Hepatocyte GF (HGF)-stimulated STAT3 mediates tubulogenesis in epithelial cells (Boccaccio et al., 1998). In remnant liver after partial hepatectomy, STAT3 participates in IL-6-dependent liver regeneration (Cressman et al., 1995). STAT3 activation is involved in IL-6-dependent proliferation through prevention of

apoptosis independently of B-cell lymphoma 2 (Bcl-2) in T cells (Takeda et al., 1998). Cytoplasmic STAT3 is involved in microtubule dynamics by interacting with a microtubule-destabilizing protein, stathmin, and antagonizing its function (Ng et al., 2006). Moreover, STAT3 is involved in skin wound healing by playing a role in EGF- and HGF-dependent motility (Sano et al., 1999).

STAT3 activation also promotes proliferative processes including cellular transformation playing a role in oncogenesis (Bromberg et al., 1999). Lymphomas, leukemias, multiple myeloma, brain, prostate, breast, lung, head, neck, ovary and pancreas cancers contain activated STAT3 (Weber-Nordt et al., 1996, Garcia et al., 1997, Bromberg, 2001, Calo et al., 2003). Activation of STAT3 appears to be associated with malignant transformation and are not found in benign lesions (Bowman et al., 2000). In myeloid leukemic cells, STAT3 activation is essential for IL-6 or LIF-mediated terminal differentiation into macrophages (Minami et al., 1996, Nakajima et al., 1996) and in progenitor B cells, STAT3 activation appears to play a crucial role in the G1 to S cell-cycle transition by upregulating cyclin D1 (Fukada et al., 1998). STAT3 activation is required and sufficient to mediate cellular transformation like for v-src transformation (Bromberg et al., 1998). More specifically, mitochondrial STAT3 appears to contribute to Ras-dependent malignant transformation by augmenting ETC activity (particularly complexes II and V) and also sustains altered glycolytic and oxidative phosphorylation activities characteristic of cancer cells (Gough et al., 2009).

STAT3 has also a role in inflammatory response mainly by mediating the effects of IL-6 and other gp130 ligands (Levy and Darnell, 2002). In macrophages and neutrophils, STAT3 activation is essential for anti-inflammatory reactions mediated by IL-10 (Takeda et al., 1999). In adult liver in response to bacterial infection, STAT3 is a mediator of induction of acute-phase genes (Alonzi et al., 2001).

As mentioned earlier STAT3 is expressed in the mitochondria where it modulates respiration exerting its actions not as a transcription factor that regulates nuclear gene expression, but rather through its localization. The precise mechanism by which STAT3 regulates complexes I and II of the ETC remains to be determined (Wegrzyn et al., 2009). In some cases, STAT3 does not require to be phosphorylated to mediate transcription. Indeed, in untransformed human mammary epithelial cells, unphosphorylated STAT3 (U-STAT3) drives expression of genes such as RANTES, IL-6, IL-8, HGF-receptor, and muscle RAS that do not respond directly to phosphorylated STAT3. Many U-STAT3-responsive genes have κB elements that are activated when U-STAT3 binds to U-nuclear factor-κB (NFκB) (Yang et al., 2005, Yang et al., 2007).

I.2 Role of the JAK2/STAT3 pathway in development

I.2.a Role of the JAK2/STAT3 pathway in the embryo development

To elucidate the *in vivo* function of JAK2, JAK2-deficient mice have been generated. $JAK2^{-/-}$ embryos are anemic and die between embryonic days 10 (E10) and E12 due to the absence of definitive erythropoiesis (fig. 6). Fetal liver myeloid progenitors fail to respond to EPO, thrombopoietin, IL-3 or GM-CSF and JAK2-deficient fibroblasts do not respond to IFN-γ meaning that JAK2 has pivotal functions for signal transduction of a set of cytokine receptors required in definitive erythropoiesis (Neubauer et al., 1998, Parganas et al., 1998).

Fig. 6: $JAK2^{+/+}$ (left side) and $JAK2^{-/-}$ embryos (right side) at day 12.5 postcoitum (Neubauer et al., 1998).

Takeda et al. (1997) produce mice lacking STAT3 by gene targeting but no viable $STAT3^{-/-}$ mice could be obtained. $STAT3^{-/-}$ embryos die between E6.5 and E7.5. STAT3 mRNA begins to be expressed exclusively in visceral endoderm around E6.0. The visceral endoderm, which covers the upper side of the egg cylinder embryo, is known to have an important function in mediating metabolic exchanges between the maternal and embryonic environments (Cross et al., 1994). Thus, the lethality may be due to defects in visceral endoderm functions, such as nutritional insufficiency. This study demonstrates that STAT3 is essential for the early development of mouse embryos. STAT3 mRNA is present in both maternal and extraembryonic tissues of the uterine epithelium during early postimplantation stages of murine development and activated STAT3 protein is present from E4.5 to E9.5 in decidual swellings of the visceral endoderm. This indicates that STAT3 is important both in preserving pregnancy and in the control of initial developmental processes (Duncan et al., 1997). Functional blockade of STAT3 before implantation reduced embryo implantation meaning that successful implantation is dependent on STAT3 phosphorylation and activation in the endometrium before implantation (Catalano et al., 2005). A reduction in STAT3 activation (alanine substituted for S^{727}) attenuates neonatal growth leading to increased perinatal mortality in mice (Shen et al., 2004) (fig. 7).

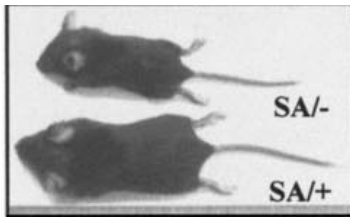

Fig. 7: $SA/^{-}$ (top) and $SA/^{+}$ (bottom) mice at postnatal day 24. $SA/^{-}$ mice have alanine substituted for S^{727} in STAT3 (the SA allele) (Shen et al., 2004).

I.2.b Role of the JAK2/STAT3 pathway in heart development

$STAT3^{-/-}$ embryos die less than one day before the embryo would have presented beating cardiomyocytes, therefore the embryonic stem (ES) cell model system aptly served as

a powerful tool for determining the role of the JAK2/STAT3 pathway in the initial differentiation pathway of cardiac cells. The essential role of the JAK2/STAT3 pathway for initial stages of cardiomyogenesis is demonstrated by using beating cardiomyocytes differentiated from ES cells in which JAK2 and STAT3 expressions and activities are elevated compared with non-beating areas from the same embryoid bodies (EBs) (fig. 8). Inhibition of JAK2 before beating significantly diminishes beating within EBs, whereas JAK2 overexpression induces beating areas. Inhibition of STAT3 causes an almost complete loss of beating areas (fig. 9) and STAT3-inhibited EBs result in lack of expression of several cardiac-specific genes (Nkx2.5, α1 subunit of the L-type calcium channel, cardiac actin) (Foshay et al., 2005).

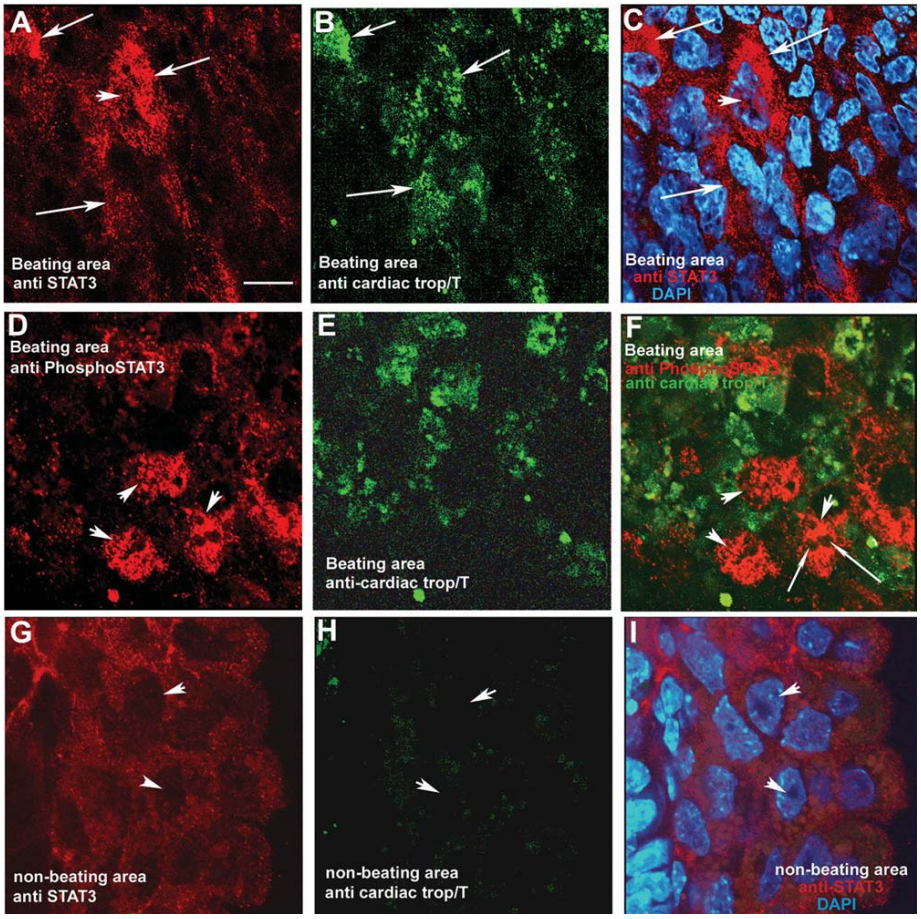

Fig. 8: Confocal microscopy reveals expression and activity of STAT3 in beating foci within embryoid bodies. (A–C): STAT3 (Rhodamine; arrows in A) is elevated in beating cardiomyocytes derived from embryonic stem cells, as shown by anti-STAT3 antibodies. Arrows in (B) show cardiac troponin T (Tnnt2) staining (fluorescein isothiocyanate) representing cardiomyocyte differentiation in cells observed in (A). (C): DAPI staining reveals each nuclei within the field of view of (A, B). (D–F): When phosphorylated on Y705, STAT3 translocates to the nucleus and becomes transcriptionally active. Using an antibody directed against Y705-phosphorylated STAT3, staining (red) was clearly observed within nuclei (arrowheads in D) of Tnnt2+ cells (green staining cells in E). Dual label of (E) anti-pSTAT3 and Tnnt2 revealed in more detail pSTAT3 residing within each cardiomyocyte nucleus (arrowheads). Nucleoli within each nucleus were devoid of pSTAT3 (thin arrows). (G–H): Within a nonbeating area, arrowheads in (G, I) point to STAT3-free nuclei, whereas in (H), anti-Tnnt2 antibodies show no signal. Scale bar in (A) = 10 µm for A–I (Foshay et al., 2005).

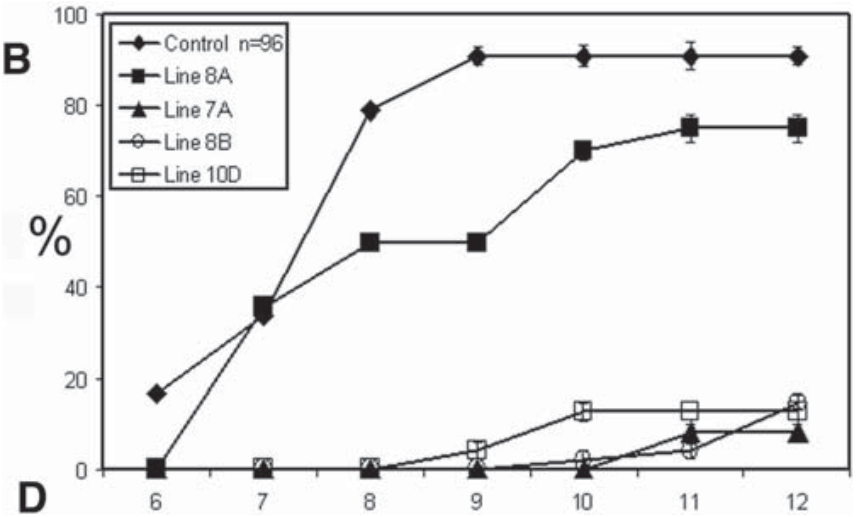

ES cell lines:

-8A: low expresser

-7A and 8B: high expressers

-10D: medium expresser of STAT3 dom/neg construct

Fig. 9: Graph shows affects of STAT3 dom/neg construct expression on cardiomyocyte differentiation from ES cells (Foshay et al., 2005)

JAK2-deficient embryos show a detectable delay in heart development which could be related to anoxia as a consequence of the reduced erythropoiesis (Parganas et al., 1998).

I.3 Regulation of the JAK2/STAT3 pathway

I.3.a Activation by hypoxia

The effect of a transient lack of oxygen on the JAK2/STAT3 pathway has been demonstrated in different cells types and tissues. In adult cardiomyocytes, in response to hypoxia JAK2 is activated and mediates apoptosis via the increased phosphorylation of STAT1 and JNK, the increase expression of Bax protein and the increase in caspase-1 and caspase-3 activities (Mascareno et al., 2005). In contrast to STAT3, STAT1 induces a pro-apoptotic signal (Stephanou and Latchman, 2005). In lung microvascular endothelial cells, JAK2 activation plays a role in xanthine dehydrogenase/oxidase (XDH/XO) activation (Wang et al., 2007a). STAT3 is activated in response to hypoxia and protects neonatal cardiomyocytes (Negoro et al., 2001) as well as adult rat hepatocytes (Terui et al., 2004) from cell death and reactive oxygen species (ROS). In addition activated STAT3 plays an

important role in hypoxia-induced cell activation and proliferation in pulmonary arterial smooth muscle cells (PASMC) (Bai et al., 2006). In response to hypoxia, activated STAT3 can also mediate VEGF release in mesenchymal stem cells (Wang et al., 2007c) and in human renal carcinoma cells in a HIF-1α-dependent manner (Jung et al., 2005). Moreover, nuclear STAT3 phosphorylation and DNA-binding activity are increased during post-anoxic reoxygenation which lead to an anti-apoptotic effect in PASMC (Zhang et al., 2005). The expression of JAK2 and STAT3 transcripts is also increased in response to hypoxia like in PASMC (Wang et al., 2005) and in the perifornical region of adult rat (Volgin and Kubin, 2006). Hypoxia can also stimulate the expression of STAT3 protein in mammary epithelial cells and human breast cancer cells (Lee et al., 2006). In v-Src–transformed cells and cancer cells with activated c-Src, under hypoxia STAT3 regulates hypoxia-inducible factor-1α (HIF-1α) protein level (Niu et al., 2008). In contrast, in retinal capillary endothelial cells, hypoxia has no effect on STAT3 Y phosphorylation or nuclear accumulation (Dudley et al., 2005) and even impairs LIF-induced STAT3 phosphorylation indicating that hypoxia inhibits self-renewal and induces early differentiation via suppression of the LIF-STAT3 signalling in ES cells (Jeong et al., 2007). It should be noticed that in the majority of the studies, cells or organs are submitted to long periods of hypoxia (from 2 to 48h).

I.3.b Activation by ischemia-reperfusion (I-R)

The major pathological condition of activation of the JAK2/STAT3 pathway is the ischemia-reperfusion. Indeed, in *in vivo* myocardial ischemia model, phosphorylation of JAK2 (Hwang et al., 2005) and STAT3 is rapidly observed (5min) and STAT3 remains activated for 7 days (El-Adawi et al., 2003). More specifically, STAT3 Y phosphorylation increases (Omura et al., 2001) in the ischemic area and in the healthy border area adjacent to the infarcted area (Negoro et al., 2000). In rat heart, Y and S STAT3 phosphorylation occur

during ischemia, remains unchanged during reperfusion and is induced by ROS (McCormick et al., 2006). The effect of I-R is also observable in other organs like in kidney where STAT3 Y phosphorylation is increased in an EGF and JAK2-dependent manner (Arany et al., 2006) ; or in brain where a transient middle cerebral artery occlusion increases JAK2 and STAT3 phosphorylation after 6-72 h of reperfusion (Satriotomo et al., 2006). In contrast, in some studies there is no activation of JAK2 (Omura et al., 2001) or STAT3 in heart subjected to prolonged ischemia followed by reperfusion (Mascareno et al., 2001) or in ventricular samples from transplant patients with heart failure due to ischemic heart disease (Ng et al., 2003). In neonatal cardiomyocytes submitted to simulated ischemia (no glucose, no O_2) followed by simulated reperfusion (10mM glucose, 21% O_2), STAT3 protein expression is not affected but overexpression of STAT3 reduced ischemia-induced apoptosis (Stephanou et al., 2000).

I.3.c Role in pre- and postconditioning

It is noteworthy that activation of the JAK2/STAT3 pathway appears as a key mechanism underlying the marked protection against I-R afforded by so-called preconditioning which includes the ischemic (IPC) and the pharmacological preconditioning (PPC) protocols.

First, the IPC is the phenomenon whereby brief and transient episodes of ischemia render the heart relatively resistant to a subsequent ischemic insult (Murry et al., 1986). The early phase of preconditioning is manifested within minutes after the ischemic stress and lasts less than 3h whereas the late phase (the so-called second window of protection) is characterized by a slower onset (≥20h) and last up to 72 hours. Both phases of preconditioning involve reduction of necrotic tissue mass, improvement of cardiac performance and reduction of arrhythmias. Activation of JAK2 and STAT3 within rat hearts exposed to three cycles of 5min of ischemia

and 5min of reperfusion followed by I-R, leads to a decrease in cardiomyocyte apoptosis and reduce myocardial infarction (Hattori et al., 2001). Nuclear STAT3 phosphorylation also increases (Lecour et al., 2005) in an IL-6-dependent manner 30min after the IPC stimulus (Dawn et al., 2004) or in a PKCε-Raf1-MEK-ERK way leading to cardioprotective effects (Xuan et al., 2005, Xuan et al., 2007). Treatment of isolated rat hearts with the coronary effluent of ischemic preconditioned hearts increases STAT3 phosphorylation which plays also a role in transferred cardioprotection (Huffman et al., 2008). In a mouse model for late IPC using six cycles of 4min of coronary occlusion followed by 4min of reperfusion, activation of JAK2 is observed concomitantly with transcriptional activation of STAT3 *in vivo* (Xuan et al., 2001, Xuan et al., 2003).

Ischemic postconditioning (IPoC) consists of brief episodes of myocardial I-R employed during reperfusion after a prolonged ischemic insult which attenuates the total I-R injury (Na et al., 1996). In a young mouse model for IPoC using three cycles of 10s of ischemia and 10s of reperfusion, an increase in STAT3 phosphorylation is observed at 10min of reperfusion and mediates a reduction of the infarct size. Interestingly, STAT3 phosphorylation is reduced in aged mice compared with young mice hearts so this may contribute to the age-related loss of IPoC (Boengler et al., 2008a). Using IPoC, expression of phosphorylated STAT3 increases in myocardial nuclear fractions (Suleman et al., 2006, Lacerda et al., 2009b) and leads to recovery of myocardial function at end-reperfusion (Goodman et al., 2008). In the same time in the cytosol, IPoC reduces phosphorylated STAT3 (Suleman et al., 2006, Lacerda et al., 2009b).

Second, the heart can be pharmacologically preconditioned for example with tumor necrosis factor-α (TNF-α) administered in a time- and dose-dependent manner (Lecour et al., 2002). In isolated rat hearts preconditioned with TNF-α given for 7min followed by a 10min wash-out period before ischemia, nuclear S phosphorylation of STAT3 increases after 5min of

reperfusion and leads to reduction of the infarct size (Lecour et al., 2005). In isolated rat heart, PC with gadolinium given 15min prior to ischemia, STAT3 phosphorylation increases and plays a role in cardioprotection by reducing infarct size (Nicolosi et al., 2008). Like IPoC, the heart can also be pharmacologically postconditioned. In isolated perfused rat hearts preconditioned with insulin given at onset of reperfusion, Y phosphorylation of STAT3 increases after 15min of reperfusion and leads to decrease in infarct size (Fuglesteg et al., 2008). In mice hearts pharmacologically postconditioned by six alternating cycles of 10s reperfusion without TNF-α, 10s reperfusion with TNF-α, an increase in phosphorylated STAT3 occurs in the nuclear fraction during the first 15min of reperfusion and leads to cardioprotection whereas in the cytosol phosphorylation level of STAT3 does not change (Lacerda et al., 2009b).

I.3.d Activation by oxidant stress

I.3.d.1 Definition of oxidant stress

Oxidant stress is defined by an imbalance between the formation of ROS and/or reactive nitrogen species (RNS) (fig. 10) and antioxidant defenses which can lead to reversible or irreversible injury. ROS are molecules or ions formed by the incomplete reduction of O_2 and have beneficial and deleterious effects. In a physiological context, ROS play a role in the regulation of signal transduction and gene expression but in a pathological situation (oxidative stress) ROS could damage nucleic acids, proteins, lipids and carbohydrates (Valko et al., 2007).

ROS (Reactive Oxygen Species)	RNS (Reactive Nitrogen Species)
▪ superoxide anion (O2•-) ▪ hydroxyl radical (OH•) ▪ hydrogen peroxide (H2O2) ▪ hypochlorous acid (HOCl)	▪ peroxynitrite (ONOO−) ▪ nitric oxide (NO•)

Fig. 10: ROS and RNS

I.3.d.2 ROS sources

After an ischemia, at reperfusion, radicals production is important (Xu et al., 2001) especially when ischemia is long (Li and Jackson, 2002). In the ischemic heart, the major ROS source are the mitochondrial electron transport chain (ETC), the nicotinamide adenine dinucleotide phosphate (NADPH) oxidases (Nox) and the enzyme XO (Zweier and Talukder, 2006) (fig. 11).

During respiration, most of the O_2 consumed is reduced to water but 1-2% is partially reduced to $O_2^{\bullet-}$. Under physiological conditions the ETC is composed of a series of electron carriers arranged spatially according to their redox potentials and organized into four complexes. The two major sites for $O_2^{\bullet-}$ production are at complexe I (NADH dehydrogenase) and III (cytochrome bc_1 complex).

The Nox, located in the plasma membrane as well as in the membrane of phagosome, is an ubiquitously distributed enzyme made up of six subunits (a GTPase and five "phox" units: $gp91^{phox}$, $p22^{phox}$, $p40^{phox}$, $p47^{phox}$ and $p67^{phox}$) (Brandes et al., 2010). The complex normally latent must be activated to assemble in the membranes. It catalyses the reaction:

$NADPH + 2O_2 \leftrightarrow NADP^+ + 2O_2^{\bullet-} + H^+$

Seven isoforms of Nox have been identified termed Nox1-5 and dual oxidase 1 and 2 (Duox 1 and 2). Nox1, Nox2 and Nox4 are the predominant isoforms expressed within the cardiovascular system but their expression profile differs between cell types, for instance

cardiomyocytes express predominantly Nox2 and Nox4. More specifically, Nox4 is the major isoform present during early stages of cardiac differentiation (Li et al., 2006).

The XO is an ubiquitous enzyme composed of two flavin molecules, two molybdenum atoms and eight iron atoms. XO is derived from XDH through posttranslational modifications and catalyses the reactions:

hypoxanthine + H_2O + O_2 $\rightleftharpoons$ xanthine + H_2O_2 and

xanthine + H_2O + O_2 $\rightleftharpoons$ uric acid + H_2O_2

NO is also produced at reperfusion (Nonami, 1997). NO synthases (NOSs) (fig. 11) are enzymes that catalyze the production of $NO^{\bullet}$ from L-Arg:

L-Arg + NADPH + H^+ + O_2 → Nω-hydroxy-Larginine + $NADP^+$ + H_2O and

Nω-hydroxy-Larginine + ½ NADPH + ½ H^+ + O_2 → L-citrulline + ½ $NADP^+$ + NO + H_2O

There are three known NOS isoforms: neuronal NOS (nNOS or NOS1), inducible NOS (iNOS or NOS2) and endothelial NOS (eNOS or NOS3). Both nNOS and eNOS are present in human cardiomyocytes (Wei et al., 1996, Guo et al., 1999), while iNOS expression appears in cardiomyocytes of failing hearts (Satoh et al., 1997).

Moreover production of both $O_2^{\bullet -}$ and NO are stimulated during reperfusion and these two species react to form peroxynitrite (Beckman et al., 1990).

Oxidant stress can also derive from ROS production by extracellular sources (i.e. paracrine effect).

I.3.d.3 Antioxidant systems

Cells possess systems to neutralize the physiological but potentially deleterious radical production, the rate of ROS remaining low. There are enzymatic and non enzymatic antioxidant systems (fig. 11).

The superoxide dismutase (SOD) catalyzes the dismutation of $O_2^{\bullet-}$ into O_2 and H_2O_2 (McCord and Fridovich, 1969). In humans, three forms of SOD are present. SOD1 is located in the cytoplasm, SOD2 in the mitochondria, and SOD3 is extracellular. SOD1 and SOD3 contain copper and zinc, whereas SOD2 has manganese in its reactive centre.

Catalase is also located in mitochondria (Bai and Cederbaum, 2001), cytoplasm (Ferrari et al., 2004) and peroxisomes and catalyzes the decomposition of H_2O_2:

$2\ H_2O_2 \rightarrow 2\ H_2O + O_2$

The glutathione redox cycle is composed of the glutathione reductase (GR) and the glutathione peroxidase (GPx), an enzyme composed of four subunits, present in extracellular fluids and in the cytosol and mitochondria (Jassem et al., 2002). There are eight different isoforms of GPx (GPx1-8) identified in humans. GPx catalyzes the reaction:

$2GSH + H_2O_2 \rightarrow GS–SG + 2H_2O$

The GR then reduces the oxidized glutathione to complete the cycle:

$GS\text{-}SG + NADPH + H^+ \rightarrow 2\ GSH + NADP^+$

The thioredoxin is an ubiquitous protein which contains a dithiol-disulfide active site and reduces other proteins by cysteine thiol-disulfide exchange.

There are also non enzymatic intracellular molecules such as ascorbic acid (vitamin C) and α-tocopherol (vitamin E). Vitamin C is water-soluble and can react with many radicals generating the ascorbyl radical anion then ascorbyl. The ascorbyl radical can react with itself to regenerate. This regeneration is also possible by NADPH or glutathione.

Vitamin E is a lipophilic compound, which allows it to localize at the membranes. It protects membrane lipids from oxidation. The α-tocopherol is reduced in radical by the exchange of an electron and reacts with ascorbic acid, which then becomes radical.

There are also antioxidants agents such as N-(2-mercaptopropionyl)-glycine (MPG) or N-acetylcysteine (NAC), both thiol-containing compounds. MPG is an analog of glutathione

and an effective scavenger of H_2O_2, $ONOO^-$ and OH•. NAC has free thiol group capable of interacting with the electrophilic groups of ROS, like OH• and H_2O_2. In addition, NAC exerts an indirect antioxidant effect related to its role as a GSH precursor (Raddatz et al., 2010).

ROS sources	**Antioxidant systems**
▪electron transport chain ▪complexe I (NADH dehydrogenase) ▪complexe III (cytochrome *bc1* complex) ▪nicotinamide adenine dinucleotide phosphate oxidase ▪xanthine oxidase ▪NO synthases	▪enzymatic ▪superoxide dismutase ▪catalase ▪gluthathione reductase/ glutathione peroxidase ▪thioredoxin ▪non enzymatic ▪ascorbic acid ▪vitamin E ▪antioxidants agents ▪MPG ▪N-acetylcysteine

Fig. 11: ROS sources and antioxidants systems

I.3.d.4 JAK2/STAT3 pathway alteration by oxidant stress

It is now well established that ROS/RNS play an important physiological role in cell signalling and many studies show the involvement of radicals in activation of the JAK2/STAT3 pathway. Indeed, in human ventricular myocytes, Ang II enhances JAK2 activity via ROS generation (Modesti et al., 2005). Same result is observed in rat vascular SMC (VSMC), where Ang II inhibits the tyrosine phosphatase SHP-1 which mediates JAK2 dephosphorylation (Shaw et al., 2003). In neonatal rat ventricular myocytes, H_2O_2 exposure increases the level of STAT3 mRNA, phophorylation and content in an Akt/NF-κB-dependent manner which leads to cell survival (Lu et al., 2008b). H_2O_2 also causes STAT3 activation within 5min independently of new protein synthesis in rat fibroblasts (Simon et al., 1998) and pheochromocytoma cells (Yu et al., 2006). In human fibroblasts, oxidized low-density lipoprotein, by generation of an intracellular oxidant stress, induces the phosphorylation of JAK2 and STAT3 which triggers STAT3 translocation into the nucleus. This activation is

prevented by addition of the antioxidant vitamin E (Simon et al., 1998, Maziere et al., 2001). In rat liver, chemically induced oxidative stress (buthionine-sulfoximine, a blocker of glutathione synthesis; phorone, a GSH depletory and nitrofurantoin, an $O_2^{\bullet-}$ generator) activates STAT3 DNA-binding capacity with some minor differences in time-course and intensity (Tacchini et al., 2002). In human liver carcinoma cells, Nox leads to cadmium-induced S phosphorylation of STAT3 and an increase in DNA-binding whereas antioxidant treatment reduces STAT3 activation. ERK contributes to this activation that could induce a protective mechanism against cadmium toxicity (Souza et al., 2009). In contrast, NO and thiol oxidants inhibit the autokinase activity of rat JAK2, presumably through oxidation of crucial dithiols to disulfides within JAK2. In murine progenitor B cells NO pre-treatment inhibits the IL-3-triggered activation of JAK2 which leads to proliferation inhibition (Duhe et al., 1998). Moreover, in neonatal rat cardiomyocytes, ROS generation via parthenolide blocks STAT3 signalling of the IL-6-type cytokines (Kurdi and Booz, 2007b). In human neuroblastoma cells, neurons from chick ciliary ganglia and retina or mouse motor neuron, treatment with H_2O_2, a NO generator or a complex I inhibitor results in a decrease in the ability of CNTF and leptin to activate STAT3 and a blockade of STAT3 translocation (Kaur et al., 2005, Jang et al., 2007). This inhibition in STAT3 activation is explained by the authors by the fact that mediators of oxidative stress have very different actions in nerve when compared with non-nerve cells.

I.4 Interactions of the JAK2/STAT3 pathway with other signalling pathways

I.4.a Interaction with the Reperfusion Injury Salvage Kinase (RISK) pathway

The RISK pathway is a group of pro-survival protein kinases including PhosphoInositide-3-Kinase (PI3K), Akt/Protein Kinase B (PKB), MEK 1/2 and ERK 1/2 capable of mediating cardioprotection at the time of myocardial reperfusion (Yellon and Baxter, 1999) (fig. 12).

Moreover, the RISK pathway is involved in the beneficial effects of protective strategies such as IPC and IPoC through different mechanisms. This may be mediated through the inhibition/phosphorylation of downstream Glycogen Synthase Kinase 3β (GSK3β), causing the protective inhibition of the mitochondrial permeability transition pore (mPTP) a critical determinant of lethal myocardial reperfusion injury (Juhaszova et al., 2004). Another mechanism involves the activation of a variety of anti-apoptotic mechanisms including the phosphorylation and inhibition of pro-apoptotic factors such as Bad and Bax, and the inhibition of cytochrome c release (Hausenloy and Yellon, 2009).

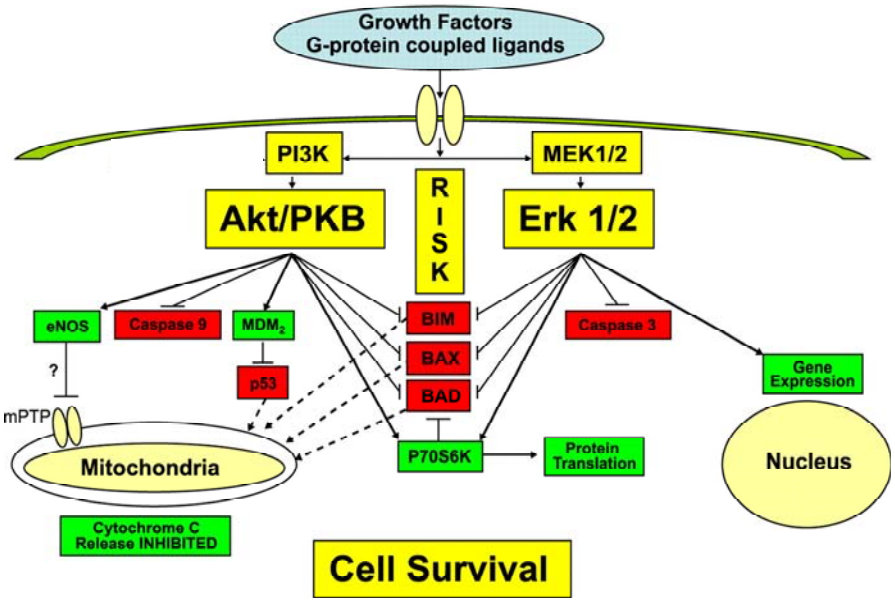

Fig. 12: Potential anti-apoptotic mechanisms through which activation of the pro-survival PI3K/Akt and ERK 1/2 kinase cascades, which comprise the RISK pathway, protect the heart against reperfusion-induced injury. Growth factors, G-protein-coupled receptor ligands and atorvastatin administered during the first few minutes of reperfusion initiate cardioprotection by activating the RISK pathway, which then protects against the apoptotic and necrotic components of reperfusion-induced cell death. The scheme portrays the important anti-apoptotic mechanisms that have been implicated in mediating cellular survival associated with the recruitment of these kinase cascades. Signalling through the PI3K/Akt and/or the MEK 1/2/ERK 1/2 cascades results in: (1) phosphorylation and inactivation of caspases 3 and 9, which inhibits apoptosis; (2) phosphorylation and inactivation of the proapoptotic proteins BIM, BAX, BAD and p53, one consequence of which is to prevent the release of mitochondrial cytochrome c in response to an apoptotic stimulus (shown by dashed arrows); (3) phosphorylation and activation of eNOS (endothelial nitric oxide synthase), producing nitric oxide which may protect by inhibiting opening of the mitochondrial permeability transition pore (mPTP); (4) phosphorylation and activation of p70S6K which can protect by inactivating BAD or regulating protein translation; and (5) regulating the expression of genes concerned with cellular survival (Hausenloy and Yellon, 2004).

Recently, the existence of an alternative pro-survival signal transduction pathway for protecting the ischemic myocardium against lethal myocardial reperfusion injury has been discovered. Lecour and co-workers have described this novel pro-survival pathway, which involves the activation of TNF and STAT3 as the Survivor Activating Factor Enhancement (SAFE) pathway. The SAFE pathway was first discovered in the setting of IPC, but its role in IPoC has been recently confirmed (Lacerda et al., 2009a, Lecour, 2009).

The JAK2/STAT3 and RISK pathways being both cardioprotective in the context of I-R injury, several studies have been performed to assess possible crosstalk (fig 13). Most studies evaluate interactions between JAK2/STAT3 and PI3K/Akt and provide controversial results.

Some studies show a dual interaction between JAK2/STAT3 and PI3K/Akt, like in neonatal rat ventricular myocytes in which cells that survive from apoptotic insults (oxidant stress) have higher levels of Akt and STAT3. Inhibition of Akt activity reduces STAT3 expression and inhibition of STAT3 diminishes Akt expression (Lu et al., 2008b). In the IPC context, STAT3 knockout mice fail to increase Akt phosphorylation. In addition, Akt phosphorylation is reduced in the presence of the JAK/STAT3 pathway inhibitor (AG490) and vice versa STAT3 phosphorylation is diminished in the presence of a PI3K/Akt inhibitor (Wortmannin) (Suleman et al., 2008a).

Other studies show only an effect of JAK2/STAT3 on PI3K/Akt like in a model for IPoC, where JAK2/STAT3 pathway may provide upstream initiation of RISK pathway signalling via PI3K/Akt activation but is insufficient to provide cardioprotection following IPoC without subsequent RISK activation (Goodman et al., 2008). Insulin-induced cardioprotection at reperfusion occurs through activation of STAT3. Inhibition of STAT3 affects activation of Akt meaning a close interaction between STAT3 and Akt in the cardioprotective signalling pathway activated by insulin treatment at reperfusion (Fuglesteg et al., 2008).

Other studies demonstrate only an effect of PI3K/Akt on JAK2/STAT3 like in an *in vivo* model of I-R together with a cell culture model (H9C2 cardiomyoblasts), where opioid-induced cardioprotection occurs via the activation of both JAK/STAT3 and PI3K/Akt pathways and STAT3 phosphorylation is dependent on PI3K activation (Gross et al., 2006). In pulmonary artery endothelial cells, STAT3 activation by carbon monoxide is dependent on PI3K/Akt pathway with subsequent attenuation of pro-apoptotic factors (Zhang et al., 2005).

By contrast in a model for IPoC, STAT3 phosphorylation does not require PI3K activation (Goodman et al., 2008) and in hearts submitted to pharmacological preconditioning with TNF-α, STAT3 activation could also be achieved independent of Akt (Suleman et al., 2008a).

The JAK2/STAT3 pathway interacts also with GSK3β, a downstream target of Akt, like in hepatocytes where STAT3 sensitizes the insulin signalling by negatively regulating GSK3β (Moh et al., 2008).

And finally STAT3 can also act on ERK 1/2. For example, in H_2O_2-treated renal cells, inhibition of JAK2 or STAT3 (by AG490 or a dominant-negative STAT3 adenovirus) ameliorates survival through restoring ERK 1/2 activation (Arany et al., 2006). By contrast, in adult ventricular myocytes, IL-6 activates independently the JAK2/STAT3 and ERK 1/2 pathways, but only JAK2/STAT3 signalling mediates the NO-associated decrease in contractility (Yu et al., 2003).

Although STAT3 is basically a transcription factor shuttling between cytoplasmic and nuclear compartments, the intracellular localization of its interactions with RISK pathway components remains unknown.

I.4.b Interaction with the NF-κB (nuclear factor kappa-B) pathway

NF-κB is a transcription factor involved in cellular responses to stimuli such as stress, cytokines, free radicals, ultraviolet irradiation, oxidized LDL, and bacterial or viral antigens

(Gilmore, 2006). NF-κB plays a key role in regulating the immune response to infection and it has been shown that it is necessary for the late phase of cardioprotection after IPC (Tranter et al., 2010). The JAK2/STAT3 and NF-κB pathways are both involved in cardioprotection in response to I-R injury, consequently some studies have evaluated possible interaction (fig. 13). In neonatal rat ventricular myocytes, cells that survive from apoptotic insults (oxidative stress) have higher levels of STAT3. Direct activation of NF-κB enhances STAT3 expression, an effect abrogated by NF-κB inhibitor, meaning that cardiomyocytes possess an apoptosis-resistant property as a cytoprotection mechanism which is likely conferred by mutual transactivation between NF-κB and JAK2/STAT3 (Lu et al., 2008b). In cardiomyocytes differentiated from murine ES cells and treated with CT-1, the activation of NF-κB requires the JAK2 phosphorylation (Sauer et al., 2004). In cancer and tumor-associated hematopoietic cells, maintenance of NF-κB activity requires STAT3 to upregulate anti-apoptotic and other oncogenic genes (Lee et al., 2009). By contrast, in murine mesangial cells, STAT3, via direct interactions with NF-κB p65, serves as a dominant-negative inhibitor of NF-κB activity to suppress indirectly cytokine (IL-1ß, LPS + IFN-γ) induction of the iNOS promoter (Yu et al., 2002).

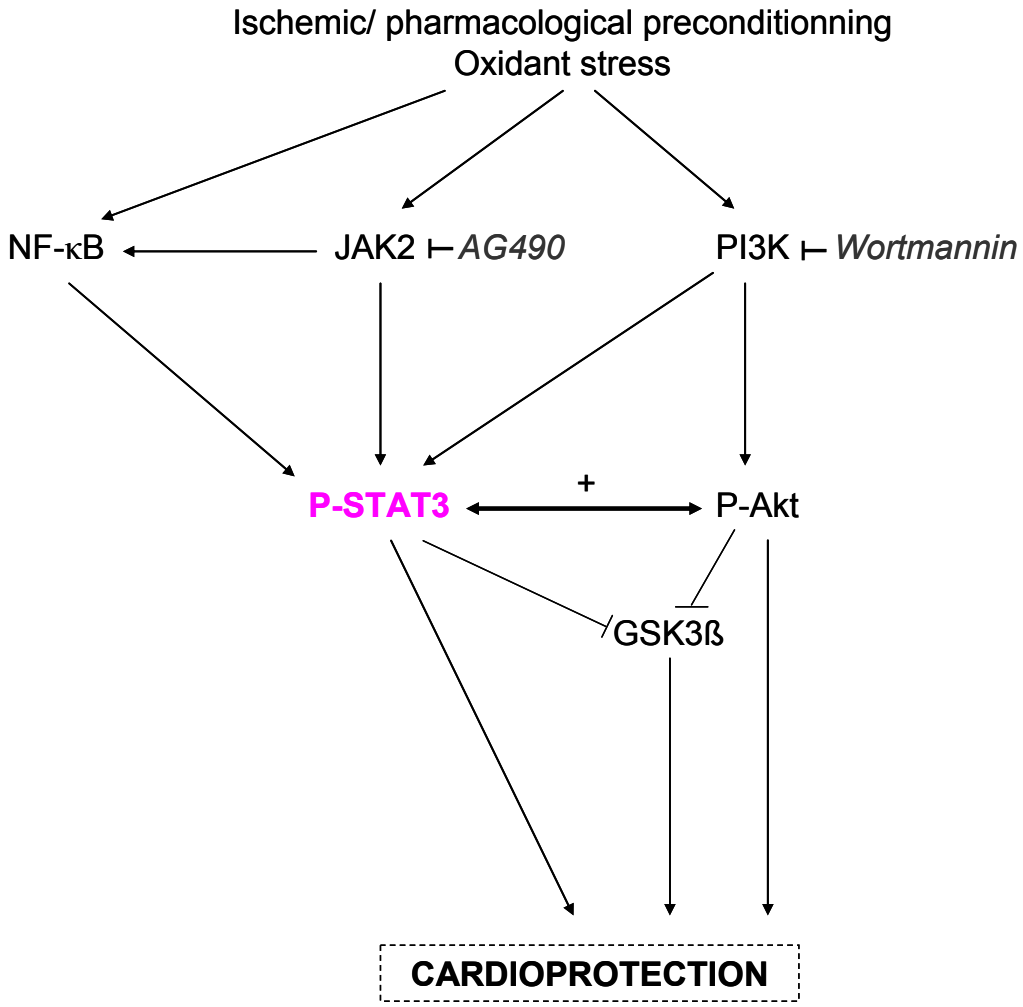

Fig. 13: Interactions between the JAK2/STAT3 and the RISK and NF-κB pathways in the context of cardioprotection. It should be noticed that GSK3β exerts its cardioprotective effect when the protein is inhibited (phosphorylated).

I.5 Role of the JAK2/STAT3 pathway in cardioprotective mechanisms

It is known that the JAK2/STAT3 pathway plays a major role in cardioprotection after I-R injury by acting on the expression of specific target genes and/or the activity of proteins. In a rat model of left anterior descending coronary artery ligation, treatment with JAK2 inhibitor reduces STAT3 phosphorylation and results in an increase in caspase-3 activity and Bax protein (Negoro et al., 2000). Caspase-3 is responsible for the cleavage of key cellular

proteins, such as cytoskeletal proteins, that leads to the typical morphological changes observed in cells undergoing apoptosis and Bax (Bcl-2-associated X protein) promotes mitochondrial outer membrane permeabilization and release of cytochrome c into the cytosol. In isolated hearts from endothelial cell-restricted STAT3 knockout mice, I-R induces greater expression of caspase-8 (Wang et al., 2007b) known to propagate the apoptotic signal by directly cleaving and activating downstream caspases. In isolated rat hearts submitted to IPC or TNF-α PC, inhibition of STAT3 activation at the time of reperfusion results in the deleterious loss of phosphorylation of the pro-apoptotic agent BAD (Bcl-2-associated death promoter) (Lecour et al., 2005). BAD phosphorylation causes the loss of BAD ability to heterodimerize with the survival proteins Bcl-xl or Bcl-2 and then leads to survival. In mouse hearts, JAK2 inhibition before the IPC abrogates completely the increase in iNOS protein and activity (Xuan et al., 2001) known to mediate late PC *in vivo* (Guo et al., 1999) as well as the upregulation of cyclooxygenase-2 (Cox-2) protein (Xuan et al., 2003), PGE_2 and/or PGI_2 being the most likely effectors of Cox-2-dependent cardioprotection (Shinmura et al., 2000). In neonatal rat STAT3 activation protects cardiomyocytes against ROS caused by hypoxia-reoxygenation through upregulation of the MnSOD gene and its anti-oxidant activity (Negoro et al., 2001). STAT consensus sequences (GAS elements) are present in the mouse iNOS, Cox-2 and MnSOD promoters (Boengler et al., 2008b) allowing STAT3 to directly control the transcription of these genes. In cardiac-specific transgenic mice expressing constitutively active STAT3 exposed to I-R, free radical scavenging enzymes metallothionein1 (MT1) and metallothionein2 (MT2) are markedly upregulated compared to nontransgenic littermates. Moreover, homozygous deletion of the MT1 and MT2 genes abrogates cardioprotective effect of STAT3 with the abolition of its ROS-scavenging effects (Oshima et al., 2005). In rat VSMC treated with H_2O_2, JAK2 inhibition abolishes H_2O_2-induced heat-shock protein 70 (HSP70) expression, a chaperone known to protect cells from ROS (Madamanchi et al.,

2001). In opioid-induced cardioprotection, inhibition of JAK2/STAT3 reduces GSK3β phosphorylation (Gross et al., 2006) and GSK3β phosphorylation/inhibition is suggested to be protective by preventing mPTP opening (Juhaszova et al., 2004). However, the protection of the cardiac electromechanical function afforded by the JAK2/STAT3 pathway under pathological conditions remains to be explored in the developing heart.

The figure 14 shows a summary of the different ways leading to the cardioprotective effect of the JAK2/STAT3 pathway.

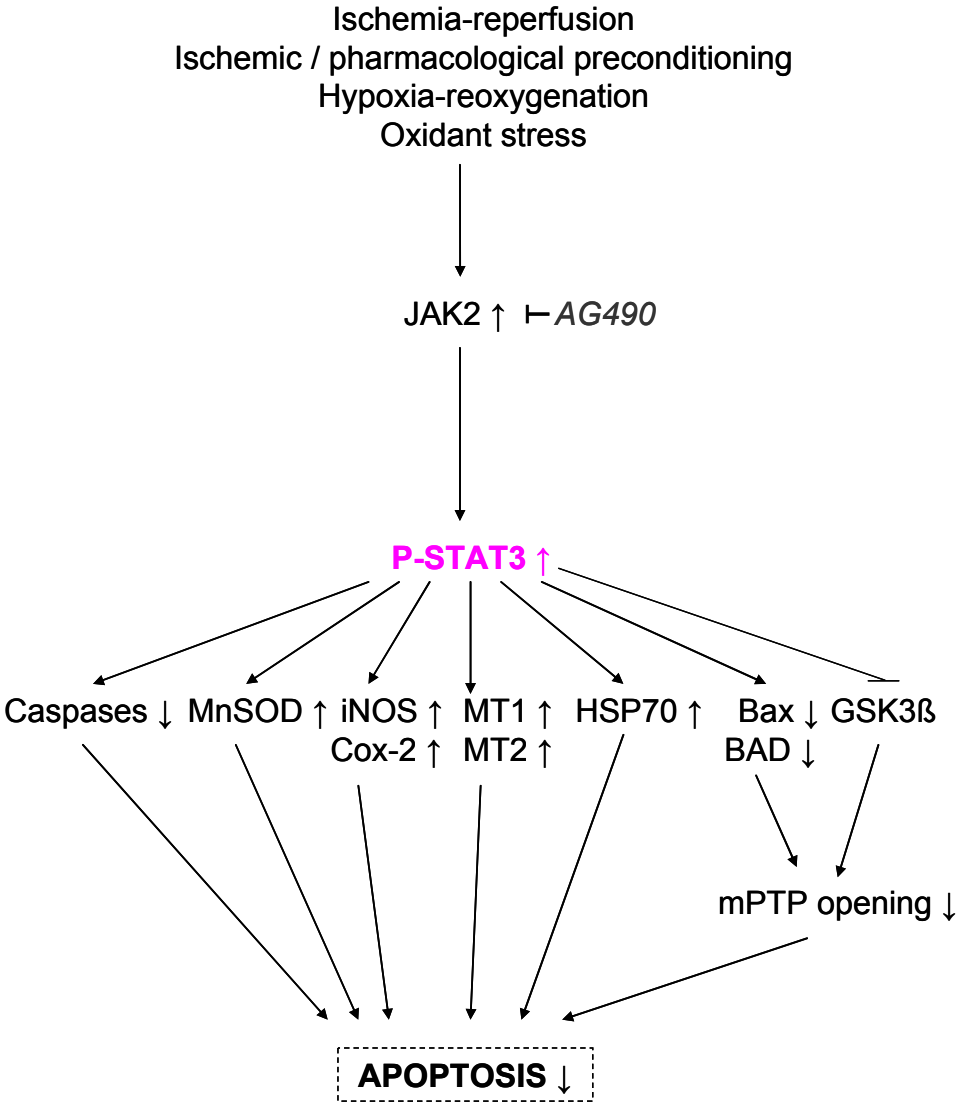

Fig. 14: Cardioprotective actions of the JAK2/STAT3 pathway.

II. The embryonic heart

II.1 Characteristics

In vertebrate embryogenesis the heart is the first organ to form and become completely functional. A correct development of the embryo absolutely requires a normal cardiogenesis. The embryo and the fetus develop normally in a relatively hypoxic environment (PO_2: 0-8kPa) (Maltepe and Simon, 1998, Burton and Jaunaiux, 2001). The 4-day-old embryonic chick heart is composed of three different regions: atria will differentiate into pacemaker tissue, ventricle into working myocardium and outflow tract into aorta and pulmonary arteries (Moorman and Christoffels, 2003). At the stage investigated, the outflow tract undergoes important morphogenetic processes (remodeling) preparing the aorticopulmonary septation which require an important physiological apoptotic activity (Sugishita et al., 2004, Barbosky et al., 2006). Indeed, in our preparation, there was 8.4 ± 1.3, 9.5 ± 0.3, and 14.5 ± 0.8% (n = 3 determinations) of apoptotic cells in atria, ventricle, and outflow tract, respectively (Gardier et al., 2010a).

Embryonic mammalian cardiomyocytes have immatures sarcoplasmic reticulum (SR) (Porter et al., 2003) and T-tubules are absent or less developed than in adult heart (Brette and Orchard, 2003). In contrast all the components required for a functional SR and excitation-contraction (E-C) coupling are expressed in the chick embryonic heart (at the 4 day stage) like ryanodine receptor 2 (Dutro et al., 1993), SR Ca^{2+}-ATPase (SERCA2) (Jorgensen and Bashir, 1984), L- and T-type voltage-dependent calcium channels (Brotto and Creazzo, 1996)and Na^{+}/Ca^{2+} exchanger (Murphy et al., 1986).

The sympathetic or parasympathetic extrinsic cardiac innervation is absent at early stages and the regulation of the cardiovascular function is directly dependent on intrinsic mechanisms at the tissue level. Embryonic heart has no myocardial vascularisation, the coronary vasculature

starting to expand only after day 32-37 in human (Reese et al., 2002), day 12 in mouse (Olivey et al., 2004) and day 5 in chick (Martinsen, 2005), oxygen and nutrients diffusing directly from the luminal blood.

The content of glycolytic and mitochondrial enzymes is lower in the rapidly growing embryonic heart than in the mature heart (Seltzer and McDougal, 1975). In the embryonic chick heart, the mitochondrial oxidative capacity is rather moderate (i.e. about half of that in the mature myocardium) but the activity of the working ventricle depends predominantly on aerobic ATP synthesis as in the adult (Romano et al., 2001). The glycogen concentration is much higher (10-20 fold) in embryonic than in adult myocardium and atria contains more glycogen than ventricle (Tuganowski et al., 1975, Romano et al., 2001).

In the embryo/fetus, the level of antioxidants is relatively low. Indeed, antioxidant enzymes like SOD and catalase appear to be lower in immature than in adult myocardium (Mover and Ar, 1997), but a high content of ascorbic acid has been found in the yolk sac as well as in liver and brain of the developing chick embryo (Surai et al., 1996). More specifically, in the 4-day-old embryonic chick heart the activity of GPx and GR as well as the normalized content of reduced glutathione are comparable to those in adult cardiac tissue (Raddatz et al. unpublished).

II.2 Response to anoxia-reoxygenation

Early cardiogenesis is severely affected even by short period of hypoxia (Ream et al., 2008) and cardiovascular function can be rapidly altered by oxygen deprivation (Jensen et al., 1999, Raddatz et al., 2006). During intrauterine life the embryo/fetus can be exposed to transient reduction of perfusion and oxygenation, like torsion of the umbilical cord, maternal hypoxaemia or acute placental dysfunction, leading to adaptative mechanisms.

In the 4-day-old chick embryo model, it has already been shown that functional (chrono-, dromo- and inotropic) disturbances and ultrastructural modifications induced by 30min of anoxia followed by 60min of reoxygenation are reversible within a period of time that depends on the developmental stage (Sedmera et al., 2002). Atrial rate, PR interval, QT duration determined from the electrocardiogram (ECG), atrial and ventricular electromechanical delay (EMD) and ventricular shortening are rapidly impaired but fully recover after about 30min of reoxygenation (Raddatz et al., 2006) (fig. 15). Tenthorey et al. (1998) demonstrate a rapid decline of ventricular contractility (i.e. decreased myocardial shortening with contracture, reduction in velocities of contraction and relaxation) during anoxia. L-type calcium channels and SR calcium release channels are implicated in the myocardial dysfunction induced by anoxia-reoxygenation (Tenthorey et al., 1998). Hearts also display different types of arrhythmias like atrial ectopy, transient sinoatrial arrest leading to cardioplegia, brady- and tachycardia, 1st, 2nd and 3rd degree atrioventricular block and intermittent bursting activity (Tenthorey et al., 1998, Sarre et al., 2005, Sarre et al., 2006). Reoxygenation causes also Wenckebach phenomenon and rare ventricular escape beats. Moreover, there is an absence of increased incidence of cell death in the embryonic myocardium submitted to various periods of anoxia (Sedmera et al., 2002).

A burst of ROS/RNS production is observable during the first 15min of reoxygenation and the reoxygenation-induced arrhythmias are related to the peak of ROS production (Rosa et al., 2003, Sarre et al., 2005). This ROS production is maximal after 10min of reoxygenation (Sarre et al., 2005) and it has just been shown that the ETC and the Nox were the main sources of ROS and that glutathione redox cycle appeared to be the major antioxidant system (Raddatz et al., 2010). In the embryonic myocardium iNOS is strongly expressed and generates NO during anoxia-reoxygenation (Terrand et al., 2003), improving recovery of E-C

coupling in the ventricle (Maury et al., 2004), but no nitrosative stress was detectable (Raddatz et al., 2010).

The myocardial dysfunction induced by anoxia-reoxygenation is also associated with a significant alteration of signalling pathways. In particular, the region-specific activation of MAPKs (p38, ERK and JNK) (Sarre et al., 2008, Gardier et al., 2010b) and stimulation of PKC and NOSs (Sarre et al., 2005) are part of the mechanisms involved in the response to anoxia-reoxygenation, with slight differences relative to the ischemic-reperfused adult heart (Hausenloy and Yellon, 2006).

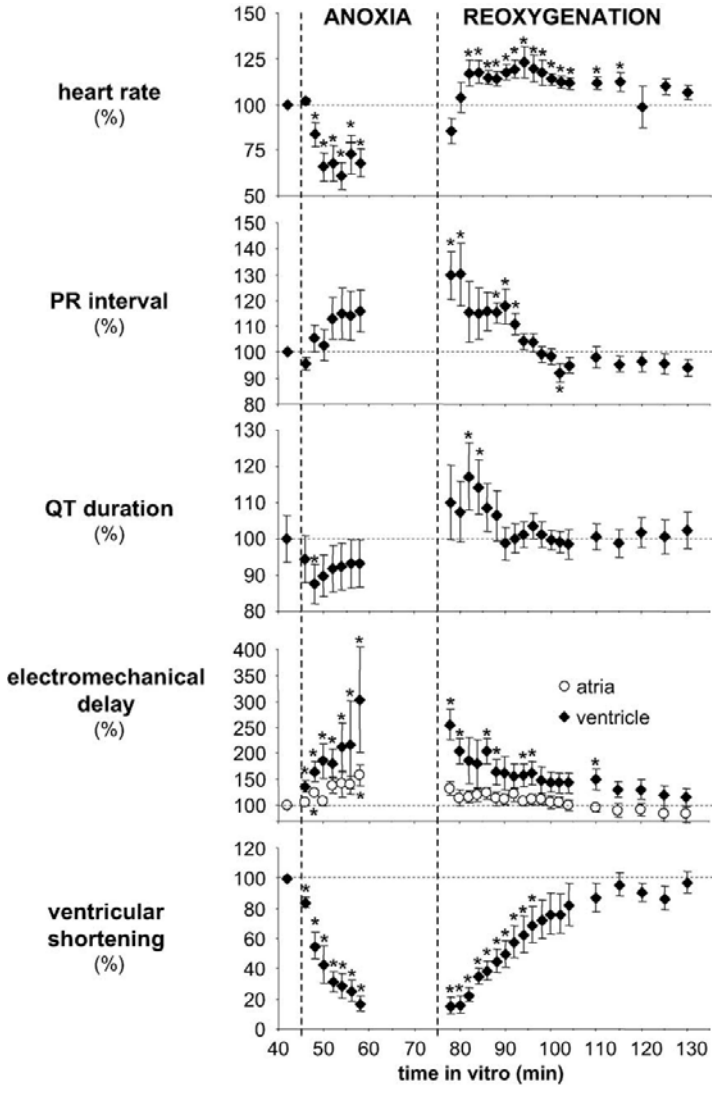

Fig. 15. Functional parameters of the isolated 4-day-old embryonic chick heart during anoxia-reoxygenation, expressed as percent changes of their preanoxic values (Raddatz et al., 2006).

II.3 Fetal programming

The JAK2/STAT3 pathway playing an important role in embryogenesis and more especially in cardiogenesis, alteration of this pathway by different stresses could have consequences on fetal programming. This is the concept that epigenetic factors in the intrauterine environment can profoundly influence the trajectory of prenatal development. Programming effects can be induced by maternal diet alterations, maternal substance abuse (e.g. alcohol, nicotine, drugs), chronic fetal hypoxia and anemia. Intrauterine programming may involve structural and functional changes in genes, cells, tissues, and whole organs (Fowden et al., 2006). There are critical time windows when developing systems are most vulnerable to adverse conditions, and these critical periods differ among systems and species. Fetal programming has permanent effects that can alter responses to stress in later life and can modify susceptibility to diseases (Nijland et al., 2008). Indeed, this phenomenon is now recognized as a possible origin of many systemic adult diseases including coronary heart disease, hypertension, stroke, atherosclerosis, pre-eclampsia and diabetes.

AIMS OF THE WORK

I. Characterization of the JAK2/STAT3 pathway in the 4-day-old chick embryonic heart

The first phase of this work characterized the JAK2/STAT3 pathway in the 4-day-old chick embryonic heart. We first checked the basal expression of JAK2 and STAT3 in atria, ventricle and outflow tract. In addition, we studied the response of the pathway to classical activation by IL-6. And finally we compared STAT3 expression in basal conditions (freshly isolated hearts) and in the culture chamber used for the experiment of anoxia-reoxygenation (after stabilization).

II. Modulation of the JAK2/STAT3 pathway by anoxia-reoxygenation and functional consequences

The second phase of this work determined the role of the JAK2/STAT3 pathway in the developing heart submitted to anoxia-reoxygenation. We therefore established the temporal profile of STAT3 phosphorylation and determined the role played by the reoxygenation-induced ROS in this activation. STAT3 being a transcription factor, we studied its transcriptional activity including expression of specific target genes. We finally examined the role of activated STAT3 in the functional recovery of the embryonic heart at reoxygenation.

III. Interaction of the JAK2/STAT3 and RISK pathways during anoxia-reoxygenation

The third phase of this work firstly assessed the temporal profile of phosphorylation of RISK pathway components (PI3K, Akt, and ERK) and their direct targets GSK3ß and

glycogen synthase (GS) and secondly assessed the crosstalk between STAT3 and RISK pathways in the nuclear and cytoplasmic compartments of the anoxic-reoxygenated embryonic heart.

IV. Effects of an exogenous oxidant stress (H_2O_2) on cardiac activity and JAK2/STAT3 pathway

The last part of this work evaluated the response of the embryonic heart to an exogenous oxidant stress (H_2O_2) in comparison with the reoxygenation-induced endogenous ROS. We assessed the functional response of the heart to H_2O_2, the level of phosphorylation, the transcriptional activity of STAT3 and the expression of specific target genes.

MATERIAL AND METHODS

I. Preparation and in vitro mounting of the heart.

Fertilized eggs from Lohman Brown hens were incubated during 96h at 38°C and 80% relative humidity to obtain stage 24HH embryo according to Hamburger and Hamilton (Hamburger and Hamilton, 1951). After opening a window in the shell, the embryo was explanted. The spontaneously beating hearts were carefully excised under a dissecting microscope (x12) from explanted embryos by section at the level of the truncus arteriosus as well as between the sinus venosus and the atria using micro-scissors. The heart was then placed in a stainless steel chamber, specially designed for this preparation (Raddatz et al., 1992) (fig. 16). Briefly this chamber was equipped with two windows for observation and two electrodes for ECG recording. The heart was placed in the culture compartment. A thin and transparent silicone membrane (15µm), highly permeable to gas (O_2, CO_2, N_2) but impermeable to liquids (RTV 141, Rhône-Poulenc) was gently placed on the heart. In these conditions, the thickness of the preparation was about 300µm. The volume of the lower compartment was approximately 300µl. The liquid of the upper compartment was removed allowing the passage of gas of selected composition. At the developmental stage investigated, the heart lacks vascularization and the myocardial oxygen requirement is met exclusively by diffusion. The culture chamber was then placed on the thermostabilized stage (37.5°C) of an inverted microscope (Olympus IMT2).

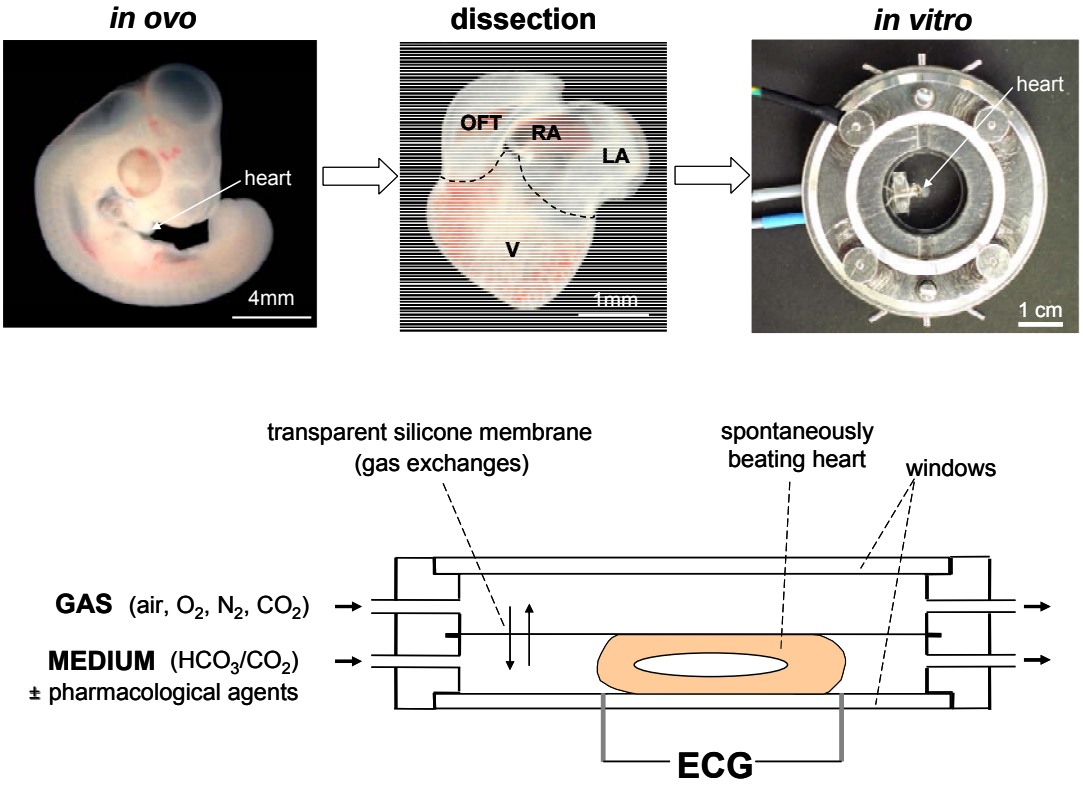

Fig. 16: From left to right, chicken embryo stage 24HH, isolated heart and culture chamber (upper panels). The lower compartment containing the heart in culture medium was separated from the upper compartment by a thin silicon membrane for gas exchanges (lower panel) (Raddatz et al., 1992). RA and LA: right and left atria, V: ventricle, OFT: outflow tract.

The standard HCO_3/CO_2 buffered medium was composed of (in mmol/L): 99.25 NaCl; 0.3 NaH_2PO_4; 10 $NaHCO_3$; 4 KCl; 0.79 $MgCl_2$; 0.75 $CaCl_2$ and 8 D-glucose. This medium was equilibrated in the chamber with 2.31% CO_2 in air containing 21% O_2 (normoxia and reoxygenation) or in N_2 (anoxia) yielding a pH of 7.4. The JAK2/STAT3 inhibitor AG490 and the PI3K/Akt inhibitor LY-294002 (Calbiochem) were reconstituted in dimethylsulfoxide (DMSO, Sigma-Aldrich). MPG (Sigma-Aldrich), AG490 and LY-294002 were diluted in the standard medium containing 0.5% and 0.006% DMSO (vehicle, V), respectively, and present throughout the experimental protocol.

II. Determination of the optimal level of myocardial oxygenation.

We have first determined the optimal level of oxygenation of the preparation to ensure a normal heart function. Under our experimental conditions 21% O_2 corresponded to 141mmHg and 8% O_2 to 54mmHg which was closer to *in ovo* environment. In a first series of experiments, hearts were submitted to steady normoxia (21% O_2) (fig. 17, protocol A) or hypoxia (8% O_2) (fig. 17, protocol B) during 165min at 37°C. In a second series of experiments hearts were equilibrated in normoxia (21% O_2) during 105min and then submitted to hypoxia (8% O_2) during 180min (fig. 17, protocol C). The reverse protocol was also tested: first hypoxia and then transition to normoxia (fig. 17, protocol D). Heart rate and atrioventricular conduction were determined after 45min of stabilization and then every hour.

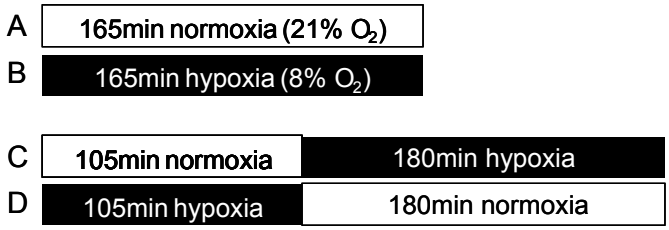

Fig. 17: Experimental protocols. Isolated hearts were submitted to normoxia (21% O_2) or hypoxia (8% O_2).

III. Experimental protocols

III.1 Exposure to interleukine-6 (IL-6).

In order to determine the effect of a cytokine known to activate the JAK2/STAT3 pathway, embryonic hearts were placed in a Petri dish (3cm of diameter) in the standard medium, stabilized 45min under normoxia and then exposed 1h to 1000 or 10000U/ml of recombinant human IL-6 (rHu-IL-6, GenScript) at 37°C (cardiac rhythmicity and contractility were not different between hearts maintained in Petri dishes and hearts mounted in the

chamber). Atrial rate was assessed throughout experiment. Ventricles were then carefully dissected on ice and stored at -80°C for subsequent determinations. We also treated rat neonatal cardiomyocytes with rHu-IL-6 as a positive control for the tyrosine phosphorylated form of STAT3 (P-Tyr STAT3).

III.2 Anoxia-reoxygenation.

After a 30min pretreament at room temperature in V, MPG [1Mm (Sarre et al., 2008)] AG490 (10µM) or LY-294002 (10µM), hearts were mounted in the chamber, stabilized 45min under normoxia and submitted to anoxia (30min) and reoxygenation (80min) (fig. 18). Control hearts were maintained under steady normoxia 60 and 90min after S, corresponding to the time points R30 and R60, respectively. At the end of the experiment atria, ventricle and outflow tract were carefully dissected on ice and stored at -80°C for subsequent determinations.

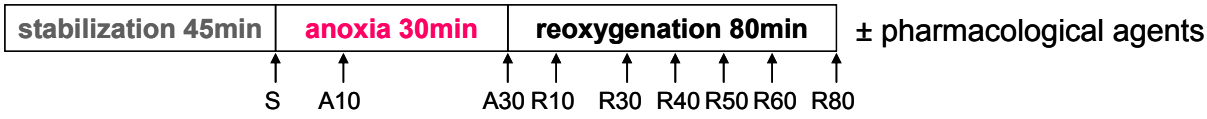

Fig. 18: Anoxia-reoxygenation protocol. Isolated hearts were stabilized 45min in normoxia and submitted to anoxia (30min) and reoxygenation (80min). Hearts were harvested after stabilization (S), 10 (A10) and 30min (A30) of anoxia and 10 (R10), 30 (R30), 40 (R40), 50 (R50), 60 (R60) and 80min (R80) of reoxygenation (time points indicated by the arrows).

III.3 Exposure to hydrogen peroxyde (H_2O_2).

With the aim of establishing the effect of an exogenous oxidant stress on the embryonic chick heart, hearts were placed in Petri dish in the standard medium, stabilized 45min under

normoxia and then exposed 1h to 50, 100, 200, 500 or 1000µM of H_2O_2 (Sigma-Aldrich) at 37°C (Gardier et al., 2010b). The proportion of hearts still beating at the end of each experiment was determined and atrial rate was assessed at 1000µM of H_2O_2. Atria, ventricle and outflow tract were then carefully dissected on ice and stored at -80°C for subsequent determinations.

IV. Protein expression and phosphorylation (JAK2, STAT3, PI3K, Akt, GSK3ß, GS, ERK).

The protein expression and level of phosphorylation of JAK2, STAT3, PI3K, Akt, GSK3ß, GS and ERK were determined by immunoblotting.

IV.1 Protein homogenate.

Six atria, three ventricles and six outflow tracts were pooled because of the small size of the hearts. Atria, ventricle and outflow tract were homogenized by sonication 3 x 2s in the ice-cold lysis buffer (in mmol/L: 20 Tris-acetate (pH 7), 270 sucrose, 1 EGTA, 1 EDTA, 50 NaF, 10 β-glycerophosphate, 1 dithiothreitol (DTT), 10 4-nitrophenyl phosphate disodium salt hexahydrate (PNPP), 1% Triton X-100 and inhibitors of proteases) and protein content was measured by the method of Bradford (Coomassie protein assay kit, Pierce) with bovine serum albumin as standard.

IV.2 Enriched nuclear and cytoplasmic fractions preparation.

Cytoplasmic and nuclear extracts were obtained as described elsewhere (Levrand et al., 2005). Twelve ventricles were homogenized in hypotonic buffer (in mmol/L): 10 HEPES (pH 7.9), 0.1 EDTA (pH 8), 0.1 EGTA (pH 8), 10 KCl, 1 DTT, 1 Na_3VO_4 and inhibitors of proteases. After addition of detergent Nonidet P-40 (0,625%) and centrifugation, supernatants containing the cytoplasmic proteins were stored at -80°C. Pellets were resuspended in hypertonic buffer (in mmol/L: 20 HEPES (pH 7.9), 400 NaCl, 1 EDTA (pH 8), 1 EGTA (pH 8), 1 DTT, 1mM Na_3VO_4 and inhibitors of proteases), centrifugated and the resulting supernatants (nuclear fractions) were collected and stored at -80 °C. Protein content was measured in each fraction by the method of Bradford.

IV.3 Immunoblotting.

Proteins from cellular extracts (20µg) were boiled with 1/3 of SDS sample buffer (in mmol/L: 150 Tris-HCl (pH 6.8), 6% SDS, 30% glycerol, 7.5% β-mercaptoethanol and 0.2% bromophenol blue), separated on 10% SDS-polyacrylamide gels (1h, 185V), and transferred to nitrocellulose membranes (2h, 100V). Membranes were probed with primary antibodies against JAK2 (1:1500); phospho-Tyr^{705}-STAT3 and phospho-GS (1:750); phospho-Ser^{727}-STAT3, phospho-PI3K, STAT3 and PI3K (1:500); phospho-Akt, phospho-GSK3β, phospho-ERK, Akt, GSK3β, GS and ERK (1:1000) diluted in 5% bovine serum albumin in tris-buffered saline tween [(TBS-T), in mmol/L: 20 Tris (pH 7.6), 150 NaCl and 0.00025% tween-20)] (overnight, 4°C). Blots were then incubated (1h, room temperature) with the secondary

antibody (1:10000, goat anti-rabbit HRP conjugated, GE Healthcare) in 1% non-fat milk in TBS-T. Immunoreactive bands were detected using the ECL western blot reagent kit (PerkinElmer). Signal was semi-quantitatively analyzed using scanning densitometry (Quantity One software, Biorad). Protein bands (phospho) were normalized to expression of the total protein in the same sample and on the same membrane. More specifically for STAT3, the phospho-α isoform (P-STAT3α) was normalized to expression of the total α isoform. Phosphorylation level at each time point of anoxia and reoxygenation was normalized to the respective preanoxic S level. We used total cell extracts from serum-starved HeLa cells prepared with IFN-α treatment (Cell Signaling Technology) as a positive control for P-Tyr STAT3, in which the α isoform was largely predominant relative to the ß isoform. Rabbit antibodies against phospho-Ser^{727}-STAT3, phospho-Tyr^{458}-PI3K, PI3K, phospho-Ser^{473}-Akt, Akt, phospho-Ser^{9}-GSK3β, GSK3β, phospho-Ser^{641}-GS, GS, phosphorylated ERK and ERK were from Cell Signaling Technology, the one against JAK2 was from Sigma-Aldrich, the one against phospho-Tyr^{705}-STAT3 was from Ab Frontier and the one against STAT3 was from Santa Cruz Biotechnology.

It should be noticed that antibodies used are not known to crossreact with avian proteins but rather with mammals. By checking protein sequences we found a high homology between the different species.

V. Recordings of electrical and contractile activities.

Electrical and contractile activities were recorded simultaneously and continuously throughout in vitro experiments according to Sarre et al, 2006.

V.1 Electrical activity.

ECG recording of the spontaneously contracting intact heart was performed using two Ag/AgCl electrodes 1.2mm apart (diameter 0.625mm) inserted into the window facing the culture compartment (fig. 16). The atrial and ventricular regions of the whole heart were placed in the immediate vicinity of these electrodes, which were connected to a differential preamplifier (gain of 2000), resulting in an output signal of 1-5V peak-to-peak. This signal was digitized and processed using a powerful data acquisition (IOX, sampling rate: 2kHz) and analysis system (ECG-Auto) developed by EMKA Technologies (France).

ECG of the heart displayed characteristic P, QRS and T components which allowed to determine PP, PR and QT intervals (ms) and amplitude of the QRS complex and T wave (mV). Atrial rate was determined from PP interval and ventricular rate from RR interval. We assessed QRS widening, reflecting a possible reduction of intraventricular conduction, by measuring the half-width of the QRS complex.

The various types of arrhythmias, their scoring, and their duration were precisely determined on the basis of continuous ECG recording. Arrhythmias were characterized according to Sarre et al. (Sarre et al., 2006) i.e. *atrial bradycardia:* regular atrial rhythm with a rate below 130bpm; *atrial tachycardia:* regular atrial rhythm with a rate superior to 200bpm; *atrial arrest:* sudden atrial pause leading to transient cardioplegia; *atrial ectopy:* atrial arrhythmias due to blocked atrial premature beats; *n:1 atrioventricular block (AVB):* sustained second-degree AVB with a constant n:1 relation between atria and ventricle during regular atrial rhythm; *second-degree AVB:* Wenckebach phenomenon during regular atrial rhythm nonrelated to atrial tachycardia with PR prolongation preceding the dropped beats; *third-degree AVB:* sustained (>20s) complete lack of AV conduction.

V.2 Contractile activity.

Adjustable phototransistors were positioned over the projected image of the investigated regions allowing detection of edge motion of the myocardial wall, that is, at the level of atrial pacemaker and ventricular apex in the intact heart (fig. 19). Simultaneously with ECG, myocardial shortening was sampled at a rate of 1kHz using the same acquisition/analysis system as described above. The maximal velocity of contraction and relaxation was calculated from the maximal positive and negative values of the first derivative of shortening and relaxation respectively.

V.3 Excitation-contraction coupling.

The EMD, reflecting the efficiency of E-C coupling, was determined at the level of atria (EMDa) and ventricle (EMDv) by measuring the delay between the electrical and mechanical events, i.e., the interval of time between the very initial phase of the P and QRS components and the initiation of contraction in the atria and ventricle, respectively (fig. 19).

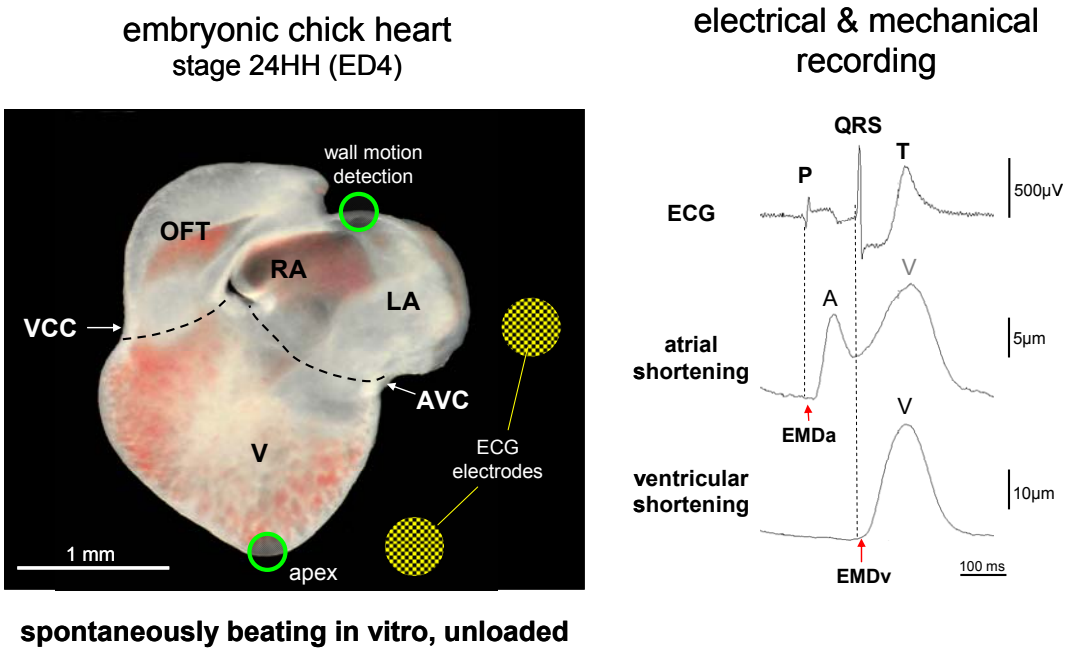

Fig. 19: Embryonic heart mounted in vitro and representative recordings of electrical and contractile activities. RA and LA: right and left atria, V: ventricle, OFT: outflow tract; AVC: atrioventricular canal; VCC: ventriculoconotruncal canal; P, QRS and T: P wave, QRS complex and T wave of ECG; EMDa and EMDv: atrial and ventricular electromechanical delay, respectively. The dotted lines indicate where hearts have been cut [modified from (Raddatz, 2007)].

VI. Electrophoretic Mobility Shift Assay (EMSA).

A STAT3 oligonucleotide probe (5′-GAT CCA TTT CCC GTA AAT CAT GGA TC-3′) was labeled with α-^{32}PdCTP using the Klenow enzyme (Roche Applied Science). It should be noticed that the probe was designed specifically for the chick. 10µg of nuclear proteins were incubated with EMSA buffer [in mmol/L: 20 HEPES (pH 7.9), 50 KCl, 0.5mM EDTA, 0.1% NP-40, 1 mg/ml bovine serum albumin, 5% glycerol and 170 µg/ml poly(dI-dC)] and the probe for 20min at room temperature. Samples were resolved on a nondenaturing polyacrylamide gel. Gels were transferred to Whatman 3M paper, dried under vacuum, and exposed to photographic films at -80°C. Densitometric analysis of autoradiographs was

performed. Negative controls were performed using either an antibody against total STAT3 or an unlabelled probe.

VII. Quantitative RT-PCR.

Twelve ventricles were homogenized in trizol (Invitrogen) and total RNA were purified by slight modifications of the method originally described by Chomczynski & Sacchi (Chomczynski and Sacchi, 1987). The reverse transcription (RT) reaction was performed using the high capacity cDNA reverse transcription kit and protocols from Applied Biosystem. Briefly, the RT was run with 1.5µg of total RNA in a reaction volume of 20µl and aliquots of this reaction mixture [(primers (150-300 mmol/l), 1× SYBR Green PCR master mix and H_2O] were used for the subsequent PCR reactions. The level of mRNA expression of three STAT3 specific target genes in the context of I-R, i.e. iNOS, MnSOD and Cox-2 were investigated and the following sequences were used: iNOS, forward: TCT TCC AGC TAA AGA GCC AAA AG, reverse: CAC GTC CAA TGT CTG TTG TTC A; MnSOD, forward: CCC ACA TCA GTG CAG AGA TCA, reverse: TGA GCT GTA ACA TCA CCT TTT GC, COX-2, forward: CACCAC CAA TGG GTG TTA AAG GTA AGA, reverse: ATA AAT TTT CTC CGC AGC AAG AA and actine, forward: TCG TAC CAC AGG TAT TGT TCT TGA C, reverse: AGA TCC CTG CCA GCC AGA T. 5ng of cDNA was laid per well. Results are calculated using the ΔCt method (Livak and Schmittgen, 2001). It should be noticed that PCR primers were designed specifically for the chick.

VIII. Statistical analysis.

Because of the very small size of the heart (circa 60µg proteins) a total of about 6100 chick embryos have been used in this study. Results are given as mean ± standard error of the mean (SEM) for immunoblotting densitometry (as otherwise indicated) and EMSA and as mean ± standard deviation (SD) for functional parameters and RT-PCR quantification. The significance of any difference between two cardiac areas, two time points or two conditions was assessed using Mann-Whitney test. The statistical significance was defined by a value of $p \leq 0.05$.

RESULTS

I. Determination of the optimal level of myocardial oxygenation

After 165min, under steady normoxia (21% O_2) more than 80% of the hearts showed a normal conduction whereas under hypoxia (8% O_2) it was the case in only 30% of the hearts (fig. 20). However the mean atrial rate was not different between normoxia and hypoxia, even after 165min. In the hearts initially exposed to normoxia, transition to hypoxia reduced by 40 and 75% the number of hearts displaying normal conduction after 1h and 3h, respectively. Conversely in the hearts initially stabilized under hypoxia, passage to normoxia leaded to a 130% increase in the proportion of the hearts with normal conduction (fig. 21). The mean atrial rate remained constant in the two different protocols. Thus, these results show clearly that an optimal oxygenation of the embryonic myocardium in our experimental model was obtained with 21% O_2.

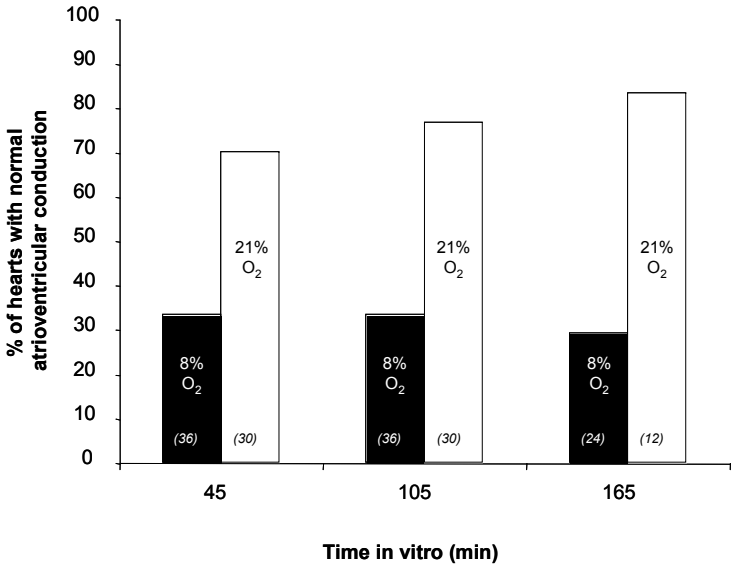

Fig. 20: Hypoxia altered the atrioventricular conduction. Effect of steady normoxia vs steady hypoxia on atrioventricular conduction of the embryonic chick heart in vitro. Percentage of hearts showing normal conduction under steady normoxia (21% O_2) or hypoxia (8% O_2) after 45, 105 and 165min (37°C). ( ): number of hearts investigated.

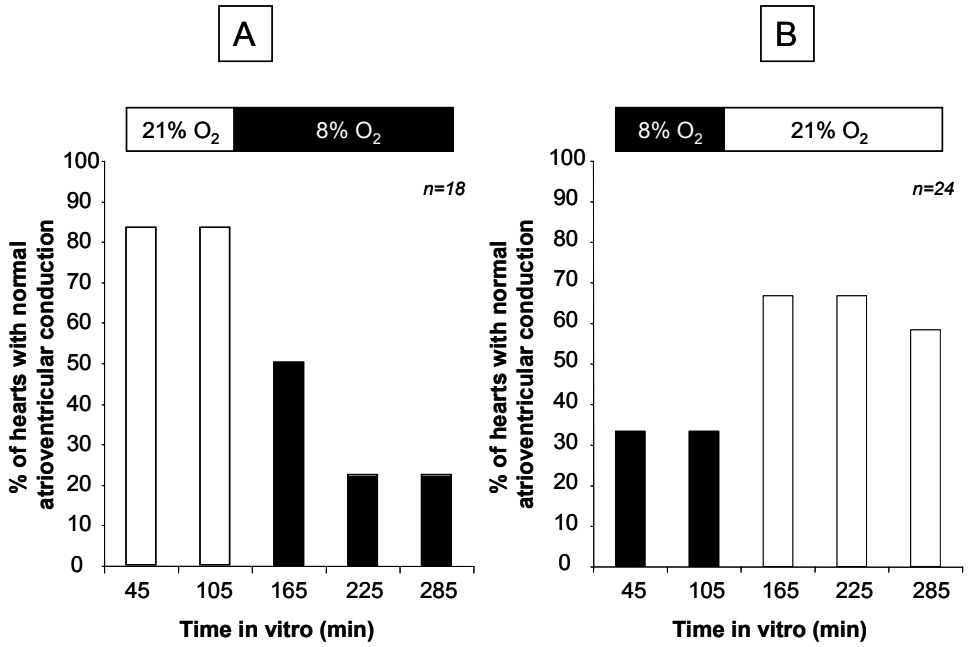

Fig. 21: Embryonic hearts recovered rather well from an hypoxic episode. Effect of transition from normoxia to hypoxia (A) and reciprocally (B) on atrioventricular conduction of the embryonic chick heart. Percentage of hearts showing normal atrioventricular conduction. n: number of hearts investigated.

II. Characterization of the JAK2/STAT3 pathway in the heart of the 4-day-old chick embryo

II.1 Basal expression of JAK2 and STAT3 in atria, ventricle and outflow tract

In freshly isolated embryonic heart, JAK2 content tended to be higher (+77%, p=0.08, n=4-9) in outflow tract compared to atria and ventricle (fig. 22). Although both α (~92kDa) and ß (~83kDa) STAT3 isoforms were expressed in the embryonic heart (fig. 23A), only the α isoform of P-Tyr STAT3 was detectable under our conditions (fig. 23B). STAT3 content, like JAK2, was significantly higher (+22%) in outflow tract compared to atria and ventricle whereas the phosphorylated STAT3α to total form ratio was higher in atria than in ventricle (+50%) and outflow tract (+35%) (fig. 23A, 23B).

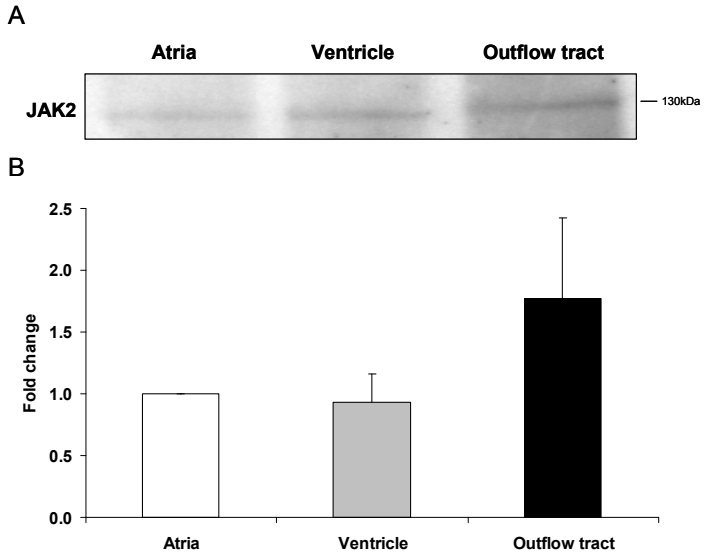

Fig. 22: Distribution of the total form of JAK2 in atria, ventricle and outflow tract of the 4-day-old embryonic heart. (A) Representative immunoblots and (B) densitometric analysis of JAK2. N=4-9 determinations for each region. Data are expressed as fold change relative to atria.

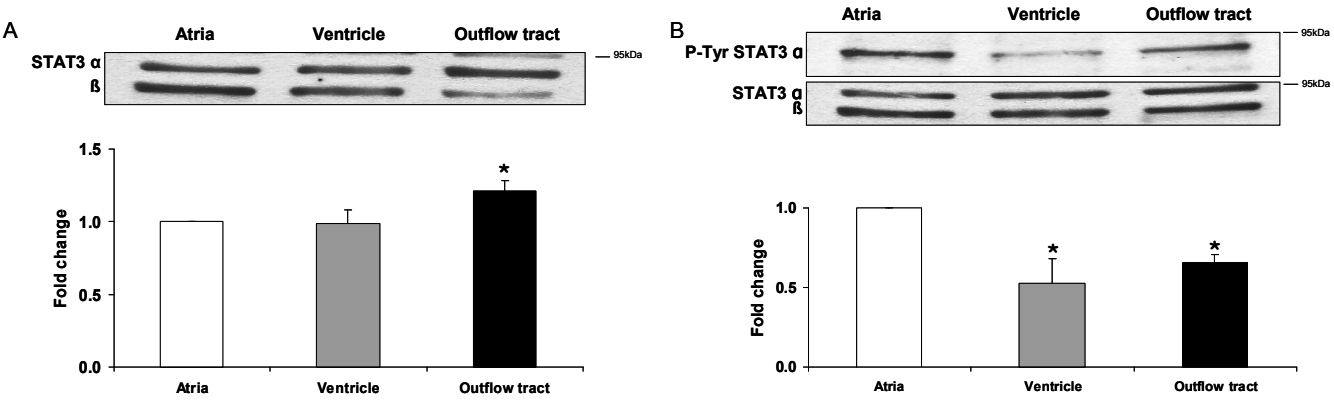

*Fig. 23: The content of STAT3 was the highest in outflow tract but the level of STAT3 phosphorylation was the highest in atria. Representative immunoblots and densitometric analysis of A) α and ß isoforms of STAT3 and B) α isoform of tyrosine phosphorylated STAT3 (P-Tyr STAT3α) normalized to STAT3α in atria, ventricle and outflow tract of the embryonic heart at stage 24HH. *: $p<0.05$ vs atria. N=6 determinations for each region*

II.2 Activation of the JAK2/STAT3 pathway by interleukine-6 in the ventricle

We wanted to check if in the 4-day-old chick embryonic heart model the JAK2/STAT3 pathway could be activated by IL-6, like it is the case in almost all cell types of adult tissues.

Atrial rate was not altered by 1h exposure to IL-6 at 1000 or 10000U/ml. Surprisingly, in the embryonic heart ventricle P-Tyr STAT3α was not altered by IL-6 stimulation whatever the concentration (fig. 24A, 24B). By contrast, neonatal rat cardiomyocytes treated with rHu-IL-6 and used as a positive control, showed an increase of P-Tyr STAT3α from 15min of exposure at 1000U/ml onward (fig. 24C). This experience shows that the concentration of rHu-IL-6 used was able to stimulate the JAK2/STAT3 pathway.

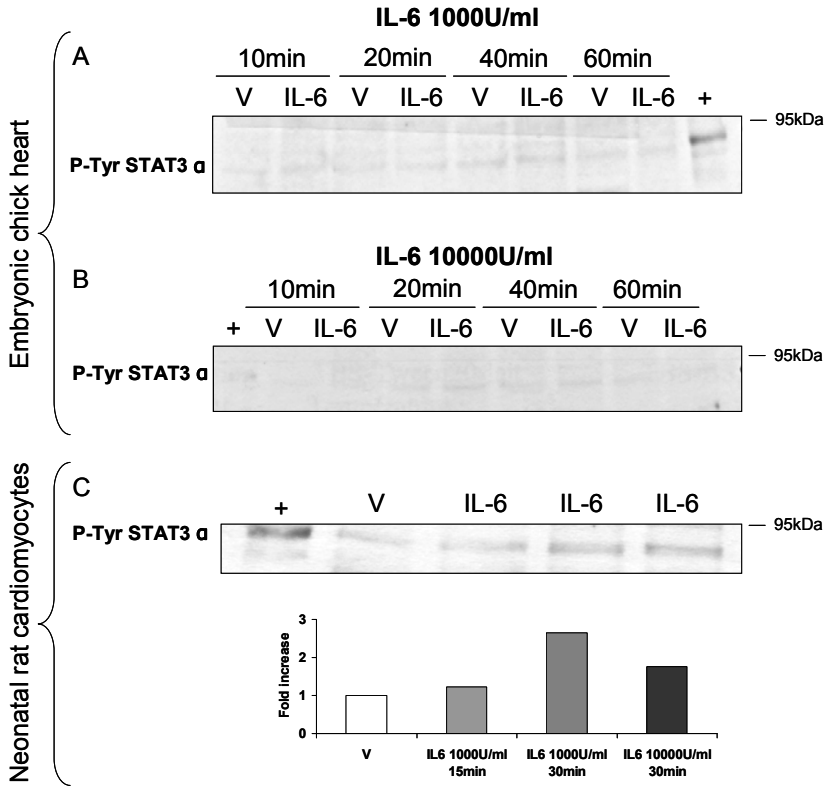

Fig. 24: P-Tyr STAT3α was not altered by IL-6 in the embryonic chick heart. Representative immunoblots of P-Tyr STAT3α in embryonic chick heart ventricle in vehicle (V) or in IL-6 at 1000 A) or 10000U/ml B) after 10, 20, 40 and 60min, n=2-4. C) Immunoblot and densitometric analysis of P-Tyr STAT3α in rat neonatal cardiomyocytes in V or in IL-6 at 1000 or 10000U/ml after 15 and 30min, n=1. +: commercial positive control for P-Tyr STAT3α.

II.3 STAT3 expression in basal and culture conditions.

We wanted to compare STAT3 basal phosphorylation in freshly isolated hearts and after *in vitro* culture. We found that in the ventricle P-Tyr STAT3α was decreased after 45min of stabilization at 37°C compared to basal expression (fig. 25A), whereas STAT3 content was not significantly different between the two conditions (fig. 25B).

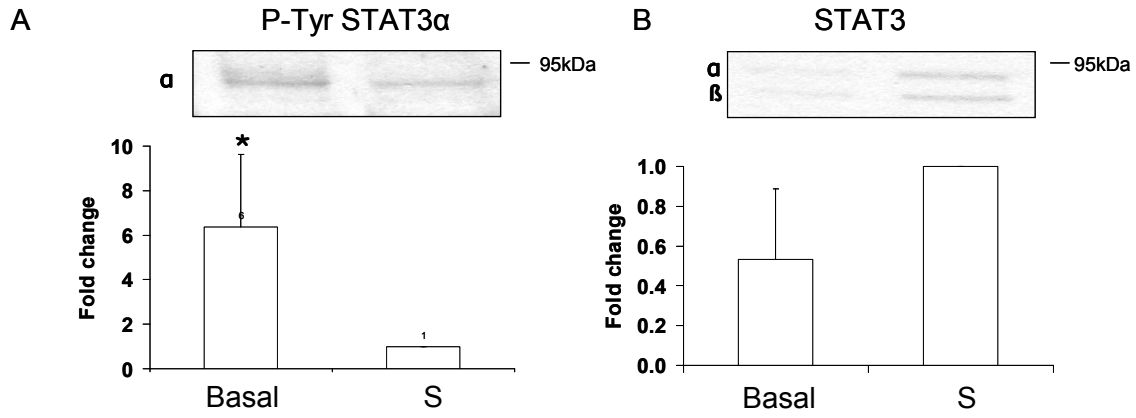

*Fig. 25: P-Tyr STAT3α was decreased after 45min of stabilization in vitro at 37°C. Representative immunoblots and densitometric analysis of A) P-Tyr STAT3α and B) α and ß isoforms of STAT3 in ventricle freshly isolated (basal) and after 45min of stabilization (S) at 37°C. Data are expressed as fold change relative to S. *: p<0.05 vs S. N=3-4 determinations.*

II.4 Discussion

Information about the myocardial JAK2 and STAT3 content at very early stages of development in the chick was lacking whereas it exists in the whole mouse embryo (Takeda et al., 1997, Neubauer et al., 1998). However, no information exists regarding the specific cardiac distribution of JAK2 and STAT3 during development. In the heart of the chick embryo at stage 24HH, JAK2 tended to be inhomogeneously distributed, the outflow tract showing the highest level of total JAK2. Unfortunately it was technically difficult to reveal

the JAK2 phosphorylated form with antibodies available on the market. Our data indicate that α and ß isoforms of STAT3 were strongly expressed in the embryonic heart but that only the α isoform was phosphorylated in this model. STAT3ß is known to have a critical developmental function (Dewilde et al., 2008). STAT3α, like its classical upstream regulator JAK2, was differentially distributed in the three cardiac regions, the highest level being found in the outflow tract. At this developmental stage the outflow tract undergoes complex apoptosis-dependent remodeling leading to a dual aortico-pulmonary circulation (Liu and Fisher, 2008). STAT3 could be involved into this morphogenetic process since it can regulate angiogenesis (Funamoto et al., 2000, Hilfiker-Kleiner et al., 2005). However, the level of STAT3α phosphorylation was the highest in the atria. The meaning of this observation will be discussed in the discussion section (paragraph V.4, page 88).

Classically the JAK2/STAT3 pathway is stimulated by type I cytokines like IL-6, IL-11 and LIF (Leonard and O'Shea, 1998). We found that in the 4-day-old chick embryonic heart the JAK2/STAT3 pathway was not activated by IL-6, like it is the case in almost all adult or neonatal tissues. This absence of response may be due to the fact that at this early developmental stage cytokine receptors are not expressed or not functional. We hypothesize that the JAK2/STAT3 pathway is differently regulated according to the developmental stage. Kinugawa et al. used ventricular myocytes from 10-day-old chick and human IL-6 so the possibility of a lack of recognition of human IL-6 by the avian IL-6 receptors can be ruled out (Kinugawa et al., 1994).

We observed that the level of STAT3α phosphorylation was decreased after 45min of stabilization at 37°C in the culture chamber compared to basal expression. Even if hearts were carefully excised from explanted embryos, such a procedure represents a strong and abrupt surgical stress for the tissue and could explain the peak of STAT3α phosphorylation observed

in just isolated hearts. It is conceivable that the period of stabilization (45min) was sufficient to recover the level of STAT3α phosphorylation *in ovo*.

III. Activation of the JAK2/STAT3 pathway in the embryonic heart submitted to anoxia-reoxygenation

In response to a temporary lack of oxygen, the embryonic heart shows reversible functional disturbances and ultrastructural modifications (Sedmera et al., 2002, Sarre et al., 2006) associated with overproduction of ROS/RNS (Sarre et al., 2005). In the adult heart, it is known that the JAK2/STAT3 pathway is implicated in protection against hypoxia-reoxygenation by controlling gene expression (Negoro et al., 2001) whereas it is still undetermined whether this pathway is involved in the response of the embryonic heart to a transient lack of oxygen. We wanted to establish to what extent STAT3 phosphorylation level is modulated by anoxia-reoxygenation.

III.1 Profile of STAT3α phosphorylation in atria, ventricle and outflow tract during anoxia-reoxygenation and role of ROS.

In the ventricle, P-Tyr STAT3α was not affected by anoxia (A10, A30) but increased between R10 and R60 and returned to basal level at R80. It should be noted that P-Tyr STAT3α was not significantly different between R10 and R60 meaning that there were not really two peaks of phosphorylation during reoxygenation (fig. 26A, 26B). By contrast, P-Ser STAT3α was not altered throughout reoxygenation (fig. 26B). It should be mentioned that phosphorylation of the ß isoform, which does not bear a serine phosphorylation site was not detectable whatever the time point. The time-matched normoxic controls at S, R30 and R60 did not exhibit change in P-Tyr STAT3α indicating that the culture conditions by themselves did not alter STAT3 activation relative to preanoxia (fig. 26B). The level of P-Tyr STAT3α was significantly decreased by the antioxidant MPG at R10 and R60, time-points at which

activation of STAT3 was the strongest, with no effect at S (fig. 26C). It should be remarked that the level of P-Tyr STAT3α in fig.26C was not the same that shown in fig. 26A, this difference could be due to the variability between experiments and/or the imunoblotting conditions.

In atria, P-Tyr STAT3α was not affected by anoxia (A10, A30) but increased between R10 and R50 and returned to basal level at R80 (fig. 27A).

In the outflow tract, P-Tyr STAT3α increased during reoxygenation but only significantly at R60 and returned to basal level at R80 (fig. 27B). We did not determine the level of P-Tyr STAT3α during anoxia (A10, A30) and at R30 and R50.

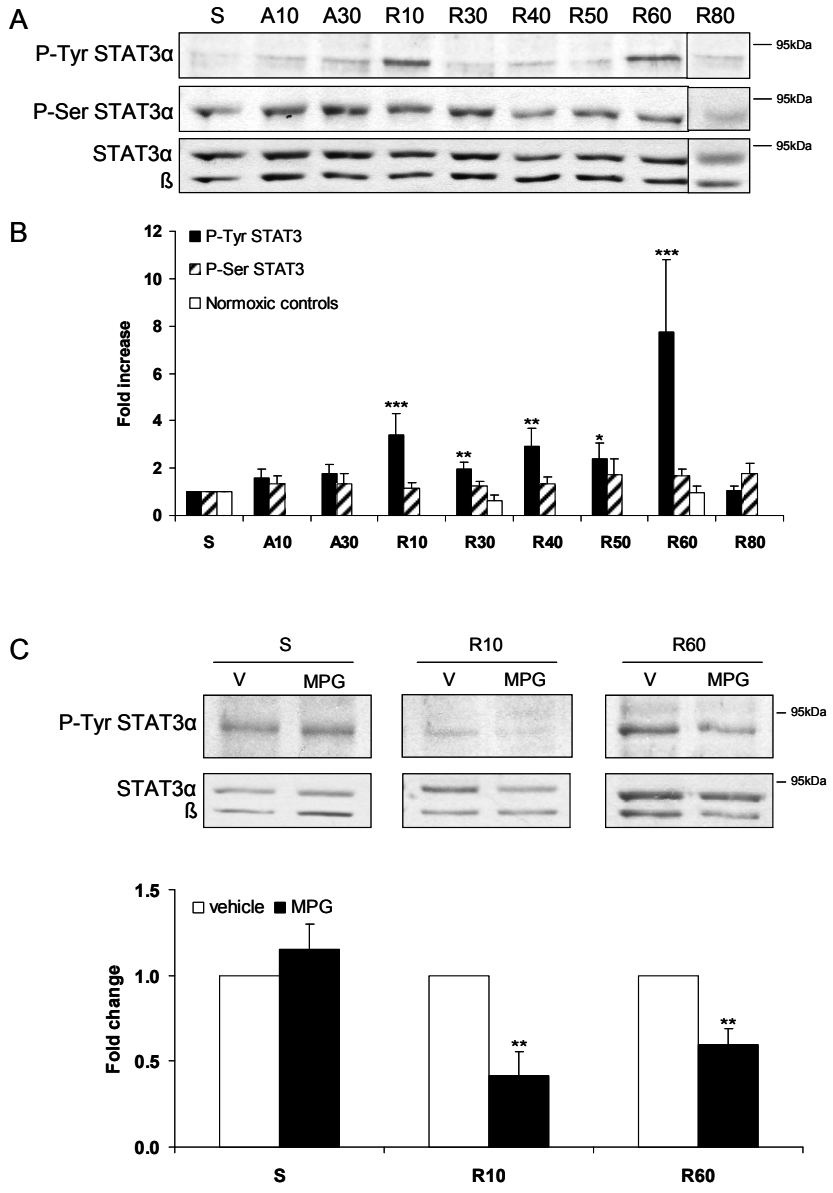

*Fig. 26: Profile of STAT3 activation in the ventricle during anoxia-reoxygenation. A) Representative immunoblots of P-Tyr STAT3α, serine phosphorylated STAT3 (P-Ser STAT3α) and STAT3α and STAT3β during anoxia (A10 and A30) and reoxygenation (R10 to R80). B) Densitometric analysis of P-STAT3α normalized to STAT3α. Black columns represent P-Tyr STAT3α, hatched columns P-Ser STAT3α and open columns P-Tyr STAT3α in time-matched normoxic controls. Data are expressed as fold increase relative to the preanoxic value (S). *: p<0.05, **: p<0.01, ***: p<0.001 vs S. N=4-9 determinations. C) Representative immunoblots of P-Tyr STAT3α, STAT3α and STAT3β (upper panels) and densitometric analysis of P-Tyr STAT3α normalized to STAT3α in vehicle (V, open columns) or in 1mM MPG (black columns) at S, R10 and R60 (lower panel). Data are expressed as fold change relative to vehicle. **: p<0.01 vs vehicle. N= 6-15 determinations.*

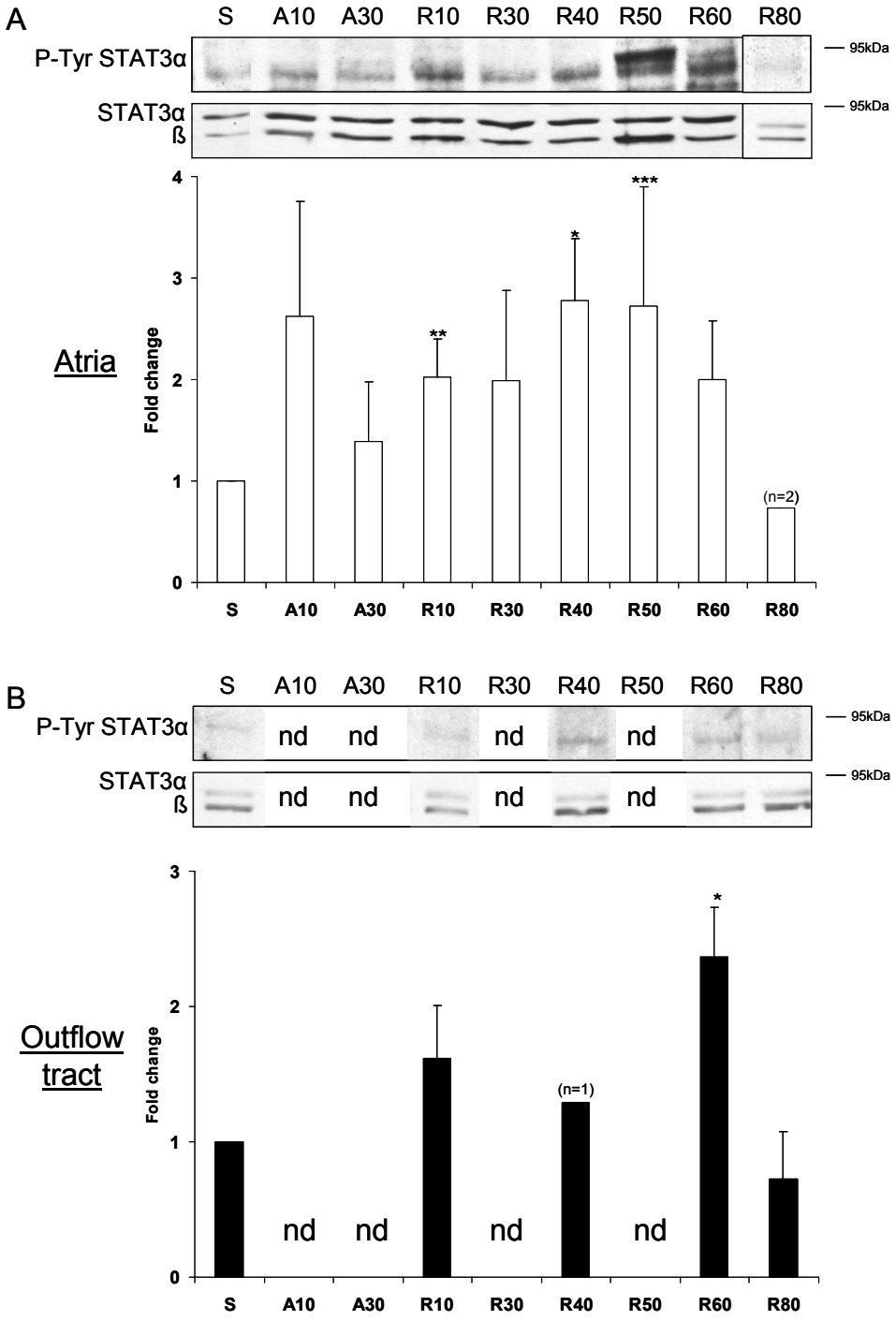

*Fig. 27: Profile of STAT3 activation in the atria and the outflow tract during anoxia-reoxygenation. Representative immunoblots of P-Tyr STAT3α and STAT3α and STAT3β and densitometric analysis of P-STAT3α normalized to STAT3α during anoxia (A10 and A30) and reoxygenation (R10 to R80) in A) atria and B) outflow tract. Data are expressed as fold change relative to the preanoxic value (S). *: p<0.05, **: p<0.01, ***: p<0.001 vs S. N=2-8 determinations for A) and n=1-4 determinations for B). Nd: not determined.*

The fig. 28 shows a summary of the temporal profile of STAT3 phosphorylation in the three cardiac regions during anoxia-reoxygenation.

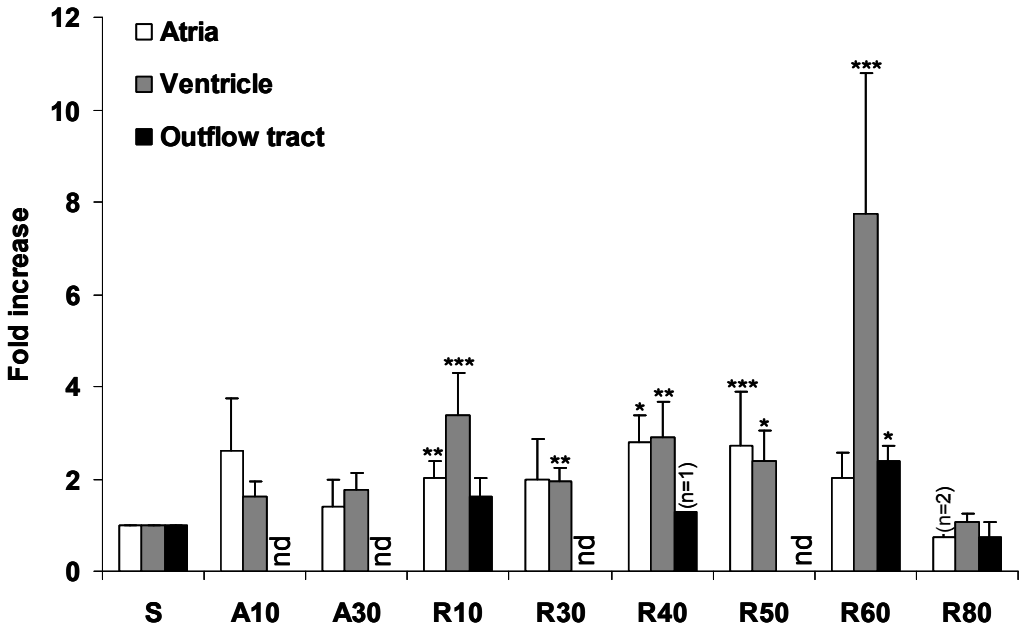

*Fig. 28: Profile of STAT3 activation in atria, ventricle and outflow tract of the embryonic heart during anoxia (A10 and A30) and reoxygenation (R10 to R80). Densitometric analysis of P-STAT3α was normalized to STAT3α. Data are expressed as fold increase relative to the preanoxic value (S). *: p<0.05, **: p<0.01, ***: p<0.001 vs S. N=1-10 determinations. Nd: not determined.*

III.2 Involvement of STAT3 in functional recovery of the embryonic heart.

STAT3 being phosphorylated during reoxygenation in the three cardiac regions we wanted to study its possible functional role by performing ECG recordings of hearts treated with the JAK2/STAT3 inhibitor (AG490).

First, we checked the effect of AG490 concentration under normoxia on the mean atrial rate and establish the dose response. AG490 at 10µM had no effect on atrial rate but from 50 to 200µM decreased the mean atrial rate and at 1mM induced cardioplegia (fig. 29A, 29B). Consequently, the concentration of 10µM of AG490 was selected for the experiments.

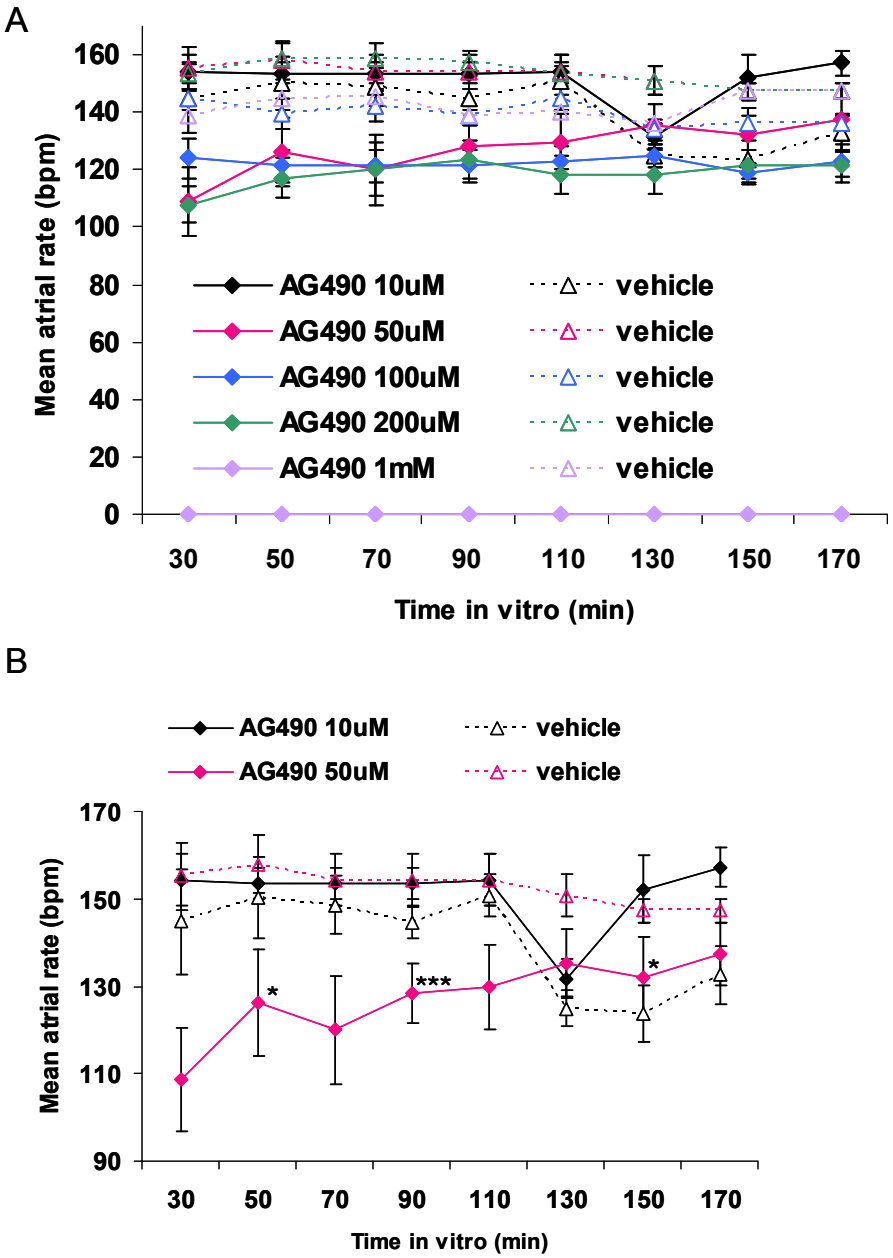

*Fig. 29: At concentrations higher than 10µM the JAK2/STAT3 inhibitor AG490 decreased the mean atrial rate under normoxia. A) Mean atrial rate of hearts in vehicle (open triangles) or in AG490 (colored diamonds) at 10 (black), 50 (pink), 100 (blue), 200 (green) or 1000µM (purple). B) For the sake of clarity, detail of experiments with AG490 at 10 (black) and 50µM (pink). *: p<0.05, ***: p<0.001 vs vehicle. Mean ± SEM, n=29-36 hearts.*

The fig. 30A illustrating the mean atrial rate relative to the preanoxic level showed that the recovery of atrial rate during reoxygenation was impaired and the coefficient of variability of the mean atrial rate was increased by JAK2/STAT3 inhibition (table 1). It should be

noticed that during the first 15min of reoxygenation the coefficient of variability of the mean atrial rate was increased in untreated hearts as well (table 1) because of the unavoidable interferences of the reoxygenation-induced arrhythmias as described elsewhere (Sarre et al., 2006). However, at R30 the RR variability was clearly higher in AG490-treated hearts (fig. 30B, 30C). None of the other electrical and mechanical parameters were affected by AG490 (table 1), i.e. atrioventricular (PR interval) and intraventricular conduction (QRS widening), QT duration and E-C coupling (EMDv). AG490 had no inotropic (shortening) or lusitropic (relaxation) effects (table 1). The types of arrhythmias (including atrial ectopy, atrioventricular block, Wenchebach) were similar in treated and untreated hearts. Furthermore, arrhythmias persisted throughout reoxygenation in 30% of the treated hearts, while they ceased at R30 in all other hearts.

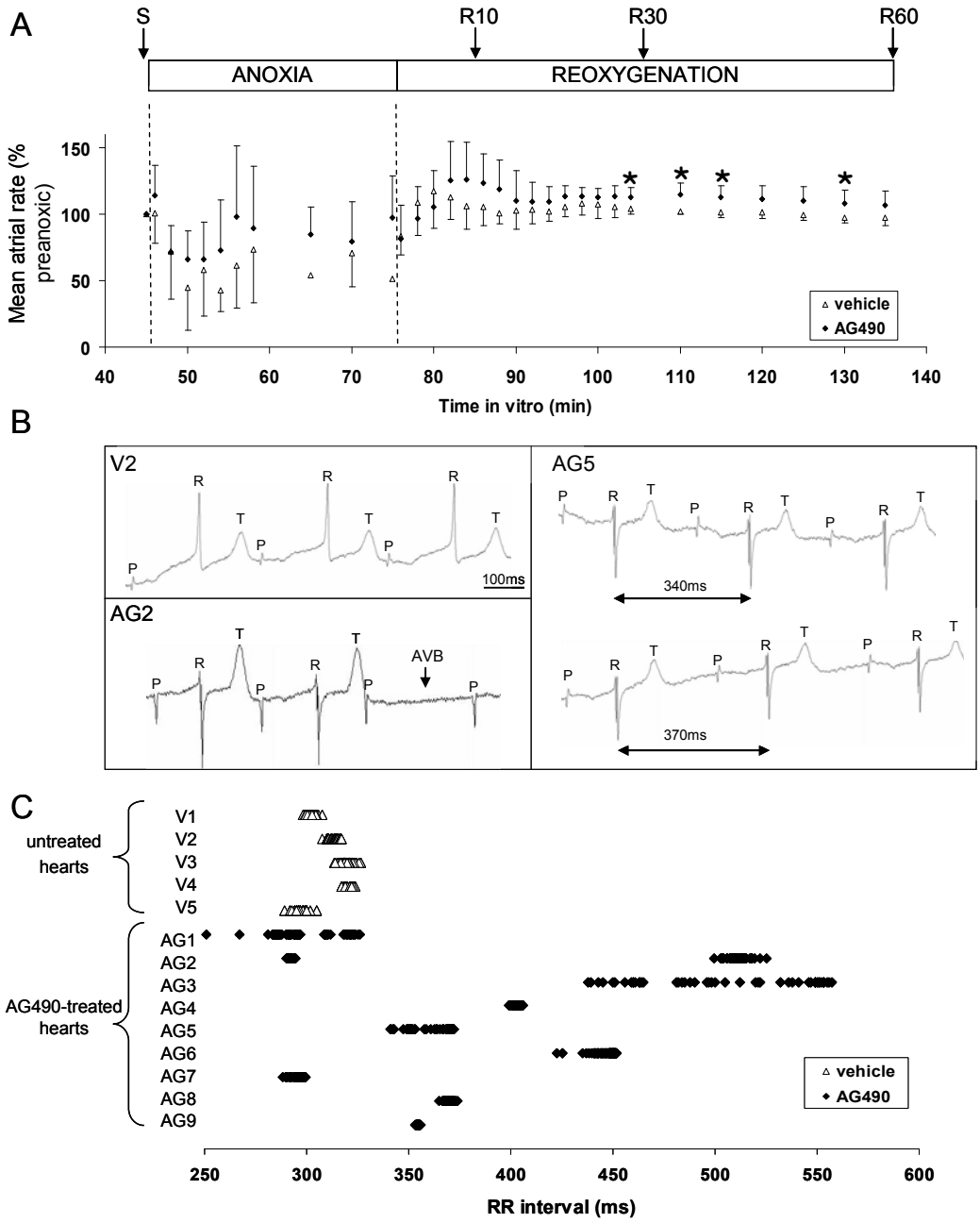

*Fig. 30: STAT3 inhibition affected recovery of atrial rhythm during reoxygenation. A) Mean atrial rate relative to the preanoxic level during anoxia-reoxygenation in vehicle (open triangles; n=5) or in 10µM AG490 (black diamonds; n=9). Note the greatest SD in treated hearts. *: p<0.05 vs vehicle. B) Representative ECGs with P, R and T components in vehicle (V2, upper left panel) or in AG490 illustrating arrhythmias i.e. PR prolongation followed by atrioventricular block AVB (AG2, lower left panel) and variations of RR interval from one cardiac cycle to another at R30 (AG5, right panel). C) Distribution of individual RR intervals in 5 untreated hearts (vehicle, V1-V5) and in 9 AG490-treated hearts (AG1-AG9) at R30. The beat to beat analysis was performed on 100 successive cycles.*

	S	R10	R30	R60
Mean atrial rate (bpm)				
v	191 ± 8	202 ± 31	198 ± 8	185 ± 8
AG	160 ± 26	193 ± 27	180 ± 33	170 ± 28
Coefficient of variability of the mean atrial rate (%)				
v	4	15	4	4
AG	16	14	18	17
PR interval (ms)				
v	133 ± 22	169 ± 34	143 ± 35	126 ± 32
AG	128 ± 33	145 ± 25	126 ± 29	119 ± 33
QT duration (ms)				
v	153 ± 10	182±5	153 ± 19	150 ± 26
AG	149 ± 12	137 ± 9	131 ± 9	139 ± 11
Contraction / relaxation velocity ratio				
v	0.96 ± 0.26	0.93 ± 0.28	1.00 ± 0.14	1.00 ± 0.21
AG	1.05 ± 0.12	0.91± 0.28	1.03 ± 0.30	1.20 ± 0.18
Ventricular shortening (µm)				
v	16.5 ± 9.6	7.8 ± 8.7	18 ± 15	10.7 ± 8.5
AG	14.1± 7.9	9.0 ± 6.2	9 ± 8	26 ± 26
EMDv (ms)				
v	26 ± 10	54±4	33±1	26±9
AG	25 ± 4	28 ± 10	25 ± 3	27 ± 5
QRS half-width (ms)				
v	3.4 ± 1.5	3.7 ± 2.0	3.2 ±0.8	4.6 ± 2.0
AG	3.0 ± 1.3	4.26 ± 2.0	3.5 ± 1.6	3.2 ± 1.5

Table 1. Functional parameters under normoxic stabilization and during reoxygenation. Electrical and mechanical parameters were systematically determined at S, R10, R30 and R60 in vehicle (V) or in 10µM AG490 (AG). Only the coefficient of variability of the mean atrial rate was different in AG490-treated hearts at S, R30 and R60. EMDv: ventricular electromechanical delay. N=3-9 determinations.

III.3 STAT3 nuclear translocation, transcriptional activity and expression of specific target genes during anoxia- reoxygenation in the ventricle.

Usually once phosphorylated, STAT3 forms homo/heterodimer with another STAT protein and can then translocate into the nucleus. We wanted to assess if this happens at reoxygenation by checking STAT3 phosphorylation level and content in nuclear and cytoplasmic compartments.

In the nuclear fraction P-Tyr STAT3α increased at R10 and tended to increase at R60 (fig. 31A) whereas STAT3 was significantly increased throughout reoxygenation (fig. 31B). By contrast, in the cytoplasmic fraction P-Tyr STAT3α and STAT3 were not affected (fig. 31C, 31D).

Generally when STAT3 is translocated into the nucleus, like every transcription factor, it binds to DNA in order to initiate the transcription of target genes. We checked by EMSA the ability of STAT3 to bind to DNA at reoxygenation.

STAT3 DNA-binding activity (fig. 31E) unexpectedly did not vary during reoxygenation as illustrated by densitometry (fig. 31F). Ventricles from hearts treated with H_2O_2 were used as a positive control and showed that STAT3 DNA-binding activity was increased (+33% in hearts treated with H_2O_2); ensuring that the technique was sensitive enough to detect any change in STAT3 DNA-binding activity (fig. 31G). A negative control of DNA-binding performed by adding an antibody against total STAT3 or an unlabelled probe to the samples showed that the upper band corresponding to STAT3 disappeared under these two conditions (fig. 31G).

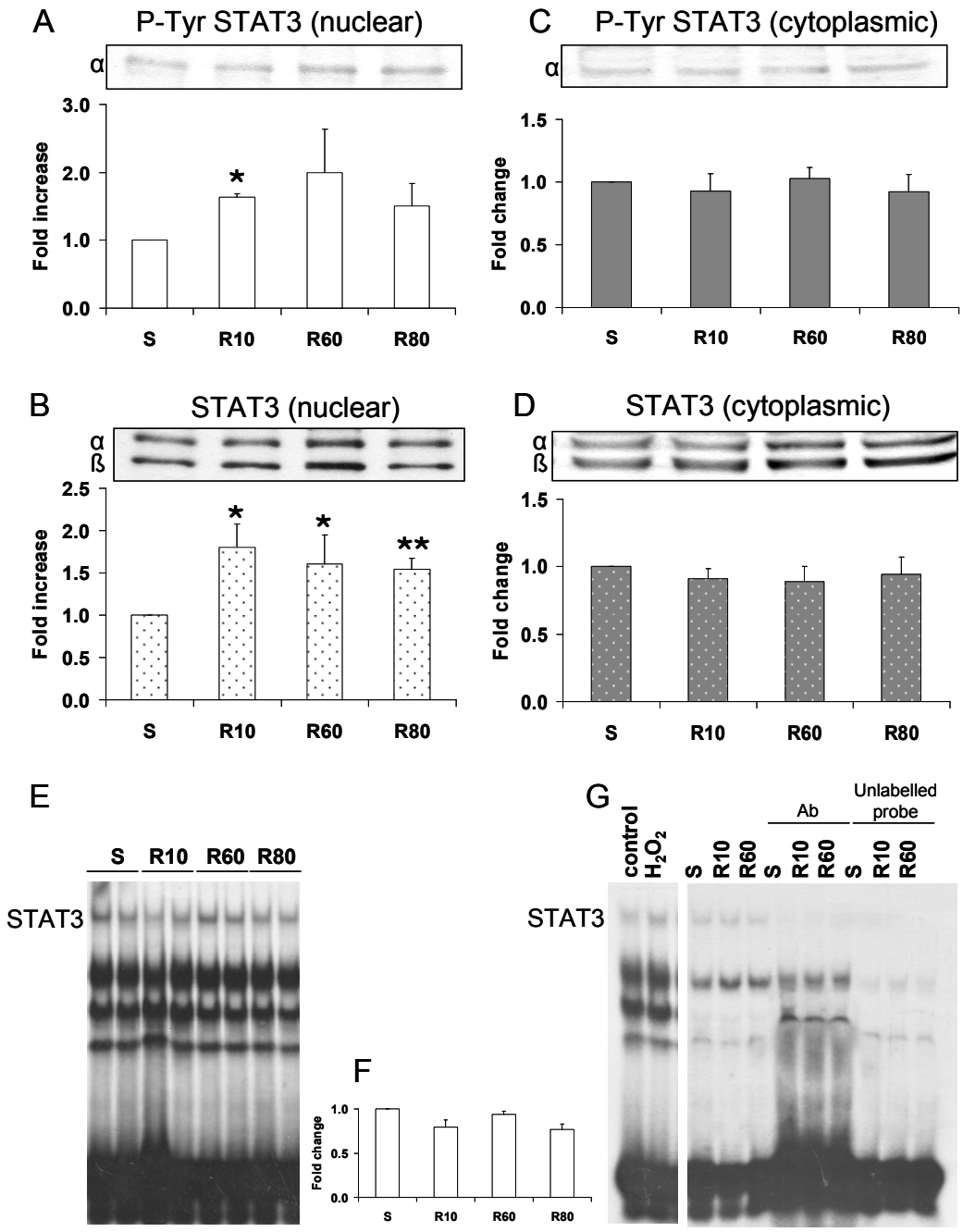

*Fig. 31: At reoxygenation STAT3 translocated into the nuclear compartment without DNA-binding activity. Representative immunoblots at S, R10, R60 and R80 and densitometric analysis of A) P-Tyr STAT3α and B) STAT3α and STAT3β in enriched nuclear fraction; C) P-Tyr STAT3α and D) STAT3α and STAT3β in cytoplasmic fraction. E) Representative EMSA of STAT3 at S, R10, R60 and R80 (duplicates) and F) densitometric analysis of STAT3. Data are expressed as fold change relative to S. G) Negative control with antibody (Ab) against STAT3 and unlabelled probe. *: $p<0.05$, **: $p<0.01$ vs S. N=4-13 determinations for A to D and n=3-6 determinations for F.*

To support our unexpected finding that STAT3 was translocated into the nucleus without binding to DNA we checked the level of mRNA expression of three known STAT3 specific target genes in the context of the response to I-R, i.e. inducible NO synthase (iNOS), manganese superoxide dismutase (MnSOD) and cyclooxygenase-2 (Cox-2). We found that the level of mRNA expression of iNOS (fig. 32A) and MnSOD (fig. 32B) was not increased even at R80. The level of mRNA expression of Cox-2 was increased at R60 and R80 but it was also the case in the time-matched normoxic controls indicating that the culture conditions could alter mRNA expression of Cox-2 relative to preanoxia (fig. 32C).

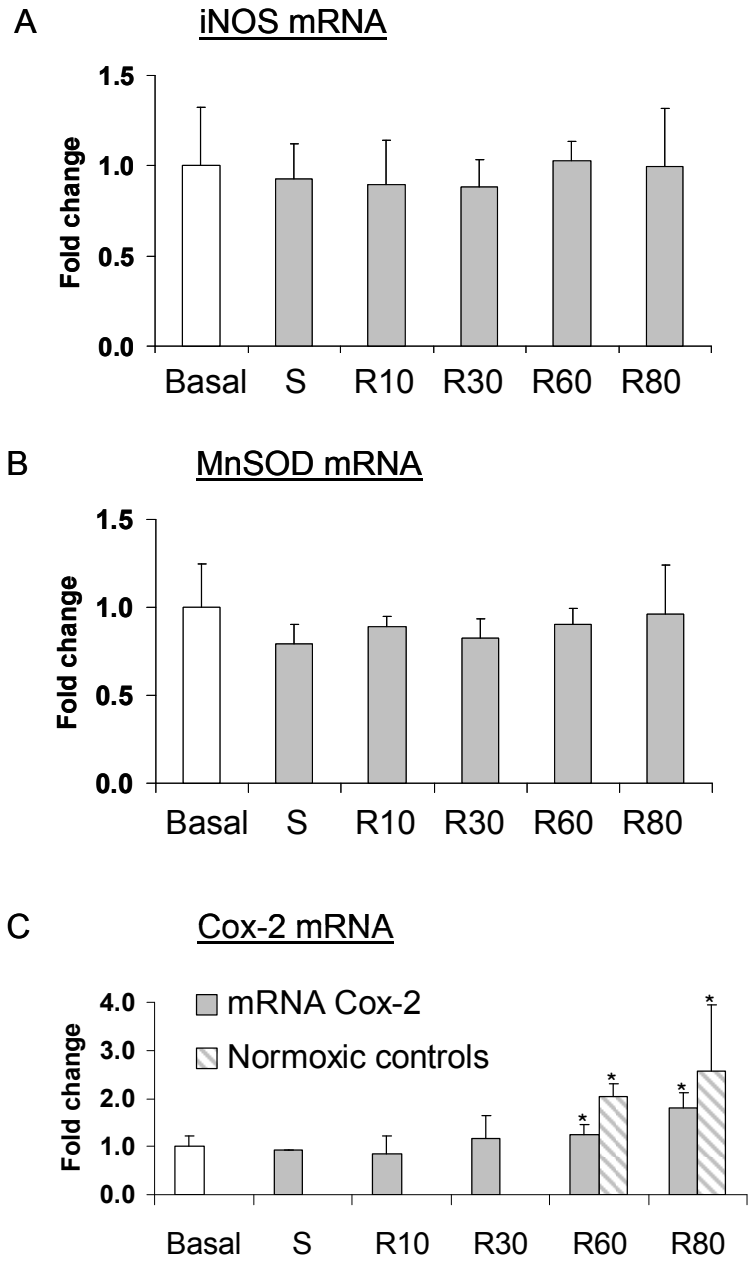

*Fig. 32: The level of mRNA expression of STAT3 target genes was not increased during the 80min of reoxygenation. Level of mRNA expression in ventricle freshly isolated (basal), at S, R10, R30, R60 and R80 of A) inducible NO synthase (iNOS), B) manganese superoxide dismutase (MnSOD) and C) cyclooxygenase-2 (Cox-2). In C) grey columns represent Cox-2 mRNA during anoxia-reoxygenation and hatched columns Cox-2 mRNA in normoxic controls. *: $p<0.05$ vs S. N=3-4 determinations.*

III.4 Discussion

Our data show that in the embryonic heart ventricle tyrosine rather than serine site was phosphorylated by reoxygenation, suggesting that STAT3 activation by other kinases like ERK 1/2, p38MAPK (Kovarik et al., 2001) or mTOR (Yonezawa et al., 2004) can be ruled out under our conditions since these pathways are known to phosphorylate preferentially serine. More specifically, although p38MAPK and ERK are activated at R10 and R30 respectively (Gardier et al., 2010b), they did not phosphorylate STAT3 on serine. Our present finding that STAT3α tyrosine phosphorylation was ROS-dependent at R10 and R60 is consistent with studies performed in neonatal cardiomyocytes (Lu et al., 2008b) and adult myocardium (McCormick et al., 2006). However, at R10 there is a strong burst of ROS whereas at R60 ROS production returns to its preanoxic level (Sarre et al., 2005) suggesting that the ROS-dependent mechanisms of STAT3 activation are different during the early (R10) and late (R60) phases of reoxygenation. This phenomenon could be partly due to chemical differences between radical species produced at R10 and R60 (i.e. superoxide anion $O_2^{\bullet-}$ being predominantly generated during early reoxygenation). In atria, STAT3α was tyrosine phosphorylated during reoxygenation like in the ventricle, and also returned to preanoxic level at the end of the reoxygenation, even if it was slightly earlier than in ventricle. Even if STAT3 phosphorylation in the outflow tract was not determined at all time points, the general pattern appears to be the same as in the ventricle, namely an increase during reoxygenation and a return to basal level at R80. Thus, in the embryonic heart STAT3 was not phosphorylated in a region-specific manner during anoxia-reoxygenation like it is the case for p38MAPK, ERK and JNK (Gardier et al., 2010b) but displayed the same temporal profile of phosphorylation in the three cardiac regions.

It has been previously shown that the embryonic heart fully recovers at R60 after anoxia (Sarre et al., 2005, Sarre et al., 2006) but the signalling pathways underlying the mechanisms of recovery remain relatively unexplored. Activated STAT3 is known to exert its late cardioprotective action (antiapoptotic properties (Lu et al., 2008b)) mainly via alteration of transcription of target genes principally induced by pre- or postconditioning. However, the short-term consequences of STAT3 activation on the electrical and mechanical activities have never been investigated in the developing, neonatal or adult failing heart. Here we provided for the first time data about the involvement of STAT3 in the functional response to a transient hypoxic stress. At R30, inhibition of JAK2/STAT3 gave rise to the highest variability of atrial rate and RR interval, suggesting that activation of STAT3 is involved in recovery of atrial and ventricular rhythm. As there are no extrinsic innervation at the embryonic stage investigated and no neurohumoral influence in the culture chamber, the fluctuations of rhythm (dysrhythmias) originated exclusively at the level of the pacemaker tissues, independently of the physiological spontaneous oscillations of heart rate reported previously (Sarre et al., 2006). These observations and the fact that arrhythmias persisted throughout reoxygenation in 30% of the AG490-treated hearts, strongly suggest that activated STAT3 can protect cardiac automaticity by interacting with pacemaking mechanisms, especially under pathological conditions. It has been previously shown that subtle modulations of L-type calcium, K_{ATP} and HCN channels can improve postanoxic recovery of the embryonic heart (Sarre et al., 2005, Bruchez et al., 2008, Sarre et al., 2010). It is conceivable that the JAK2/STAT3 pathway may directly or indirectly control finely these ion channels affecting membrane potential, and contributing to protect pacemaker activity under adverse conditions. However, the present findings show clearly that activated STAT3 had no dromo-, ino- and lusitropic effects in the anoxic-reoxygenated embryonic heart since atrioventricular (PR) and intraventricular (QRS widening) conduction, ventricular

contractility (shortening) and relaxation (ratio contraction/relaxation velocity) as well as E-C coupling (EMDv) were not affected by STAT3 inhibition. Additionally, the types of arrhythmias during anoxia and reoxygenation previously documented (Sarre et al., 2006) were similar in untreated and AG490-treated hearts. It should be noticed that the isolated embryonic heart displays noticeable interindividual variations of the functional parameters and ECGs performed in similar conditions can also modestly differ in morphology from one experiment to another (Sarre et al., 2005). Such variations could be due to slight interindividual differences in developmental stage, three-dimensional geometry of the hearts in the chamber and vicinity of the recording electrodes.

In addition to its direct or indirect involvement in heart function, the transcription factor STAT3 should also control expression of specific target genes. At R10 activation of STAT3 observed in homogenate of ventricle principally reflected what took place in the nuclear compartment since only the nuclear STAT3α tyrosine phosphorylation increased significantly. At R60 nuclear P-Tyr STAT3α was above the preanoxic level and the rise in nuclear STAT3 observed at R10 persisted throughout reoxygenation suggesting that translocated STAT3 remained in the nuclear compartment. Furthermore, the fact that mRNA level of specific STAT3 target genes including iNOS, MnSOD and Cox-2 known to be involved in cardioprotection (Negoro et al., 2001, Bolli et al., 2003, Sarre et al., 2005) remained stable throughout reoxygenation corroborates the finding that translocated STAT3 had no detectable transcriptional activity. Additionally, the level of STAT3 phosphorylation on serine remained constant throughout all experimental protocols (~2h), STAT3 requiring phosphorylation on both sites (tyrosine and serine) to be maximally active in the assembly of active transcription complexes (Wen et al., 1995b).

IV. Interaction of the JAK2/STAT3 and RISK pathways in the embryonic heart submitted to anoxia-reoxygenation

As activated STAT3 was not linked to DNA, interaction with other signalling pathways could not be ruled out, in particular with the RISK pathway. We first checked if proteins of this pathway were modulated by anoxia-reoxygenation.

IV.1 Phosphorylation of PI3K, Akt, GSK3ß, GS and ERK2 in the ventricle.

The temporal pattern of phosphorylation varied from one component of the RISK pathway to another. PI3K and Akt phosphorylation peaked at R10 (fig. 33A, 33B) while GSK3β and GS phosphorylation increased at R10 and R60 (fig. 33C, 33D). Relative to other proteins, ERK2 phosphorylation was delayed at R60 (fig. 33E).

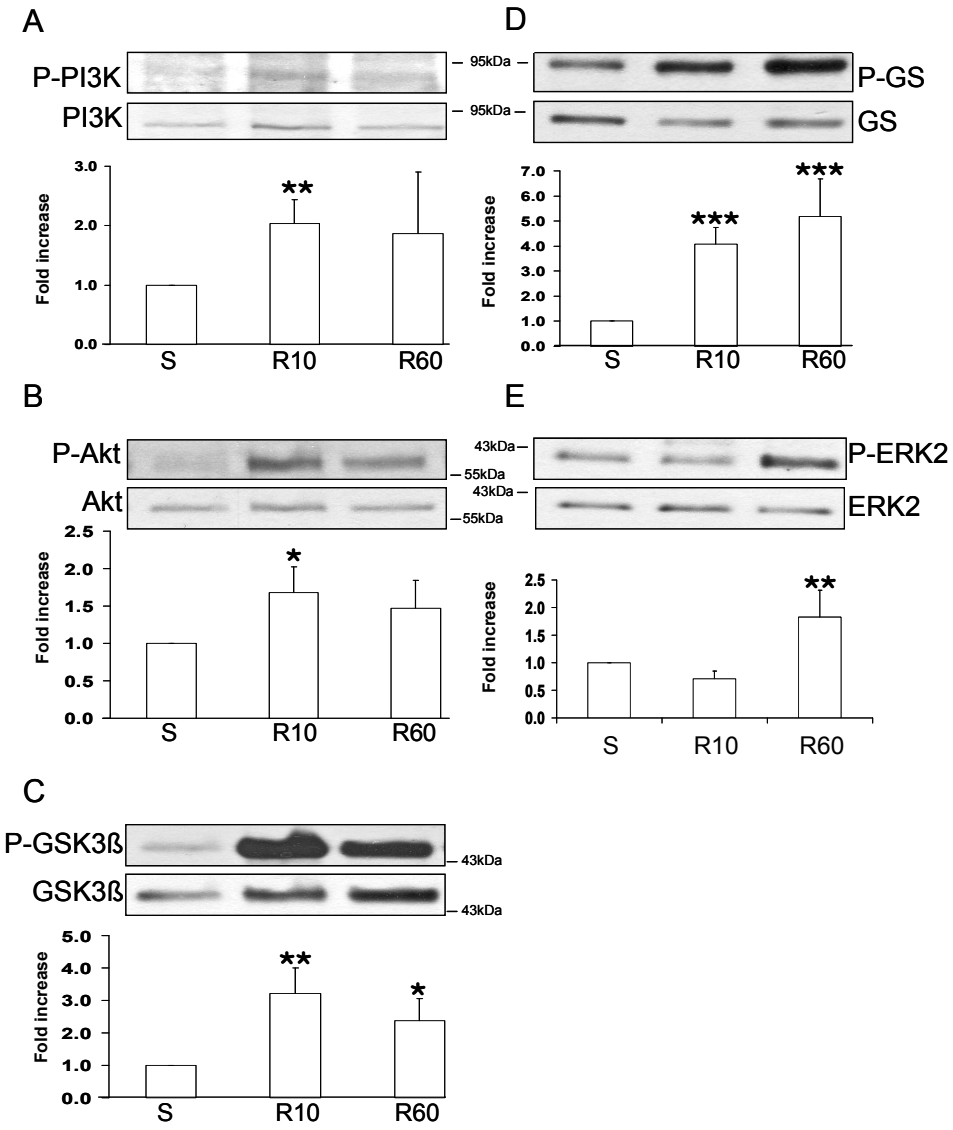

*Fig. 33: Profile of PI3K, Akt, GSK3ß, GS and ERK2 activation in the ventricle during post-anoxic reoxygenation. Representative immunoblots and densitometry of phosphorylated PI3K, Akt, GSK3ß, GS and ERK2 (A, B, C, D and E, respectively) normalized to total protein in homogenates at S, R10 and R60. Data are expressed as fold increase relative to S. *: p<0.05, **: p<0.01, ***: p<0.001 vs S. N=5-12 determinations.*

IV.2 Crosstalk between STAT3 and RISK pathways in nuclear and cytoplasmic compartments in the ventricle.

Using histone H1 and GAPDH as specific markers of enriched nuclear and cytoplasmic fractions respectively, we found that phosphorylated and total forms of PI3K, Akt, GS and

ERK2 were restricted to cytoplasm. Basal level of phosphorylated GSK3ß was markedly higher in the nuclear fraction than in the cytoplasmic fraction whereas the total form of GSK3ß was comparable in the two compartments (fig. 34).

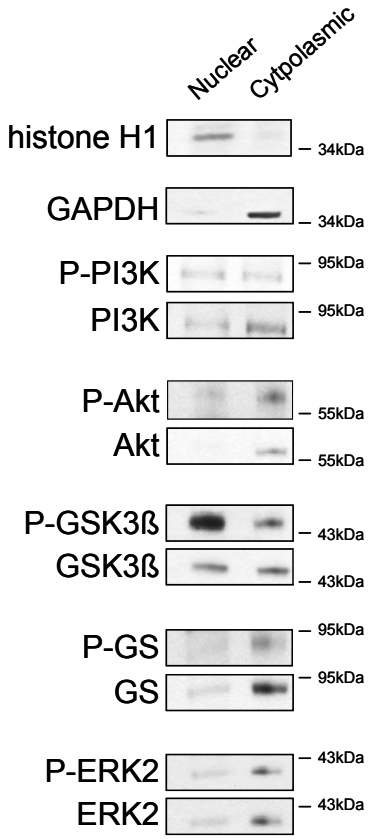

Figure 34: Distribution and level of phosphorylation of PI3K, Akt, GSK3ß, GS and ERK2 in nuclear and cytoplasmic fractions of the ventricle. Representative immunoblots of basal content of phosphorylated and total forms of PI3K, Akt, GSK3ß, GS and ERK2 in enriched nuclear and cytoplasmic fractions of the ventricle. Histone H1 was used as a nuclear marker and GAPDH as a cytoplasmic marker (upper panels).

The possibility of interaction between RISK and JAK2/STAT3 pathways was assessed pharmacologically by blocking the JAK2/STAT3 pathway with AG490. As expected, AG490 significantly decreased P-Tyr STAT3α and P-Akt at R10 and R60 as well (fig. 35A, 35C). AG490 reduced GS (fig. 35D) and ERK2 (fig. 35E) phosphorylation at R10 only with no effect on PI3K phosphorylation (fig. 35B).

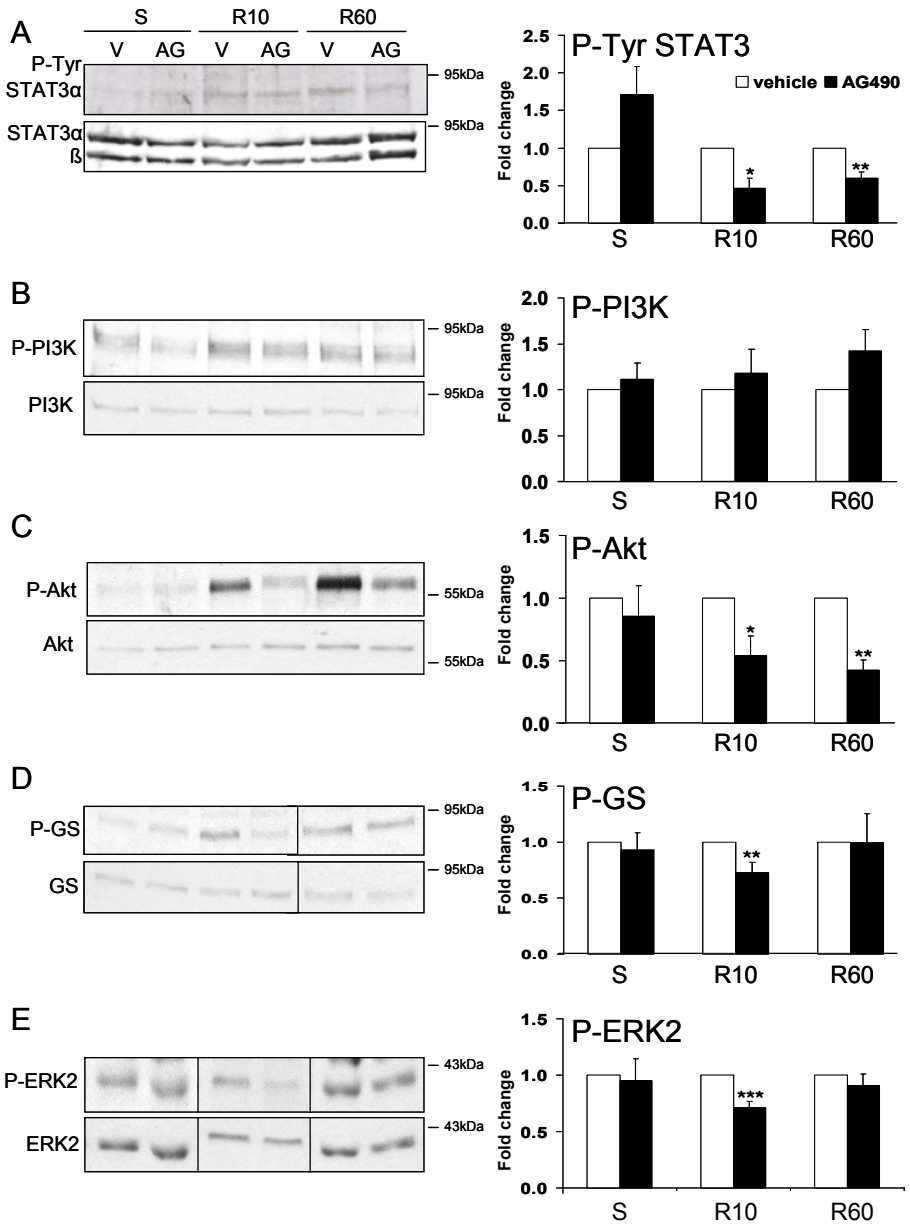

*Fig. 35: JAK2/STAT3 inhibition by AG490 significantly reduced reoxygenation-induced phosphorylation of Akt, GS and ERK2. On left panels, immunoblots of phosphorylated Tyr STAT3α, PI3K, Akt, GS and ERK2 (A, B, C, D, and E, respectively) in vehicle (V) or in 10μM AG490 (AG) at S, R10 and R60 in homogenates. On right panels, densitometric analysis of phosphorylated proteins normalized to total protein and to vehicle (open columns) in 10μM AG490 (black columns,) at S, R10 and R60. Data are expressed relative to vehicle. *: p<0.05, **: p<0.01, ***: p<0.001 vs vehicle. N=4-11 determinations.*

GSK3β being the only protein of the RISK pathway present in the nuclear compartment, together with STAT3, we checked separately the effect of STAT3 inhibition on the

phosphorylation level of nuclear GSK3β. Nuclear and cytoplasmic P-GSK3β significantly increased between S and R10 while GSK3β did not vary (fig. 36A). GSK3β phosphorylation was decreased by AG490 in the nuclear fraction at R10 (fig. 36B) but remained unchanged in the cytoplasmic fraction (fig. 36C).

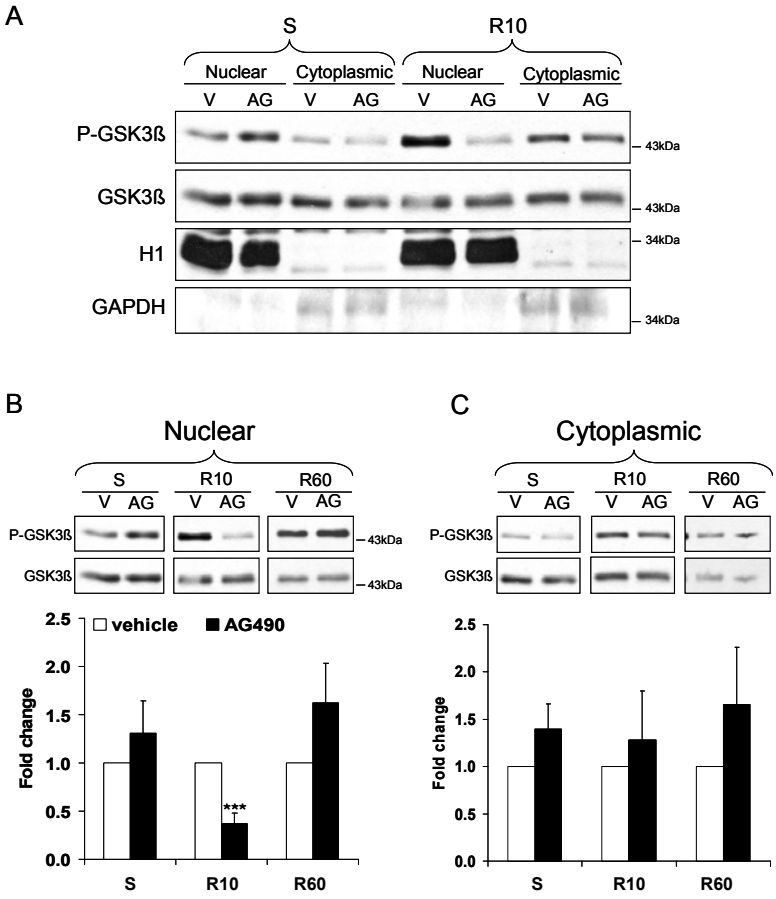

*Fig. 36: Reoxygenation-induced phosphorylation/inhibition of GSKβ in the nuclear compartment depended on JAK2/STAT3 activation. A) Representative immunoblots of P-GSK3β and GSK3β in enriched nuclear and cytoplasmic fractions in vehicle (V) or in 10μM AG490 (AG) at S and R10. Histone H1 was used as a nuclear marker and GAPDH as a cytoplasmic marker. B) Representative immunoblots (upper panels) and densitometric analysis (lower panels) of phosphorylated GSK3β in enriched nuclear fraction and C) in cytoplasmic fraction in vehicle (V, open columns) and in AG490 (AG, black columns) at S, R10 and R60. Data are expressed as fold change relative to vehicle. ***: p<0.001 vs vehicle. N=3-6 determinations.*

The possible effect of PI3K/Akt on STAT3 phosphorylation was evaluated pharmacologically using LY-294002, a common PI3K/Akt pathway inhibitor. As expected, LY-294002 decreased P-Akt by 55% at R10 (fig. 37A) but did not affect P-Tyr STAT3α (fig. 37B).

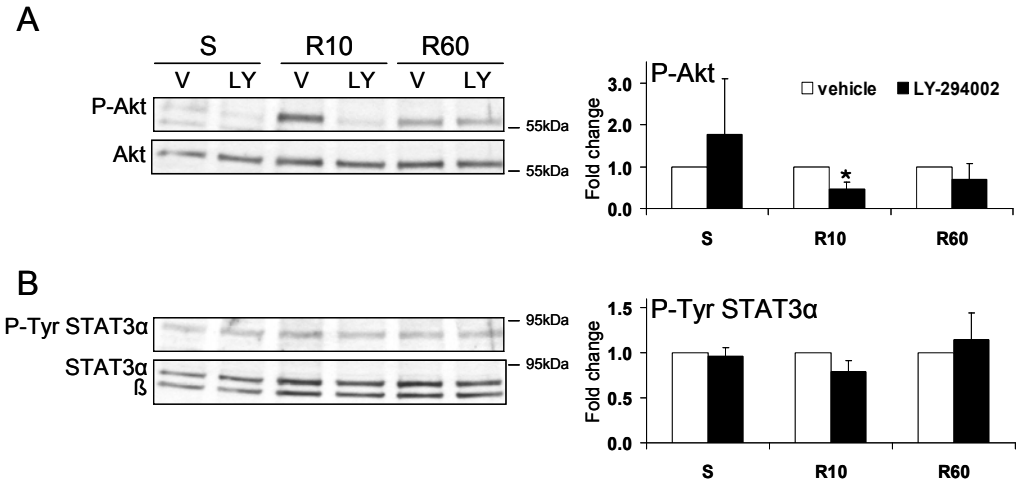

*Fig. 37: PI3K/Akt inhibition by LY-294002 did not affect reoxygenation-induced phosphorylation of STAT3. On left panels, immunoblots of phosphorylated and total forms of A) Akt and B) STAT3 in vehicle (V) or in 10μM LY-294002 (LY) at S, R10 and R60 in homogenates. On right panels, densitometric analysis of phosphorylated A) Akt and B) Tyr STAT3α normalized to total protein in 10μM LY-294002 (black columns) and expressed relative to vehicle (open columns) at S, R10 and R60 in homogenates. *p<0.05 vs vehicle. N=3 determinations.*

IV.3 Discussion

Unexpectedly, we found that activated STAT3 did not bind to DNA in response to a transient hypoxia but could interact with other signalling pathways. We focused our attention on the RISK pathway which is able to mediate cardioprotection at the time of myocardial reperfusion (Yellon and Baxter, 1999). It is still unknown whether the survival kinases of the RISK pathway are activated by anoxia-reoxygenation as opposed to ischemia-reperfusion. The profile of phosphorylation shows that in the ventricle, PI3K, Akt and ERK2 were differently modulated during the early (R10) and late (R60) phases of reoxygenation.

Phosphorylation of PI3K, Akt and GSK3β was maximal at R10 whereas activation of ERK2 was delayed at R60 as previously described (Gardier et al., 2010b). Regarding ERK, as previously shown, only the p42 isoform (ERK2) is detectable in the embryonic and adult chicken heart, in contrast to neonatal and adult murine heart. Furthermore, GS which is a downstream target of GSK3β, was strongly phosphorylated/inhibited from R10 onward, despite the fact that the phosphorylated form of GSK3β was inactive. Other kinases such as PKA, AMPK, CK1 or CK2 (Marks et al., 2009) may phosphorylate/inhibit GS, reducing glycogen storage which is known to be specially important and to play a cardioprotective role in the embryonic myocardium (Romano et al., 2001).

In the embryonic ventricle, only STAT3 and GSK3β were present both in the nuclear and cytoplasmic fractions. PI3K, Akt, GS and ERK2 were restricted to the cytoplasm in the developing myocardium, whereas in neonatal and adult cardiomyocytes PI3K (Rubio et al., 2009), Akt (Miyamoto et al., 2009) and ERK 1/2 (Pantos et al., 2007) are also detected in the nuclear compartment. These observations suggest that the cytoplasm-nucleus shuttling of proteins, including transcription factors, may well depend on the level of differentiation and maturation of the cardiomyocytes. The inhibition of the JAK2/STAT3 pathway by AG490 significantly decreased the reoxygenation-induced STAT3 phosphorylation as expected, which validates this pharmacological approach to interfere rapidly with the JAK2/STAT3 pathway. The AG490-mediated reduction of phosphorylation of Akt, ERK2 and nuclear GSK3β indicates clearly that activation of the JAK2/STAT3 pathway can modulate RISK components upon reoxygenation (R10) both in the cytoplasmic (Akt and ERK2) and nuclear (GSK3β) compartments. We checked the presence of ERK2 in the nuclear compartment in basal conditions whereas ERK 1/2 translocates into the nucleus only when it is phosphorylated. At R10 we found an interaction between ERK2 and STAT3 in homogenate but did not assess specifically the effect of AG490 on ERK2 phosphorylation in nucleus and

cytoplasm because ERK2 was not phosphorylated at R10 and consequently not present in the nucleus. The transient inhibitory effect of STAT3 on nuclear GSK3β in the first 10 minutes of reoxygenation may be determinant as GSK3β is known to regulate many transcription factors and modulate cellular functions (Meares and Jope, 2007). In H_2O_2-treated neonatal (Lu et al., 2008b) and ischemic-reperfused adult (Gross et al., 2006, Fuglesteg et al., 2008, Goodman et al., 2008) cardiomyocytes STAT3 inhibition reduces also Akt and GSK3β phosphorylation but the intracellular localization is not established. However, our results show that a preferential and predominant interaction between JAK2/STAT3 pathway and Akt persists throughout reoxygenation since AG490 leads to strong inactivation of Akt up to R60, which is not the case for GSK3ß, ERK2 and GS. Whatever the time point investigated, reoxygenation-induced activation of PI3K was unrelated with JAK2/STAT3 pathway in the embryonic heart like in an ischemic-reperfused heart model (Goodman et al., 2008), although such a dissociation remains controversial (Suleman et al., 2008a). The mechanisms by which activation of JAK2/STAT3 pathway phosphorylates GS at R10 and might transiently reduce glycogen synthesis remain to be elucidated. At R10, it appears that there is no dual interaction between PI3K/Akt and JAK2/STAT3 pathways in the embryonic heart. Such an interaction remains controversial in neonatal and adult cardiomyocytes and depends on the type of pathological situation such as ischemic (Suleman et al., 2008b) and pharmacological pre- (Gross et al., 2006, Suleman et al., 2008b) and postconditioning (Goodman et al., 2008) and oxidant stress (Lu et al., 2008a). As STAT3 activation improved recovery of heart rhythm during reoxygenation, a crosstalk between JAK2/STAT3 and RISK pathways may directly or indirectly take part in this protection.

V. Tolerance of the embryonic heart to exogenous H_2O_2 and activation of the JAK2/STAT3 pathway

V.1 Effect of H_2O_2 on heart function.

In response to a transient lack of oxygen, the embryo shows reversible functional disorders (Sedmera et al., 2002) associated with overproduction of ROS/RNS (Sarre et al., 2005) and in neonatal and adult heart the JAK2/STAT3 pathway is stimulated in response to oxidant stress (Modesti et al., 2005, Lu et al., 2008b). To what extent the response of the embryonic heart to an exogenous oxidant stress (H_2O_2) is different from the response to a reoxygenation-induced endogenous stress is still unknown.

We established the dose-response curve in the three cardiac regions to H_2O_2. At concentrations $\leq$500µM of H_2O_2, cardiac activity was not significantly altered but was markedly affected at 1mM. Indeed, spontaneous atrial activity was lost in 45% of the hearts and atrioventricular propagation persisted in only 34% (fig. 38A). The mean atrial rate in hearts submitted to 1mM H_2O_2 rapidly decreased after 15min (-25%) and this negative chronotropic effect continued onward (fig. 38B).

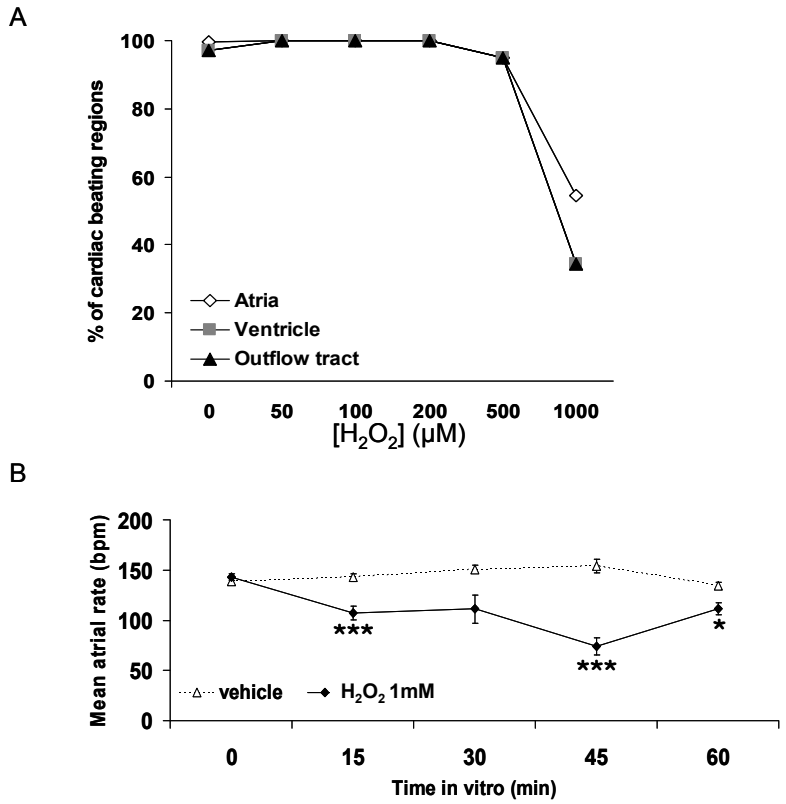

*Fig. 38: Atria was the most resistant to H_2O_2. A) Percentage of beating atria (open diamonds), ventricle (grey squares) and outflow tract (black triangles) after 1h exposure to H_2O_2 at concentrations ranging between 50 and 1000µM. N=20-75 hearts. B) Mean atrial rate in vehicle (open triangles) or in H_2O_2 1mM (black diamonds). *: p<0.05, ***: p<0.001 vs vehicle. N=10-76 hearts.*

V.2 STAT3 phosphorylation in atria, ventricle and outflow tract after exposure to H_2O_2.

In order to determine to what extent STAT3 is stimulated by H_2O_2, as in adult myocardium, hearts were exposed to concentrations ranging from 50 to 1000µM.

Whatever the cardiac region examined P-Tyr STAT3α did not significantly increase after 1h of exposure to H_2O_2 at concentrations ≤500µM (fig. 39A, 39B, 39C), except at 200µM in the ventricle (fig. 39B). It should be noticed that there was a large variability in these experiments.

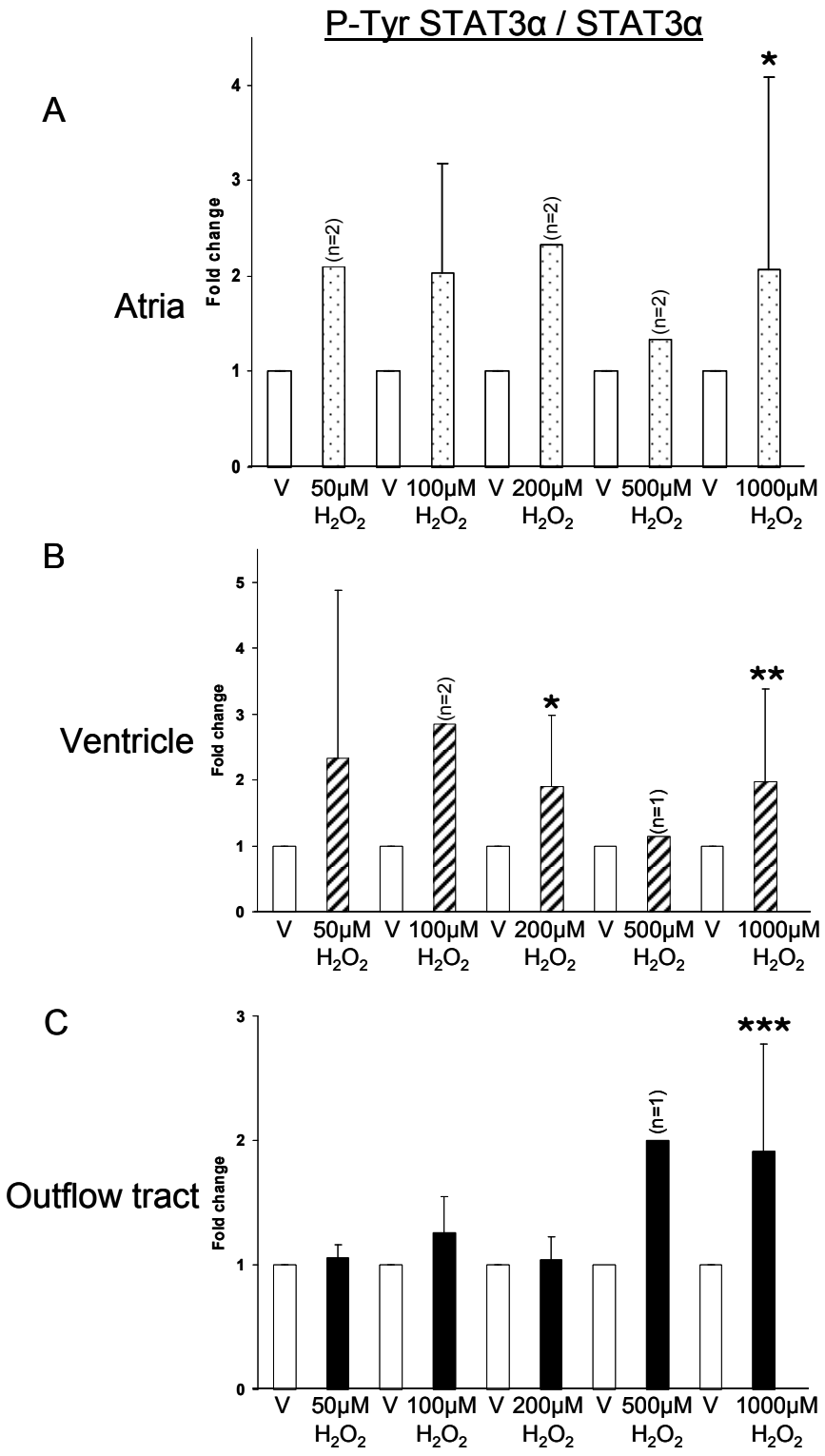

*Fig. 39: STAT3 phosphorylation was increased by severe exogenous oxidant stress. Densitometric analysis of P-Tyr STAT3α normalized to STAT3α in vehicle (V, open columns) or in H_2O_2 at 50, 100, 200, 500 and 1000μM (dotted, hatched and black columns) after 1h in A) atria, B) ventricle and C) ouftlow tract. Data are expressed as fold change relative to vehicle. Mean ± SD. *: p<0.05, **: p<0.01, ***: p<0.001 vs vehicle. N=1-14 determinations.*

By contrast, at 1mM of H_2O_2 P-Tyr STAT3α was increased in the three cardiac regions studied (fig. 40A, 40B).

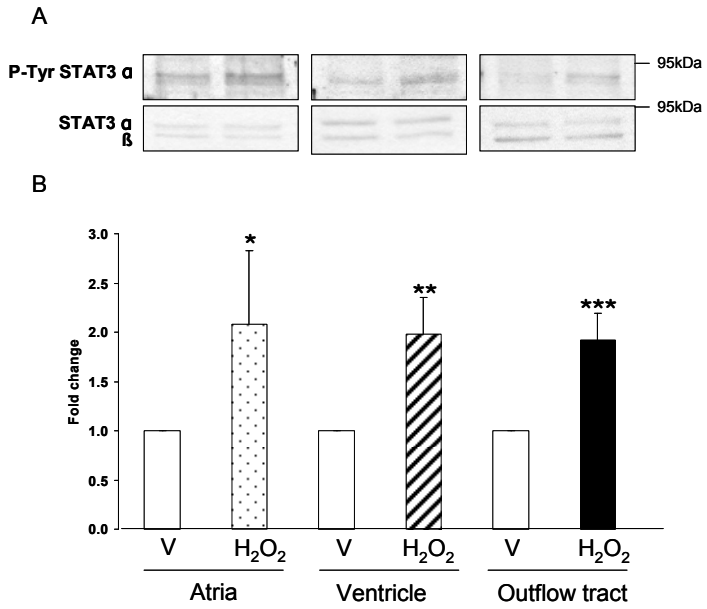

*Fig. 40: STAT3α phosphorylation was increased in all the parts of the embryonic heart exposed to H_2O_2. A) Representative immunoblots of P-Tyr STAT3α, STAT3α and STAT3β and B) densitometric analysis of P-Tyr STAT3α normalized to STAT3α in vehicle (V, open columns) or in 1mM H_2O_2 (dotted, hatched and black columns) after 1h in atria, ventricle and outflow tract respectively. Data are expressed as fold change relative to vehicle. *: p<0.05, **: p<0.01, ***: p<0.001 vs vehicle. N=7-14 determinations.*

More specifically in the ventricle, a time course showed that P-Tyr STAT3α was increased only after 1h of exposure to 1mM of H_2O_2 (fig. 41A, 41B).

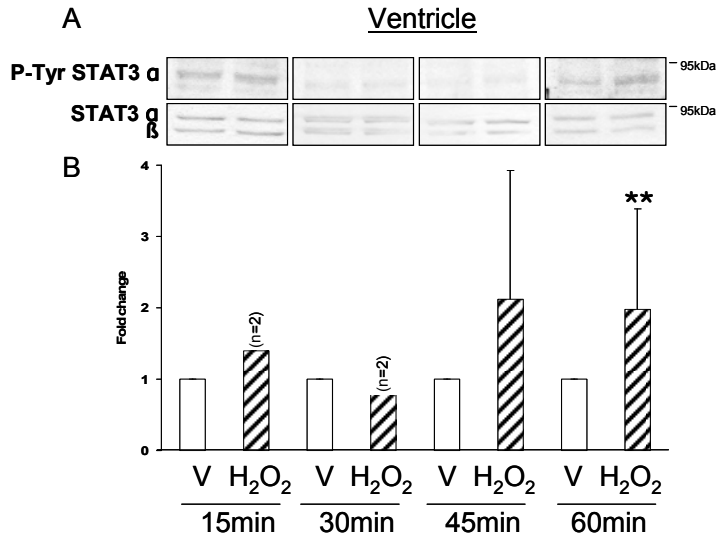

*Fig. 41: STAT3 phosphorylation was increased in ventricle only after 1h exposure to H_2O_2. A) Representative immunoblots of P-Tyr STAT3α, STAT3α and STAT3β and B) densitometric analysis of P-Tyr STAT3α normalized to STAT3α in vehicle (V, open columns) or in H_2O_2 1mM (hatched columns) after 15, 30, 45 and 60min. Data are expressed as fold change relative to vehicle. Mean ± SD. **: p<0.01 vs vehicle. N=2-14 determinations.*

V.3 STAT3 transcriptional activity and expression of specific target genes after exposure to H_2O_2 in the ventricle.

H_2O_2 inducing phosphorylation of STAT3, we wanted to know whether STAT3 transcriptional activity could be also modified.

STAT3 DNA-binding activity detected by EMSA (fig. 42A) was significantly increased after 1h exposure to 1mM of H_2O_2 as illustrated by densitometry (fig. 42B) but the level of mRNA expression of iNOS (fig. 43A), MnSOD (fig. 43B) and Cox-2 (fig. 43C) was not increased.

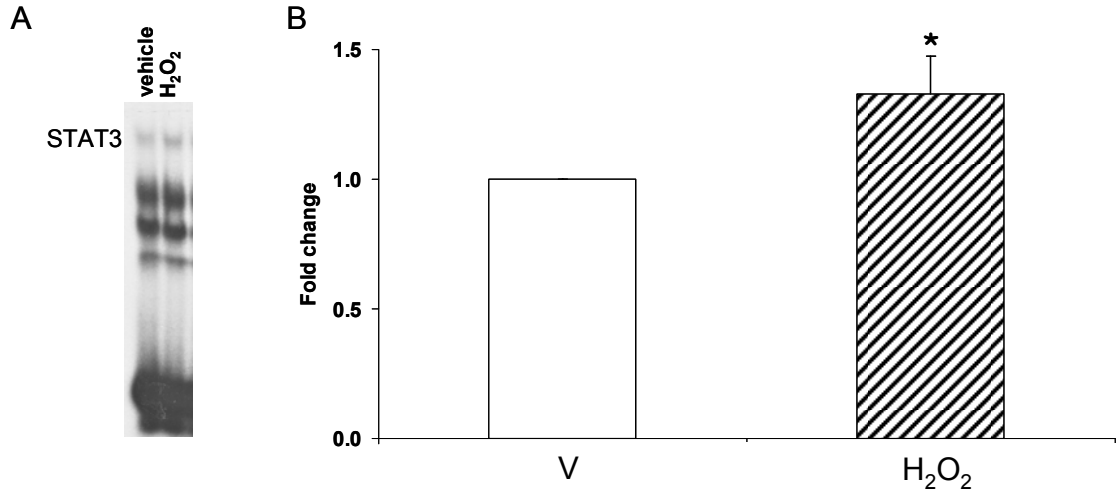

*Fig. 42: STAT3 DNA-binding activity was increased by H_2O_2. A) Representative EMSA of STAT3 and B) densitometric analysis of STAT3 after 1h in vehicle (open column) or in 1mM H_2O_2 (hatched column) in ventricle. Data are expressed as fold change relative to vehicle. *: $p<0.05$ vs S. N=4 determinations.*

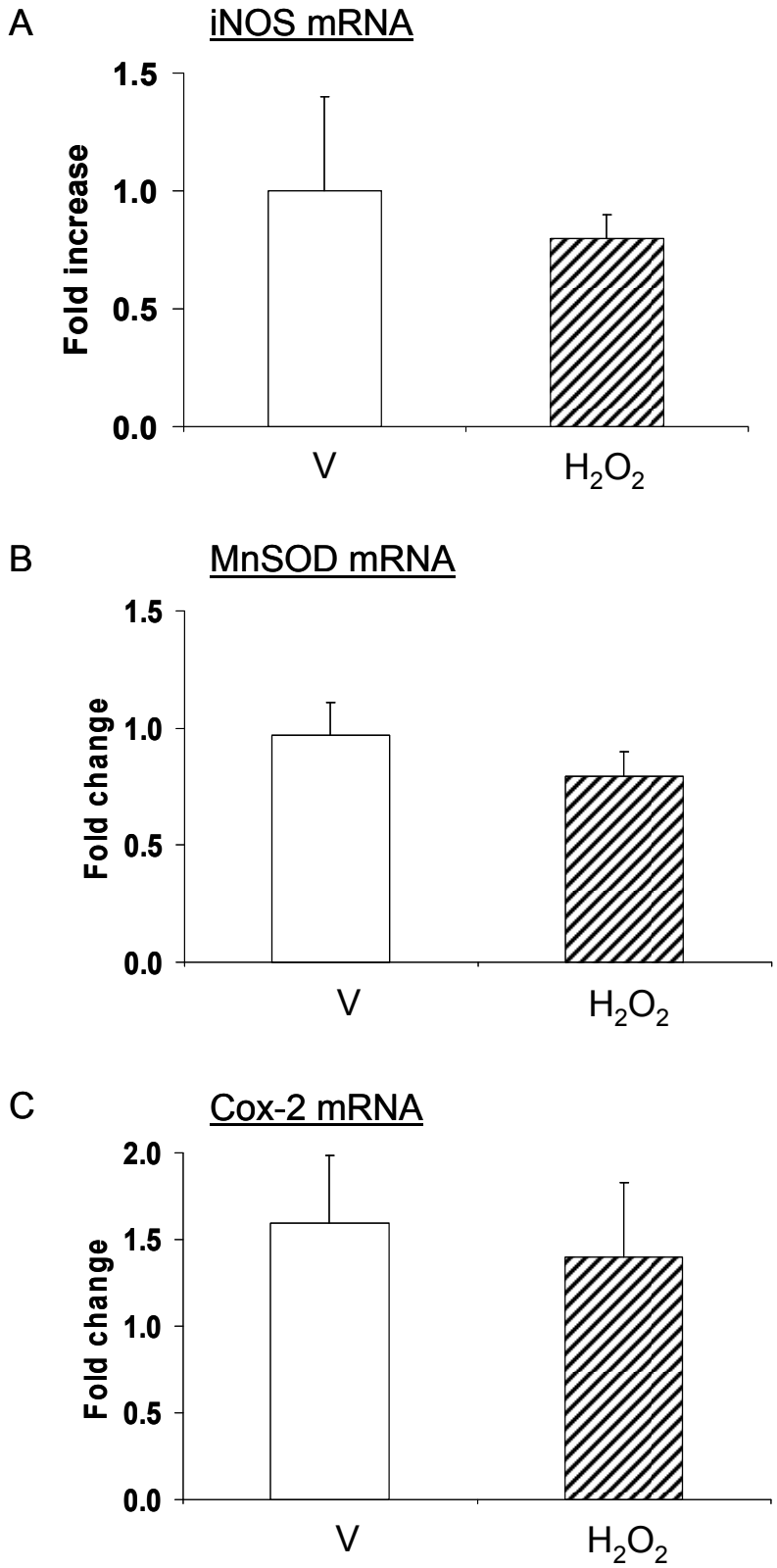

Fig. 43: The level of mRNA expression of STAT3 target genes was not increased by H_2O_2. Level of mRNA expression in ventricle of A) inducible NO synthase (iNOS), B) manganese superoxide dismutase (MnSOD) and C) cyclooxygenase-2 (Cox-2) in vehicle (V, open columns) or in 1mM H_2O_2 (hatched columns) after 1h. Data are expressed as fold change relative to vehicle. N=3-4 determinations.

V.4 Discussion

It has been shown that in neonatal and adult heart the JAK2/STAT3 pathway is activated in response to oxidant stress (Ang II-mediated or H_2O_2) (Modesti et al., 2005, Lu et al., 2008b). Nevertheless whether the response of the embryonic heart to exogenous oxidant stress (H_2O_2) resembles the response to reoxygenation-induced oxyradicals is still undertermined.

Surprisingly, an especially severe oxidant stress was necessary to significantly affect embryonic heart function since H_2O_2 at the highest concentration (1mM) decreased atrial pacemaker activity and impaired atrioventricular conduction, whereas lower concentrations had no detectable effect. By comparison, in adult rats, 100µM of H_2O_2 is sufficient to decrease contractile function in a time-dependent manner (Lakomkin et al., 2007). In neonatal cardiac myocytes only 5min of exposure to H_2O_2 at 50µM decreased contraction amplitude (Sabri et al., 1998). Our observations unexpectedly suggest that the embryonic heart is more resistant to an oxidant stress than newborn or adult hearts. Furthermore, atria appears to be more resistant than the ventricle and the outflow tract to a potentially deleterious oxidant stress. It is conceivable that the high resistance of atrial activity to oxyradicals (like H_2O_2) could be related to the high basal level of STAT3 phosphorylation in this area. At the same developmental stage, a comparable differential resistance to H_2O_2 (assessed by tissue viability and caspase-3/7 activity) between atria, ventricle and outflow tract has been observed at nanomolar concentrations (Fisher, 2007). The mean atrial rate was decreased by an exogenous oxidant stress from 15min whereas it was increased during the first 10 to 12min of reoxygenation reaching a maximum (slight tachycardia) before returning to its preanoxic value (Sarre, 2006).

Oxidants, such as H_2O_2, are known to activate intracellular signal transduction pathways (Fruehauf and Meyskens, 2007). STAT3 tyrosine phosphorylation increased in response to a

severe oxidant stress (1h H_2O_2 1mM) in the three investigated cardiac regions in our model. By contrast, in neonatal ventricular myocytes only 70µM of H_2O_2 are sufficient to increase STAT3 tyrosine phosphorylation (Lu et al., 2008b). Taken together our data and these observations indicate that the embryonic heart is less sensitive than neonatal or adult hearts to oxyradicals (as well as H_2O_2). More specifically in the ventricle, STAT3 tyrosine phosphorylation was increased only after 1h of exposure to H_2O_2 whereas in neonatal cardiac fibroblasts, it reaches a peak after only 15min of exposure and returns to a near-basal level by 1h (Wang et al., 2002). These data suggest that in the embryonic myocardium STAT3 activation by a severe oxidant stress is delayed relative to newborn rats or that this activation is maintained during time. We can also hypothesize that the increase observed in STAT3 tyrosine phosphorylation is the result of an inhibition of tyrosine phosphatases, known to be extremely sensitive to oxidative stress. As expected, STAT3 DNA-binding activity was increased after 1h exposure to H_2O_2. Same results are found in lymphocytes, where the DNA-binding increases after 30min of exposure to H_2O_2 (Carballo et al., 1999). By contrast, in neonatal cardiac fibroblasts, even if STAT3 is phosphorylated, the DNA-binding is not altered even after 2h of exposure to H_2O_2 (Wang et al., 2002). These differences might be explained by the fact that contrary to the adult, the ventricle of the 4-day-old embryonic chick heart is mostly composed of proliferating and differentiating cardiomyocytes and mesenchymal cells with only few endothelial and epicardial cells and no differentiated fibroblasts (Sedmera et al., 2000). The fact that mRNA level of specific STAT3 target genes iNOS, MnSOD and Cox-2 was not altered by 1h exposure to H_2O_2 suggests that such exposure may be too short to enhance expression of theses genes or that none of these three genes are responsive to H_2O_2. These observations illustrate the remarkable tolerance of the embryonic heart to strong oxidant stress.

CONCLUSIONS AND PERSPECTIVES

In the context of current advances in fetal and neonatal medicine, this work provides a first step in understanding the modulation of JAK2/STAT3 pathway in the fetal heart submitted to intrauterine oxygen deprivation. The experimental approach has been biochemical (immunoblotting), molecular (EMSA and RT-PCR), functional (ECG and contractility) and pharmacological (antioxidant, JAK2/STAT3 and PI3K/Akt pathways inhibitors).

For the first time in the developing heart, the myocardial JAK2 and STAT3 proteins and their inhomogeneous distribution and phosphorylation between the different cardiac regions have been investigated. Moreover we showed that in the developing heart the JAK2/STAT3 pathway is not activated by IL-6, like it is classically the case in almost all adult or neonatal tissues.

This work also demonstrates that the JAK2/STAT3 pathway plays a complex role in the myocardial response to anoxia-reoxygenation during a critical period of cardiogenesis and that this role is different during the early and late phases of reoxygenation. The reoxygenation-activated transcription factor STAT3 translocates into the nucleus but does not bind to DNA and can also interact rapidly with various signalling proteins of the RISK pathway differently in nuclear and cytoplasmic compartments (fig. 44). Furthermore, the fact that STAT3 activation improved post-anoxic recovery of cardiac rhythm illustrates the potential role that STAT3 plays in the protection of the cardiovascular function against a transient oxygen lack.

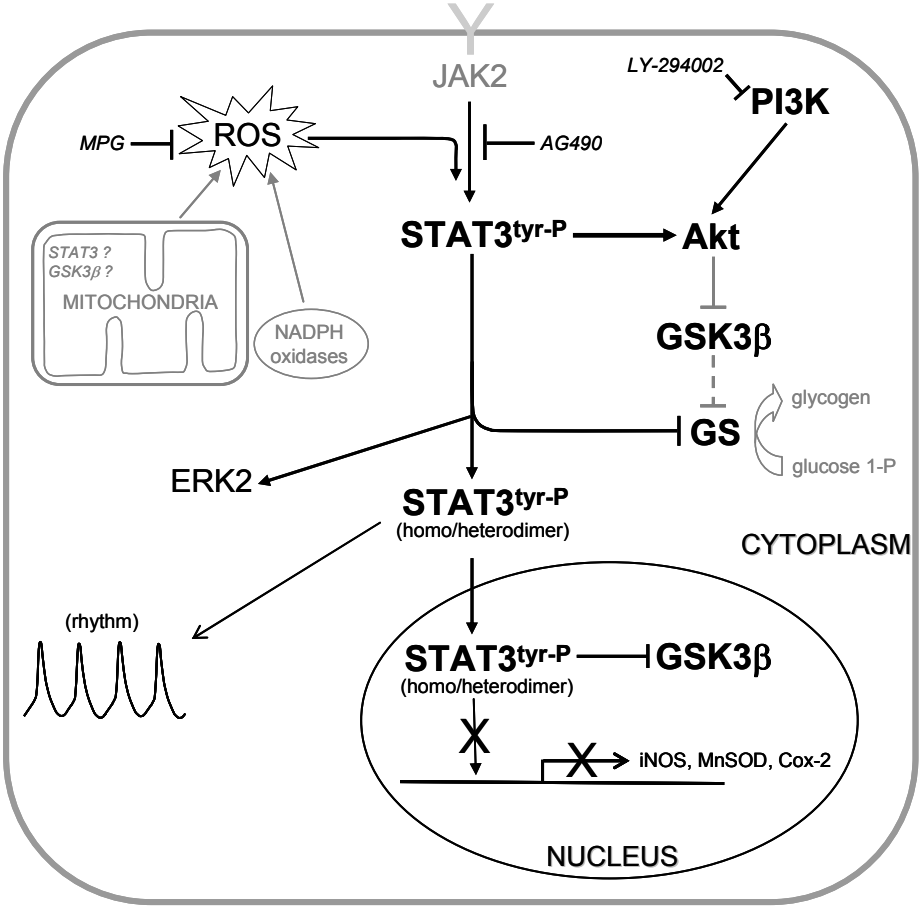

Fig. 44. Schematic representation based on our findings and illustrating STAT3 activation and its possible interaction with the RISK pathway components during the early phase of reoxygenation (10min) in the embryonic ventricle. In the cytoplasm, mitochondria- and NADPH oxidase-derived ROS stimulate the JAK2/STAT3 pathway which in turn activates Akt and ERK2 and inhibits GS. Activated STAT3 translocates into the nucleus and induces GSK3β inhibition without binding to DNA. Activation of STAT3 stabilized cardiac rhythm. Arrow, activation; T-shaped symbol, inhibition. Pharmacological agents used are indicated in italics. Dotted lines indicate putative activation/inhibition. Representations in light grey were not explored in the present work.

Finally this work shows that the embryonic heart is remarkably resistant to a potentially deleterious oxidant stress and that the atrial region is the most resistant. The response of the JAK2/STAT3 pathway to reoxygenation-induced oxyradicals is different from the response to exogenous oxidant stress which increases STAT3 DNA-binding activity.

To complete our experimental approach of the JAK2/STAT3 pathway, the role of JAK2 remains to be assessed in the embryonic heart to identify the possible molecular trigger of JAK2 activation under hypoxic conditions or oxidative stress.

Although this study focused exclusively on the ventricle, it would be necessary to find out about a possible correlation between the regional differences in myocardial tolerance to anoxia-reoxygenation and the differential activation of the JAK2/STAT3 and RISK pathways along the heart tube. Especially in the outflow tract in which a deleterious environment during early development can lead to congenital cardiac malformations and dysfunction (e.g. tetralogy of Fallot, the most common heart defect in children).

The subtle mechanisms by which STAT3 activation reduced arrhythmias during reoxygenation deserve to be investigated at the level of the ion channels known to be involved in pacemaking during early cardiogenesis.

A surprising finding of this work was that the developing heart displayed remarkable endogenous capabilities to cope with a strong oxidant stress (H_2O_2), especially in the sinoatrial region. As little is known about the mechanisms underlying this tolerance, we suggest investigating whether the high basal level of STAT3 phosphorylation can regulate some target genes involved in the protection against oxyradicals.

Furthermore, it would be interesting to elucidate the mechanisms involved in early and late phases of reoxygenation.

The findings of the present work give new insights into the cellular mechanisms involved in the adaptative response of the developing heart to oxygen deprivation during early fetal life and could be useful in the context of the fetal medicine.

REFERENCES

Aaronson DS, Horvath CM (A road map for those who don't know JAK-STAT. Science 296:1653-1655.2002).

Akira S (Functional roles of STAT family proteins: lessons from knockout mice. Stem Cells 17:138-146.1999).

Alonzi T, Maritano D, Gorgoni B, Rizzuto G, Libert C, Poli V (Essential role of STAT3 in the control of the acute-phase response as revealed by inducible gene inactivation [correction of activation] in the liver. Mol Cell Biol 21:1621-1632.2001).

Arany I, Megyesi JK, Nelkin BD, Safirstein RL (STAT3 attenuates EGFR-mediated ERK activation and cell survival during oxidant stress in mouse proximal tubular cells. Kidney Int 70:669-674.2006).

Bai J, Cederbaum AI (Mitochondrial catalase and oxidative injury. Biol Signals Recept 10:189-199.2001).

Bai L, Yu Z, Qian G, Qian P, Jiang J, Wang G, Bai C (SOCS3 was induced by hypoxia and suppressed STAT3 phosphorylation in pulmonary arterial smooth muscle cells. Respir Physiol Neurobiol 152:83-91.2006).

Barbosky L, Lawrence DK, Karunamuni G, Wikenheiser JC, Doughman YQ, Visconti RP, Burch JB, Watanabe M (Apoptosis in the developing mouse heart. Dev Dyn 235:2592-2602.2006).

Beckman JS, Beckman TW, Chen J, Marshall PA, Freeman BA (Apparent hydroxyl radical production by peroxynitrite: implications for endothelial injury from nitric oxide and superoxide. Proc Natl Acad Sci U S A 87:1620-1624.1990).

Bhattacharya S, Schindler C (Regulation of Stat3 nuclear export. J Clin Invest 111:553-559.2003).

Boccaccio C, Ando M, Tamagnone L, Bardelli A, Michieli P, Battistini C, Comoglio PM (Induction of epithelial tubules by growth factor HGF depends on the STAT pathway. Nature 391:285-288.1998).

Boengler K, Buechert A, Heinen Y, Roeskes C, Hilfiker-Kleiner D, Heusch G, Schulz R (Cardioprotection by ischemic postconditioning is lost in aged and STAT3-deficient mice. Circ Res 102:131-135.2008a).

Boengler K, Hilfiker-Kleiner D, Drexler H, Heusch G, Schulz R (The myocardial JAK/STAT pathway: from protection to failure. Pharmacol Ther 120:172-185.2008b).

Boeuf H, Hauss C, Graeve FD, Baran N, Kedinger C (Leukemia inhibitory factor-dependent transcriptional activation in embryonic stem cells. J Cell Biol 138:1207-1217.1997).

Bolli R, Dawn B, Xuan YT (Role of the JAK-STAT pathway in protection against myocardial ischemia/reperfusion injury. Trends Cardiovasc Med 13:72-79.2003).

Bonni A, Sun Y, Nadal-Vicens M, Bhatt A, Frank DA, Rozovsky I, Stahl N, Yancopoulos GD, Greenberg ME (Regulation of gliogenesis in the central nervous system by the JAK-STAT signaling pathway. Science 278:477-483.1997).

Bowman T, Garcia R, Turkson J, Jove R (STATs in oncogenesis. Oncogene 19:2474-2488.2000).

Brandes RP, Weissmann N, Schroder K (NADPH oxidases in cardiovascular disease. Free Radic Biol Med 49:687-706.2010).

Brette F, Orchard C (T-tubule function in mammalian cardiac myocytes. Circ Res 92:1182-1192.2003).

Brierley MM, Fish EN (Stats: multifaceted regulators of transcription. J Interferon Cytokine Res 25:733-744.2005).

Bromberg JF (Activation of STAT proteins and growth control. Bioessays 23:161-169.2001).
Bromberg JF, Horvath CM, Besser D, Lathem WW, Darnell JE, Jr. (Stat3 activation is required for cellular transformation by v-src. Mol Cell Biol 18:2553-2558.1998).
Bromberg JF, Wrzeszczynska MH, Devgan G, Zhao Y, Pestell RG, Albanese C, Darnell JE, Jr. (Stat3 as an oncogene. Cell 98:295-303.1999).
Brotto MA, Creazzo TL (Ca2+ transients in embryonic chick heart: contributions from Ca2+ channels and the sarcoplasmic reticulum. Am J Physiol 270:H518-525.1996).
Bruchez P, Sarre A, Kappenberger L, Raddatz E (The L-Type Ca+ and KATP channels may contribute to pacing-induced protection against anoxia-reoxygenation in the embryonic heart model. J Cardiovasc Electrophysiol 19:1196-1202.2008).
Buettner R, Mora LB, Jove R (Activated STAT signaling in human tumors provides novel molecular targets for therapeutic intervention. Clin Cancer Res 8:945-954.2002).
Burton GJ, Jaunaiux E (Maternal vascularisation of the human placenta: does the embryo develop in a hypoxic environment? Gynecol Obstet Fertil 29:503-508.2001).
Caldenhoven E, van Dijk TB, Solari R, Armstrong J, Raaijmakers JA, Lammers JW, Koenderman L, de Groot RP (STAT3beta, a splice variant of transcription factor STAT3, is a dominant negative regulator of transcription. J Biol Chem 271:13221-13227.1996).
Calo V, Migliavacca M, Bazan V, Macaluso M, Buscemi M, Gebbia N, Russo A (STAT proteins: from normal control of cellular events to tumorigenesis. J Cell Physiol 197:157-168.2003).
Carballo M, Conde M, El Bekay R, Martin-Nieto J, Camacho MJ, Monteseirin J, Conde J, Bedoya FJ, Sobrino F (Oxidative stress triggers STAT3 tyrosine phosphorylation and nuclear translocation in human lymphocytes. J Biol Chem 274:17580-17586.1999).
Catalano RD, Johnson MH, Campbell EA, Charnock-Jones DS, Smith SK, Sharkey AM (Inhibition of Stat3 activation in the endometrium prevents implantation: a nonsteroidal approach to contraception. Proc Natl Acad Sci U S A 102:8585-8590.2005).
Chakraborty A, White SM, Schaefer TS, Ball ED, Dyer KF, Tweardy DJ (Granulocyte colony-stimulating factor activation of Stat3 alpha and Stat3 beta in immature normal and leukemic human myeloid cells. Blood 88:2442-2449.1996).
Chomczynski P, Sacchi N (Single-step method of RNA isolation by acid guanidinium thiocyanate-phenol-chloroform extraction. Anal Biochem 162:156-159.1987).
Cressman DE, Diamond RH, Taub R (Rapid activation of the Stat3 transcription complex in liver regeneration. Hepatology 21:1443-1449.1995).
Cross JC, Werb Z, Fisher SJ (Implantation and the placenta: key pieces of the development puzzle. Science 266:1508-1518.1994).
Dawn B, Xuan YT, Guo Y, Rezazadeh A, Stein AB, Hunt G, Wu WJ, Tan W, Bolli R (IL-6 plays an obligatory role in late preconditioning via JAK-STAT signaling and upregulation of iNOS and COX-2. Cardiovasc Res 64:61-71.2004).
Dawson MA, Bannister AJ, Gottgens B, Foster SD, Bartke T, Green AR, Kouzarides T (JAK2 phosphorylates histone H3Y41 and excludes HP1alpha from chromatin. Nature 461:819-822.2009).
Decker T, Kovarik P (Serine phosphorylation of STATs. Oncogene 19:2628-2637.2000).
Dewilde S, Vercelli A, Chiarle R, Poli V (Of alphas and betas: distinct and overlapping functions of STAT3 isoforms. Front Biosci 13:6501-6514.2008).
Dudley AC, Thomas D, Best J, Jenkins A (A VEGF/JAK2/STAT5 axis may partially mediate endothelial cell tolerance to hypoxia. Biochem J 390:427-436.2005).

Duhe RJ, Evans GA, Erwin RA, Kirken RA, Cox GW, Farrar WL (Nitric oxide and thiol redox regulation of Janus kinase activity. Proc Natl Acad Sci U S A 95:126-131.1998).

Duncan SA, Zhong Z, Wen Z, Darnell JE, Jr. (STAT signaling is active during early mammalian development. Dev Dyn 208:190-198.1997).

Dutro SM, Airey JA, Beck CF, Sutko JL, Trumble WR (Ryanodine receptor expression in embryonic avian cardiac muscle. Dev Biol 155:431-441.1993).

El-Adawi H, Deng L, Tramontano A, Smith S, Mascareno E, Ganguly K, Castillo R, El-Sherif N (The functional role of the JAK-STAT pathway in post-infarction remodeling. Cardiovasc Res 57:129-138.2003).

Ferrari R, Guardigli G, Mele D, Percoco GF, Ceconi C, Curello S (Oxidative stress during myocardial ischaemia and heart failure. Curr Pharm Des 10:1699-1711.2004).

Fisher SA (The developing embryonic cardiac outflow tract is highly sensitive to oxidant stress. Dev Dyn 236:3496-3502.2007).

Fornerod M, Ohno M, Yoshida M, Mattaj IW (CRM1 is an export receptor for leucine-rich nuclear export signals. Cell 90:1051-1060.1997).

Foshay K, Rodriguez G, Hoel B, Narayan J, Gallicano GI (JAK2/STAT3 directs cardiomyogenesis within murine embryonic stem cells in vitro. Stem Cells 23:530-543.2005).

Fowden AL, Giussani DA, Forhead AJ (Intrauterine programming of physiological systems: causes and consequences. Physiology 21:29-37.2006).

Fruehauf JP, Meyskens FL, Jr. (Reactive oxygen species: a breath of life or death? Clin Cancer Res 13:789-794.2007).

Fuglesteg BN, Suleman N, Tiron C, Kanhema T, Lacerda L, Andreasen TV, Sack MN, Jonassen AK, Mjos OD, Opie LH, Lecour S (Signal transducer and activator of transcription 3 is involved in the cardioprotective signalling pathway activated by insulin therapy at reperfusion. Basic Res Cardiol 103:444–453.2008).

Fukada T, Ohtani T, Yoshida Y, Shirogane T, Nishida K, Nakajima K, Hibi M, Hirano T (STAT3 orchestrates contradictory signals in cytokine-induced G1 to S cell-cycle transition. EMBO J 17:6670-6677.1998).

Funamoto M, Fujio Y, Kunisada K, Negoro S, Tone E, Osugi T, Hirota H, Izumi M, Yoshizaki K, Walsh K, Kishimoto T, Yamauchi-Takihara K (Signal transducer and activator of transcription 3 is required for glycoprotein 130-mediated induction of vascular endothelial growth factor in cardiac myocytes. J Biol Chem 275:10561-10566.2000).

Garcia R, Yu CL, Hudnall A, Catlett R, Nelson KL, Smithgall T, Fujita DJ, Ethier SP, Jove R (Constitutive activation of Stat3 in fibroblasts transformed by diverse oncoproteins and in breast carcinoma cells. Cell Growth Differ 8:1267-1276.1997).

Gardier S, Pedretti S, Sarre A, Raddatz E (Transient anoxia and oxyradicals induce a region-specific activation of MAPKs in the embryonic heart. Mol Cell Biochem 340:239-247.2010a).

Gardier S, Pedretti S, Sarre A, Raddatz E (Transient anoxia and oxyradicals induce a region-specific activation of MAPKs in the embryonic heart. Mol Cell Biochem 340:239–247.2010b).

Gilmore TD (Introduction to NF-kappaB: players, pathways, perspectives. Oncogene 25:6680-6684.2006).

Goodman MD, Koch SE, Fuller-Bicer GA, Butler KL (Regulating RISK: a role for JAK-STAT signaling in postconditioning? Am J Physiol Heart Circ Physiol 295:H1649-1656.2008).

Gorlich D, Kutay U (Transport between the cell nucleus and the cytoplasm. Annu Rev Cell Dev Biol 15:607-660.1999).

Gough DJ, Corlett A, Schlessinger K, Wegrzyn J, Larner AC, Levy DE (Mitochondrial STAT3 supports Ras-dependent oncogenic transformation. Science 324:1713-1716.2009).

Gross ER, Hsu AK, Gross GJ (The JAK/STAT pathway is essential for opioid-induced cardioprotection: JAK2 as a mediator of STAT3, Akt, and GSK-3 beta. Am J Physiol Heart Circ Physiol 291:H827-834.2006).

Guo Y, Jones WK, Xuan YT, Tang XL, Bao W, Wu WJ, Han H, Laubach VE, Ping P, Yang Z, Qiu Y, Bolli R (The late phase of ischemic preconditioning is abrogated by targeted disruption of the inducible NO synthase gene. Proc Natl Acad Sci U S A 96:11507-11512.1999).

Hamburger V, Hamilton HL (A series of normal stages in the development of the chick embryo. 1951. Dev Dyn 195:231-272.1951).

Hattori R, Maulik N, Otani H, Zhu L, Cordis G, Engelman RM, Siddiqui MA, Das DK (Role of STAT3 in ischemic preconditioning. J Mol Cell Cardiol 33:1929-1936.2001).

Hausenloy DJ, Yellon DM (New directions for protecting the heart against ischaemia-reperfusion injury: targeting the Reperfusion Injury Salvage Kinase (RISK)-pathway. Cardiovasc Res 61:448-460.2004).

Hausenloy DJ, Yellon DM (Survival kinases in ischemic preconditioning and postconditioning. Cardiovasc Res 70:240-253.2006).

Hausenloy DJ, Yellon DM (Cardioprotective growth factors. Cardiovasc Res 83:179-194.2009).

Hilfiker-Kleiner D, Limbourg A, Drexler H (STAT3-mediated activation of myocardial capillary growth. Trends Cardiovasc Med 15:152-157.2005).

Huffman LC, Koch SE, Butler KL (Coronary effluent from a preconditioned heart activates the JAK-STAT pathway and induces cardioprotection in a donor heart. Am J Physiol Heart Circ Physiol 294:H257-262.2008).

Hwang YC, Shaw S, Kaneko M, Redd H, Marrero MB, Ramasamy R (Aldose reductase pathway mediates JAK-STAT signaling: a novel axis in myocardial ischemic injury. Faseb J 19:795-797.2005).

Jang EH, Park CS, Lee SK, Pie JE, Kang JH (Excessive nitric oxide attenuates leptin-mediated signal transducer and activator of transcription 3 activation. Life Sci 80:609-617.2007).

Jassem W, Fuggle SV, Rela M, Koo DD, Heaton ND (The role of mitochondria in ischemia/reperfusion injury. Transplantation 73:493-499.2002).

Jensen A, Garnier Y, Berger R (Dynamics of fetal circulatory responses to hypoxia and asphyxia. Eur J Obstet Gynecol Reprod Biol 84:155-172.1999).

Jeong CH, Lee HJ, Cha JH, Kim JH, Kim KR, Kim JH, Yoon DK, Kim KW (Hypoxia-inducible factor-1 alpha inhibits self-renewal of mouse embryonic stem cells in Vitro via negative regulation of the leukemia inhibitory factor-STAT3 pathway. J Biol Chem 282:13672-13679.2007).

Jorgensen AO, Bashir R (Temporal appearance and distribution of the Ca2+ + Mg2+ ATPase of the sarcoplasmic reticulum in developing chick myocardium as determined by immunofluorescence labeling. Dev Biol 106:156-165.1984).

Juhaszova M, Zorov DB, Kim SH, Pepe S, Fu Q, Fishbein KW, Ziman BD, Wang S, Ytrehus K, Antos CL, Olson EN, Sollott SJ (Glycogen synthase kinase-3beta mediates convergence of protection signaling to inhibit the mitochondrial permeability transition pore. J Clin Invest 113:1535-1549.2004).

Jung JE, Lee HG, Cho IH, Chung DH, Yoon SH, Yang YM, Lee JW, Choi S, Park JW, Ye SK, Chung MH (STAT3 is a potential modulator of HIF-1-mediated VEGF expression in human renal carcinoma cells. FASEB J 19:1296-1298.2005).

Kaur N, Lu B, Monroe RK, Ward SM, Halvorsen SW (Inducers of oxidative stress block ciliary neurotrophic factor activation of Jak/STAT signaling in neurons. J Neurochem 92:1521-1530.2005).

Keller BB, Liu LJ, Tinney JP, Tobita K (Cardiovascular developmental insights from embryos. Ann N Y Acad Sci 1101:377-388.2007).

Kim DJ, Tremblay ML, Digiovanni J (Protein tyrosine phosphatases, TC-PTP, SHP1, and SHP2, cooperate in rapid dephosphorylation of Stat3 in keratinocytes following UVB irradiation. PLoS One 5:e10290.2010).

Kinugawa K, Takahashi T, Kohmoto O, Yao A, Aoyagi T, Momomura S, Hirata Y, Serizawa T (Nitric oxide-mediated effects of interleukin-6 on [Ca2+]i and cell contraction in cultured chick ventricular myocytes. Circ Res 75:285-295.1994).

Kojima H, Sasaki T, Ishitani T, Iemura S, Zhao H, Kaneko S, Kunimoto H, Natsume T, Matsumoto K, Nakajima K (STAT3 regulates Nemo-like kinase by mediating its interaction with IL-6-stimulated TGFbeta-activated kinase 1 for STAT3 Ser-727 phosphorylation. Proc Natl Acad Sci U S A 102:4524-4529.2005).

Kovarik P, Mangold M, Ramsauer K, Heidari H, Steinborn R, Zotter A, Levy DE, Muller M, Decker T (Specificity of signaling by STAT1 depends on SH2 and C-terminal domains that regulate Ser727 phosphorylation, differentially affecting specific target gene expression. EMBO J 20:91-100.2001).

Kurdi M, Booz GW (Can the protective actions of JAK-STAT in the heart be exploited therapeutically? Parsing the regulation of interleukin-6-type cytokine signaling. J Cardiovasc Pharmacol 50:126-141.2007a).

Kurdi M, Booz GW (Evidence that IL-6-type cytokine signaling in cardiomyocytes is inhibited by oxidative stress: parthenolide targets JAK1 activation by generating ROS. J Cell Physiol 212:424-431.2007b).

Kurdi M, Booz GW (JAK redux: a second look at the regulation and role of JAKs in the heart. Am J Physiol Heart Circ Physiol 297:H1545-1556.2009).

Lacerda L, Somers S, Opie LH, Lecour S (Ischaemic postconditioning protects against reperfusion injury via the SAFE pathway. Cardiovasc Res 84:201-208.2009a).

Lacerda L, Somers S, Opie LH, Lecour S (Ischemic postconditioning protects against reperfusion injury via the SAFE pathway. Cardiovasc Res 84:201-208.2009b).

Lakomkin VL, Kapel'ko VI, Lankin VZ, Konovalova GG, Kaminnyi AI (Effect of beta-hydroxy-beta-methylglutaryl coenzyme A reductase inhibitor atorvastatin on contractility of the isolated rat heart under normal conditions and during oxidative stress. Bull Exp Biol Med 143:408-410.2007).

Lecour S (Activation of the protective Survivor Activating Factor Enhancement (SAFE) pathway against reperfusion injury: Does it go beyond the RISK pathway? J Mol Cell Cardiol 47:32-40.2009).

Lecour S, Smith RM, Woodward B, Opie LH, Rochette L, Sack MN (Identification of a novel role for sphingolipid signaling in TNF alpha and ischemic preconditioning mediated cardioprotection. J Mol Cell Cardiol 34:509-518.2002).

Lecour S, Suleman N, Deuchar GA, Somers S, Lacerda L, Huisamen B, Opie LH (Pharmacological preconditioning with tumor necrosis factor-alpha activates signal transducer and activator of transcription-3 at reperfusion without involving classic prosurvival kinases (Akt and extracellular signal-regulated kinase). Circulation 112:3911-3918.2005).

Lee H, Herrmann A, Deng JH, Kujawski M, Niu G, Li Z, Forman S, Jove R, Pardoll DM, Yu H (Persistently activated Stat3 maintains constitutive NF-kappaB activity in tumors. Cancer Cell 15:283-293.2009).

Lee MY, Joung YH, Lim EJ, Park JH, Ye SK, Park T, Zhang Z, Park DK, Lee KJ, Yang YM (Phosphorylation and activation of STAT proteins by hypoxia in breast cancer cells. Breast 15:187-195.2006).

Leonard WJ, O'Shea JJ (Jaks and STATs: biological implications. Annu Rev Immunol 16:293-322.1998).

Levrand S, Pesse B, Feihl F, Waeber B, Pacher P, Rolli J, Schaller MD, Liaudet L (Peroxynitrite is a potent inhibitor of NF-{kappa}B activation triggered by inflammatory stimuli in cardiac and endothelial cell lines. J Biol Chem 280:34878-34887.2005).

Levy DE, Darnell JE, Jr. (Stats: transcriptional control and biological impact. Nat Rev Mol Cell Biol 3:651-662.2002).

Lew DJ, Decker T, Strehlow I, Darnell JE (Overlapping elements in the guanylate-binding protein gene promoter mediate transcriptional induction by alpha and gamma interferons. Mol Cell Biol 11:182-191.1991).

Li C, Jackson RM (Reactive species mechanisms of cellular hypoxia-reoxygenation injury. Am J Physiol Cell Physiol 282:C227-241.2002).

Li J, Stouffs M, Serrander L, Banfi B, Bettiol E, Charnay Y, Steger K, Krause KH, Jaconi ME (The NADPH oxidase NOX4 drives cardiac differentiation: Role in regulating cardiac transcription factors and MAP kinase activation. Mol Biol Cell 17:3978-3988.2006).

Lim CP, Cao X (Structure, function, and regulation of STAT proteins. Mol Biosyst 2:536-550.2006).

Liu H, Fisher SA (Hypoxia-inducible transcription factor-1alpha triggers an autocrine survival pathway during embryonic cardiac outflow tract remodeling. Circ Res 102:1331-1339.2008).

Liu L, McBride KM, Reich NC (STAT3 nuclear import is independent of tyrosine phosphorylation and mediated by importin-alpha3. Proc Natl Acad Sci U S A 102:8150-8155.2005).

Livak KJ, Schmittgen TD (Analysis of relative gene expression data using real-time quantitative PCR and the 2(-Delta Delta C(T)) Method. Methods 25:402-408.2001).

Lobie PE, Ronsin B, Silvennoinen O, Haldosen LA, Norstedt G, Morel G (Constitutive nuclear localization of Janus kinases 1 and 2. Endocrinology 137:4037-4045.1996).

Lu Y, Zhou J, Xu C, Lin H, Xiao J, Wang Z, Yang B (JAK/STAT and PI3K/AKT pathways form a mutual transactivation loop and afford resistance to oxidative stress-induced apoptosis in cardiomyocytes. Cell Physiol Biochem 21:305-314.2008a).

Lu Y, Zhou J, Xu C, Lin H, Xiao J, Wang Z, Yang B (JAK/STAT and PI3K/AKT Pathways Form a Mutual Transactivation Loop and Afford Resistance to Oxidative Stress-Induced Apoptosis in Cardiomyocytes. Cell Physiol Biochem 21:305-314.2008b).

Ma J, Cao X (Regulation of Stat3 nuclear import by importin alpha5 and importin alpha7 via two different functional sequence elements. Cell Signal 18:1117-1126.2006).

Madamanchi NR, Li S, Patterson C, Runge MS (Reactive oxygen species regulate heat-shock protein 70 via the JAK/STAT pathway. Arterioscler Thromb Vasc Biol 21:321-326.2001).

Maltepe E, Simon MC (Oxygen, genes, and development: an analysis of the role of hypoxic gene regulation during murine vascular development. J Mol Med 76:391-401.1998).

Maritano D, Sugrue ML, Tininini S, Dewilde S, Strobl B, Fu X, Murray-Tait V, Chiarle R, Poli V (The STAT3 isoforms alpha and beta have unique and specific functions. Nat Immunol 5:401-409.2004).

Marks F, Klingmüller U, Müller-Decker K (2009) Cellular signal processing: Garland Science. 194-196.

Martinsen BJ (Reference guide to the stages of chick heart embryology. Dev Dyn 233:1217-1237.2005).

Mascareno E, Beckles DL, Siddiqui MA (Janus kinase-2 signaling mediates apoptosis in rat cardiomyocytes. Vascul Pharmacol 43:327-335.2005).

Mascareno E, El-Shafei M, Maulik N, Sato M, Guo Y, Das DK, Siddiqui MA (JAK/STAT signaling is associated with cardiac dysfunction during ischemia and reperfusion. Circulation 104:325-329.2001).

Maury P, Sarre A, Terrand J, Rosa A, Kucera P, Kappenberger L, Raddatz E (Ventricular but not atrial electro-mechanical delay of the embryonic heart is altered by anoxia-reoxygenation and improved by nitric oxide. Mol Cell Biochem 265:141-149.2004).

Maziere C, Conte MA, Maziere JC (Activation of JAK2 by the oxidative stress generated with oxidized low-density lipoprotein. Free Radic Biol Med 31:1334-1340.2001).

McCord JM, Fridovich I (Superoxide dismutase. An enzymic function for erythrocuprein (hemocuprein). J Biol Chem 244:6049-6055.1969).

McCormick J, Barry SP, Sivarajah A, Stefanutti G, Townsend PA, Lawrence KM, Eaton S, Knight RA, Thiemermann C, Latchman DS, Stephanou A (Free radical scavenging inhibits STAT phosphorylation following in vivo ischemia/reperfusion injury. Faseb J 20:2115-2117.2006).

McGaffin KR, Sun CK, Rager JJ, Romano LC, Zou B, Mathier MA, O'Doherty RM, McTiernan CF, O'Donnell CP (Leptin signalling reduces the severity of cardiac dysfunction and remodelling after chronic ischaemic injury. Cardiovasc Res 77:54-63.2008).

Meares GP, Jope RS (Resolution of the nuclear localization mechanism of glycogen synthase kinase-3: functional effects in apoptosis. J Biol Chem 282:16989-17001.2007).

Minami M, Inoue M, Wei S, Takeda K, Matsumoto M, Kishimoto T, Akira S (STAT3 activation is a critical step in gp130-mediated terminal differentiation and growth arrest of a myeloid cell line. Proc Natl Acad Sci U S A 93:3963-3966.1996).

Miyamoto S, Rubio M, Sussman MA (Nuclear and mitochondrial signalling Akts in cardiomyocytes. Cardiovasc Res 82:272-285.2009).

Modesti A, Bertolozzi I, Gamberi T, Marchetta M, Lumachi C, Coppo M, Moroni F, Toscano T, Lucchese G, Gensini GF, Modesti PA (Hyperglycemia activates JAK2 signaling pathway in human failing myocytes via angiotensin II-mediated oxidative stress. Diabetes 54:394-401.2005).

Moh A, Zhang W, Yu S, Wang J, Xu X, Li J, Fu XY (STAT3 sensitizes insulin signaling by negatively regulating glycogen synthase kinase-3 beta. Diabetes 57:1227-1235.2008).

Moorman AF, Christoffels VM (Cardiac chamber formation: development, genes, and evolution. Physiol Rev 83:1223-1267.2003).

Mover H, Ar A (Antioxidant enzymatic activity in embryos and placenta of rats chronically exposed to hypoxia and hyperoxia. Comp Biochem Physiol C Pharmacol Toxicol Endocrinol 117:151-157.1997).

Murphy E, Wheeler DM, LeFurgey A, Jacob R, Lobaugh LA, Lieberman M (Coupled sodium-calcium transport in cultured chick heart cells. Am J Physiol 250:C442-452.1986).

Murry CE, Jennings RB, Reimer KA (Preconditioning with ischemia: a delay of lethal cell injury in ischemic myocardium. Circulation 74:1124-1136.1986).

Na HS, Kim YI, Yoon YW, Han HC, Nahm SH, Hong SK (Ventricular premature beat-driven intermittent restoration of coronary blood flow reduces the incidence of reperfusion-

induced ventricular fibrillation in a cat model of regional ischemia. Am Heart J 132:78-83.1996).

Nakajima K, Yamanaka Y, Nakae K, Kojima H, Ichiba M, Kiuchi N, Kitaoka T, Fukada T, Hibi M, Hirano T (A central role for Stat3 in IL-6-induced regulation of growth and differentiation in M1 leukemia cells. EMBO J 15:3651-3658.1996).

Negoro S, Kunisada K, Fujio Y, Funamoto M, Darville MI, Eizirik DL, Osugi T, Izumi M, Oshima Y, Nakaoka Y, Hirota H, Kishimoto T, Yamauchi-Takihara K (Activation of signal transducer and activator of transcription 3 protects cardiomyocytes from hypoxia/reoxygenation-induced oxidative stress through the upregulation of manganese superoxide dismutase. Circulation 104:979-981.2001).

Negoro S, Kunisada K, Tone E, Funamoto M, Oh H, Kishimoto T, Yamauchi-Takihara K (Activation of JAK/STAT pathway transduces cytoprotective signal in rat acute myocardial infarction. Cardiovasc Res 47:797-805.2000).

Neubauer H, Cumano A, Muller M, Wu H, Huffstadt U, Pfeffer K (Jak2 deficiency defines an essential developmental checkpoint in definitive hematopoiesis. Cell 93:397-409.1998).

Ng DC, Court NW, dos Remedios CG, Bogoyevitch MA (Activation of signal transducer and activator of transcription (STAT) pathways in failing human hearts. Cardiovasc Res 57:333-346.2003).

Ng DC, Lin BH, Lim CP, Huang G, Zhang T, Poli V, Cao X (Stat3 regulates microtubules by antagonizing the depolymerization activity of stathmin. J Cell Biol 172:245-257.2006).

Nicolosi AC, Strande JL, Hsu A, Fu X, Su J, Gross GJ, Baker JE (Gadolinium limits myocardial infarction in the rat: dose-response, temporal relations and mechanisms. J Mol Cell Cardiol 44:345-351.2008).

Nijland MJ, Ford SP, Nathanielsz PW (Prenatal origins of adult disease. Curr Opin Obstet Gynecol 20:132-138.2008).

Nilsson J, Bjursell G, Kannius-Janson M (Nuclear Jak2 and transcription factor NF1-C2: a novel mechanism of prolactin signaling in mammary epithelial cells. Mol Cell Biol 26:5663-5674.2006).

Niu G, Briggs J, Deng J, Ma Y, Lee H, Kortylewski M, Kujawski M, Kay H, Cress WD, Jove R, Yu H (Signal transducer and activator of transcription 3 is required for hypoxia-inducible factor-1alpha RNA expression in both tumor cells and tumor-associated myeloid cells. Mol Cancer Res 6:1099-1105.2008).

Niwa H, Burdon T, Chambers I, Smith A (Self-renewal of pluripotent embryonic stem cells is mediated via activation of STAT3. Genes Dev 12:2048-2060.1998).

Nonami Y (The role of nitric oxide in cardiac ischemia-reperfusion injury. Jpn Circ J 61:119-132.1997).

Olivey HE, Compton LA, Barnett JV (Coronary vessel development: the epicardium delivers. Trends Cardiovasc Med 14:247-251.2004).

Omura T, Yoshiyama M, Ishikura F, Kobayashi H, Takeuchi K, Beppu S, Yoshikawa J (Myocardial ischemia activates the JAK-STAT pathway through angiotensin II signaling in in vivo myocardium of rats. J Mol Cell Cardiol 33:307-316.2001).

Oshima Y, Fujio Y, Nakanishi T, Itoh N, Yamamoto Y, Negoro S, Tanaka K, Kishimoto T, Kawase I, Azuma J (STAT3 mediates cardioprotection against ischemia/reperfusion injury through metallothionein induction in the heart. Cardiovasc Res 65:428-435.2005).

Pantos C, Xinaris C, Mourouzis I, Malliopoulou V, Kardami E, Cokkinos DV (Thyroid hormone changes cardiomyocyte shape and geometry via ERK signaling pathway:

potential therapeutic implications in reversing cardiac remodeling? Mol Cell Biochem 297:65-72.2007).

Parganas E, Wang D, Stravopodis D, Topham DJ, Marine JC, Teglund S, Vanin EF, Bodner S, Colamonici OR, van Deursen JM, Grosveld G, Ihle JN (Jak2 is essential for signaling through a variety of cytokine receptors. Cell 93:385-395.1998).

Park OK, Schaefer LK, Wang W, Schaefer TS (Dimer stability as a determinant of differential DNA binding activity of Stat3 isoforms. J Biol Chem 275:32244-32249.2000).

Petosa C, Schoehn G, Askjaer P, Bauer U, Moulin M, Steuerwald U, Soler-Lopez M, Baudin F, Mattaj IW, Muller CW (Architecture of CRM1/Exportin1 suggests how cooperativity is achieved during formation of a nuclear export complex. Mol Cell 16:761-775.2004).

Piuhola J, Kerkela R, Keenan JI, Hampton MB, Richards AM, Pemberton CJ (Direct cardiac actions of erythropoietin (EPO): effects on cardiac contractility, BNP secretion and ischaemia/reperfusion injury. Clin Sci (Lond) 114:293-304.2008).

Porter GA, Jr., Makuck RF, Rivkees SA (Intracellular calcium plays an essential role in cardiac development. Dev Dyn 227:280-290.2003).

Pranada AL, Metz S, Herrmann A, Heinrich PC, Muller-Newen G (Real time analysis of STAT3 nucleocytoplasmic shuttling. J Biol Chem 279:15114-15123.2004).

Raddatz E (2007) Biologie et pathologie du coeur et des vaisseaux: John Libbey Eurotext. 203.

Raddatz E, Gardier S, Sarre A (Physiopathology of the embryonic heart (with special emphasis on hypoxia and reoxygenation). Ann Cardiol Angeiol (Paris) 55:79-89.2006).

Raddatz E, Servin M, Kucera P (Oxygen uptake during early cardiogenesis of the chick. Am J Physiol 262:H1224-1230.1992).

Raddatz E, Thomas AC, Sarre A, Benathan M (Differential contribution of mitochondria, NADPH-oxidases and glycolysis to region-specific oxidant stress in the anoxic-reoxygenated embryonic heart. Am J Physiol Heart Circ Physiol.2010).

Ream M, Ray AM, Chandra R, Chikaraishi DM (Early fetal hypoxia leads to growth restriction and myocardial thinning. Am J Physiol Regul Integr Comp Physiol 295:R583-595.2008).

Reese DE, Mikawa T, Bader DM (Development of the coronary vessel system. Circ Res 91:761-768.2002).

Reich NC, Liu L (Tracking STAT nuclear traffic. Nat Rev Immunol 6:602-612.2006).

Romano R, Rochat AC, Kucera P, De Ribaupierre Y, Raddatz E (Oxidative and glycogenolytic capacities within the developing chick heart. Pediatr Res 49:363-372.2001).

Rosa A, Maury JP, Terrand J, Lyon X, Kucera P, Kappenberger L, Raddatz E (Ectopic pacing at physiological rate improves postanoxic recovery of the developing heart. Am J Physiol Heart Circ Physiol 284:H2384-2392.2003).

Rubio M, Avitabile D, Fischer K, Emmanuel G, Gude N, Miyamoto S, Mishra S, Schaefer EM, Brown JH, Sussman MA (Cardioprotective stimuli mediate phosphoinositide 3-kinase and phosphoinositide dependent kinase 1 nuclear accumulation in cardiomyocytes. J Mol Cell Cardiol 47:96-103.2009).

Sabri A, Byron KL, Samarel AM, Bell J, Lucchesi PA (Hydrogen peroxide activates mitogen-activated protein kinases and Na+-H+ exchange in neonatal rat cardiac myocytes. Circ Res 82:1053-1062.1998).

Sano S, Itami S, Takeda K, Tarutani M, Yamaguchi Y, Miura H, Yoshikawa K, Akira S, Takeda J (Keratinocyte-specific ablation of Stat3 exhibits impaired skin remodeling, but does not affect skin morphogenesis. EMBO J 18:4657-4668.1999).

Sarre A (2006) Physiopathology of the anoxic-reoxygenated embryonic heart: protective role of NO and KATP channel. In: Department of Physiology: University of Lausanne.

Sarre A, Gardier S, Maurer F, Bonny C, Raddatz E (Modulation of the c-Jun N-terminal kinase activity in the embryonic heart in response to anoxia-reoxygenation: involvement of the Ca2+ and mitoKATP channels. Mol Cell Biochem 313:133-138.2008).

Sarre A, Lange N, Kucera P, Raddatz E (mitoKATP channel activation in the postanoxic developing heart protects E-C coupling via NO-, ROS-, and PKC-dependent pathways. Am J Physiol Heart Circ Physiol 288:H1611-1619.2005).

Sarre A, Maury P, Kucera P, Kappenberger L, Raddatz E (Arrhythmogenesis in the developing heart during anoxia-reoxygenation and hypothermia-rewarming: an in vitro model. J Cardiovasc Electrophysiol 17:1350-1359.2006).

Sarre A, Pedretti S, Gardier S, Raddatz E (Specific inhibition of HCN channels slows rhythm differently in atria, ventricle and outflow tract and stabilizes conduction in the anoxic-reoxygenated embryonic heart model. Pharmacol Res 61:85-91.2010).

Sato N, Kawai T, Sugiyama K, Muromoto R, Imoto S, Sekine Y, Ishida M, Akira S, Matsuda T (Physical and functional interactions between STAT3 and ZIP kinase. Int Immunol 17:1543-1552.2005).

Satoh M, Nakamura M, Tamura G, Makita S, Segawa I, Tashiro A, Satodate R, Hiramori K (Inducible nitric oxide synthase and tumor necrosis factor-alpha in myocardium in human dilated cardiomyopathy. J Am Coll Cardiol 29:716-724.1997).

Satriotomo I, Bowen KK, Vemuganti R (JAK2 and STAT3 activation contributes to neuronal damage following transient focal cerebral ischemia. J Neurochem 98:1353-1368.2006).

Sauer H, Neukirchen W, Rahimi G, Grunheck F, Hescheler J, Wartenberg M (Involvement of reactive oxygen species in cardiotrophin-1-induced proliferation of cardiomyocytes differentiated from murine embryonic stem cells. Exp Cell Res 294:313-324.2004).

Schaefer TS, Sanders LK, Park OK, Nathans D (Functional differences between Stat3alpha and Stat3beta. Mol Cell Biol 17:5307-5316.1997).

Schieffer B, Luchtefeld M, Braun S, Hilfiker A, Hilfiker-Kleiner D, Drexler H (Role of NAD(P)H oxidase in angiotensin II-induced JAK/STAT signaling and cytokine induction. Circ Res 87:1195-1201.2000).

Sedmera D, Kucera P, Raddatz E (Developmental changes in cardiac recovery from anoxia-reoxygenation. Am J Physiol Regul Integr Comp Physiol 283:R379-388.2002).

Sedmera D, Pexieder T, Vuillemin M, Thompson RP, Anderson RH (Developmental patterning of the myocardium. Anat Rec 258:319-337.2000).

Seltzer JL, McDougal DB, Jr. (Enzyme levels in chick embryo heart and brain from 1 to 21 days of development. Dev Biol 42:95-100.1975).

Shaw S, Wang X, Redd H, Alexander GD, Isales CM, Marrero MB (High glucose augments the angiotensin II-induced activation of JAK2 in vascular smooth muscle cells via the polyol pathway. J Biol Chem 278:30634-30641.2003).

Shen Y, Schlessinger K, Zhu X, Meffre E, Quimby F, Levy DE, Darnell JE, Jr. (Essential role of STAT3 in postnatal survival and growth revealed by mice lacking STAT3 serine 727 phosphorylation. Mol Cell Biol 24:407-419.2004).

Shi X, Zhang H, Paddon H, Lee G, Cao X, Pelech S (Phosphorylation of STAT3 serine-727 by cyclin-dependent kinase 1 is critical for nocodazole-induced mitotic arrest. Biochemistry 45:5857-5867.2006).

Shinmura K, Tang XL, Wang Y, Xuan YT, Liu SQ, Takano H, Bhatnagar A, Bolli R (Cyclooxygenase-2 mediates the cardioprotective effects of the late phase of ischemic

preconditioning in conscious rabbits. Proc Natl Acad Sci U S A 97:10197-10202.2000).

Simon AR, Rai U, Fanburg BL, Cochran BH (Activation of the JAK-STAT pathway by reactive oxygen species. Am J Physiol 275:C1640-1652.1998).

Souza V, Escobar Mdel C, Bucio L, Hernandez E, Gomez-Quiroz LE, Gutierrez Ruiz MC (NADPH oxidase and ERK1/2 are involved in cadmium induced-STAT3 activation in HepG2 cells. Toxicol Lett 187:180-186.2009).

Stephanou A, Brar BK, Scarabelli TM, Jonassen AK, Yellon DM, Marber MS, Knight RA, Latchman DS (Ischemia-induced STAT-1 expression and activation play a critical role in cardiomyocyte apoptosis. J Biol Chem 275:10002-10008.2000).

Stephanou A, Latchman DS (Opposing actions of STAT-1 and STAT-3. Growth Factors 23:177-182.2005).

Sugishita Y, Watanabe M, Fisher SA (Role of myocardial hypoxia in the remodeling of the embryonic avian cardiac outflow tract. Dev Biol 267:294-308.2004).

Suleman N, Opie LH, Lecour S (Ischemic postconditioning confers cardioprotection via phosphorylation of STAT-3. Journal of Molecular and Cellular Cardiology 40:977.2006).

Suleman N, Somers S, Smith R, Opie LH, Lecour S (Dual activation of STAT-3 and Akt is required during the trigger phase of ischaemic preconditioning. Cardiovasc Res 79:127-133.2008a).

Suleman N, Somers S, Smith R, Opie LH, Lecour SC (Dual activation of STAT-3 and Akt is required during the trigger phase of ischaemic preconditioning. Cardiovasc Res 79:127-133.2008b).

Surai PF, Noble RC, Speake BK (Tissue-specific differences in antioxidant distribution and susceptibility to lipid peroxidation during development of the chick embryo. Biochim Biophys Acta 1304:1-10.1996).

Tacchini L, Fusar-Poli D, Bernelli-Zazzera A (Activation of transcription factors by drugs inducing oxidative stress in rat liver. Biochem Pharmacol 63:139-148.2002).

Takeda K, Clausen BE, Kaisho T, Tsujimura T, Terada N, Forster I, Akira S (Enhanced Th1 activity and development of chronic enterocolitis in mice devoid of Stat3 in macrophages and neutrophils. Immunity 10:39-49.1999).

Takeda K, Kaisho T, Yoshida N, Takeda J, Kishimoto T, Akira S (Stat3 activation is responsible for IL-6-dependent T cell proliferation through preventing apoptosis: generation and characterization of T cell-specific Stat3-deficient mice. J Immunol 161:4652-4660.1998).

Takeda K, Noguchi K, Shi W, Tanaka T, Matsumoto M, Yoshida N, Kishimoto T, Akira S (Targeted disruption of the mouse Stat3 gene leads to early embryonic lethality. Proc Natl Acad Sci U S A 94:3801-3804.1997).

Tenthorey D, de Ribaupierre Y, Kucera P, Raddatz E (Effects of verapamil and ryanodine on activity of the embryonic chick heart during anoxia and reoxygenation. J Cardiovasc Pharmacol 31:195-202.1998).

Terrand J, Felley-Bosco E, Courjault-Gautier F, Rochat AC, Kucera P, Raddatz E (Postanoxic functional recovery of the developing heart is slightly altered by endogenous or exogenous nitric oxide. Mol Cell Biochem 252:53-63.2003).

Terui K, Enosawa S, Haga S, Zhang HQ, Kuroda H, Kouchi K, Matsunaga T, Yoshida H, Engelhardt JF, Irani K, Ohnuma N, Ozaki M (Stat3 confers resistance against hypoxia/reoxygenation-induced oxidative injury in hepatocytes through upregulation of Mn-SOD. J Hepatol 41:957-965.2004).

Thornburg KL, O'Tierney PF, Louey S (Review: The placenta is a programming agent for cardiovascular disease. Placenta 31 Suppl:S54-59.2010).

Tranter M, Ren X, Forde T, Wilhide ME, Chen J, Sartor MA, Medvedovic M, Jones WK (NF-kappaB driven cardioprotective gene programs; Hsp70.3 and cardioprotection after late ischemic preconditioning. J Mol Cell Cardiol.2010).

Tuganowski W, Samek D, Glenc F (Glycogen content in human embryonic heart. Recent Adv Stud Cardiac Struct Metab 8:179-180.1975).

Ushijima R, Sakaguchi N, Kano A, Maruyama A, Miyamoto Y, Sekimoto T, Yoneda Y, Ogino K, Tachibana T (Extracellular signal-dependent nuclear import of STAT3 is mediated by various importin alphas. Biochem Biophys Res Commun 330:880-886.2005).

Valko M, Leibfritz D, Moncol J, Cronin MT, Mazur M, Telser J (Free radicals and antioxidants in normal physiological functions and human disease. Int J Biochem Cell Biol 39:44-84.2007).

Volgin DV, Kubin L (Chronic intermittent hypoxia alters hypothalamic transcription of genes involved in metabolic regulation. Auton Neurosci 126-127:93-99.2006).

Wang G, Qian P, Jackson FR, Qian G, Wu G (Sequential activation of JAKs, STATs and xanthine dehydrogenase/oxidase by hypoxia in lung microvascular endothelial cells. Int J Biochem Cell Biol.2007a).

Wang GS, Qian GS, Zhou DS, Zhao JQ (JAK-STAT signaling pathway in pulmonary arterial smooth muscle cells is activated by hypoxia. Cell Biol Int 29:598-603.2005).

Wang M, Zhang W, Crisostomo P, Markel T, Meldrum KK, Fu XY, Meldrum DR (Endothelial STAT3 plays a critical role in generalized myocardial proinflammatory and proapoptotic signaling. Am J Physiol Heart Circ Physiol 293:H2101-2108.2007b).

Wang M, Zhang W, Crisostomo P, Markel T, Meldrum KK, Fu XY, Meldrum DR (STAT3 mediates bone marrow mesenchymal stem cell VEGF production. J Mol Cell Cardiol 42:1009-1015.2007c).

Wang Z, Jiang B, Brecher P (Selective inhibition of STAT3 phosphorylation by sodium salicylate in cardiac fibroblasts. Biochem Pharmacol 63:1197-1207.2002).

Weber-Nordt RM, Egen C, Wehinger J, Ludwig W, Gouilleux-Gruart V, Mertelsmann R, Finke J (Constitutive activation of STAT proteins in primary lymphoid and myeloid leukemia cells and in Epstein-Barr virus (EBV)-related lymphoma cell lines. Blood 88:809-816.1996).

Wegrzyn J, Potla R, Chwae YJ, Sepuri NB, Zhang Q, Koeck T, Derecka M, Szczepanek K, Szelag M, Gornicka A, Moh A, Moghaddas S, Chen Q, Bobbili S, Cichy J, Dulak J, Baker DP, Wolfman A, Stuehr D, Hassan MO, Fu XY, Avadhani N, Drake JI, Fawcett P, Lesnefsky EJ, Larner AC (Function of mitochondrial Stat3 in cellular respiration. Science 323:793-797.2009).

Wei C, Jiang S, Lust JA, Daly RC, McGregor CG (Genetic expression of endothelial nitric oxide synthase in human atrial myocardium. Mayo Clin Proc 71:346-350.1996).

Wen W, Meinkoth JL, Tsien RY, Taylor SS (Identification of a signal for rapid export of proteins from the nucleus. Cell 82:463-473.1995a).

Wen Z, Zhong Z, Darnell JE, Jr. (Maximal activation of transcription by Stat1 and Stat3 requires both tyrosine and serine phosphorylation. Cell 82:241-250.1995b).

Wong M, Fish EN (RANTES and MIP-1alpha activate stats in T cells. J Biol Chem 273:309-314.1998).

Xu Z, Cohen MV, Downey JM, Vanden Hoek TL, Yao Z (Attenuation of oxidant stress during reoxygenation by AMP 579 in cardiomyocytes. Am J Physiol Heart Circ Physiol 281:H2585-2589.2001).

Xuan YT, Guo Y, Han H, Zhu Y, Bolli R (An essential role of the JAK-STAT pathway in ischemic preconditioning. Proc Natl Acad Sci U S A 98:9050-9055.2001).

Xuan YT, Guo Y, Zhu Y, Han H, Langenbach R, Dawn B, Bolli R (Mechanism of cyclooxygenase-2 upregulation in late preconditioning. J Mol Cell Cardiol 35:525-537.2003).

Xuan YT, Guo Y, Zhu Y, Wang OL, Rokosh G, Bolli R (Endothelial nitric oxide synthase plays an obligatory role in the late phase of ischemic preconditioning by activating the protein kinase C epsilon p44/42 mitogen-activated protein kinase pSer-signal transducers and activators of transcription1/3 pathway. Circulation 116:535-544.2007).

Xuan YT, Guo Y, Zhu Y, Wang OL, Rokosh G, Messing RO, Bolli R (Role of the protein kinase C-epsilon-Raf-1-MEK-1/2-p44/42 MAPK signaling cascade in the activation of signal transducers and activators of transcription 1 and 3 and induction of cyclooxygenase-2 after ischemic preconditioning. Circulation 112:1971-1978.2005).

Yang J, Chatterjee-Kishore M, Staugaitis SM, Nguyen H, Schlessinger K, Levy DE, Stark GR (Novel roles of unphosphorylated STAT3 in oncogenesis and transcriptional regulation. Cancer Res 65:939-947.2005).

Yang J, Liao X, Agarwal MK, Barnes L, Auron PE, Stark GR (Unphosphorylated STAT3 accumulates in response to IL-6 and activates transcription by binding to NFkappaB. Genes Dev 21:1396-1408.2007).

Ye F, Chen HZ, Xie X, Ye DF, Lu WG, Ding ZM (Vascular endothelial growth factor (VEGF) and ovarian carcinoma cell supernatant activate signal transducers and activators of transcription (STATs) via VEGF receptor-2 (KDR) in human hemopoietic progenitor cells. Gynecol Oncol 94:125-133.2004).

Yellon DM, Baxter GF (Reperfusion injury revisited: is there a role for growth factor signaling in limiting lethal reperfusion injury? Trends Cardiovasc Med 9:245-249.1999).

Yonezawa K, Yoshino KI, Tokunaga C, Hara K (Kinase activities associated with mTOR. Curr Top Microbiol Immunol 279:271-282.2004).

Yu HM, Zhi JL, Cui Y, Tang EH, Sun SN, Feng JQ, Chen PX (Role of the JAK-STAT pathway in protection of hydrogen peroxide preconditioning against apoptosis induced by oxidative stress in PC12 cells. Apoptosis 11:931-941.2006).

Yu X, Kennedy RH, Liu SJ (JAK2/STAT3, not ERK1/2, mediates interleukin-6-induced activation of inducible nitric-oxide synthase and decrease in contractility of adult ventricular myocytes. J Biol Chem 278:16304-16309.2003).

Yu Z, Zhang W, Kone BC (Signal transducers and activators of transcription 3 (STAT3) inhibits transcription of the inducible nitric oxide synthase gene by interacting with nuclear factor kappaB. Biochem J 367:97-105.2002).

Zhang X, Shan P, Alam J, Fu XY, Lee PJ (Carbon monoxide differentially modulates STAT1 and STAT3 and inhibits apoptosis via a phosphatidylinositol 3-kinase/Akt and p38 kinase-dependent STAT3 pathway during anoxia-reoxygenation injury. J Biol Chem 280:8714-8721.2005).

Zhong Z, Wen Z, Darnell JE, Jr. (Stat3 and Stat4: members of the family of signal transducers and activators of transcription. Proc Natl Acad Sci U S A 91:4806-4810.1994).

Zweier JL, Talukder MA (The role of oxidants and free radicals in reperfusion injury. Cardiovasc Res 70:181-190.2006).

ANNEXES

This work resulted in the following articles:

-S. Pedretti and E. Raddatz *«STAT3α interacts with nuclear GSK3ß and cytoplasmic RISK pathway and stabilizes rhythm in the anoxic-reoxygenated embryonic heart»*, Basic Research in Cardiology, January 2011

-S. Gardier, S. Pedretti, A. Sarre and E. Raddatz *«Transient anoxia and oxyradicals induce a region-specific activation of MAPKs in the early septating embryonic heart»*, Molecular and Cellular Biochemistry, July 2010; 340(1-2):239-47

-A. Sarre, S. Pedretti, S. Gardier and E. Raddatz *«Specific inhibition of HCN channels slows rhythm differently in atria, ventricle and outflow tract and stabilizes conduction in the anoxic-reoxygenated embryonic heart model»*, Pharmacological Research, January 2010; 61(1):85-91

Basic Res Cardiol
DOI 10.1007/s00395-011-0152-5

ORIGINAL CONTRIBUTION

STAT3α interacts with nuclear GSK3beta and cytoplasmic RISK pathway and stabilizes rhythm in the anoxic-reoxygenated embryonic heart

Sarah Pedretti · Eric Raddatz

Received: 12 October 2010 / Revised: 23 December 2010 / Accepted: 13 January 2011

Abstract Activation of the Janus Kinase 2/Signal Transducer and Activator of Transcription 3 (JAK2/STAT3) pathway is known to play a key role in cardiogenesis and to afford cardioprotection against ischemia–reperfusion in adult. However, involvement of JAK2/STAT3 pathway and its interaction with other signaling pathways in developing heart transiently submitted to anoxia remains to be explored. Hearts isolated from 4-day-old chick embryos were submitted to anoxia (30 min) and reoxygenation (80 min) with or without the antioxidant MPG, the JAK2/STAT3 inhibitor AG490 or the PhosphoInositide-3-Kinase (PI3K)/Akt inhibitor LY-294002. Time course of phosphorylation of STAT3$\alpha^{tyrosine705}$ and Reperfusion Injury Salvage Kinase (RISK) proteins [PI3K, Akt, Glycogen Synthase Kinase 3beta (GSK3beta), Extracellular signal-Regulated Kinase 2 (ERK2)] was determined in homogenate and in enriched nuclear and cytoplasmic fractions of the ventricle. STAT3 DNA-binding was determined. The chrono-, dromo- and inotropic disturbances were also investigated by electrocardiogram and mechanical recordings. Phosphorylation of STAT3α^{tyr705} was increased by reoxygenation, reduced ($\sim$50%) by MPG or AG490 but not affected by LY-294002. STAT3 and GSK3beta were detected both in nuclear and cytoplasmic fractions while PI3K, Akt and ERK2 were restricted to cytoplasm. Reoxygenation led to nuclear accumulation of STAT3 but unexpectedly without DNA-binding. AG490 decreased the reoxygenation-induced phosphorylation of Akt and ERK2 and phosphorylation/inhibition of GSK3beta in the nucleus, exclusively. Inhibition of JAK2/STAT3 delayed recovery of atrial rate, worsened variability of cardiac cycle length and prolonged arrhythmias as compared to control hearts. Thus, besides its nuclear translocation without transcriptional activity, oxyradicals-activated STAT3α can rapidly interact with RISK proteins present in nucleus and cytoplasm, without dual interaction, and reduce the anoxia–reoxygenation-induced arrhythmias in the embryonic heart.

Keywords JAK2/STAT3 pathway · Anoxia–reoxygenation · Embryonic heart · Oxyradicals · RISK pathway

Introduction

Although the embryo and the fetus develop normally in a relatively hypoxic environment [7, 31], cardiovascular function can be rapidly impaired by an accidental and transient intrauterine lack of oxygen [21] with possible long-term deleterious consequences. In the embryonic heart, the chrono-, dromo- and inotropic disturbances induced by anoxia–reoxygenation [39, 48] are associated with overproduction of Reactive Oxygen Species (ROS) and significant alterations of signaling pathways. In particular, the region-specific activation of Mitogen-Activated Protein Kinases (MAPKs) [12, 43] such as p38MAPK, extracellular signal-regulated kinase (ERK2) and c-jun N-terminal kinase (JNK) and stimulation of protein kinase C and nitric oxide synthases [44] are part of the mechanisms involved in the response to anoxia–reoxygenation,

Electronic supplementary material The online version of this article (doi:10.1007/s00395-011-0152-5) contains supplementary material, which is available to authorized users.

S. Pedretti (✉) · E. Raddatz
Department of Physiology, Faculty of Biology and Medicine, University of Lausanne, Rue du Bugnon 7, 1005 Lausanne, Switzerland
e-mail: sarah.pedretti@unil.ch

Published online: 29 January 2011

with slight differences relative to the ischemic-reperfused adult heart [18]. In addition to these signaling pathways, the Janus Kinase 2/Signal Transducer and Activator of Transcription 3 (JAK2/STAT3) pathway is also activated by ischemia–reperfusion [1, 19]. JAK2 is a receptor-associated cytosolic protein which mediates signals to the nucleus by the subsequent phosphorylation/activation of STAT3 transcription factor. STAT3 can be phosphorylated on tyrosine^{705} by JAK upon activation and on serine^{727} mainly by ERK and p38MAPK [24]. It should also be noticed that expression of STAT3 is necessary for normal embryogenesis [53] and that JAK2/STAT3 activation is a prerequisite for the differentiation of embryonic stem cells into spontaneously beating cardiomyocytes [10]. Moreover, the JAK2/STAT3 pathway affords protection against reperfusion-induced injury in neonatal [51] and adult [19, 37] cardiomyocytes and can interact with other pathways including the Reperfusion Injury Salvage Kinase (RISK) pathway [11, 13, 15, 17, 30]. The RISK pathway is a group of pro-survival protein kinases including PhosphoInositide-3-Kinase (PI3K), Akt/PKB, Glycogen Synthase Kinase 3beta (GSK3beta) and ERK1/2 which confers cardioprotection when activated at reperfusion but not in all species [50]. Although STAT3 is basically a transcription factor shuttling between cytoplasmic and nuclear compartments, the intracellular localization of its interactions with RISK pathway components as well as its role in cardiac function under pathological conditions remains to be explored. This work aimed (1) to establish the temporal profile of phosphorylation, the mechanisms of activation and the transcriptional activity of STAT3, (2) to assess the crosstalk between STAT3 and RISK pathway in the nuclear and the cytoplasmic compartments, and (3) to examine the role of activated STAT3 in the functional recovery of the anoxic-reoxygenated embryonic heart.

Materials and methods

Reagents

Dimethylsulfoxide (DMSO) and antioxidant N2-mercaptopropionylglycine (MPG) were purchased from Sigma–Aldrich, JAK2/STAT3 inhibitor AG490 and PI3K/Akt inhibitor LY-294002 from Calbiochem and proteases inhibitors from Roche Biosciences. Rabbit antibody against phospho-Tyr^{705}-STAT3 was from Ab Frontier. Antibodies against phospho-Ser^{727}-STAT3, phospho-Tyr^{458}-PI3K, PI3K, phospho-Ser^{473}-Akt, Akt, phospho-Ser^{9}-GSK3beta, GSK3beta, phospho-Ser^{641}-GS, GS, phosphorylated ERK and ERK were from Cell Signaling Technology. Antibody against STAT3 was from Santa Cruz Biotechnology and the secondary antibody (goat anti-rabbit HRP conjugated) was from GE Healthcare. The enhanced chemiluminescence (ECL) western blot reagent kit was from PerkinElmer and films from GE Healthcare.

Preparation and in vitro mounting of the heart

Fertilized eggs from Lohman Brown hens were incubated during 96 h at 38°C and 90% relative humidity to obtain stage 24HH embryo (according to Hamburger and Hamilton [16]). The spontaneously beating hearts were carefully excised from explanted embryos by section at the level of the truncus arteriosus as well as between the sinus venosus and the atria. As previously described [45], the hearts were then placed in the culture compartment of a stainless steel chamber equipped with two windows for observation and maintained under controlled conditions on the thermostabilized stage (37.5°C) of an inverted microscope (IMT2 Olympus, Tokyo, Japan). Briefly, the incubation compartment (300 µL) was separated from the gas compartment by a 15 µm transparent and gas-permeable silicone membrane (RTV 141, Rhône-Poulenc, Lyon, France). Thus, PO_2 at the tissue level was strictly controlled and rapidly modified (within less than 5 s) by flushing high-grade gas of selected composition through the gas compartment. The standard HCO_3/CO_2 buffered tyrode (supp. file) medium was equilibrated in the chamber with 2.31% CO_2 in air containing 19.5% O_2 (normoxia and reoxygenation) or in N_2 (anoxia) yielding a pH of 7.4. AG490 was reconstituted in DMSO. MPG, AG490 and LY-294002 were diluted in tyrode containing 0.5, 0.006 and 0.006% DMSO (vehicle), respectively, and present throughout the experimental protocol.

Anoxia–reoxygenation protocol

After a 30 min pretreatment at room temperature in vehicle, MPG (1 mM), AG490 (10 µM) or LY-294002 (10 µM), hearts were mounted in the chamber, stabilized 45 min under normoxia and submitted to anoxia (30 min) and reoxygenation (80 min). The hearts were harvested after stabilization (S), 10 (A10) and 30 min (A30) of anoxia and 10 (R10), 30 (R30), 40 (R40), 50 (R50), 60 (R60) and 80 min (R80) of reoxygenation. Control hearts were maintained under steady normoxia 60 and 90 min after S, corresponding to the time points R30 and R60, respectively. At the end of the experiment, the ventricles were carefully dissected on ice and stored at −80°C for subsequent determinations.

Protein homogenate

For each sample, three ventricles were pooled because of the very small size of hearts. Ventricles were homogenized

by sonication 3 × 2 s in the ice-cold lysis buffer (supp. file) and protein content was measured by the method of Bradford (Coomassie protein assay kit, Pierce) with bovine serum albumin as standard.

Immunoblotting

Proteins from cellular extracts (20 µg) were boiled with 1/3 of SDS sample buffer (supp. file), separated on 10% SDS-polyacrylamide gels (1 h, 185 V), and transferred to nitrocellulose membranes (2 h, 100 V). The equal loading in the membranes was systematically verified by performing Red Ponceau and by determining densitometry of total proteins and GAPDH. Membranes were probed with primary antibodies against phospho-Tyr^{705}-STAT3 and phospho-GS (1:750); phospho-Ser^{727}-STAT3, phospho-PI3K, STAT3 and PI3K (1:500); phospho-Akt, phospho-GSK3beta, phospho-ERK, Akt, GSK3beta, GS and ERK (1:1,000) diluted in 5% bovine serum albumin in tris-buffered saline tween (TBS-T, supp. file) (overnight, 4°C). Blots were then incubated (1 h, room temperature) with the secondary antibody (1:10,000) in 1% non-fat milk in TBS-T. Immunoreactive bands were detected using the ECL western blot reagent kit. Signal was semi-quantitatively analyzed using scanning densitometry (Quantity One software, Biorad). Bands of phosphorylated proteins were normalized to the total protein in the same sample and in the same membrane. More specifically for STAT3, the phospho-α isoform (P-STAT3α) was normalized to the total α isoform. Phosphorylation level at each time point of anoxia and reoxygenation was normalized to the respective preanoxic S level. We used total cell extracts from serum-starved HeLa cells prepared with IFN-α treatment (Cell Signaling Technology) as a positive control for P-Tyr STAT3, in which the α isoform was largely predominant relative to the beta isoform.

Enriched nuclear and cytoplasmic fractions preparation

Cytoplasmic and nuclear extracts were obtained as described elsewhere [27]. Twelve ventricles were homogenized in hypotonic buffer (supp. file). After addition of detergent Nonidet P-40 (0,625%) and centrifugation, supernatants containing the cytoplasmic proteins were stored at −80°C. Pellets were resuspended in hypertonic buffer (supp. file), centrifugated and the resulting supernatants (nuclear fractions) were collected and stored at −80°C. Protein content was measured by the method of Bradford.

Electrophoretic mobility shift assay

A STAT3 oligonucleotide probe (supp. file) was labeled with α-^{32}PdCTP using the Klenow enzyme (Roche Applied Science). 10 µg of nuclear proteins were incubated with EMSA buffer (supp. file) and the probe for 20 min at room temperature. Samples were resolved on a nondenaturing polyacrylamide gel. Gels were transferred to Whatman 3 M paper, dried under vacuum, and exposed to photographic films at −80°C with intensifying screens. Densitometric analysis of autoradiographs was performed. A negative control was performed using either an antibody against STAT3 or an unlabeled probe. Ventricles isolated from hearts treated with H_2O_2 at 1 mM for 1 h were used as a positive control for STAT3.

Quantitative RT-PCR

Twelve ventricles were homogenized in trizol (Invitrogen) and total RNA were purified by slight modifications of the method originally described by Chomczynski & Sacchi [8]. The reverse transcription (RT) reaction was performed using the High capacity cDNA Reverse Transcription Kit and protocols from Applied Biosystem (ABI, Foster City, CA, USA). Briefly, the RT was run with 1.5 µg of total RNA in a reaction volume of 20 µl and aliquots of this reaction mixture (supp. file) were used for the subsequent PCR reactions. 5 ng of cDNA was laid per well. Results are calculated using the ΔCt method [29].

Recording of electrical and contractile activities

Electrical and contractile activities were recorded simultaneously and continuously throughout in vitro experiments as previously described [45]. The PR and RR intervals, the QT duration, the ventricular apical shortening and the electromechanical delay (EMDv) were determined as previously described [45]. The maximal velocity of contraction and relaxation was calculated from the maximal positive and negative values of the first derivative of shortening and relaxation, respectively. Atrial rate was determined by measuring the delay between two P waves and the RR interval by the delay between peaks of two successive QRS complexes. We also assessed QRS widening, reflecting a possible reduction of ventricular conduction, by measuring the half-width of the QRS complex.

Statistical analysis

Because of the very small size of the heart (circa 60 µg proteins) a total of about 2,300 chick embryos have been used in this study. Results are given as mean ± standard error of the mean (SEM) for immunoblotting densitometry and as mean ± standard deviation (SD) for functional parameters. The significance of any difference between two time points or two conditions was assessed using Mann–Whitney test. The statistical significance was defined by a value of $p \leq 0.05$.

Results

Profile of STAT3 phosphorylation and STAT3 nuclear translocation during anoxia–reoxygenation

Only the α isoform of P-Tyr STAT3 was detectable under our conditions although both α (~92 kDa) and beta (~83 kDa) STAT3 isoforms were expressed in the ventricle (Fig. 1a). P-Tyr STAT3α was not affected by anoxia (A10, A30) but increased during the first 60 min of reoxygenation (from R10 to R60) and returned to basal level at R80 (Fig. 1b). It should be noted that P-Tyr STAT3α increase was more pronounced at R10 and R60. By contrast, P-Ser STAT3α was not altered throughout reoxygenation compared to preanoxic level (Fig. 1b), the beta isoform bearing no serine phosphorylation site. The time-matched normoxic controls at S, R30 and R60 did not exhibit change in P-Tyr STAT3α indicating that the culture conditions did not alter STAT3 activation relative to preanoxia (Fig. 1b). In the nuclear fraction P-Tyr STAT3α increased at R10 and tend to increase at R60 ($p = 0.095$) (Fig. 1c) whereas STAT3 was significantly increased

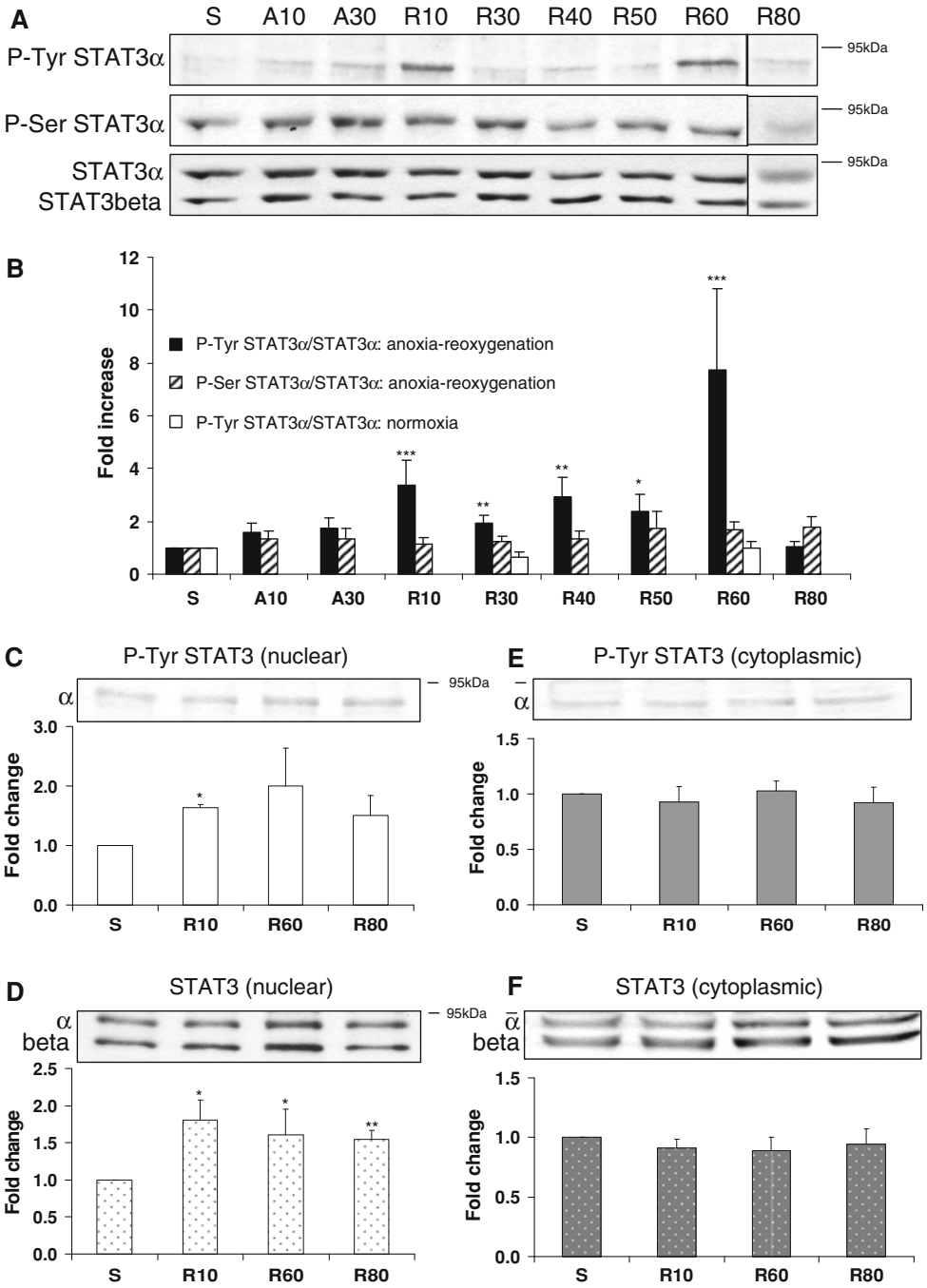

Fig. 1 Profile of STAT3α activation in homogenates, nuclear and cytoplasmic fractions of the ventricle during anoxia–reoxygenation. **a** Representative immunoblots of the α isoform of tyrosine phosphorylated STAT3 (P-Tyr STAT3α), serine phosphorylated STAT3 (P-Ser STAT3α) and α and beta isoforms of STAT3 during anoxia (A10 and A30) and reoxygenation (R10 to R80) in homogenates. **b** Densitometric analysis of P-STAT3α normalized to STAT3α. *Black columns* represent P-Tyr STAT3α and *hatched columns* P-Ser STAT3α during anoxia–reoxygenation and *open columns* P-Tyr STAT3α in normoxic controls at matching time-points S, R30 and R60. Representative immunoblots at S, R10, R60 and R80 and densitometric analysis of P-Tyr STAT3α (**c**) and STAT3α and STAT3beta (**d**) in enriched nuclear fraction; P-Tyr STAT3α (**e**) and STAT3α and STAT3beta (**f**) in cytoplasmic fraction. Data are expressed as fold change relative to the preanoxic value (S). $*p < 0.05$, $**p < 0.01$, $***p < 0.001$ versus S. $N = 4$–9 determinations for **b** and $N = 4$–13 determinations for **c**–**f**

throughout reoxygenation (Fig. 1d). By contrast, in the cytoplasmic fraction P-Tyr STAT3α and STAT3 were not affected (Fig. 1e, f). As total STAT3 increased in the nuclear fraction (Fig. 1d), P-Tyr STAT3α obtained in both fractions was not corrected for total STAT3 in Fig. 1c, e.

Involvement of STAT3 in functional recovery of the anoxic-reoxygenated embryonic heart

The recovery of atrial rate during reoxygenation was impaired and the coefficient of variability of the mean atrial rate was worsened by JAK2/STAT3 inhibition (Fig. 2a; Table 1). It should be noticed that during the first 15 min of reoxygenation the coefficient of variability of the mean atrial rate was increased in untreated hearts as well because of the unavoidable interferences of the reoxygenation-induced arrhythmias as described elsewhere [45]. However, at R30 the beat-to-beat variability of RR was clearly higher in AG490-treated hearts (Fig. 2b, c). All the other electrical and mechanical parameters were not significantly affected by AG490 (Table 1), i.e. atrioventricular (PR interval) and intraventricular conduction (QRS widening), QT duration and excitation–contraction coupling (EMDv). AG490 had no inotropic (shortening) or lusitropic (relaxation) effects. The types of arrhythmias (including atrial ectopy, atrioventricular block, Wenchebach) were similar in treated and untreated hearts. Furthermore, arrhythmias persisted throughout reoxygenation in 30% of

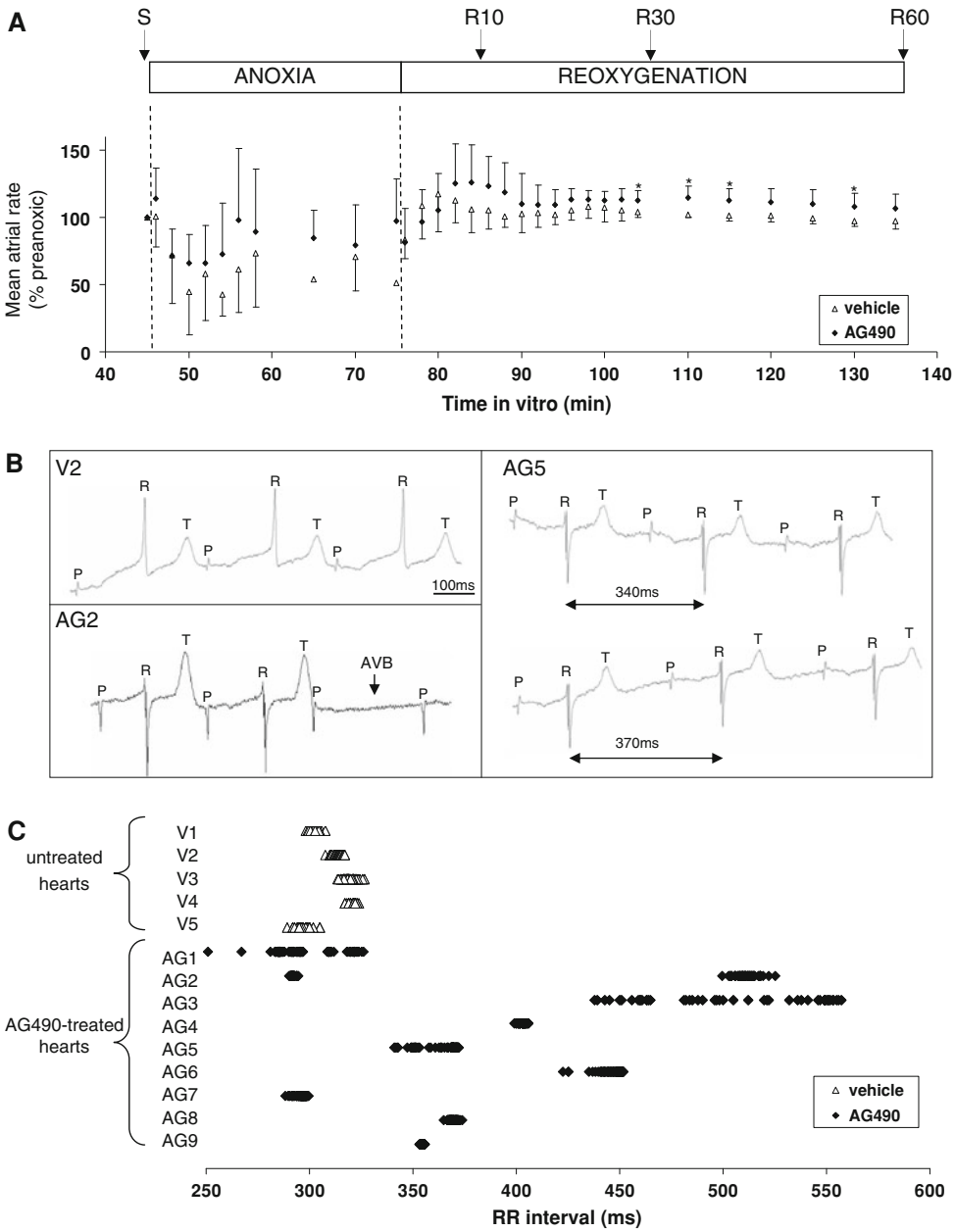

Fig. 2 STAT3 inhibition affected recovery of atrial rhythm during reoxygenation. **a** Mean atrial rate during anoxia–reoxygenation relative to the preanoxic level in vehicle (*open triangles*, $n = 5$) or in 10 μM AG490 (*black diamonds*, $n = 9$), mean ± SD. Note the greatest SD in treated hearts throughout reoxygenation. $^{*}p < 0.05$ versus vehicle. **b** Representative ECGs with P, R and T components in vehicle (V2, *upper left panel*) or in AG490 illustrating arrhythmias, i.e. PR prolongation followed by atrioventricular block (AVB; AG2, *lower left panel*) and variations of RR interval from one cardiac cycle to another at R30 (AG5, *right panel*). **c** Distribution of individual RR intervals in five untreated hearts (vehicle, V1–V5) and in nine AG490-treated hearts (AG1–AG9) at R30. The beat-to-beat analysis was performed on 100 successive cycles

Table 1 Functional parameters under normoxia and during reoxygenation

	S	R10	R30	R60
Mean atrial rate (bpm)				
v	191 ± 8	202 ± 31	198 ± 8	185 ± 8
AG	160 ± 26	193 ± 27	180 ± 33	170 ± 28
Coefficient of variability of the mean atrial rate (%)				
v	4	15	4	4
AG	16	14	18	17
PR interval (ms)				
v	133 ± 22	169 ± 34	143 ± 35	126 ± 32
AG	128 ± 33	145 ± 25	126 ± 29	119 ± 33
QT duration (ms)				
v	153 ± 10	182 ± 5	153 ± 19	150 ± 26
AG	149 ± 12	137 ± 9	131 ± 9	139 ± 11
Contraction/relaxation velocity ratio				
v	0.96 ± 0.26	0.93 ± 0.28	1.00 ± 0.14	1.00 ± 0.21
AG	1.05 ± 0.12	0.91 ± 0.28	1.03 ± 0.30	1.20 ± 0.18
Ventricular shortening (μm)				
v	16.5 ± 9.6	7.8 ± 8.7	18 ± 15	10.7 ± 8.5
AG	14.1 ± 7.9	9.0 ± 6.2	9 ± 8	26 ± 26
EMDv (ms)				
v	26 ± 10	54 ± 4	33 ± 1	26 ± 9
AG	25 ± 4	28 ± 10	25 ± 3	27 ± 5
QRS half-width (ms)				
v	3.4 ± 1.5	3.7 ± 2.0	3.2 ± 0.8	4.6 ± 2.0
AG	3.0 ± 1.3	4.26 ± 2.0	3.5 ± 1.6	3.2 ± 1.5

Electrical and mechanical parameters were not different in vehicle (V) and in 10 μM AG490 (AG) at S, R10, R30 and R60. However, the interindividual coefficient of variability of the mean atrial rate appeared to be the highest in AG490-treated group at S, R30 and R60. Mean ± SD; Mann–Whitney test, $N = 3$–9 determinations

EMDv ventricular electromechanical delay

the treated hearts, while they ceased at R30 in all other hearts.

ROS-dependent STAT3α activation during post-anoxic reoxygenation

The level of P-Tyr STAT3α was significantly decreased by MPG at R10 and R60, time-points at which activation of STAT3 was the strongest, with no effect at S (Fig. 3). The level of P-Tyr STAT3α at R10 in Fig. 3 was lower than that shown in Fig. 1a, this effect was due to variability between experiments and/or the conditions of immunoblotting.

STAT3 DNA-binding

STAT3 DNA-binding activity determined by EMSA (Fig. 4a) did not vary during reoxygenation as illustrated by densitometry (Fig. 4b). Ventricles from hearts treated with H_2O_2 were used as a positive control to show that the technique was sensitive enough to detect any change in STAT3 DNA-binding activity in this embryonic tissue (+33% in hearts treated with H_2O_2) (Fig. 4c). A negative control of DNA-binding performed by adding an antibody against STAT3 or an unlabeled probe to the samples showed that the upper band corresponding to STAT3 disappeared under these two conditions (Fig. 4c). The unexpected finding that STAT3 was translocated without DNA-binding was supported by the fact that the level of mRNA expression of three STAT3 specific target genes in the context of ischemia–reperfusion, i.e. inducible NO synthase (iNOS), manganese superoxide dismutase (MnSOD) and cyclooxygenase-2 (Cox-2), was not increased even at R80 (data not shown).

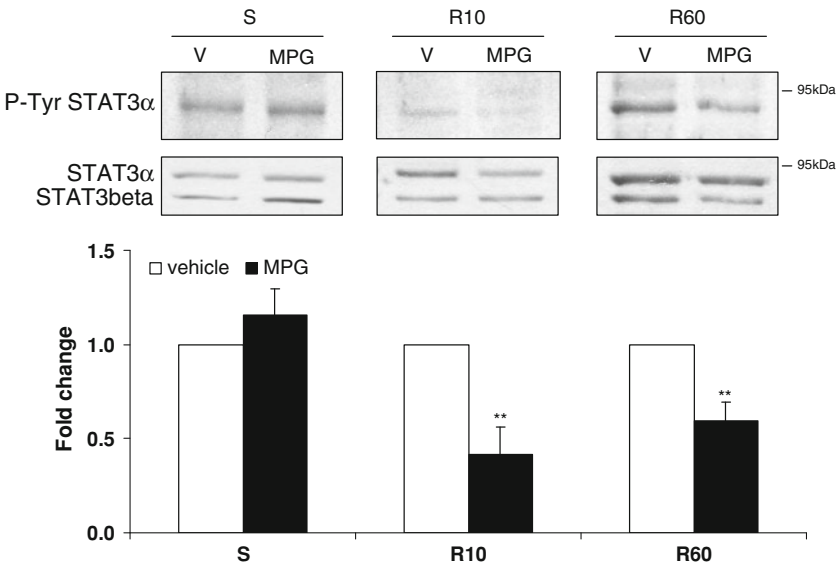

Fig. 3 ROS-dependent STAT3α activation in the ventricle during post-anoxic reoxygenation. Immunoblots of P-Tyr STAT3α, STAT3α and STAT3beta in vehicle (V) or in 1 mM MPG at S, R10 and R60 in homogenates (*upper panels*). Densitometric analysis of P-Tyr STAT3α normalized to STAT3α in 1 mM MPG (*black columns*) and expressed as fold change relative to vehicle (*open columns*) at S, R10 and R60 in homogenates (*lower panel*). $^{**}p < 0.01$ vs vehicle. $N = 6$–15 determinations

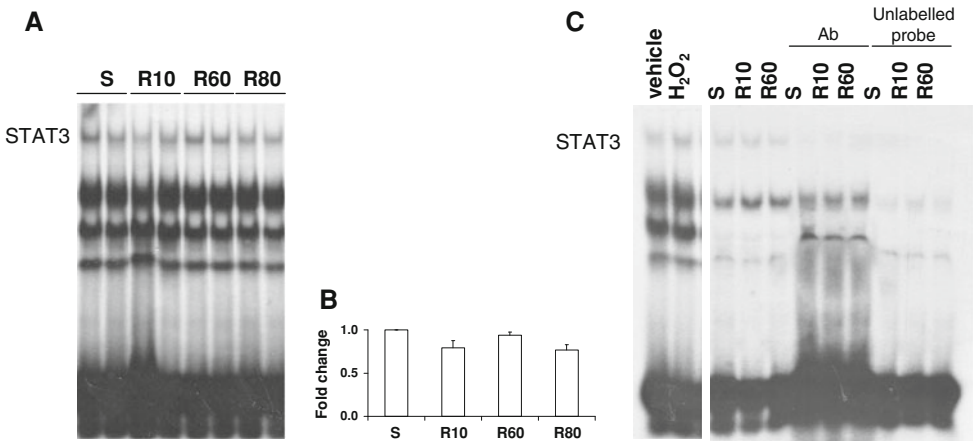

Fig. 4 At reoxygenation STAT3 did not bind to DNA. **a** Representative EMSA of STAT3 at S, R10, R60 and R80 (duplicates) and **b** densitometric analysis of STAT3 in EMSA. **c** On the *left panel*, positive control with ventricles isolated from hearts treated with H_2O_2 at 1 mM for 1 h and on the *right panel* negative control with antibody (Ab) against STAT3 and unlabeled probe at S, R10 and R60. $N = 3$–4 determinations

Distribution of PI3K, Akt, GSK3beta, glycogen synthase (GS) and ERK2 and possible crosstalk with STAT3

Using histone H1 and GAPDH as specific markers of enriched nuclear and cytoplasmic fractions, respectively, we found that phosphorylated and total forms of PI3K, Akt, GS and ERK2 were restricted to cytoplasm. Basal level of phosphorylated GSK3beta was markedly higher in the nuclear fraction than in the cytoplasmic fraction whereas the total form of GSK3beta was comparable in the two compartments (Fig. 5). The temporal pattern of phosphorylation varied from one component of the RISK pathway to another. PI3K and Akt phosphorylation peaked at R10 (Fig. 6a, b) while GSK3beta as well as GS phosphorylation was increased at R10 and R60 (Fig. 6c, d). Relative to the latest proteins, ERK2 phosphorylation was delayed at R60 (Fig. 6e). The possibility of interaction between RISK and JAK2/STAT3 pathways was assessed pharmacologically by AG490, a common JAK2/STAT3 pathway inhibitor. As expected, AG490 significantly decreased P-Tyr STAT3α and P-Akt at R10 and R60 as well (Fig. 7a, c). AG490 reduced GS (Fig. 7d) and ERK2 (Fig. 7e) phosphorylation at R10 only with no effect on PI3K phosphorylation (Fig. 7b). GSK3beta being the only protein of the RISK pathway present in the nuclear compartment, together with STAT3, we checked separately the effect of STAT3 inhibition on the phosphorylation level of nuclear GSK3beta (Fig. 8). Nuclear and cytoplasmic P-GSK3beta significantly increased between S and R10 while GSK3beta did not vary (Fig. 8a). GSK3beta phosphorylation was decreased by AG490 in the nuclear fraction at R10 (Fig. 8b) but remained unchanged in the cytoplasmic fraction (Fig. 8c). The possible effect of PI3K/Akt on STAT3 phosphorylation was evaluated pharmacologically using LY-294002, a common PI3K/Akt pathway inhibitor. As expected, LY-294002 decreased P-Akt by 55% at R10 (Fig. 9a) but did not affect P-Tyr STAT3α (Fig. 9b).

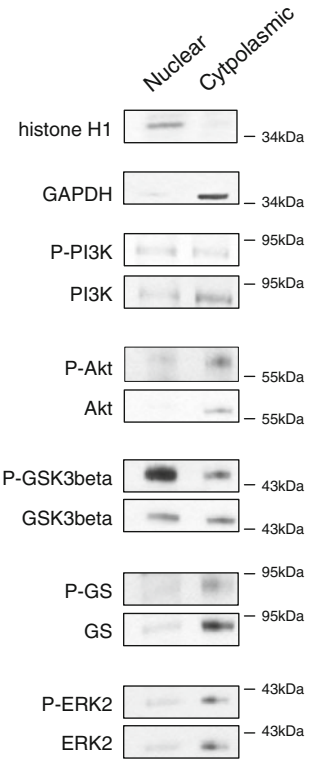

Fig. 5 Distribution and level of phosphorylation of PI3K, Akt, GSK3beta, GS and ERK2 in nuclear and cytoplasmic fractions of the ventricle. Representative immunoblots of basal content of phosphorylated and total forms of PI3K, Akt, GSK3beta, GS and ERK2 in enriched nuclear and cytoplasmic fractions of the ventricle. Histone H1 was used as a nuclear marker and GAPDH as a cytoplasmic marker (*upper panels*)

Discussion

To the best of our knowledge, this is the first time that the modulation of the JAK2/STAT3 pathway by a transient anoxic stress and its functional consequences are explored during early cardiogenesis. Our main findings indicate that (1) reoxygenation induces ROS-dependent phosphorylation

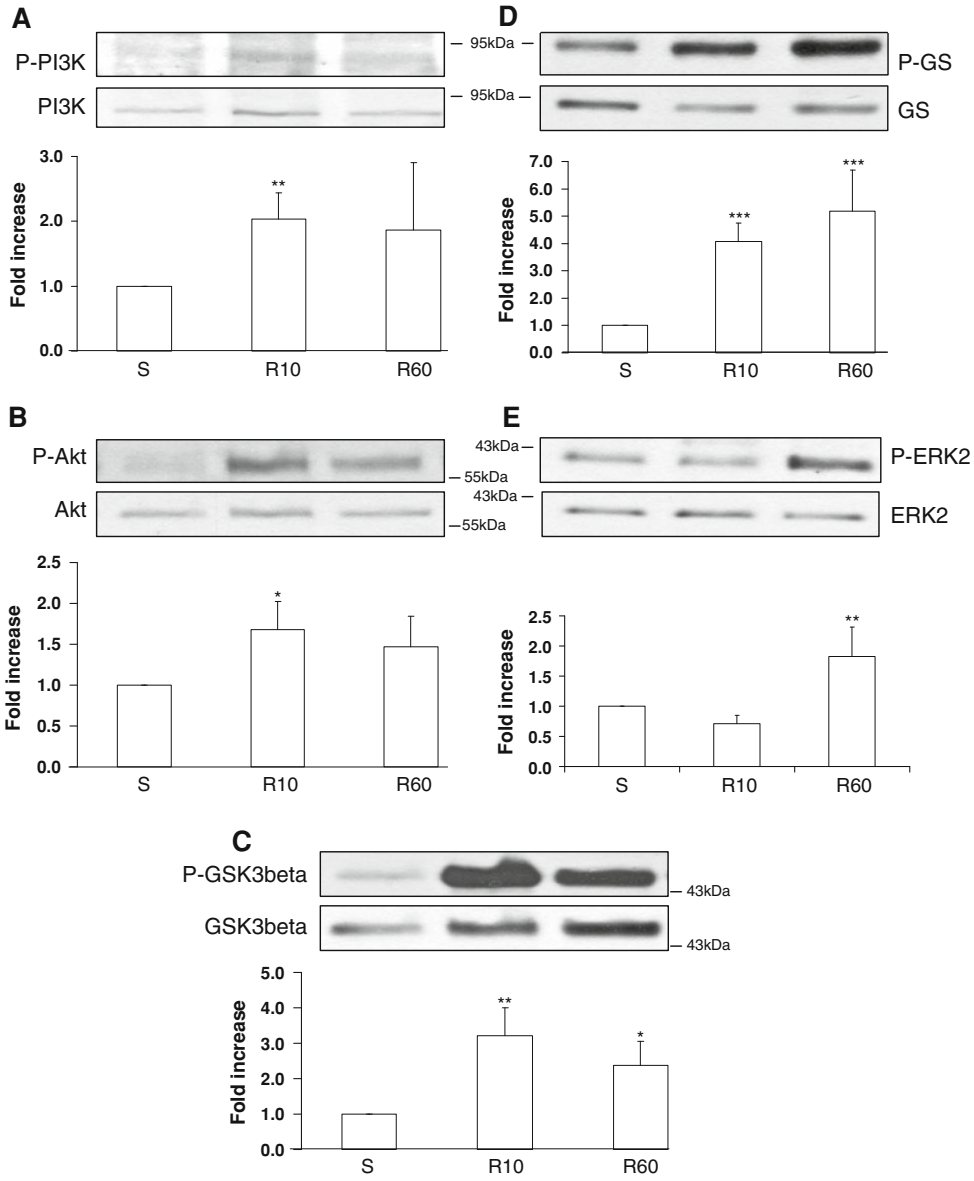

Fig. 6 Profile of PI3K, Akt, GSK3beta, GS and ERK2 activation in the ventricle during post-anoxic reoxygenation. Representative immunoblots and densitometry of phosphorylated PI3K, Akt, GSK3beta, GS and ERK2 (**a**–**e**, respectively) normalized to total protein in homogenates at S, R10 and R60. Data are expressed as fold increase relative to S. $*p < 0.05$, $**p < 0.01$, $***p < 0.001$ vs S. $N = 5$–12 determinations

of Tyr-STAT3α but not Ser-STAT3α, (2) P-Tyr STAT3α translocates into the nuclear compartment without binding to DNA and inhibits GSK3beta, (3) phosphorylation of STAT3α activates Akt and ERK2 and inhibits GS in the cytoplasmic compartment, (4) there is no dual interaction of STAT3 with proteins of the RISK pathway, and (5) activation of the JAK2/STAT3 pathway reduces the reoxygenation-induced arrhythmias.

Characteristics and limitations of the model

In the embryonic ventricle, only STAT3 and GSK3beta appeared to be present both in the nuclear and cytoplasmic fractions. PI3K, Akt, GS and ERK2 were restricted to the cytoplasm, whereas in neonatal and adult cardiomyocytes PI3K [42], Akt [35] and ERK [38] are detected also in the nuclear compartment. These observations suggest that the cytoplasm–nucleus shuttling of proteins, including transcription factors, may well depend on the level of differentiation and maturation of the cardiomyocytes. We were able to detect JAK2 by immunoblotting (not shown) but it was technically difficult to reveal its phosphorylated form with antibodies available on the market. AG490, a tyrosine kinase inhibitor which reduces JAK2 activity, significantly decreased the reoxygenation-induced STAT3 phosphorylation as expected, which validates this pharmacological approach to rapidly interfere with the JAK2/STAT3 pathway. Regarding ERK, as previously shown [12], only the p42 isoform (ERK2) is detectable in the embryonic and adult chicken heart, in contrast to neonatal and adult murine heart. As mentioned elsewhere [44], the isolated embryonic heart displays noticeable interindividual

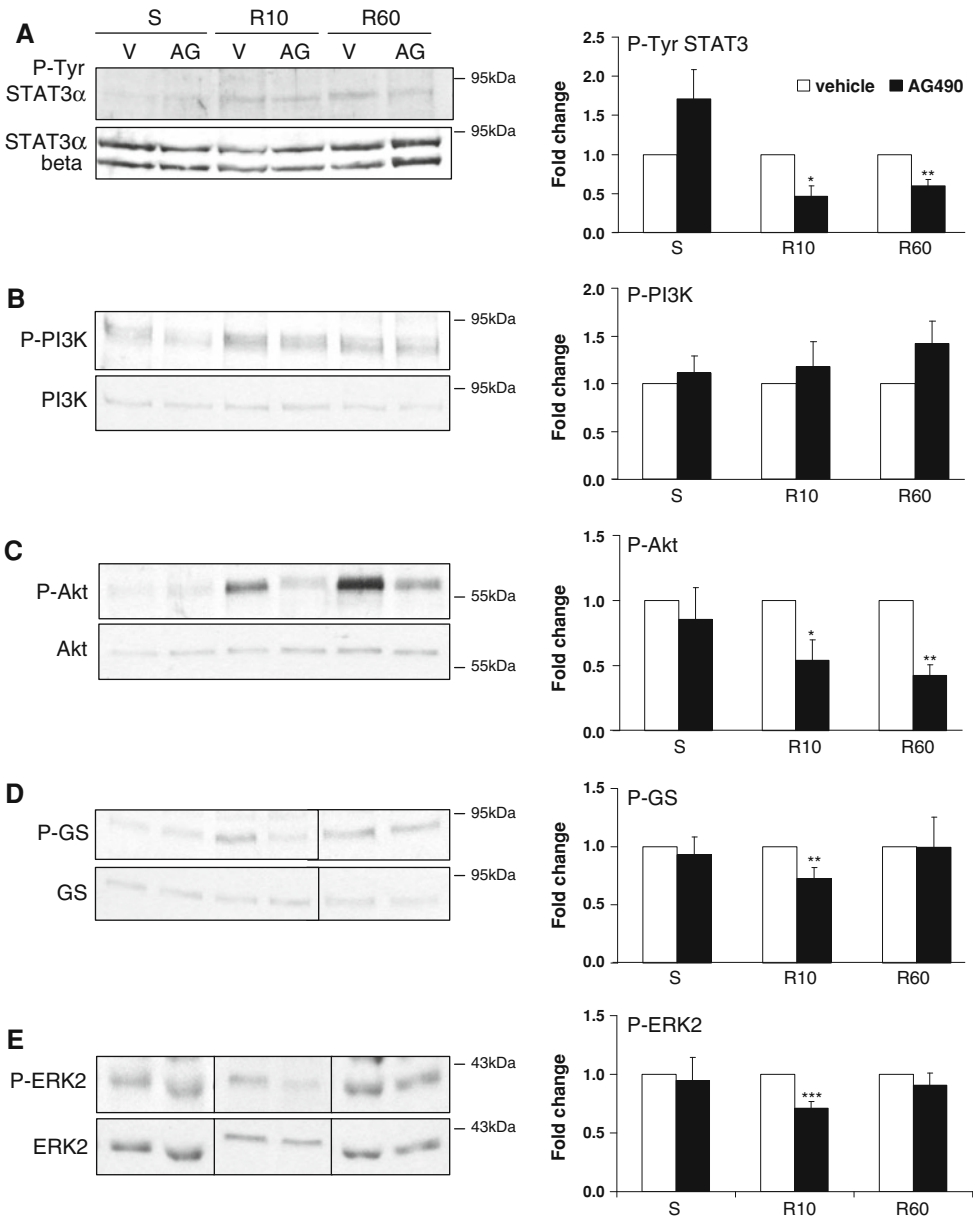

Fig. 7 JAK2/STAT3 inhibition significantly reduced reoxygenation-induced phosphorylation of Akt, GS and ERK2. On *left panels*, immunoblots of phosphorylated Tyr STAT3α, PI3K, Akt, GS and ERK2 (**a**–**e**, respectively) in vehicle (V) or in 10 μM AG490 (AG) at S, R10 and R60 in homogenates. On *right panels*, densitometric analysis of phosphorylated Tyr STAT3α, PI3K, Akt, GS and ERK2 (**a**–**e**, respectively) normalized to total protein in 10 μM AG490 (*black columns*) and expressed relative to vehicle (*open columns*) at S, R10 and R60 in homogenates. $*p < 0.05$, $**p < 0.01$, $***p < 0.001$ vs vehicle. $N = 4$–11 determinations

variations of the functional parameters and ECGs performed in similar conditions can also modestly differ in morphology from one experiment to another. Such variations could be due to slight interindividual differences in developmental stage, three-dimensional geometry of the hearts mounted in the chamber and variable vicinity of the recording electrodes. It is also conceivable that intrinsic oscillations of activation of signaling pathways in the embryonic cardiomyocytes [23], combined with variable rate of proliferation and differentiation in the different cell populations, could partly contribute to increase the inter-individual variations of STAT3 phosphorylation determined at a given time point (specially at R60). A significant variability of the phosphorylation level of signaling proteins such as JNK, p38 and ERK2, has also been observed in the same experimental setting [12, 43]. It should be noticed that, contrary to the adult, the ventricle of the 4-day old embryonic chick heart is mostly composed of proliferating and differentiating cardiomyocytes with few endothelial and epicardial cells and no fibroblasts [49].

STAT3 phosphorylation and translocation during anoxia–reoxygenation

The full-length STAT, the α isoform, can undergo alternative splicing at the 3′ end gene transcripts leading to shorter beta isoform with truncated C-terminal domain (lacking 48 amino acids) [28]. STAT3α and STAT3beta are distinctly different in their activation, transcriptional activities, and biological functions [47]. Our data indicate

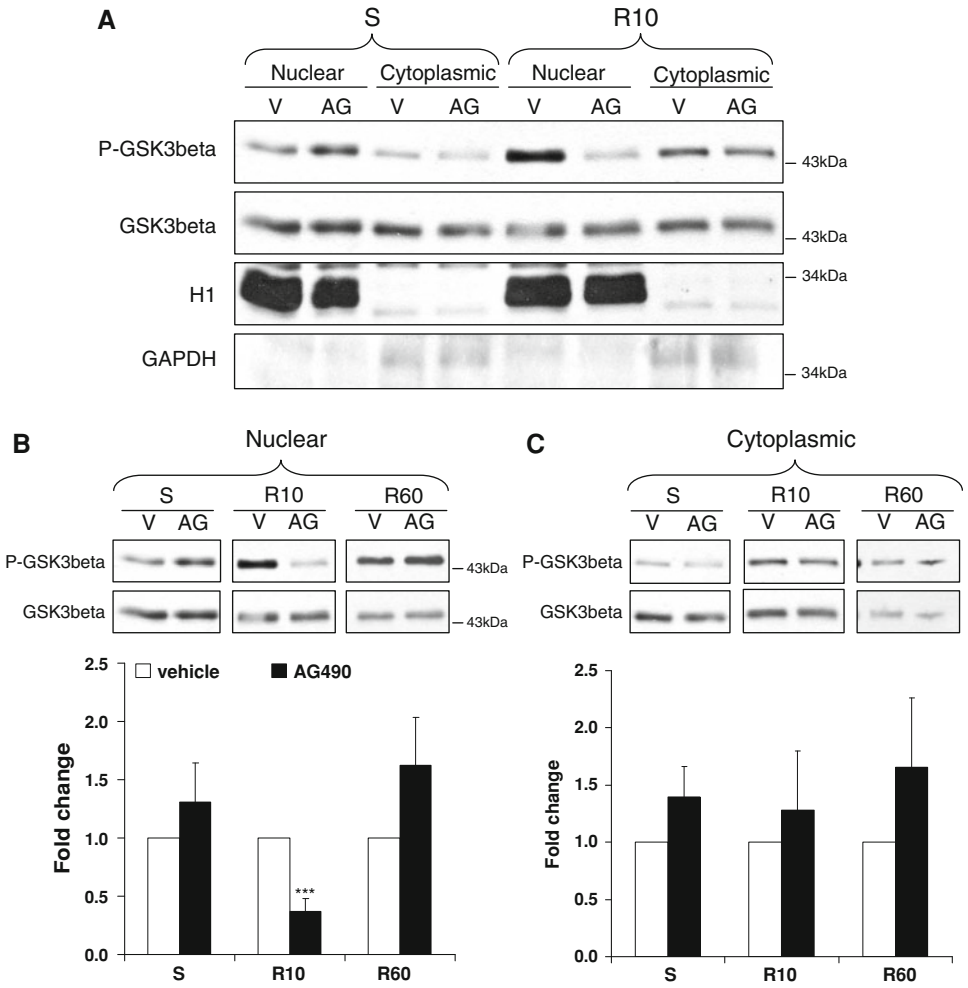

Fig. 8 Reoxygenation-induced phosphorylation/inhibition of GSK3beta in the nuclear compartment depended on JAK2/STAT3 activation. **a** Representative immunoblots of P-GSK3beta and GSK3beta in enriched nuclear and cytoplasmic fractions in vehicle (*V*) or in 10 μM AG490 (*AG*) at S and R10. Histone H1 was used as a nuclear marker and GAPDH as a cytoplasmic marker. **b** Representative immunoblots (*upper panels*) and densitometric analysis (*lower panels*) of phosphorylated GSK3beta in enriched nuclear fraction and **c** in cytoplasmic fraction in AG490 (AG, *black columns*) and expressed as fold change relative to vehicle (V, *open columns*) at S, R10 and R60. $***p < 0.001$ versus vehicle. $N = 3$–6 determinations

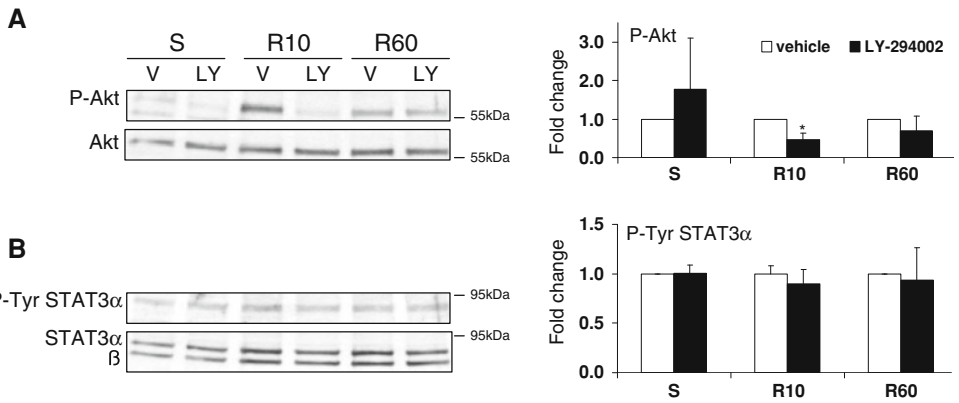

Fig. 9 PI3K/Akt inhibition by LY-294002 did not affect reoxygenation-induced phosphorylation of STAT3. On *left panels*, immunoblots of phosphorylated and total forms of **a** Akt and **b** STAT3 in vehicle (V) or in 10 μM LY-294002 (LY) at S, R10 and R60 in homogenates. On right panels, densitometric analysis of phosphorylated **a** Akt and **b** Tyr STAT3α normalized to total protein in 10 μM LY-294002 (*black columns*) and expressed relative to vehicle (*open columns*) at S, R10 and R60 in homogenates. $*p < 0.05$ versus vehicle. $N = 3$ determinations

that α and beta isoforms of STAT3 are strongly expressed in the embryonic heart but that only the α isoform is responsive to post-anoxic reoxygenation whereas STAT3beta is known to have a critical developmental function [9] which was not investigated in this work. As tyrosine rather than serine site was phosphorylated by

reoxygenation, the possibility of STAT3 activation by MAPKs [24] can be ruled out under our conditions since serine is preferentially phosphorylated by these pathways. More specifically, although p38MAPK and ERK2 are known to be activated at R10 and R30, respectively [12], they did not phosphorylate $STAT3^{Ser727}$. At R10 activation of STAT3 observed in homogenate principally reflected what took place in the nuclear compartment since only nuclear P-Tyr STAT3α increased significantly as in pharmacological postconditioned adult murine hearts [26]. At R60 nuclear P-Tyr STAT3α tended to remain higher than the preanoxic level and the rise in nuclear STAT3 observed at R10 persisted throughout reoxygenation suggesting that translocated STAT3 was sequestered in the nuclear compartment. An increase in nuclear phosphorylated STAT3 is observed also in the ethanolamine-induced protection of the adult heart against ischemia–reperfusion injury [22].

The presence of mitochondrial STAT3 in our preparation cannot be ruled out since STAT3 is known to be present in mitochondria of several tissues [2, 14, 55] and it has also recently been shown that mitochondrial activated STAT3 contributes to cardioprotection by stimulation of respiration and inhibition of mPTP opening [4]. However, in embryonic myocardium mitochondria are scarce and not fully differentiated by contrast with adult tissue and their contribution to the cellular content of STAT3, if any, should be minor.

Involvement of the JAK2/STAT3 pathway in cardiac rhythm

We have previously shown that the embryonic heart fully recovers at R60 [44] but the signaling pathways underlying the mechanisms of recovery remain relatively unexplored. Activated STAT3 is known to exert its late cardioprotective action (e.g., antiapoptotic properties [30]) mainly via alteration of transcription of target genes principally induced by pre- or postconditioning [3]. However, the short-term consequences of STAT3 activation on the electrical and mechanical activities have never been investigated, including those in the developing heart. At R30, inhibition of JAK2/STAT3 gave rise to the highest variability of atrial rate and RR interval, indicating that activation of STAT3 is involved in recovery of atrial and ventricular rhythm. As there are no extrinsic innervation at the embryonic stage investigated and no neurohumoral influence in the culture chamber, the fluctuations of rhythm (dysrhythmias) originated exclusively at the level of the pacemaker tissues, independently of the physiological spontaneous oscillations of heart rate reported previously [45]. These observations and the fact that arrhythmias persisted throughout reoxygenation in 30% of the AG-treated hearts, strongly suggest that activated STAT3 can protect cardiac automaticity by interacting with pacemaking mechanisms, especially under pathological conditions. We have previously shown that subtle modulation of L-type calcium, K_{ATP} and HCN channels can improve postanoxic recovery of the embryonic heart [6, 44, 46, 54]. It is conceivable that crosstalk between JAK2/STAT3 and RISK pathways may directly or indirectly control finely these ion channels affecting membrane potential, and contributing to protect pacemaker rate under adverse conditions. However, our present findings show clearly that activated STAT3 has no dromo-, ino- and lusitropic effects in the anoxic-reoxygenated embryonic heart since atrioventricular (PR) and intraventricular (QRS widening) conduction, ventricular contractility (shortening) and relaxation (ratio contraction/relaxation velocity) as well as excitation–contraction coupling (EMDv) were not affected by STAT3 inhibition. Additionally, the types of arrhythmias during anoxia and reoxygenation we previously documented [45] were similar in untreated and AG-treated hearts.

ROS-dependent STAT3α activation during post-anoxic reoxygenation

Our present finding that STAT3α phosphorylation on tyrosine was ROS-dependent at R10 and R60 is consistent with our preliminary data showing that exogenous H_2O_2 also activates STAT3 [Pedretti et al. (personal communication)] and with studies performed in neonatal cardiomyocytes [30] and adult myocardium [33]. However, at R10 there is a strong burst of ROS whereas at R60 ROS production returns to its preanoxic level [44] suggesting that the ROS-dependent mechanisms of STAT3 activation are different during the early (R10) and late (R60) phases of reoxygenation. This phenomenon could be partly due to chemical differences between radical species produced at R10 and R60 (i.e. superoxide anion $O_2^{\bullet -}$ being predominantly generated during early reoxygenation) and to variations of the relative contribution of mitochondrial and extramitochondrial (mainly NADPH oxidases) sources of oxyradicals throughout reoxygenation [40]. This issue deserves further investigation. The concept of the ROS-mediated protection is also verified in permeabilized cardiac muscle fibers in which the mitochondrial tolerance to anoxia–reoxygenation is improved by TNFα through ROS production [25].

STAT3 DNA-binding during anoxia–reoxygenation

After its activation STAT3 is known to dimerize and subsequently translocate into the nuclear compartment, where it can modulate expression of specific target genes [20] including iNOS, MnSOD and Cox-2 known to be

involved in cardioprotection [5, 36, 44]. The facts that STAT3 DNA-binding activity was not altered and that mRNA level of these genes remained stable throughout reoxygenation indicate that translocated STAT3 had no detectable transcriptional activity. Additionally, the level of STAT3 phosphorylation on serine remained constant throughout the experimental protocol (~2 h), STAT3 requiring phosphorylation on both sites (tyrosine and serine) to be maximally active in the assembly of active transcription complexes [56]. As activated STAT3 was not linked to DNA, we investigated the possible interaction with other signaling pathways, in particular with the RISK pathway.

Crosstalk between JAK2/STAT3 and RISK pathways

It is still unknown to what extent the survival kinases of the RISK pathway are activated by anoxia–reoxygenation as opposed to ischemia–reperfusion. The temporal profile of phosphorylation shows that components of the RISK pathway (ERK and PI3K-Akt-GSK3beta cascade) were differently modulated during the early (R10) and late (R60) phases of reoxygenation. Phosphorylation of PI3K, Akt and GSK3beta was maximal at R10 whereas activation of ERK2 was delayed at R60 as previously described [12]. The AG490-mediated reduction of phosphorylation of Akt, ERK2 and nuclear GSK3beta indicates clearly that activation of the JAK2/STAT3 pathway can modulate RISK components upon reoxygenation (R10) both in the cytoplasmic (Akt and ERK2) and nuclear (GSK3beta) compartments. We checked the presence of ERK2 in the nuclear compartment in basal conditions whereas ERK2 translocates into the nucleus only when it is phosphorylated. At R10 we found an interaction between ERK2 and STAT3 in homogenate but did not assess specifically the effect of AG490 on ERK2 phosphorylation in nucleus and cytoplasm because ERK2 was not phosphorylated at R10 and consequently not present in the nucleus. The strong basal phosphorylation/inhibition of GSK3beta in the nuclear compartment might be a characteristic of the rapidly growing embryonic ventricle. The additional inhibitory effect of STAT3 on nuclear GSK3beta in the first 10 min of reoxygenation may be determinant as GSK3beta is known to regulate many transcription factors and modulate cellular functions [34]. In H_2O_2-treated neonatal [30] and ischemic-reperfused adult [11, 13, 15] cardiomyocytes STAT3 inhibition reduces also Akt and GSK3beta phosphorylation but the intracellular localization has not yet been established. However, our results show that a preferential and predominant interaction between JAK2/STAT3 pathway and Akt persists throughout reoxygenation since AG490 leads to strong inactivation of Akt up to R60, which is not the case for GSK3beta, ERK2 and GS. Whatever the time point investigated, reoxygenation-induced activation of PI3K was unrelated with JAK2/STAT3 pathway in the embryonic heart like an ischemic-reperfused heart model [13], although such a dissociation remains controversial [52]. Furthermore, GS which is a downstream target of GSK3beta, was strongly phosphorylated/inhibited from R10 onward, despite the fact that the phosphorylated form of GSK3beta was inactive. Consequently, other kinases such as PKA, AMPK, CK1 or CK2 [32] may phosphorylate/inhibit GS, reducing glycogen storage which is known to be specially important in the embryonic myocardium and to play a cardioprotective role [41]. The mechanisms by which activation of JAK2/STAT3 pathway phosphorylate GS at R10 and might transiently reduce glycogen synthesis are beyond the scope of this work. At R10, it appears that there is no dual interaction between PI3K/Akt and JAK2/STAT3 pathways in the embryonic heart. Such an interaction remains controversial in neonatal and adult cardiomyocytes and depends on the type of pathological situation such as ischemic [52] and pharmacological pre- [15, 52] and postconditioning [13] and oxidant stress [30]. Regarding

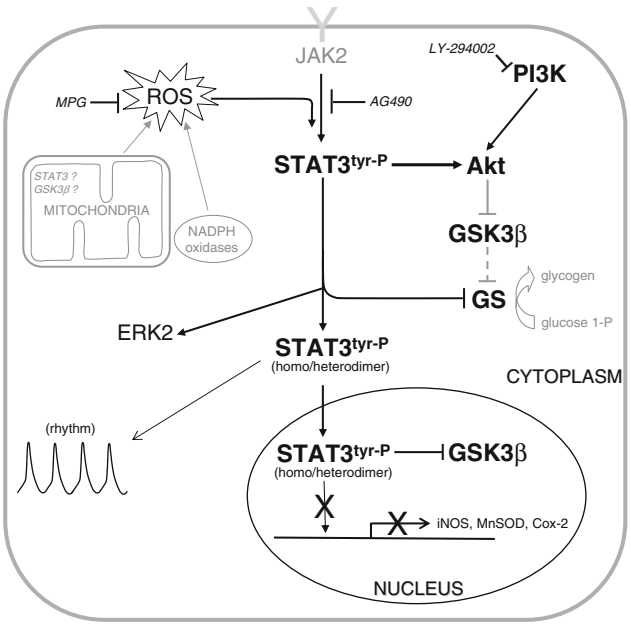

Fig. 10 Schematic representation based on our findings and illustrating STAT3 activation and its possible interaction with the RISK pathway components during the early phase of reoxygenation (10 min) in the embryonic ventricle. In the cytoplasm, mitochondria- and NADPH oxidase-derived ROS stimulate the JAK2/STAT3 pathway which in turn activates Akt and ERK2 and inhibits GS. Activated STAT3 translocates into the nucleus and induces GSK3beta inhibition without binding to DNA. Activation of STAT3 stabilized cardiac rhythm. *Arrow*, activation; *T-shaped symbol*, inhibition. Pharmacological agents used are indicated in *italics*. *Dotted lines* indicate putative activation/inhibition. Representations in *light gray* were not explored in the present work

the importance and the relevance of the RISK pathway, it should be noticed that Skyschally et al. [50] showed that, in hearts of larger mammals like pigs, RISK activation might not be necessary for postconditioning.

In conclusion, this study shows for the first time that the JAK2/STAT3 pathway plays a complex role in the myocardial response to anoxia–reoxygenation during a critical period of cardiogenesis. Indeed, besides its nuclear translocation, the reoxygenation-activated transcription factor STAT3 is also capable of interacting rapidly with various signaling proteins of the RISK pathway present in distinct cellular compartments (Fig. 10). Furthermore, the fact that STAT3 activation improved post-anoxic recovery of cardiac rhythm illustrates the potential role that STAT3 could play in the protection of cardiovascular function in a developing organism. Our findings might be of relevance to better understand the adaptative response of the heart to intermittent, transient or chronic oxygen deprivation during early fetal life, a relatively unexplored area.

Acknowledgments We thank Dr Stéphany Gardier, Dr Noureddine Loukili, Dr Joëlle Rolli and Dr Alexandre Sarre for their advices, Anne-Catherine Thomas for her skillful technical assistance and Dr Antoinette Defaux for providing the histone H1 antibody. This work was supported by the Swiss National Science Foundation, [3100A0-105901].

Conflict of interest None declared.

References

1. Ananthakrishnan R, Hallam K, Li Q, Ramasamy R (2005) JAK-STAT pathway in cardiac ischemic stress. Vascul Pharmacol 43:353–356. doi:10.1016/j.vph.2005.08.020
2. Boengler K, Heusch G, Schulz R (2010) Mitochondria in post-conditioning. Antioxid Redox Signal 2010 Sep 29. [epub ahead of print] doi:10.1089/ars.2010.3309
3. Boengler K, Hilfiker-Kleiner D, Drexler H, Heusch G, Schulz R (2008) The myocardial JAK/STAT pathway: from protection to failure. Pharmacol Ther 120:172–185. doi:10.1016/j.pharmthera.2008.08.002
4. Boengler K, Hilfiker-Kleiner D, Heusch G, Schulz R (2010) Inhibition of permeability transition pore opening by mitochondrial STAT3 and its role in myocardial ischemia/reperfusion. Basic Res Cardiol 105:771–785. doi:10.1007/s00395-010-0124-1
5. Bolli R, Dawn B, Xuan YT (2003) Role of the JAK-STAT pathway in protection against myocardial ischemia/reperfusion injury. Trends Cardiovasc Med 13:72–79. doi:S1050173802002300X
6. Bruchez P, Sarre A, Kappenberger L, Raddatz E (2008) The L-Type Ca+ and KATP channels may contribute to pacing-induced protection against anoxia–reoxygenation in the embryonic heart model. J Cardiovasc Electrophysiol 19:1196–1202. doi:10.1111/j.1540-8167.2008.01218.x
7. Burton GJ, Jaunaiux E (2001) Maternal vascularisation of the human placenta: does the embryo develop in a hypoxic environment? Gynecol Obstet Fertil 29:503–508. doi:10.1016/S1297-9589(01)00179-5
8. Chomczynski P, Sacchi N (1987) Single-step method of RNA isolation by acid guanidinium thiocyanate–phenol–chloroform extraction. Anal Biochem 162:156–159. doi:10.1006/abio.1987.99990003-2697(87)90021-2
9. Dewilde S, Vercelli A, Chiarle R, Poli V (2008) Of alphas and betas: distinct and overlapping functions of STAT3 isoforms. Front Biosci 13:6501–6514. doi:10.2741/3170
10. Foshay K, Rodriguez G, Hoel B, Narayan J, Gallicano GI (2005) JAK2/STAT3 directs cardiomyogenesis within murine embryonic stem cells in vitro. Stem Cells 23:530–543. doi:10.1634/stemcells.2004-0293
11. Fuglesteg BN, Suleman N, Tiron C, Kanhema T, Lacerda L, Andreasen TV, Sack MN, Jonassen AK, Mjos OD, Opie LH, Lecour S (2008) Signal transducer and activator of transcription 3 is involved in the cardioprotective signalling pathway activated by insulin therapy at reperfusion. Basic Res Cardiol 103:444–453. doi:10.1007/s00395-008-0728-x
12. Gardier S, Pedretti S, Sarre A, Raddatz E (2010) Transient anoxia and oxyradicals induce a region-specific activation of MAPKs in the embryonic heart. Mol Cell Biochem 340:239–247. doi:10.1007/s11010-010-0423-8
13. Goodman MD, Koch SE, Fuller-Bicer GA, Butler KL (2008) Regulating RISK: a role for JAK-STAT signaling in postconditioning? Am J Physiol Heart Circ Physiol 295:H1649–H1656. doi:10.1152/ajpheart.00692.2008
14. Gough DJ, Corlett A, Schlessinger K, Wegrzyn J, Larner AC, Levy DE (2009) Mitochondrial STAT3 supports Ras-dependent oncogenic transformation. Science 324:1713–1716. doi:10.1126/science.1171721
15. Gross ER, Hsu AK, Gross GJ (2006) The JAK/STAT pathway is essential for opioid-induced cardioprotection: JAK2 as a mediator of STAT3, Akt, and GSK-3 beta. Am J Physiol Heart Circ Physiol 291:H827–H834. doi:10.1152/ajpheart.00003.2006
16. Hamburger V, Hamilton H (1951) A series of normal stages in the development of the chick embryo. J Morphol 88:49–92. doi:10.1002/aja.1001950404
17. Hausenloy DJ, Lecour S, Yellon DM (2010) RISK and SAFE pro-survival signalling pathways in ischaemic postconditioning: two sides of the same coin. Antioxid Redox Signal 2010 Oct 26 [epub ahead of print]. doi:10.1089/ars.2010.3360
18. Hausenloy DJ, Yellon DM (2006) Survival kinases in ischemic preconditioning and postconditioning. Cardiovasc Res 70:240–253. doi:10.1016/j.cardiores.2006.01.017
19. Heusch G, Boengler K, Schulz R (2008) Cardioprotection: nitric oxide, protein kinases, and mitochondria. Circulation 118:1915–1919. doi:10.1161/CIRCULATIONAHA.108.805242
20. Imada K, Leonard WJ (2000) The Jak-STAT pathway. Mol Immunol 37:1–11. doi:S0161589000000183
21. Jensen A, Garnier Y, Berger R (1999) Dynamics of fetal circulatory responses to hypoxia and asphyxia. Eur J Obstet Gynecol Reprod Biol 84:155–172. doi:S030121159800325X
22. Kelly RF, Lamont KT, Somers S, Hacking D, Lacerda L, Thomas P, Opie LH, Lecour S (2010) Ethanolamine is a novel STAT-3 dependent cardioprotective agent. Basic Res Cardiol 105:763–770. doi:10.1007/s00395-010-0125-0
23. Ko ML, Shi L, Grushin K, Nigussie F, Ko GY (2010) Circadian profiles in the embryonic chick heart: L-type voltage-gated calcium channels and signaling pathways. Chronobiol Int 27:1673–1696. doi:10.3109/07420528.2010.514631
24. Kurdi M, Booz GW (2007) Can the protective actions of JAK-STAT in the heart be exploited therapeutically? Parsing the regulation of interleukin-6-type cytokine signaling. J Cardiovasc Pharmacol 50:126–141. doi:10.1097/FJC.0b013e318068dd4900005344-200708000-00005

25. Lacerda L, McCarthy J, Mungly SF, Lynn EG, Sack MN, Opie LH, Lecour S (2010) TNFalpha protects cardiac mitochondria independently of its cell surface receptors. Basic Res Cardiol 105:751–762. doi:10.1007/s00395-010-0113-4
26. Lacerda L, Somers S, Opie LH, Lecour S (2009) Ischemic postconditioning protects against reperfusion injury via the SAFE pathway. Cardiovasc Res 84:201–208. doi:10.1093/cvr/cvp274
27. Levrand S, Pesse B, Feihl F, Waeber B, Pacher P, Rolli J, Schaller MD, Liaudet L (2005) Peroxynitrite is a potent inhibitor of NF-{kappa}B activation triggered by inflammatory stimuli in cardiac and endothelial cell lines. J Biol Chem 280:34878–34887. doi:10.1074/jbc.M501977200
28. Lim CP, Cao X (2006) Structure, function, and regulation of STAT proteins. Mol Biosyst 2:536–550. doi:10.1039/b606246f
29. Livak KJ, Schmittgen TD (2001) Analysis of relative gene expression data using real-time quantitative PCR and the 2(-Delta Delta C(T)) Method. Methods 25:402–408. doi:10.1006/meth.2001.1262S1046-2023(01)91262-9
30. Lu Y, Zhou J, Xu C, Lin H, Xiao J, Wang Z, Yang B (2008) JAK/STAT and PI3 K/AKT pathways form a mutual transactivation loop and afford resistance to oxidative stress-induced apoptosis in cardiomyocytes. Cell Physiol Biochem 21:305–314. doi:10.1159/000129389
31. Maltepe E, Simon MC (1998) Oxygen, genes, and development: an analysis of the role of hypoxic gene regulation during murine vascular development. J Mol Med 76:391–401. doi:10.1007/s001090050231
32. Marks F, Klingmüller U, Müller-Decker K (2009) Cellular signal processing. Garland Science, New York, pp 194–196
33. McCormick J, Barry SP, Sivarajah A, Stefanutti G, Townsend PA, Lawrence KM, Eaton S, Knight RA, Thiemermann C, Latchman DS, Stephanou A (2006) Free radical scavenging inhibits STAT phosphorylation following in vivo ischemia/reperfusion injury. Faseb J 20:2115–2117. doi:10.1096/fj.06-6188fje
34. Meares GP, Jope RS (2007) Resolution of the nuclear localization mechanism of glycogen synthase kinase-3: functional effects in apoptosis. J Biol Chem 282:16989–17001. doi:10.1074/jbc.M700610200
35. Miyamoto S, Rubio M, Sussman MA (2009) Nuclear and mitochondrial signalling Akts in cardiomyocytes. Cardiovasc Res 82:272–285. doi:10.1093/cvr/cvp087
36. Negoro S, Kunisada K, Fujio Y, Funamoto M, Darville MI, Eizirik DL, Osugi T, Izumi M, Oshima Y, Nakaoka Y, Hirota H, Kishimoto T, Yamauchi-Takihara K (2001) Activation of signal transducer and activator of transcription 3 protects cardiomyocytes from hypoxia/reoxygenation-induced oxidative stress through the upregulation of manganese superoxide dismutase. Circulation 104:979–981. doi:10.1161/hc3401.095947
37. Negoro S, Kunisada K, Tone E, Funamoto M, Oh H, Kishimoto T, Yamauchi-Takihara K (2000) Activation of JAK/STAT pathway transduces cytoprotective signal in rat acute myocardial infarction. Cardiovasc Res 47:797–805. doi:S0008-6363(00)00138-3
38. Pantos C, Xinaris C, Mourouzis I, Malliopoulou V, Kardami E, Cokkinos DV (2007) Thyroid hormone changes cardiomyocyte shape and geometry via ERK signaling pathway: potential therapeutic implications in reversing cardiac remodeling? Mol Cell Biochem 297:65–72. doi:10.1007/s11010-006-9323-3
39. Raddatz E, Gardier S, Sarre A (2006) Physiopathology of the embryonic heart (with special emphasis on hypoxia and reoxygenation). Ann Cardiol Angeiol (Paris) 55:79–89. doi:10.1016/j.ancard.2006.02.007
40. Raddatz E, Thomas AC, Sarre A, Benathan M (2010) Differential contribution of mitochondria, NADPH-oxidases and glycolysis to region-specific oxidant stress in the anoxic-reoxygenated embryonic heart. Am J Physiol Heart Circ Physiol 2010 Dec 30 [epub ahead of print]. doi:10.1152/ajpheart.00827.2010
41. Romano R, Rochat AC, Kucera P, De Ribaupierre Y, Raddatz E (2001) Oxidative and glycogenolytic capacities within the developing chick heart. Pediatr Res 49:363–372. doi:0031-3998/01/4903-0363
42. Rubio M, Avitabile D, Fischer K, Emmanuel G, Gude N, Miyamoto S, Mishra S, Schaefer EM, Brown JH, Sussman MA (2009) Cardioprotective stimuli mediate phosphoinositide 3-kinase and phosphoinositide dependent kinase 1 nuclear accumulation in cardiomyocytes. J Mol Cell Cardiol 47:96–103. doi:10.1016/j.yjmcc.2009.02.022
43. Sarre A, Gardier S, Maurer F, Bonny C, Raddatz E (2008) Modulation of the c-Jun N-terminal kinase activity in the embryonic heart in response to anoxia–reoxygenation: involvement of the Ca2+ and mitoKATP channels. Mol Cell Biochem 313:133–138. doi:10.1007/s11010-008-9750-4
44. Sarre A, Lange N, Kucera P, Raddatz E (2005) mitoKATP channel activation in the postanoxic developing heart protects E-C coupling via NO-, ROS-, and PKC-dependent pathways. Am J Physiol Heart Circ Physiol 288:H1611–H1619. doi:10.1152/ajpheart.00942.2004
45. Sarre A, Maury P, Kucera P, Kappenberger L, Raddatz E (2006) Arrhythmogenesis in the developing heart during anoxia–reoxygenation and hypothermia–rewarming: an in vitro model. J Cardiovasc Electrophysiol 17:1350–1359. doi:10.1111/j.1540-8167.2006.00637.x
46. Sarre A, Pedretti S, Gardier S, Raddatz E (2010) Specific inhibition of HCN channels slows rhythm differently in atria, ventricle and outflow tract and stabilizes conduction in the anoxic-reoxygenated embryonic heart model. Pharmacol Res 61:85–91. doi:10.1016/j.phrs.2009.09.007
47. Schaefer TS, Sanders LK, Park OK, Nathans D (1997) Functional differences between Stat3alpha and Stat3beta. Mol Cell Biol 17:5307–5316. doi:0270-7306/97/$04.0010
48. Sedmera D, Kucera P, Raddatz E (2002) Developmental changes in cardiac recovery from anoxia–reoxygenation. Am J Physiol Regul Integr Comp Physiol 283:R379–R388. doi:10.1152/ajpregu.00534.2001
49. Sedmera D, Pexieder T, Vuillemin M, Thompson RP, Anderson RH (2000) Developmental patterning of the myocardium. Anat Rec 258:319–337. doi:10.1002/(SICI)1097-0185(20000401)258:4<319:AID-AR1>3.0.CO;2-O
50. Skyschally A, van Caster P, Boengler K, Gres P, Musiolik J, Schilawa D, Schulz R, Heusch G (2009) Ischemic postconditioning in pigs: no causal role for RISK activation. Circ Res 104:15–18. doi:10.1161/CIRCRESAHA.108.186429
51. Stephanou A, Brar BK, Knight RA, Latchman DS (2000) Opposing actions of STAT-1 and STAT-3 on the Bcl-2 and Bcl-x promoters. Cell Death Differ 7:329–330. doi:10.1038/sj.cdd.4400656
52. Suleman N, Somers S, Smith R, Opie LH, Lecour S (2008) Dual activation of STAT-3 and Akt is required during the trigger phase of ischaemic preconditioning. Cardiovasc Res 79:127–133. doi:10.1093/cvr/cvn067
53. Takeda K, Noguchi K, Shi W, Tanaka T, Matsumoto M, Yoshida N, Kishimoto T, Akira S (1997) Targeted disruption of the mouse Stat3 gene leads to early embryonic lethality. Proc Natl Acad Sci USA 94:3801–3804. doi:0027-8424y97y943801-4$2.00y0
54. Tenthorey D, de Ribaupierre Y, Kucera P, Raddatz E (1998) Effects of verapamil and ryanodine on activity of the embryonic chick heart during anoxia and reoxygenation. J Cardiovasc Pharmacol 31:195–202. doi:00005344-199802000-00004
55. Wegrzyn J, Potla R, Chwae YJ, Sepuri NB, Zhang Q, Koeck T, Derecka M, Szczepanek K, Szelag M, Gornicka A, Moh A, Moghaddas S, Chen Q, Bobbili S, Cichy J, Dulak J, Baker DP,

Wolfman A, Stuehr D, Hassan MO, Fu XY, Avadhani N, Drake JI, Fawcett P, Lesnefsky EJ, Larner AC (2009) Function of mitochondrial Stat3 in cellular respiration. Science 323:793–797. doi:10.1126/science.1164551

56. Wen Z, Zhong Z, Darnell JE Jr (1995) Maximal activation of transcription by Stat1 and Stat3 requires both tyrosine and serine phosphorylation. Cell 82:241–250. doi:0092-8674(95)90311-9

Mol Cell Biochem (2010) 340:239–247
DOI 10.1007/s11010-010-0423-8

Transient anoxia and oxyradicals induce a region-specific activation of MAPKs in the embryonic heart

Stephany Gardier · Sarah Pedretti · Alexandre Sarre · Eric Raddatz

Received: 26 August 2009 / Accepted: 26 February 2010 / Published online: 21 March 2010

Abstract We have previously reported in the early septating embryonic heart that electromechanical disturbances induced by anoxia-reoxygenation are distinct in atria, ventricle, and outflow tract, and are attenuated in ventricle by opening of mitochondrial K_{ATP} (mitoK_{ATP}) channels. Here, we assessed the regional activation of mitogen-activated protein kinases (MAPKs) ERK, p38, and JNK in response to anoxia-reoxygenation and H_2O_2. Hearts isolated from 4-day-old chick embryos were subjected to 30-min anoxia and 60-min reoxygenation or exposed to H_2O_2 (50 μM–1 mM). The temporal pattern of activation of ERK, p38, and JNK in atria, ventricle, and outflow tract was determined using immunoblotting and/or kinase assay. The effect of the mitoK_{ATP} channel opener diazoxide (50 μM) on JNK phosphorylation was also analyzed. Under basal conditions, total ERK and JNK were homogeneously distributed within the heart, whereas total p38 was the lowest in outflow tract. The phosphorylated/total form ratio of each MAPK was similar in all regions. Phosphorylation of ERK increased in atria and ventricle at the end of reoxygenation without change in outflow tract. Phosphorylation of p38 was augmented by anoxia in the three regions, and returned to basal level at the end of reoxygenation except in the outflow tract. JNK activity was not altered by anoxia-reoxygenation in atria and outflow tract. In ventricle, however, the diazoxide-inhibitable peak of JNK activity known to occur during reoxygenation was not accompanied by a change in phosphorylation level. H_2O_2 over 500 μM impaired cardiac function, phosphorylated ERK in all the regions and p38 in atria and outflow tract, but did not affect JNK phosphorylation. At a critical stage of early cardiogenesis, anoxia, reoxygenation, exogenous H_2O_2 and opening of mitoK_{ATP} channels can subtly modulate ERK, p38, and JNK pathways in a region-specific manner.

Keywords p38 MAP kinase · ERK · JNK · Anoxia-reoxygenation · Embryonic heart · Oxyradicals

S. Gardier · S. Pedretti · A. Sarre · E. Raddatz
Department of Physiology, Faculty of Biology and Medicine, University of Lausanne, Lausanne, Switzerland

S. Gardier (✉)
Faculty of Medicine, University of Geneva, 1 Rue Michel Servet, 1211 Geneve 4, Switzerland
e-mail: stephany.gardier@hcuge.ch

Introduction

The embryonic/fetal heart develops and operates normally in a relatively hypoxic intrauterine environment, but reacts rapidly to oxygen lack [1–3]. Oxygen deprivation during critical periods of embryogenesis impairs heart development and function, resulting in growth retardation and increasing the risk of cardiovascular disease in adulthood [4–6]. Maternal hypoxemia, reduction in umbilical blood flow or placental dysfunction can rapidly lead to acute or chronic ischemia and/or hypoxia. Although the post-ischemic fetal heart seems to recover faster than the adult heart [7, 8], the tolerance of the embryonic heart to hypoxia and its capacity to recover during reoxygenation remain under debate. Moreover, the functional and developmental consequences of oxygen lack may vary from one cardiac region to another since the tissue properties and the fate of each part of the heart are different. Atria differentiate at older stages into pacemaker tissue, ventricle into working myocardium and outflow tract into aorta and pulmonary artery. In previous works, we have precisely characterized the electrical and contractile disturbances induced by

anoxia and reoxygenation in the heart isolated from 4-day-old chick embryos [9, 10]. Arrhythmias and myocardial stunning observed at reoxygenation are associated with a burst of reactive oxygen species (ROS) [9], and recovery of excitation–contraction coupling in the ventricle is improved by pharmacological activation of the mitochondrial K_{ATP} (mitoK_{ATP}) channels, via PKC, NO-, and ROS-dependent mechanisms. However, the signaling pathways underlying the response to anoxia-reoxygenation remain unclear in the embryonic heart.

Mitogen-activated protein kinases (MAPKs), which belong to a highly conserved family of serine/threonine kinases, are present in all eukaryotic cells and are signaling proteins that play a key role in response to a wide range of stress [11]. The three best-characterized MAPKs, extracellular signal-regulated protein kinase (ERK), c-jun NH_2-terminal kinase (JNK), and p38 MAPK have been involved in a vast array of physiopathological mechanisms in cardiac cells [12–15], and are notably implicated in ischemia–reperfusion injury and in pre- and post-conditioning mechanisms [16–19]. Previous studies, mainly focused on newborn or adult models [12], have reported conflicting data, and the involvement of MAPKs pathways in the response of the fetal heart to limiting oxygen levels has been poorly investigated. We have recently shown in the ventricle of the embryonic chick heart that JNK pathway is involved in the response to anoxia-reoxygenation and that reoxygenation-induced peak of JNK activity was ROS-independent and tightly related to the open-state of the mitoK_{ATP} channel [20]. Regarding the response to oxygen deprivation and reoxygenation, some differential sensitivity is expected within the embryonic heart since anoxic tolerance [9], energy metabolism [21], Ca^{2+} handling [22, 23], myofilaments [24], oxidative stress [25], sensitivity to NO [26], and electrical [27] and contractile [10] properties vary from one cardiac region to another. These important developmental, structural, and functional differences combined with the fact that activation of MAPKs depends on the nature of the stimuli and the cell-type [28] lead us to hypothesize that ERK, p38, and JNK pathways display distinct spatio-temporal patterns of activation in response to a transient anoxic stress. The main goal of the present work was to investigate the expression and the profile of activation of ERK, p38, and JNK in atria, ventricle and outflow tract of the embryonic heart submitted to anoxia, reoxygenation, and oxidant stress.

Methods

Reagents

All standard chemicals, as well as dimethylsulfoxide (DMSO), hydrogen peroxide (H_2O_2), and mitoK_{ATP} channel opener diazoxide were analytical grade and purchased from Sigma-Aldrich. [γ-^{33}P] ATP was from Amersham Biosciences and inhibitors of proteases from Roche Biosciences. Rabbit antibodies against phosphorylated-ERK1/2, phosphorylated-p38, phosphorylated-JNK1/2, total-ERK1/2, total-p38, total-JNK1/2 were purchased from Cell Signaling Technology. The antibody against α-actin was from Sigma-Aldrich and the secondary antibody (goat anti-rabbit HRP conjugated) was from GE Healthcare. The enhanced chemiluminescence (ECL) western blot reagent kit was from Pierce and the films from GE Healthcare.

Preparation and in vitro mounting of the heart

Because of the minute size of the heart (circa 60 µg proteins) and its parts at the stage investigated, a total of about 1000 chick embryos were utilized in this study. All experiments were performed in accordance with the guidelines of the local veterinary authority. Fertilized eggs from Lohman Brown hens were incubated during 96 h at 38°C and 95% relative humidity to obtain stage 24 HH embryo (according to Hamburger and Hamilton [29]). The spontaneously beating hearts were carefully excised from explanted embryos by section at the level of the truncus arteriosus as well as between the sinus venosus and the atria. The hearts were then placed in the culture compartment of an airtight chamber.

The stainless steel chamber was equipped with two windows for observation and maintained under controlled conditions on the thermostabilized stage (37.5°C) of an inverted microscope (IMT2 Olympus, Tokyo, Japan) as previously detailed [10]. Briefly, the culture compartment (300 µl) was separated from the gas compartment by a 15 µm transparent and gas-permeable silicone membrane (RTV 141, Rhône-Poulenc, Lyon, France). Thus, pO_2 at the tissue level could be strictly controlled and rapidly modified (within less than 5 s) by flushing high-grade gas of selected composition through the gas compartment. At this developmental stage, the heart lacks vascularization and the myocardial oxygen requirement is met exclusively by diffusion.

The culture medium was standard HCO_3/CO_2 buffered Tyrode medium, equilibrated in the chamber with 2.31% CO_2 in air (normoxia and reoxygenation) or in N_2 (anoxia) yielding a pH of 7.4. Diazoxide was diluted in this medium containing 0.5% DMSO (vehicle) and present throughout the experimental protocol.

Anoxia-reoxygenation protocol

After a 30 min preincubation at room temperature in vehicle or in diazoxide (50 µM), hearts were mounted in vitro and stabilized 45 min under normoxia at 37°C, and then submitted to strict anoxia during 30 min, followed by

60 min of reoxygenation. The hearts were harvested after the period of normoxic stabilization, after 30 min of anoxia and after 10, 30, and 60 min of reoxygenation. Atria, ventricle, and outflow tract of each heart were carefully dissected on ice and stored at -80°C for subsequent determinations.

Hydrogen peroxide (H_2O_2) exposure

The hearts were placed in a Petri dish in the standard medium, stabilized 45 min under normoxia and then exposed 1 h to 50, 100, 200, 500 or 1000 μM of H_2O_2 at 37°C. Cardiac rhythmicity and contractility were not different in hearts cultured in Petri dishes or in hearts mounted in culture chamber. The critical H_2O_2 concentration that impaired cardiac function was obtained by determining the proportion of hearts still beating at the end of each experiment. Atria, ventricle, and outflow tract were then carefully dissected on ice and stored at -80°C for subsequent determinations.

Protein extract preparation

Atria, ventricles, and outflow tracts were homogenized by sonication 3 × 2 s in the ice-cold lysis buffer. For each sample six atria, three ventricles, and six outflow tracts were pooled. Insoluble material was removed by 5 min centrifugation at 10,000×*g* and protein content was measured by the method of Bradford (Coomassie protein assay kit, Pierce) with bovine serum albumin as standard.

Immunoblotting

Proteins from whole cellular extracts (20 μg) were boiled with 33 vol.% of SDS sample buffer, separated on 10% SDS-polyacrylamide gels, and transferred to nitrocellulose membranes, which were probed with primary antibodies against MAPKs (1:1000) or against α-actine (1:5000) diluted in 5% bovine serum albumin in TBS-T (overnight, 4°C). The blots were then incubated (1 h, room temperature) with secondary antibody (1:10000) in 1% non-fat milk powder in TBS-T. Immunoreactive bands were detected with enhanced chemiluminescent procedure using SuperSignal West Dura Extended Duration Substrate (Pierce, Rockford, IL, USA). The signal was semi-quantitatively analyzed using scanning densitometry (Quantity-One software, Biorad).

Protein bands were normalized to total-MAPKs or α-actin content in the same sample. In turn, the resulting densitometric ratio obtained during anoxia and reoxygenation was normalized to an internal control (the respective preanoxic ratio), and reported as fold increase. Thus, all the values >1 indicate a level of phosphorylation higher than the preanoxic level.

Kinase assay

JNK activity was determined according to a published method [30] with minor modifications [20]. Soluble protein extracts (30 μg) were incubated for 3 h at 4°C in the presence of 1 μg GST-c-Jun$_{(1–219)}$ bound to glutathione-agarose beads as both JNK-specific ligand and substrate. The beads were washed three times in washing buffer, and twice in kinase buffer. Kinase reaction was carried out for 30 min at 30°C in 20 μl of kinase buffer containing 5 μCi [γ-^{33}P]ATP. Reaction products were resolved by 12% SDS-polyacrylamide gel electrophoresis, gels were dried, and phosphorylation signals were visualized by autoradiography and quantitated by PhosphoImager (Quantity-One 1.4.0, Biorad) and normalized to the respective preanoxic control level.

Statistical analysis

Results are given as mean ± standard error of the mean (SEM). Statistical analysis was performed using Statistica 8.0 Software. Differences between time-points were determined by Kruskal-Wallis test followed by multiple comparisons post-hoc test. The significance of any difference between two conditions was assessed by Mann–Whitney test. The statistical significance was defined by a value of $P \leq 0.05$.

Results

Inhomogeneous MAPKs distribution under basal conditions

Under basal conditions (i.e., just dissected heart) the content of total form of ERK (p42) and JNK (p54) was similar in the three regions of the heart (Fig. 1a, b). However, in the outflow tract, the content of total form of p38 was lower than in atria and ventricle, and expression of p46 isoform of JNK was not detectable. In the three regions of embryonic heart p44 isoform of ERK was not expressed.

The phosphorylated to total form ratio of ERK, p38, and JNK was not significantly different in atria, ventricle, and outflow tract (Fig. 1b). Ventricle contained more α-actin than atria and outflow tract for the same quantity of protein (Fig. 1c).

Exogenous H_2O_2 phosphorylated MAPKs differently in atria, ventricle, and outflow tract

In order to determine to what extent myocardial MAPKs can be stimulated by H_2O_2, hearts were exposed to a concentration ranging from 50 μM to 1 mM. Cardiac

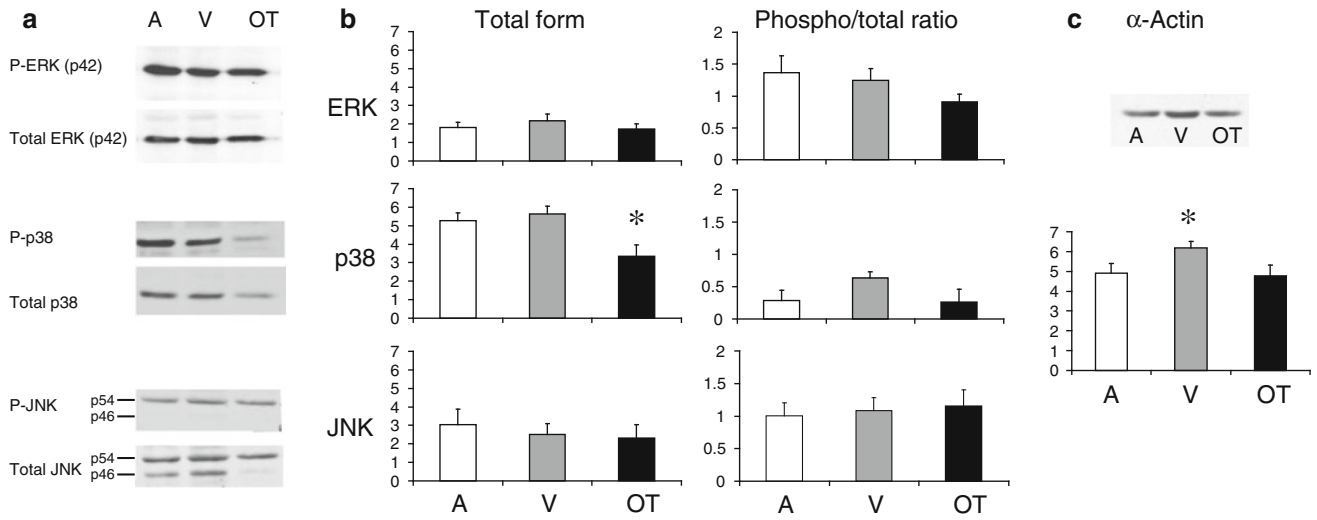

Fig. 1 Basal distribution of MAPKs and actin in atria (A), ventricle (V), and outflow tract (OT) of the embryonic chick heart at stage 24HH. **a** Representative immunoblots for phosphorylated and total ERK, p38, and JNK. **b** Densitometric analysis (arbitrary units) of total form and the phosphorylated to total form ratio. **c** Actin content. Only p38 (**a**, **b**) and JNKp46 (**a**) were inhomogeneously expressed. The phospho/total ratio was the lowest for p38 in the three regions. The content of α-actin was the highest in ventricle. The same quantity of protein was loaded in each lane of all the immunoblots (20 μg). $n = 4$–10 determinations; * $P < 0.05$ vs. A or V

function was clearly impaired by H_2O_2 at a rather high concentration (1 mM) which was subsequently used to assess its effects on the level of MAPK phosphorylation (Fig. 2a). Compared to controls, H_2O_2 promoted ERK phosphorylation in the whole heart, and significantly increased p38 phosphorylation only in atria and outflow tract. Surprisingly, the level of JNK phosphorylation was not altered by 1 mM H_2O_2, whatever the investigated region (Fig. 2b).

Anoxia-reoxygenation activated MAPKs differently in atria, ventricle, and outflow tract

The Fig. 3 shows the spatio-temporal modulation of the MAPKs in the embryonic heart subjected to anoxia and reoxygenation.

ERK phosphorylation

ERK phosphorylation increased during reoxygenation in atria and ventricle with a maximum reached at 60 min. In the outflow tract, reoxygenation did not alter significantly ERK phosphorylation.

p38 MAP kinase phosphorylation

After 30 min of anoxia, the level of p38 phosphorylation was about four-fold higher in the outflow tract than in atria and ventricle. During reoxygenation, the most important variations of p38 phosphorylation were observed in ventricle with a significant decrease at 60 min. A similar phenomenon was observed in the outflow tract but without statistical significance, most probably due to the large variability of the data. It should be noticed, however, that p38 remained activated in the outflow tract throughout reoxygenation, i.e., above its preanoxic level.

JNK activity versus phosphorylation

As determined by kinase assay, JNK activity increased in atria, ventricle, and outflow tract after 30 min of reoxygenation, but not significantly in atria and outflow tract (values reported for the ventricle are taken from our previous work [20]). Surprisingly, in contrast to activity, the level of JNK phosphorylation in the ventricle was not increased by reoxygenation (Fig. 4). Additionally, opening of the mitoK_{ATP} channels by diazoxide markedly reduced ventricular JNK activity during reoxygenation [20] but did not alter the level of phosphorylation (Fig. 4). These data show clearly that JNK activity did not parallel the level of JNK phosphorylation in the embryonic heart.

Discussion

To the best of our knowledge, this is the first time that distribution and activation of ERK, JNK, and p38 MAPK are explored in the three regions of an embryonic heart model submitted to a transient anoxic stress. Our main findings show that activation of MAPKs can be differentially modulated by anoxia-reoxygenation and by exogenous H_2O_2 in a region-specific manner.

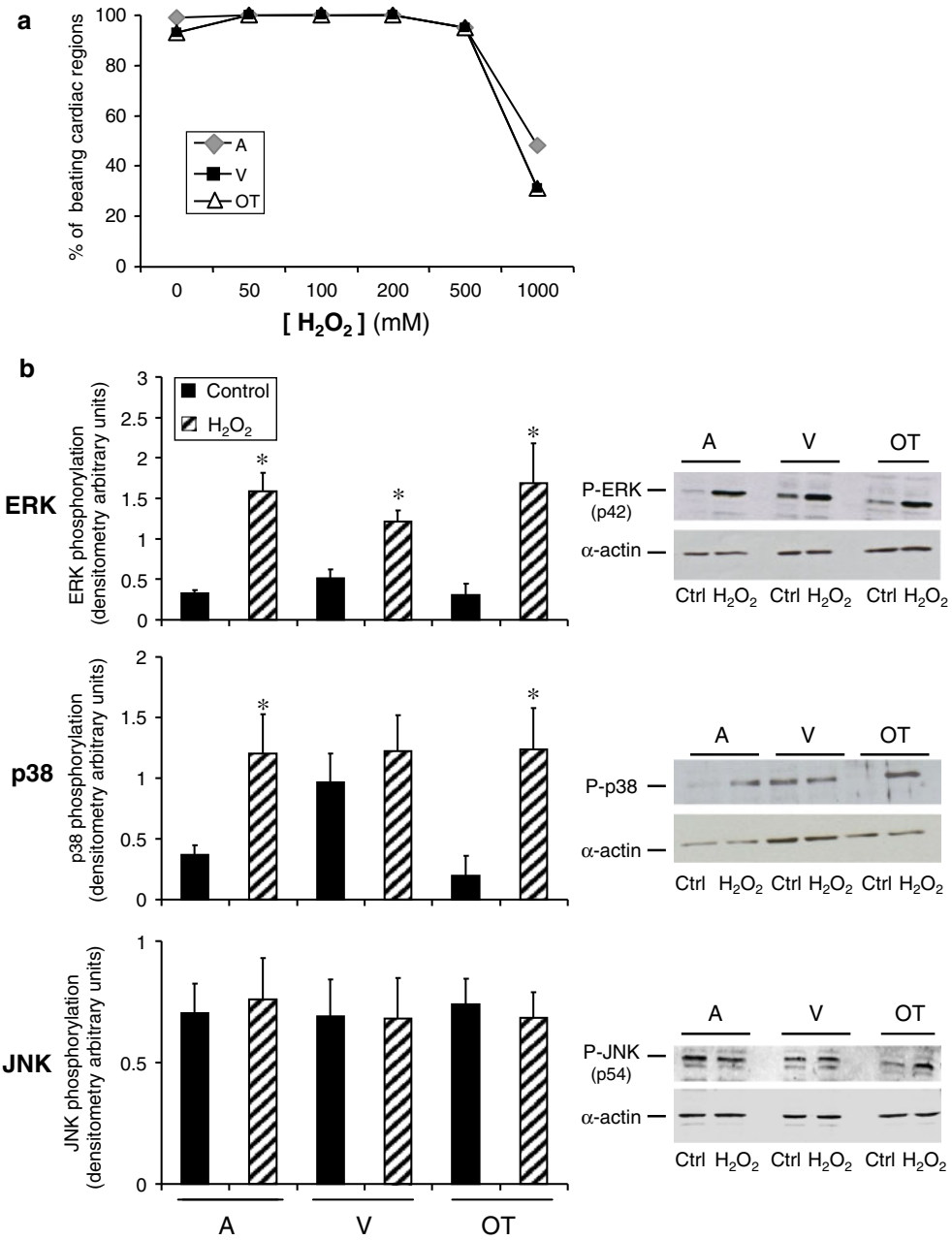

Fig. 2 Effects of H_2O_2 on contractile function and MAPKs phosphorylation. **a** A concentration of H_2O_2 higher than 500 μM was required to significantly affect contractions of A, V, and OT ($n = 100$ hearts). **b** H_2O_2 markedly increased phosphorylation of ERK and p38 specially in A and OT without modifying the level of JNK phosphorylation. Hearts were exposed to H_2O_2 1 h at 37°C. * $P < 0.05$ vs. control. $n = 5$ determinations

ERK and JNK were homogeneously distributed within the embryonic heart, whereas basal p38 expression was appreciably lower in the outflow tract relative to atria and ventricle (Fig. 1). It should be noticed that only the p42 isoform of ERK was detectable in the embryonic heart (Fig. 1a), alike in the adult chicken heart and different from neonatal and adult murine heart where both p42 and p44 isoforms were identifiable (not shown). Regarding p38 MAP kinase activation, the outflow tract appears also to be a unique part of the embryonic heart since it displayed both the lowest protein expression of p38 and the highest p38 responsiveness to anoxia and reoxygenation (Fig. 3). It should be mentioned that, at the stage investigated (24HH), the outflow tract undergoes important morphogenetic processes (remodeling) preparing the aorticopulmonary septation [31] which require an important physiological apoptotic activity [32, 33]. Indeed, in our preparation, there was 8.4 ± 1.3, 9.5 ± 0.3, and 14.5 ± 0.8% ($n = 3$ determinations) of apoptotic cells in atria, ventricle, and outflow tract, respectively (Pedretti and Yang, personal communication). Such a high level of apoptotic activity could partly explain that expression of p38 MAPK, which otherwise has been shown to display anti-apoptotic properties [12, 28], was the lowest in outflow tract. As expected, the highest relative amount of α-actin was found in the ventricle and was certainly due to the large number of proliferating and

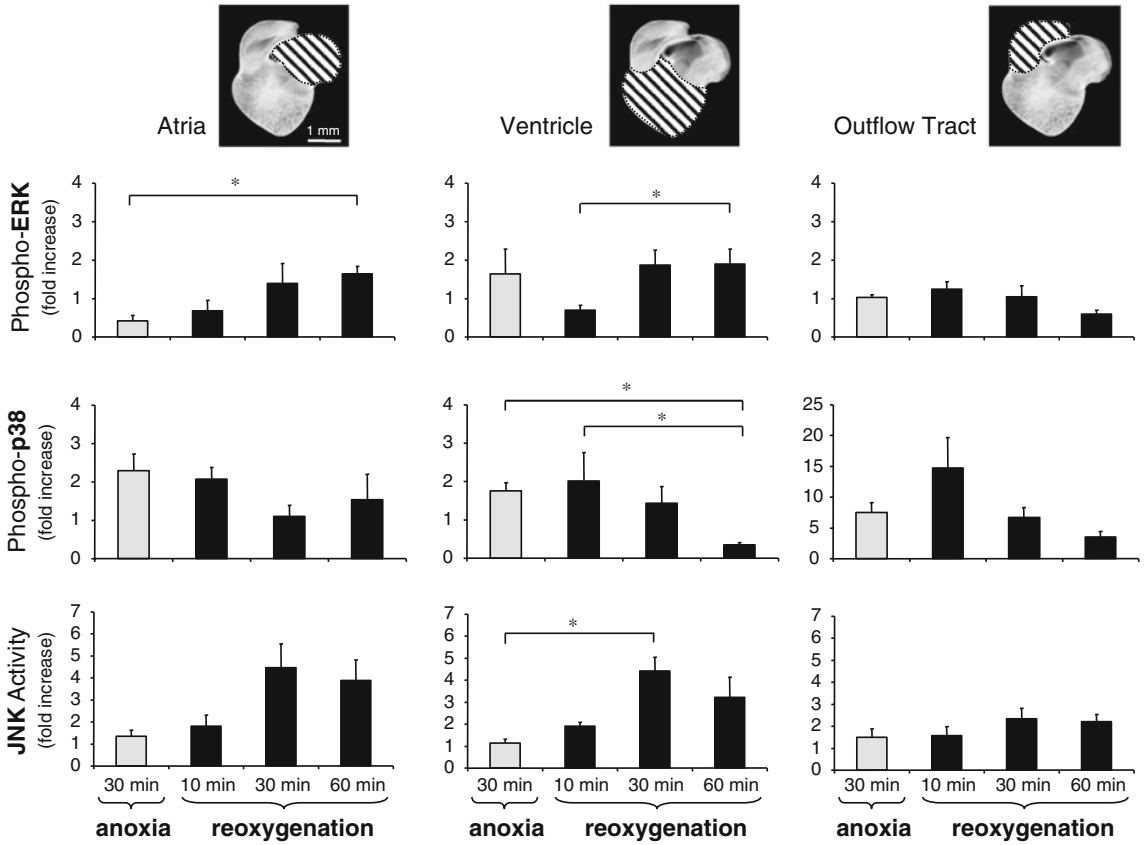

Fig. 3 Phosphorylation level of ERK and p38 MAPK and activity of JNK after 30 min of anoxia and 10, 30, and 60 min of reoxygenation in atria, ventricle, and outflow tract (hatched cardiac regions in *upper panel*). ERK, p38, and JNK displayed a characteristic profile of activation in each investigated region (see text). All values are expressed as fold increase relative to the preanoxic value obtained after 45 min of in vitro stabilization. * $P < 0.05$, $n = 3$–15 determinations for each column. Values reported for JNK activity in ventricle are taken from our previous work [20]

differentiating contractile myocytes in the developing compact and trabecular myocardial layers.

It is generally accepted that MAPKs are activated by ROS, especially by hydrogen peroxide (H_2O_2) [34, 35], although the degree and the time course of activation can differ according to the species, tissue, and cell-type [28, 36]. We sought to determine in atria, ventricle, and outflow tract to what extent exposure to a concentration of H_2O_2 sufficient to impair cardiac function, could also activate MAPKs. Under our experimental conditions the cardiac function was not altered by concentration of $H_2O_2 < 1$ mM whereas in fetal, newborn, and adult [37–39] cardiomyocytes contractions are already altered at 0.05 or 0.1 mM H_2O_2. Our data and these observations clearly indicate that the embryonic myocardium is less sensitive to this radical than the post-natal myocardium. This is corroborated by the fact that the functional recovery of the embryonic heart is rapidly completed after the reoxygenation-induced burst of ROS [9].

The most important effect of 1 mM H_2O_2 on ERK and p38 phosphorylation was observed in atria and outflow tract, which is consistent with the fact that 50% of atria stopped to beat at this concentration of H_2O_2 (Fig. 2a) and with the high sensitivity of the outflow tract to oxidative stress [40]. In the ventricle, the reoxygenation-induced peak of JNK activity is ROS-independent [20], and the present data show that JNK phosphorylation was not augmented by H_2O_2, whatever the region investigated (Fig. 2), demonstrating that JNK phosphorylation is not modulated even by the high oxidant stress induced by H_2O_2 exposure. These observations are in line with data obtained in adult myocardium showing that JNK is not activated by H_2O_2 at concentration as high as 500 μM [41] or by exposure to a pro-oxidant hyperoxia [42].

Relative to the other investigated MAPKs, ERK was modestly activated during anoxia and reoxygenation, suggesting that ERK is not a key element of the embryonic heart response to such a stress. ERK being not a stress kinase but mostly associated with cell proliferation and differentiation, it is not surprising that this pathway displayed such minor alteration under our experimental conditions. The low responsiveness of ERK to reoxygenation

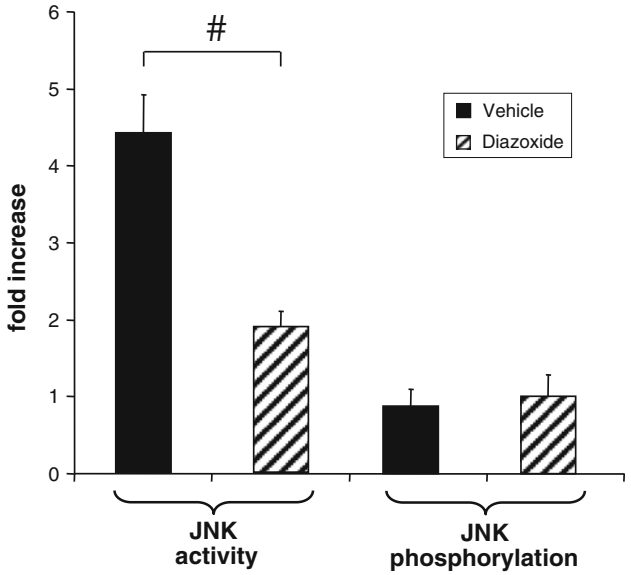

Fig. 4 After 30 min reoxygenation JNK phosphorylation did not parallel JNK activity in the ventricle. Reoxygenation strongly stimulated JNK activity but had no effect on JNK phosphorylation. Pharmacological opening of the mitoK$_{ATP}$ channel (diazoxide 50 μM) decreased the reoxygenation-induced JNK activity, but did not affect JNK phosphorylation. Values reported for JNK activity are taken from our previous work [20]. All values are expressed as fold increase relative to preanoxia value. $^{\#}$ $P < 0.05$ vs. vehicle; $n = 4$–10 determinations

suggests that the endogenous burst of ROS induced by reoxygenation is too short and/or too weak to strongly activate the kinase, in contrast to the severe exogenous oxidant stress generated by H_2O_2 which markedly increased ERK phosphorylation. It should also be noticed that ERK activity measured in the ventricle did not vary during anoxia-reoxygenation (Sarre and Maurer, personal communication).

Since the publication of Bogoyevith et al. [43] in 1996, several studies confirmed that p38 is strongly activated in heart by ischemia and involved in response to hypoxia and anoxia, but whether it displays a beneficial or a detrimental role remains under debate [44, 45]. In the present study, although the basal level of p38 expression was not homogeneous within the heart (Fig. 1b), anoxia increased phosphorylation in the three cardiac regions relative to preanoxic levels, especially in the outflow tract, (Fig. 3). Studies performed in adult [46, 47] and embryonic [9] cardiomyocytes showing that ROS production is totally abolished under strict anoxia, indicate that the observed anoxic increase of phospho-p38 was ROS-independent. The phosphorylation levels and kinase activities determined in this work displayed important interindividual variations which might be due to slight differences in developmental stage and/or to the relative sensitivity of the used techniques, including immunoblotting and kinase assay. Nevertheless, the greatest coefficient of variability of the level of p38 phosphorylation was consistently observed in ventricle and outflow tract after 10 min of reoxygenation. This suggests that during such a brief period of time, when ROS production is maximal, crucial cellular alterations may occur in these regions.

Although reoxygenation induces a calcium-dependent peak of JNK activity in the ventricle [20], we did not found the same pattern for JNK phosphorylation. Such a dissociation between JNK activity and phosphorylation could be partly related to the regulatory role played by scaffold proteins associated to JNK, e.g., JIP1, Sab, and Gst [48–50]. This important facet of JNK modulation is beyond the scope of our study. Likewise, an upward trend in JNK activity was observed in atria and outflow tract after 30–40 min reoxygenation, but without statistical significance.

We have previously shown that pharmacological opening of mitoK$_{ATP}$ channels not only reduces the reoxygenation-induced peak of JNK activity [20] but also improves ventricular recovery through a ROS-dependent mechanism [9]. However, in the present study, we found that diazoxide did not reduce JNK phosphorylation in ventricle, indicating that the modulation of JNK activity by the open-state of the mitoK$_{ATP}$ channels is not related to phosphorylation of the kinase, but rather to the level of intracellular calcium [20] and/or to alteration of JNK-interacting proteins (see above).

In conclusion, this study demonstrates for the first time that ERK, p38, and JNK show a characteristic distribution in the embryonic heart and are differentially modulated by anoxia-reoxygenation, exogenous oxyradicals, and mitochondrial K$_{ATP}$ channels in a region-specific manner. Even if the functional role of these MAP kinases remains to be clarified in such a model, our findings provide a first step in understanding the modulation of the signal transduction cascades in the developing heart subjected to oxygen lack and reoxygenation.

Acknowledgments The collaboration of Fabienne Maurer, Christophe Bonny, and Miguel Van Bemmelen, is gratefully acknowledged. We thank Anne-Catherine Thomas for her skillful technical assistance. This work was supported by the Swiss National Science Foundation n°3100A0-105901.

References

1. Ostadal B, Ostadalova I, Dhalla NS (1999) Development of cardiac sensitivity to oxygen deficiency: comparative and ontogenetic aspects. Physiol Rev 79:635–659
2. Raddatz E, Gardier S, Sarre A (2006) Physiopathology of the embryonic heart (with special emphasis on hypoxia and reoxygenation). Ann Cardiol Angeiol (Paris) 55:79–89
3. Jensen A, Garnier Y, Berger R (1999) Dynamics of fetal circulatory responses to hypoxia and asphyxia. Eur J Obstet Gynecol Reprod Biol 84:155–172

4. Sharma SK, Lucitti JL, Nordman C, Tinney JP, Tobita K, Keller BB (2005) Impact of hypoxia on early chick embryo growth and cardiovascular function. Pediatr Res 59:116–120
5. Fowden AL, Giussani DA, Forhead AJ (2006) Intrauterine programming of physiological systems: causes and consequences. Physiology 21:29–37
6. Ream M, Ray AM, Chandra R, Chikaraishi DM (2008) Early fetal hypoxia leads to growth restriction and myocardial thinning. Am J Physiol Regul Integr Comp Physiol 295:R583–R595
7. Agata N, Kato Y, Tanaka H, Shigenobu K (1994) Differential effects of hypoxia on electrical and mechanical activities of isolated ventricular muscles from fetal and adult guinea-pigs. Gen Pharmacol 25:15–18
8. Kasuya Y, Matsuki N, Shigenobu K (1977) Changes in sensitivity to anoxia of the cardiac action potential plateau during chick embryonic development. Dev Biol 58:124–133
9. Sarre A, Lange N, Kucera P, Raddatz E (2005) mitoK_{ATP} channel activation in the postanoxic developing heart protects E-C coupling via NO-, ROS-, and PKC-dependent pathways. Am J Physiol Heart Circ Physiol 288:H1611–H1619
10. Sarre A, Maury P, Kucera P, Kappenberger L, Raddatz E (2006) Arrhythmogenesis in the developing heart during anoxia-reoxygenation and hypothermia-rewarming: an in vitro model. J Cardiovasc Electrophysiol 17:1350–1359
11. Raman M, Chen W, Cobb MH (2007) Differential regulation and properties of MAPKs. Oncogene 26:3100–3112
12. Wang Y (2007) Mitogen-activated protein kinases in heart development and diseases. Circulation 116:1413–1423
13. Bogoyevitch MA (2000) Signalling via stress-activated mitogen-activated protein kinases in the cardiovascular system. Cardiovasc Res 45:826–842
14. Liberatore CM, Yutzey KE (2004) MAP kinase activation in avian cardiovascular development. Dev Dyn 230:773–780
15. Ravingerova T, Barancik M, Strniskova M (2003) Mitogen-activated protein kinases: a new therapeutic target in cardiac pathology. Mol Cell Biochem 247:127–138
16. Bell RM, Clark JE, Hearse DJ, Shattock MJ (2007) Reperfusion kinase phosphorylation is essential but not sufficient in the mediation of pharmacological preconditioning: characterisation in the bi-phasic profile of early and late protection. Cardiovasc Res 73:153–163
17. Hausenloy DJ, Yellon DM (2006) Survival kinases in ischemic preconditioning and postconditioning. Cardiovasc Res 70: 240–253
18. Schulz R (2005) A new paradigm: cross talk of protein kinases during reperfusion saves life!. Am J Physiol Heart Circ Physiol 288:H1–H2
19. Tenhunen O, Soini Y, Ilves M, Rysa J, Tuukkanen J, Serpi R et al (2006) p38 kinase rescues failing myocardium after myocardial infarction: evidence for angiogenic and anti-apoptotic mechanisms. FASEB J 20:1907–1909
20. Sarre A, Gardier S, Maurer F, Bonny C, Raddatz E (2008) Modulation of the c-Jun N-terminal kinase activity in the embryonic heart in response to anoxia-reoxygenation: involvement of the Ca^{2+} and mitoK_{ATP} channels. Mol Cell Biochem 313:133–138
21. Romano R, Rochat AC, Kucera P, De Ribaupierre Y, Raddatz E (2001) Oxidative and glycogenolytic capacities within the developing chick heart. Pediatr Res 49:363–372
22. Moorman AF, Schumacher CA, de Boer PA, Hagoort J, Bezstarosti K, van den Hoff MJ et al (2000) Presence of functional sarcoplasmic reticulum in the developing heart and its confinement to chamber myocardium. Dev Biol 223:279–290
23. Tenthorey D, de Ribaupierre Y, Kucera P, Raddatz E (1998) Effects of verapamil and ryanodine on activity of the embryonic chick heart during anoxia and reoxygenation. J Cardiovasc Pharmacol 31:195–202
24. Franco D, Gallego A, Habets PE, Sans-Coma V, Moorman AF (2002) Species-specific differences of myosin content in the developing cardiac chambers of fish, birds, and mammals. Anat Rec 268:27–37
25. Raddatz E, Thomas AC (2002) Heterogeneity of oxydant stress in the reoxygenated developing heart. J Mol Cell Cardiol 34:A52
26. Maury P, Sarre A, Terrand J, Rosa A, Kucera P, Kappenberger L et al (2004) Ventricular but not atrial electro-mechanical delay of the embryonic heart is altered by anoxia-reoxygenation and improved by nitric oxide. Mol Cell Biochem 265:141–149
27. Shrier A, Clay JR (1982) Comparison of the pacemaker properties of chick embryonic atrial and ventricular heart cells. J Membr Biol 69:49–56
28. Zarubin T, Han J (2005) Activation and signaling of the p38 MAP kinase pathway. Cell Res 15:11–18
29. Hamburger V, Hamilton H (1951) A series of normal stages in the development of the chick embryo. J Morphol 88:49–92
30. Larsen CM, Wadt KA, Juhl LF, Andersen HU, Karlsen AE, Su MS et al (1998) Interleukin-1beta-induced rat pancreatic islet nitric oxide synthesis requires both the p38 and extracellular signal-regulated kinase 1/2 mitogen-activated protein kinases. J Biol Chem 273:15294–15300
31. Martinsen BJ (2005) Reference guide to the stages of chick heart embryology. Dev Dyn 233:1217–1237
32. Sugishita Y, Leifer DW, Agani F, Watanabe M, Fisher SA (2004) Hypoxia-responsive signaling regulates the apoptosis-dependent remodeling of the embryonic avian cardiac outflow tract. Dev Biol 273:285–296
33. Barbosky L, Lawrence DK, Karunamuni G, Wikenheiser JC, Doughman YQ, Visconti RP et al (2006) Apoptosis in the developing mouse heart. Dev Dyn 235:2592–2602
34. Lee K, Esselman WJ (2002) Inhibition of PTPs by H(2)O(2) regulates the activation of distinct MAPK pathways. Free Radic Biol Med 33:1121–1132
35. Guyton KZ, Liu Y, Gorospe M, Xu Q, Holbrook NJ (1996) Activation of mitogen-activated protein kinase by H_2O_2. Role in cell survival following oxidant injury. J Biol Chem 271:4138–4142
36. Griendling KK, Sorescu D, Lassegue B, Ushio-Fukai M (2000) Modulation of protein kinase activity and gene expression by reactive oxygen species and their role in vascular physiology and pathophysiology. Arterioscler Thromb Vasc Biol 20:2175–2183
37. Barsacchi R, Camici P, Bottigli U, Salvadori PA, Pelosi G, Maiorino M et al (1983) Correlation between hydroperoxide-induced chemiluminescence of the heart and its function. Biochim Biophys Acta 762:241–247
38. Sabri A, Byron KL, Samarel AM, Bell J, Lucchesi PA (1998) Hydrogen peroxide activates mitogen-activated protein kinases and Na^{+}-H^{+} exchange in neonatal rat cardiac myocytes. Circ Res 82:1053–1062
39. Nakamura TY, Goda K, Okamoto T, Kishi T, Nakamura T, Goshima K (1993) Contractile and morphological impairment of cultured fetal mouse myocytes induced by oxygen radicals and oxidants. Correlation with intracellular Ca^{2+} concentration. Circ Res 73:758–770
40. Fisher SA (2007) The developing embryonic cardiac outflow tract is highly sensitive to oxidant stress. Dev Dyn 236:3496–3502
41. Knight RJ, Buxton DB (1996) Stimulation of c-Jun kinase and mitogen-activated protein kinase by ischemia and reperfusion in the perfused rat heart. Biochem Biophys Res Commun 218:83–88
42. Ruusalepp A, Czibik G, Flatebo T, Vaage J, Valen G (2007) Myocardial protection evoked by hyperoxic exposure involves signaling through nitric oxide and mitogen activated protein kinases. Basic Res Cardiol 102:318–326

43. Bogoyevitch MA, Gillespie-Brown J, Ketterman AJ, Fuller SJ, Ben-Levy R, Ashworth A et al (1996) Stimulation of the stress-activated mitogen-activated protein kinase subfamilies in perfused heart. p38/RK mitogen-activated protein kinases and c-Jun N-terminal kinases are activated by ischemia/reperfusion. Circ Res 79:162–173
44. Bassi R, Heads R, Marber MS, Clark JE (2008) Targeting p38-MAPK in the ischaemic heart: kill or cure? Curr Opin Pharmacol 8:141–146
45. Clerk A, Sugden PH (2006) Inflame my heart (by p38-MAPK). Circ Res 99:455–458
46. Hoffman DL, Salter JD, Brookes PS (2007) Response of mitochondrial reactive oxygen species generation to steady-state oxygen tension: implications for hypoxic cell signaling. Am J Physiol Heart Circ Physiol 292:H101–H108
47. Wang W, Fang H, Groom L, Cheng A, Zhang W, Liu J et al (2008) Superoxide flashes in single mitochondria. Cell 134:279–290
48. Nihalani D, Wong HN, Holzman LB (2003) Recruitment of JNK to JIP1 and JNK-dependent JIP1 phosphorylation regulates JNK module dynamics and activation. J Biol Chem 278:28694–28702
49. Adler V, Yin Z, Fuchs SY, Benezra M, Rosario L, Tew KD et al (1999) Regulation of JNK signaling by GSTp. EMBO J 18:1321–1334
50. Wiltshire C, Gillespie DA, May GH (2004) Sab (SH3BP5), a novel mitochondria-localized JNK-interacting protein. Biochem Soc Trans 32:1075–1077

Pharmacological Research 61 (2010) 85–91

Contents lists available at ScienceDirect

Pharmacological Research

journal homepage: www.elsevier.com/locate/yphrs

Specific inhibition of HCN channels slows rhythm differently in atria, ventricle and outflow tract and stabilizes conduction in the anoxic-reoxygenated embryonic heart model

Alexandre Sarre, Sarah Pedretti, Stephany Gardier, Eric Raddatz*

Department of Physiology, Faculty of Biology and Medicine, 7 rue du Bugnon, CH-1005 Lausanne, Switzerland

ARTICLE INFO

Article history:
Received 15 January 2009
Received in revised form
29 September 2009
Accepted 29 September 2009

Keywords:
Ivabradine
Heart
Embryo
Anoxia-reoxygenation
Electrocardiogram
HCN channels

ABSTRACT

The hyperpolarization-activated cyclic nucleotide-gated (HCN) channels are expressed in pacemaker cells very early during cardiogenesis. This work aimed at determining to what extent these channels are implicated in the electromechanical disturbances induced by a transient oxygen lack which may occur in utero.

Spontaneously beating hearts or isolated ventricles and outflow tracts dissected from 4-day-old chick embryos were exposed to a selective inhibitor of HCN channels (ivabradine 0.1–10 μM) to establish a dose–response relationship. The effects of ivabradine on electrocardiogram, excitation–contraction coupling and contractility of hearts submitted to anoxia (30 min) and reoxygenation (60 min) were also determined. The distribution of the predominant channel isoform, HCN4, was established in atria, ventricle and outflow tract by immunoblotting.

Intrinsic beating rate of atria, ventricle and outflow tract was 164 ± 22 (n = 10), 78 ± 24 (n = 8) and 40 ± 12 bpm (n = 23, mean ± SD), respectively. In the whole heart, ivabradine (0.3 μM) slowed the firing rate of atria by 16% and stabilized PR interval. These effects persisted throughout anoxia-reoxygenation, whereas the variations of QT duration, excitation–contraction coupling and contractility, as well as the types and duration of arrhythmias were not altered. Ivabradine (10 μM) reduced the intrinsic rate of atria and isolated ventricle by 27% and 52%, respectively, whereas it abolished activity of the isolated outflow tract. Protein expression of HCN4 channels was higher in atria and ventricle than in the outflow tract.

Thus, HCN channels are specifically distributed and control finely atrial, ventricular and outflow tract pacemakers as well as conduction in the embryonic heart under normoxia and throughout anoxia-reoxygenation.

1. Introduction

Hyperpolarization-activated cyclic nucleotide-gated (HCN) channels are expressed in nodal, atrial and ventricular tissues, carry the pacemaker funny current (*If*) and control the rate of diastolic depolarization of the sinoatrial node in the adult heart [1,2]. Selective inhibition of these channels slows the cardiac rate [3] without any effect on contractility [4] and can protect against ischemia-induced myocardial injury [5–7]. HCN channels, including the predominant HCN4 isoform, are expressed very early during cardiogenesis and are required for pacemaker activity [8–10]. Pacemaker locus differentiates in the posterior segment of the primitive tubular heart [11,12] and strong *If* current can be generated by hyperpolarization in ventricular cardiomyocytes from the chick (3-day-old) and the mouse (9.5-day-old) embryo [13–15], in contrast to adult ventricular myocytes. Furthermore, hierarchy of intrinsic rhythmicity within the embryonic heart is illustrated by the fact that dissected atria, ventricle and outflow tract beat spontaneously and regularly at their respective firing rate, i.e. atria > ventricle > outflow tract [16]. This observation suggests that membrane density and/or properties of the HCN channels, besides non-HCN pacing mechanisms, might vary from one cardiac region to another.

Throughout the embryonic and fetal life, occasional transient or prolonged reduction in oxygen availability can lead to reversible or irreversible cardiac arrhythmias, threatening fetal growth. The mechanisms underlying hypoxia-induced rhythm abnormalities in the developing heart remain poorly understood and deserve to be investigated. We have previously shown that anoxia and reoxygenation induce rapid and severe electrical and mechanical disturbances in the 4–5-day-old embryonic chick heart model [16,17]. Arrhythmic activity of isolated atria persists throughout anoxia and upon reoxygenation, whereas activity of isolated ventricles rapidly ceases under anoxia and resumes late after reoxygenation. Whether HCN channels are involved in such disturbances

* Corresponding author. Tel.: +41 21 692 5526; fax: +41 21 692 5505.
E-mail address: eric.raddatz@unil.ch (E. Raddatz).

1043-6618/$ – see front matter © 2010 Elsevier Ltd. All rights reserved.
doi:10.1016/j.phrs.2009.09.007

and whether their inhibition has beneficial consequences, as in the adult heart, remains to be explored.

This study mainly aimed at examining the contribution of the HCN channels to pacemaker activity and conduction in the embryonic heart as well as investigating their role in cardiac dysfunction induced by anoxia and reoxygenation.

2. Material and methods

2.1. Reagents

Standard chemicals were purchased from Sigma (Sigma Aldrich, Buchs, Switzerland). The specific inhibitor of HCN channels ivabradine was kindly provided by Servier (France).

2.2. Preparation and in vitro mounting of the heart

Fertilized eggs from Lohman Brown hens were incubated during 96 h at 38 °C and 95% relative humidity to obtain stage 24HH embryos (according to Hamburger and Hamilton [18]). Hearts were carefully excised from embryos and dissected in order to isolate ventricles and outflow tracts. Spontaneously beating hearts or the isolated parts were placed in the culture compartment of a stainless steel airtight chamber. Such device was equipped with two windows for observation as well as measurements and maintained under controlled conditions on the thermostabilized stage (37.5 °C) of an inverted microscope (IMT2 Olympus, Tokyo, Japan) as previously described in detail [17]. Briefly, the culture compartment (300 μl) was separated from the gas compartment by a 15 μm transparent and gas-permeable silicone membrane (RTV 141, Rhône-Poulenc, Lyon, France). Hearts, ventricles and outflow tracts were slightly flattened by the silicone membrane and the resulting thickness of the myocardial tissue facing the gas compartment was approximately 300 μm. Thus, pO_2 at the tissue level could be strictly controlled and rapidly modified (within less than 5 s) by flushing high-grade gas of selected composition through the gas compartment. At this developmental stage, the heart lacks coronary vascularization and the myocardial oxygen requirement is met exclusively by diffusion.

The HCO_3/CO_2 buffered medium was composed of (in mM): 99.25 NaCl; 0.3 NaH_2PO_4; 10 $NaHCO_3$; 4 KCl; 0.79 $MgCl_2$; 0.75 $CaCl_2$; 8 D(+)glucose. This culture medium was equilibrated in the chamber with 2.31% CO_2 in air (normoxia and reoxygenation) or in N_2 (anoxia) yielding a pH of 7.4. Ivabradine was dissolved in the culture medium just before experiments.

2.3. Recording of electrical and contractile activity

Electrical and contractile activities were recorded simultaneously and continuously throughout in vitro experiments as previously described [16].

2.3.1. Electrical activity

ECG recordings of the spontaneously contracting intact hearts were performed using two Ag/AgCl electrodes 1.2 mm apart (diameter 0.625 mm) inserted into the window facing the culture compartment. The atrial and ventricular regions of the heart were placed in the immediate vicinity of these electrodes, which were connected to a differential preamplifier (gain of 2000), resulting in an output signal of 1–5 V peak to peak. This signal was digitized and processed using a powerful data acquisition (IOX, sampling rate: 2 kHz) and analysis system (ECG-Auto) developed by EMKA Technologies (France). ECG displayed characteristic P, QRS and T components, which allowed to assess the beating rate from RR interval (beats/min, bpm), PR interval (ms) and QT duration (ms). Corrected QT (QTc) was calculated using Bazett's formula ($QT/RR^{1/2}$).

2.3.2. Contractile activity

Adjustable phototransistors were positioned over the projected image of the investigated regions allowing detection of edge motion of the myocardial wall, i.e. at the level of atrial pacemaker and ventricular apex of the intact heart. Simultaneously with ECG, myocardial shortening was sampled at a rate of 1 kHz using the same acquisition/analysis system as described above. The actual ventricular shortening at the apex (μm) was determined using video recordings performed just before anoxia and at the end of reoxygenation.

2.3.3. Excitation–contraction coupling

The electromechanical delay (EMD, ms), reflecting the efficiency of excitation–contraction (E–C) coupling, was determined at the level of the right atrium and at the apex of the ventricle by measuring the delay between the very initial phase of the P and QRS components and the initiation of contraction in atrium and ventricle, respectively, as previously described [16].

2.4. Experimental protocols

2.4.1. Dose–response curve

Whole hearts, isolated ventricles and outflow tracts were pretreated with ivabradine at room temperature during 30 min, mounted in the culture chamber and exposed to normoxia during 1 h in the absence (control) or the presence of ivabradine. The tested concentrations of ivabradine ranged from 0.1 to 10 μM. The spontaneous beating rate was determined at the end of the protocol.

2.4.2. Anoxia-reoxygenation protocol

Whole hearts (pretreated or not with 0.3 μM ivabradine) were placed in the chamber, stabilized during 45 min under normoxia and submitted to anoxia (30 min) followed by reoxygenation (60 min). Ivabradine (0.3 μM) was present throughout anoxia-reoxygenation and electrical (ECG) as well as contractile activities were continuously recorded.

2.5. Western Blotting of HCN4 channels

A total of 84 hearts have been used and carefully dissected into atria, ventricle and outflow tract. Six atria, 3 ventricles and 6 outflow tracts were pooled for each sample preparation. Protein extracts were generated from the dissected regions using a lysis buffer (in mM: 20 Tris-acetate (pH 7), 270 sucrose, 1 EGTA, 1 EDTA, 50 NaF, 10 β-glycerophosphate, 10 dithiothreitol (DTT), 10 4-nitrophenyl phosphate disodium salt hexahydrate (PNPP), 1% Triton X-100 and inhibitors of proteases). Insoluble material was removed by a 5 min centrifugation at 10,000 g. Protein concentration was determined by the Bradford method. Samples were denatured in sample buffer (6 min, 95 °C), 20 μg of protein were loaded per lane, separated on 10% SDS-polyacrylamide gels, and transferred to nitrocellulose membranes. Membranes were blocked (overnight at 4 °C) with 5% non-fat milk in PBS and probed (2 h at room temperature) with rabbit polyclonal antibody against HCN4 1:200 (Alomone Labs, Jerusalem, Israel) or GAPDH 1:1000 (Abcam, Cambridge, UK). A control fusion protein was used as control antigen. Anti-HCN4 antibody was preincubated with the antigen (for negative control) into PBS–5% non-fat dry milk for 1 h. After 4 washes in 0.1% Tween 20 PBS the membranes were incubated in 1:10,000 dilution of horseradish peroxidase-conjugated anti-rabbit IgG (Amersham Biosciences) in PBS containing 5% non-fat milk (1 h, room temperature) and then washed 4 times.

Immunoreactive bands were detected with enhanced chemiluminescent procedure using ECL Western Blotting Analysis System (Amersham Biosciences). Autoradiograms were scanned and densitometric analysis performed with Quantity One software (Biorad). Protein bands were normalized using GAPDH in the same sample as reference.

2.6. Statistical analysis

All values are reported as mean ± standard error of the mean (SEM) unless otherwise indicated. The significance of any difference between two groups was assessed with Student *t*-test or repeated measures ANOVA (to compare rates of recovery), while differences in the dose–response of ivabradine were determined using one-way ANOVA completed by Tukey's post hoc test using SPSS software. Mann–Whitney test was used to compare slopes of the PR–RR relationship. The statistical significance was defined by a value of $p < 0.05$.

3. Results

3.1. HCN4 channels are differentially expressed within the embryonic chick heart

Immunoblotting shows that expression of the predominant isoform HCN4 was higher in atria and ventricle than in the outflow tract of the embryonic chick heart (Fig. 1). The specificity of the anti-HCN4 antibody was controlled by immunoblotting with the anti-HCN4 antibody preincubated with the corresponding antigen. The band normally found at about 160 kDa, corresponding to HCN4, disappeared completely in the presence of the antigen (not shown).

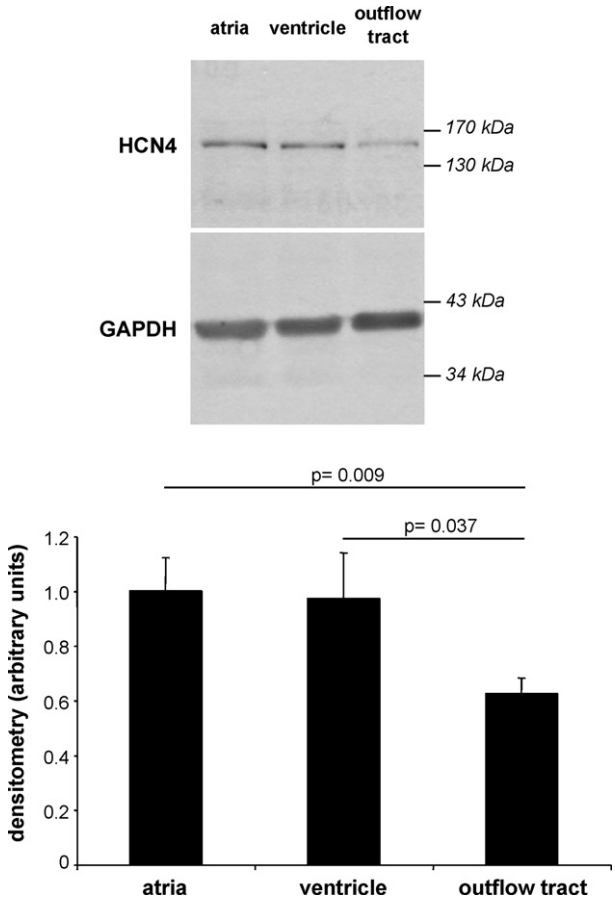

Fig. 1. Representative immunoblot of the HCN4 channel and GAPDH (*upper panel*) and quantitative densitometry of HCN4 corrected for GAPDH (*lower panel*) showing that HCN4 was inhomogeneously distributed in the embryonic chick heart at stage 24HH. Bars represent the mean ± SEM from 14, 12 and 11 independent determinations for atria, ventricle and outflow tract, respectively.

3.2. Dose–response curve for ivabradine was different in atria, ventricle and outflow tract

In vitro, all atria (in whole hearts) and dissected ventricles beat at their intrinsic rate, whereas only about 25% of the dissected outflow tracts beat spontaneously and regularly. Under normoxia, the intrinsic beating rate of the untreated atria, isolated ventricles and outflow tract was 164 ± 22 ($n = 10$), 78 ± 24 ($n = 8$) and 40 ± 12 bpm ($n = 23$, mean ± SD), respectively, and remained stable in vitro. The dose–response curves (Fig. 2) show that inhibition of HCN channels by 1 μM ivabradine significantly ($p < 0.01$) slowed the firing rate of atria (dropping to 134 ± 17 bpm, $n = 6$) and ventricle (dropping to 39 ± 19 bpm, $n = 7$) respectively. The highest concentration of ivabradine (10 μM) further decreased moderately atrial rate, had no additional effect on ventricular rhythm but completely stopped spontaneous activity of the outflow tract (Fig. 2). Thus, the maximal inhibitory effect of ivabradine is achieved at 0.3–1 and 10 μM in ventricle and outflow tract, respectively. Since the ventricular rate was already altered at a low concentration of ivabradine (0.3 μM), we investigated the functional consequences of HCN inhibition during anoxia-reoxygenation at this concentration only.

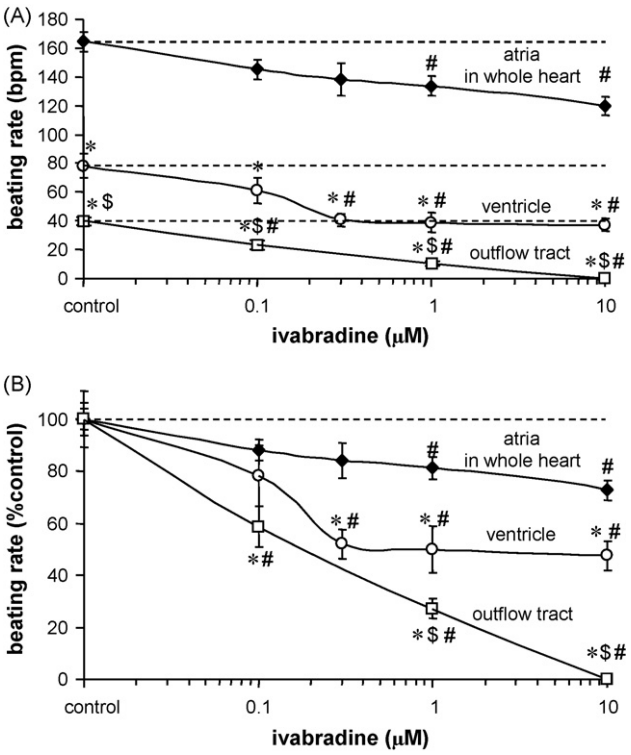

Fig. 2. Dose–response curves of whole hearts (black diamonds), dissected ventricles (open circles) and outflow tracts (open squares) treated with ivabradine under normoxia. The spontaneous beating rate of atria, isolated ventricles and outflow tracts was expressed as raw data (A) or as percent of the respective control value representing ivabradine efficiency (B). Control: untreated preparation; broken lines indicate the control level; bpm: beats per min.; mean ± SEM; $n = 4$–11 for atria and ventricle; $n = 9$–23 for outflow tract; *: $p < 0.01$ dissected ventricle or outflow tract versus atria in whole heart; $: $p < 0.01$ outflow tract versus ventricle; #: $p < 0.01$ versus respective control.

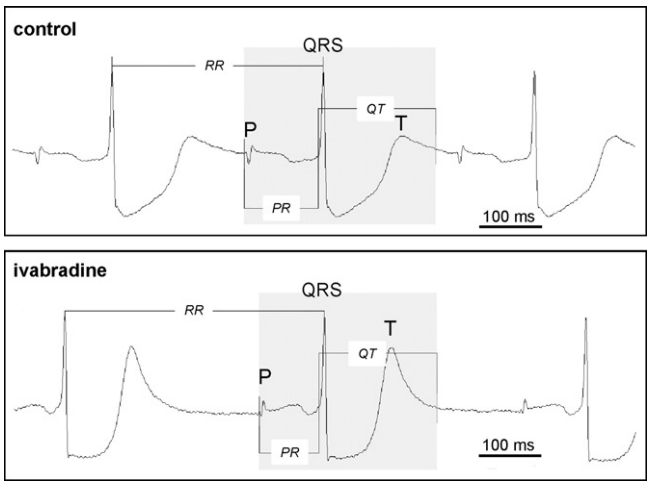

Fig. 3. Representative ECGs illustrating the P, QRS and T components of the embryonic chick heart spontaneously beating in vitro under normoxia and showing how RR, PR and QT intervals have been analysed in control and ivabradine (0.3 μM) treated hearts.

3.3. Inhibition of HCN channels had a bradycardic effect associated with a stabilization of conduction without affecting the pattern of arrhythmias throughout anoxia-reoxygenation

Under preanoxic conditions, ivabradine (0.3 μM) reduced atrial rate and PR interval by 20%, but did not alter QT duration, ventricular EMD and ventricular shortening (Figs. 3 and 4). It should be noticed that the preanoxic atrial rate of untreated hearts (186 ± 9 bpm, $n = 5$, Fig. 4) was slightly higher than heart rate of the controls of the dose–response experiments (164 ± 7 bpm, $n = 10$, Fig. 2) although it did not reach statistical significance. Such a difference between the two series of experiments, combined with a higher coefficient of variability of atrial rate at 0.3 μM ivabradine in Fig. 2 (18%; $n = 5$) than that in Fig. 4 (12%; $n = 5$), could explain that the bradycardic effect of 0.3 μM ivabradine on atria was significant during preanoxia ($p = 0.03$) but not under the conditions of the dose–response determination ($p = 0.09$). As we recently described [16], anoxia induced bradycardia, atrial ectopy, 1st, 2nd and 3rd degree A-V blocks as well as transient arrests followed by bursting activity. Reoxygenation triggered also Wenckebach phenomenon and ventricular escape beats. All hearts fully recovered after 30–50 min of reoxygenation. Relative to control after 10 min anoxia, ivabradine augmented the mean atrial rate measured during bursts of activity with no effect on other functional parameters (Fig. 4). During reoxygenation, ivabradine shortened PR interval with respect to untreated hearts. Nevertheless, the types, incidence and duration of arrhythmias were not significantly affected by ivabradine (Table 1). Relative to control, ivabradine did not alter QTc neither under normoxia (0.25 ± 0.02 and 0.28 ± 0.03 s, in control and treated group, respectively, $n = 5$) nor throughout reoxygenation (peaking after 9 min of reoxygenation at 0.35 ± 0.07 and 0.30 ± 0.02 s in control and ivabradine, respectively). However, the mean of all the QTcs which were possible to determine, i.e. in the absence of AV blocks, at 11, 13, 20, 25 and 30 min of anoxia (see Fig. 4), was longer in the ivabradine group (0.28 ± 0.06 s, $n = 17$) than in the control group (0.23 ± 0.04 s, $n = 16$; ± SD) ($p = 0.006$). Furthermore, as previously described [19], atrial EMD was longer than ventricular EMD under baseline condition (i.e. 19.9 ± 0.9 ms vs 12.1 ± 1.8 ms) and was not significantly affected by reoxygenation and ivabradine (not shown).

Table 1
Inhibition of HCN channels by ivabradine (0.3 μM) did not significantly influence the pattern of arrhythmias in the embryonic heart during anoxia and reoxygenation; time is given in minutes; mean ± SD; $n = 5$ for each condition.

	Anoxia				Reoxygenation				
	First atrial arrest	First ventricular arrest	Duration of AV blocks	Duration of cardioplegia	Atrial resumption	Ventricular resumption	Duration of AV blocks	Duration of Wenckebach	End of arrhythmias
Control	12.3 ± 10.9	3.4 ± 2.0	11.8 ± 8.9	7.5 ± 9.3	1.5 ± 1.6	3.0 ± 2.2	11.9 ± 9.7	14.7 ± 17.1	33 ± 15
Ivabradine	3.0 ± 1.4	2.7 ± 1.3	6.4 ± 4.8	15.8 ± 3.2	0.8 ± 0.6	1.4 ± 0.8	10.7 ± 5.0	8.0 ± 11.6	25 ± 9

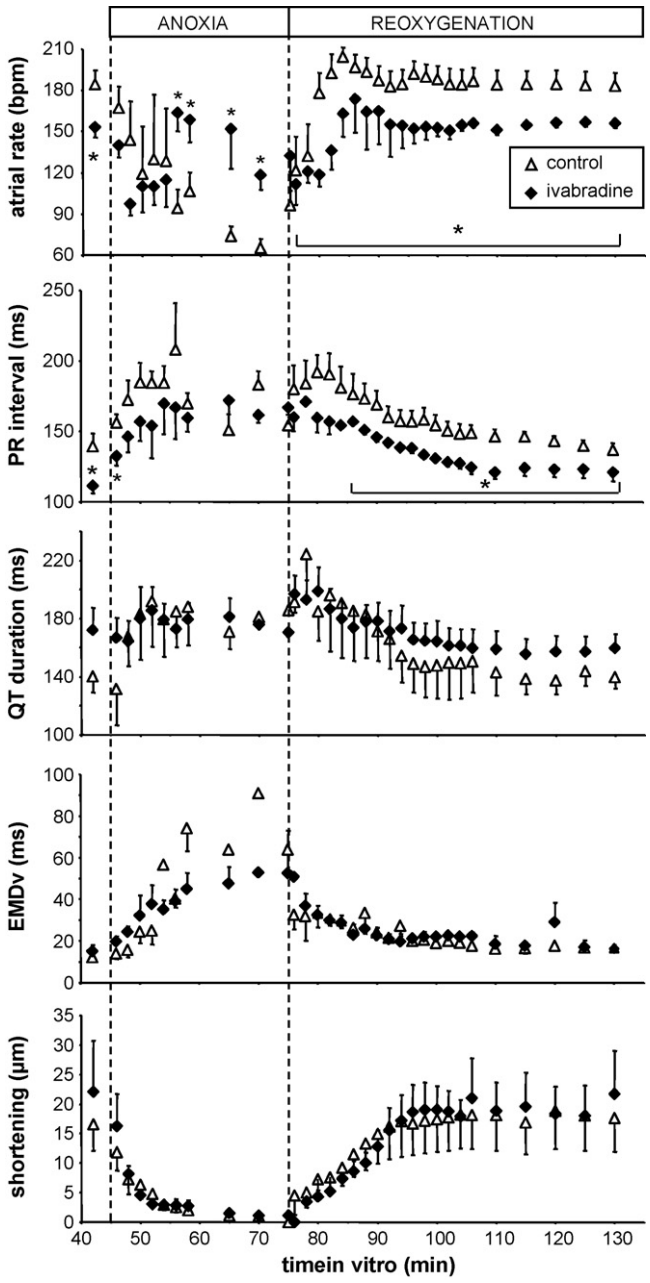

Fig. 4. In the whole heart, ivabradine decreased atrial rate and shortened PR interval under normoxia (preanoxia) and throughout reoxygenation. By contrast, QT duration, ventricular electromechanical delay (EMDv) and ventricular shortening were not affected. Mean ± SEM; $n = 5$ for each condition; *: $p < 0.05$ versus control.

3.4. Correlation between heart rate and atrio-ventricular conduction

Fig. 5 clearly shows that atrio-ventricular conduction under normoxia depended on beating rate since the longer the RR interval, the shorter the PR interval, regardless if ivabradine was applied or not. Furthermore, a beat-to-beat analysis performed in individual hearts revealed that specific inhibition of HCN channels by ivabradine stabilized conduction, specially when RR varied between 370 and 475 ms, i.e. between 160 and 130 bpm. Indeed, the individual slope PR/RR (250 data points per heart) was significantly higher in the control group (0.53 ± 0.27, $n = 5$) than in the ivabradine treated group (0.10 ± 0.04, $n = 5$) ($p = 0.032$). However, during anoxia and reoxygenation no significant correlation could be properly established between PR and RR intervals, most likely due to major electromechanical disturbances, including numerous AV blocks (see Table 1).

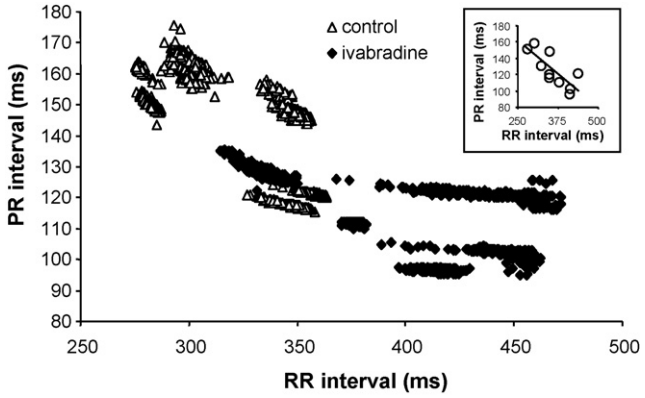

Fig. 5. Beat-to-beat analysis performed in individual hearts showing that the relationship between PR interval and RR interval under normoxic conditions is different in control and ivabradine treated hearts, the PR interval being stabilized by ivabradine. The general linear relationship between PR interval and RR interval is shown in the inset regardless if ivabradine was applied or not ($r^2 = 0.62$). Each beat-to-beat analysis was performed on 250 successive preanoxic cardiac cycles; Ivabradine, 0.3 µM; r^2: coefficient of determination of the linear regression; $n = 5$ hearts in each group.

4. Discussion

4.1. Dose–response curve for ivabradine

The inhibition of the *If* current by ivabradine is known to be specific, selective and use-dependent at concentrations lower than 10 µM. However, at higher concentrations unspecific currents, such as calcium currents (L and T type) that play an important functional role in the embryonic heart, are also inhibited [3]. For this reason, dose–response curves have been determined within the range of 0.1–10 µM of ivabradine. Interestingly, ivabradine lowered embryonic atrial rate in the very same range of concentrations (1–3 µM) and to the same extent (~20%) than in adult sinoatrial node cells [4,20], corresponding to half-block concentrations for HCN1 and HCN4 subtypes [20,21]. These observations indicate that the pharmacological modulation of HCN channels could be similar in embryonic and adult pacemaker cells, which deserves to be further investigated. Although ivabradine (1 µM) decreased the beating rate by about 40 bpm both in atria and ventricle (equal effect), it was more efficient in ventricle than in atria, i.e. a drop of frequency of 50% versus 20%. Furthermore, compared with other regions, ivabradine had a stronger inhibitory effect on spontaneous activity of the outflow tract, even at the lowest concentration.

Concentrations of ivabradine higher than 0.3 µM decreased further atrial rate but had no additional effect on ventricular rhythm, suggesting that non-HCN pacing mechanisms, such as sodium–calcium exchanger [22] and intracellular calcium release [23,24], can also contribute to pacemaker current more markedly in the ventricle than in atria of the embryonic heart. Our experiments showing that spontaneous contractions of the isolated outflow tract were totally abolished by ivabradine, in contrast to atria and ventricle, support the hypothesis that pacemaking activity in this part of the heart rely on HCN channels exclusively, and including at least HCN4.

Under normoxia, ivabradine had a negative chronotropic effect without any inotropic effect, alike in adult sinoatrial myocytes [4]. Thus, the fact that inhibition of HCN channels slowed the

spontaneous beating rate differently in the three cardiac regions and that the HCN4 isoform was inhomogenously distributed, suggest a subtle gradient of density and/or properties of HCN channels along the developing heart.

4.2. Anoxia-reoxygenation

The embryonic heart at the investigated stage is not innervated by the autonomic nervous system and no neurohumoral influence exists under our in vitro conditions. Thus, the observed changes of pacemaker rate during anoxia-reoxygenation were exclusively regulated at the cardiomyocytes level.

In addition to its negative chronotropic effect, inhibition of HCN channels appears to stabilize atrio-ventricular conduction, especially when heart rate is below 160 bpm, under normoxia (Fig. 5) as well as during anoxia and reoxygenation (Fig. 4). To our knowledge, such a dromotropic effect of HCN channel inhibition has not been reported in adult heart [5,25]. It should be noticed that this PR interval stabilizing effect can be clearly observed with ivabradine, but it may not be exclusively due to HCN inhibition.

It has been shown [26] that if HCN channels are blocked, cells tend to hyperpolarize more which in turn relieves inactivation of more Ca^{2+} and/or Na^{+} channels involved in action potential propagation and consequently improves conduction. This hypothesis is strongly supported by the evident correlation observed between PR interval and RR interval. A complementary interpretation is that Ca^{2+} reuptake into sarcoplasmic reticulum and transsarcolemmal Ca^{2+} extrusion, taking place during a significantly prolonged diastole (+25%), could somewhat lower basal diastolic intracellular calcium relative to untreated hearts. This is consistent with a slight enhancement of gap junction permeability by a lower intracellular Ca^{2+}. Indeed, although there is no specialized conduction system at the stage investigated, various connexins (e.g. Cx43) forming gap junctions are expressed and functional during early cardiogenesis [27,28]. Furthermore, alike in adult heart, decreasing heart rate reduces myocardial oxygen consumption in the embryonic chick heart at stage 24HH [29], which is known to protect heart function especially during an ischemic/hypoxic episode. Remarkably, during anoxia and reoxygenation, inhibition of HCN channels did not affect ventricular depolarization–repolarization (QT duration), excitation–contraction coupling (EMD) and contractility (shortening) and had no additional proarrhythmic effects as those observed in the adult mouse heart model at highly unspecific ivabradine concentrations [30]. During the last 20 min of anoxia QTc was 23% longer in ivabradine treated hearts than in control hearts but no additional arrhythmias were observed. Although a longer QTc puts an adult heart at increased risk for arrhythmias, it does not seem to be the case in the minute embryonic heart at stage 24HH in which the compact myocardium of the ventricle is very thin (200–300 μm) and action potential duration quite uniform in space.

Although a tendency toward a shorter time to resumption in atria and ventricle of treated hearts relative to control hearts can be observed in Table 1, there was no significant difference between the experimental groups. It should be noticed that the relatively important interindividual variability of the investigated parameters is probably due to slight differences in developmental stage, level of differentiation, cardiac dimensions and degree of flattening of the hearts in the culture compartment as previously discussed [17]. Moreover, the unavoidable arrhythmic activity induced by anoxia and reoxygenation was also responsible for a great variability. For example, in Fig. 4, the fact that atrial rate during anoxia was the average rate determined during bursts of activity contributed to increase interindividual variability. Nevertheless, the preanoxic PR and QT values were within the range found in our previous work [16].

4.3. Distribution of the HCN4 channel

The antibody against HCN4 identified a band at about 160 kDa, corresponding to molecular weight of HCN4 which predominates over the other HCN isoforms in the adult sinoatrial node [31]. Our data provide the first direct evidence that the HCN4 channel, considered as the predominant isoform during early cardiogenesis [8–10], is inhomogeneously distributed within the heart of the chick embryo, i.e. atria = ventricle > outflow tract. Ivabradine at 10 μM reduced the beating rate in both atria and ventricle by about 40 bpm but abolished spontaneous activity of the outflow tract. These findings support the concept that the low intrinsic beating rate of the outflow tract can be attributed to the low density of HCN4 channels. As the fate of the outflow tract is to differentiate at older stages into aorta and pulmonary artery rather than spontaneously contracting myocardium, it is not surprising that this otherwise slowly conducting region exhibited the lowest HCN4 expression.

The possibility that other subtypes of HCN channels (i.e. HCN1, 2) blocked by ivabradine and known to be present in the adult heart [2], are expressed in the embryonic heart and play a role in atrial and ventricular pacemaking cannot be ruled out. Furthermore, the spatial distribution of HCN4 drastically changes throughout cardiac development [8,32] and HCN4 can heteromerize with HCN2 to form functional pacemaker channels in the embryonic heart [33].

5. Conclusion

The gradient of intrinsic beating rate within the embryonic heart model, the differential efficiency of ivabradine in the sinoatrial region, ventricle and outflow tract and the characteristic distribution of the predominant HCN4 isoform along the heart, indicate that HCN channels play an important role in the fine control of the rate of diastolic depolarization in all cardiac regions. Moreover, our findings show that HCN channels can be involved in the chrono- and dromotropic responses to transient oxygen deprivation without affecting E–C coupling or contractility.

Acknowledgements

We thank Anne-Catherine Thomas for her skillful technical assistance. Supported by the Swiss Heart Foundation and the Swiss National Science Foundation no. 3100A0-105901. Servier (France) kindly provided ivabradine.

References

[1] Bucchi A, Barbuti A, Baruscotti M, Difrancesco D. Heart rate reduction via selective 'funny' channel blockers. Curr Opin Pharmacol 2007;7:208–13.
[2] Siu CW, Lieu DK, Li RA. HCN-encoded pacemaker channels: from physiology and biophysics to bioengineering. J Membr Biol 2006;214:115–22.
[3] DiFrancesco D, Camm JA. Heart rate lowering by specific and selective I(f) current inhibition with ivabradine: a new therapeutic perspective in cardiovascular disease. Drugs 2004;64:1757–65.
[4] Bois P, Bescond J, Renaudon B., Lenfant J. Mode of action of bradycardic agent, S 16257, on ionic currents of rabbit sinoatrial node cells. Br J Pharmacol 1996;118:1051–7.
[5] Berdeaux A. Preclinical results with I(f) current inhibition by ivabradine. Drugs 2007;67(Suppl. 2):25–33.
[6] Ferrari R, Cargnoni A, Ceconi C. Anti-ischaemic effect of ivabradine. Pharmacol Res 2006;53:435–9.
[7] Vilaine JP. The discovery of the selective I(f) current inhibitor ivabradine A new therapeutic approach to ischemic heart disease. Pharmacol Res 2006;53:424–34.
[8] Mommersteeg MT, Hoogaars WM, Prall OW, de Gier-de Vries C, Wiese C, Clout DE, et al. Molecular pathway for the localized formation of the sinoatrial node. Circ Res 2007;100:354–62.
[9] Stieber J, Herrmann S, Feil S, Loster J, Feil R, Biel M, et al. The hyperpolarization-activated channel HCN4 is required for the generation of pacemaker action potentials in the embryonic heart. Proc Natl Acad Sci USA 2003;100:15235–40.
[10] Harzheim D, Pfeiffer KH, Fabritz L, Kremmer E, Buch T, Waisman A, et al. Cardiac pacemaker function of HCN4 channels in mice is confined to embryonic development and requires cyclic AMP. EMBO J 2008;27:692–703.

[11] Kamino K, Hirota A, Fujii S. Localization of pacemaking activity in early embryonic heart monitored using voltage-sensitive dye. Nature 1981;290:595–7.
[12] Van Mierop LH. Location of pacemaker in chick embryo heart at the time of initiation of heartbeat. Am J Physiol 1967;212:407–15.
[13] Satoh H, Sperelakis N. Identification of the hyperpolarization-activated inward current in young embryonic chick heart myocytes. J Dev Physiol 1991;15:247–52.
[14] Satoh H, Sperelakis N. Hyperpolarization-activated inward current in embryonic chick cardiac myocytes: developmental changes and modulation by isoproterenol and carbachol. Eur J Pharmacol 1993;240:283–90.
[15] Yasui K, Liu W, Opthof T, Kada K, Lee JK, Kamiya K, et al. I(f) current and spontaneous activity in mouse embryonic ventricular myocytes. Circ Res 2001;88:536–42.
[16] Sarre A, Maury P, Kucera P, Kappenberger L, Raddatz E. Arrhythmogenesis in the developing heart during anoxia-reoxygenation and hypothermia-rewarming: an in vitro model. J Cardiovasc Electrophysiol 2006;17:1350–9.
[17] Rosa A, Maury JP, Terrand J, Lyon X, Kucera P, Kappenberger L, et al. Ectopic pacing at physiological rate improves postanoxic recovery of the developing heart. Am J Physiol Heart Circ Physiol 2003;284:H2384–92.
[18] Hamburger V, Hamilton H. A series of normal stages in the development of the chick embryo. J Morphol 1951;88:49–92.
[19] Sarre A, Lange N, Kucera P, Raddatz E. mitoKATP channel activation in the postanoxic developing heart protects E-C coupling via NO-, ROS-, and PKC-dependent pathways. Am J Physiol Heart Circ Physiol 2005;288:H1611–9.
[20] Bucchi A, Tognati A, Milanesi R, Baruscotti M, Difrancesco D. Properties of ivabradine-induced block of HCN1 and HCN4 channels. J Physiol 2006;572:335–46.
[21] El Chemaly A, Magaud C, Patri S, Jayle C, Guinamard R, Bois P. The heart rate-lowering agent ivabradine inhibits the pacemaker current I in human atrial myocytes. J Cardiovasc Electrophysiol 2007;18:1190–6.
[22] Shepherd N, Graham V, Trevedi B, Creazzo TL. Changes in regulation of sodium/calcium exchanger of avian ventricular heart cells during embryonic development. Am J Physiol Cell Physiol 2007;292:C1942–50.
[23] Mery A, Aimond F, Menard C, Mikoshiba K, Michalak M, Puceat M. Initiation of embryonic cardiac pacemaker activity by inositol 1,4,5-trisphosphate-dependent calcium signaling. Mol Biol Cell 2005;16:2414–23.
[24] Yang HT, Tweedie D, Wang S, Guia A, Vinogradova T, Bogdanov K, et al. The ryanodine receptor modulates the spontaneous beating rate of cardiomyocytes during development. Proc Natl Acad Sci USA 2002;99:9225–30.
[25] Thollon C, Bidouard JP, Cambarrat C, Lesage L, Reure H, Delescluse I, et al. Stereospecific in vitro and in vivo effects of the new sinus node inhibitor (+)-S 16257. Eur J Pharmacol 1997;339:43–51.
[26] Park K, Lee S, Kang SJ, Choi S, Shin KS. Hyperpolarization-activated currents control the excitability of principal neurons in the basolateral amygdala. Biochem Biophys Res Commun 2007;361:718–24.
[27] Veenstra RD. Developmental changes in regulation of embryonic chick heart gap junctions. J Membr Biol 1991;119:253–65.
[28] Wiens D, Jensen L, Jasper J, Becker J. Developmental expression of connexins in the chick embryo myocardium and other tissues. Anat Rec 1995;241:541–53.
[29] Romano R, Rochat AC, Kucera P, De Ribaupierre Y, Raddatz E. Oxidative and glycogenolytic Capacities within the developing chick heart. Pediatr Res 2001;49:363–72.
[30] Stieber J, Wieland K, Stockl G, Ludwig A, Hofmann F. Bradycardic and proarrhythmic properties of sinus node inhibitors. Mol Pharmacol 2006;69:1328–37.
[31] Brioschi C, Micheloni S, Tellez JO, Pisoni G, Longhi R, Moroni P, et al. Distribution of the pacemaker HCN4 channel mRNA and protein in the rabbit sinoatrial node. J Mol Cell Cardiol 2009;47:221–7.
[32] Garcia-Frigola C, Shi Y, Evans SM. Expression of the hyperpolarization-activated cyclic nucleotide-gated cation channel HCN4 during mouse heart development. Gene Expr Patterns 2003;3:777–83.
[33] Whitaker GM, Angoli D, Nazzari H, Shigemoto R, Accili EA. HCN2 and HCN4 isoforms self-assemble and co-assemble with equal preference to form functional pacemaker channels. J Biol Chem 2007;282:22900–9.